NGU Report 2002.014

Sedimentological descriptions and results of analytical tests of sediment cores from fjords and lakes in northwest Western Norway

Geological Survey of Norway
N-7441 Trondheim, Norway
Tel.: 47 73 90 40 00
Telefax 47 73 92 16 20

REPORT

Report no.: 2002.014 | ISSN 0800-3416 | Grading: Open

Title: Sedimentological descriptions and results of analytical tests of sediment cores from fjords and lakes in northwest Western Norway

Authors:
Aivo Lepland, Reidulv Bøe, Eivind Sønstegaard, Haflidi Haflidason, Connie Hovland, Heidi Olsen and Runar Sandnes

Client:
Norsk Hydro ASA, NGU

County:
Sogn og Fjordane, Møre og Romsdal

Commune:
Eid, Volda, Ørsta

Map-sheet name (M=1:250.000)
Årdal, Ålesund

Map-sheet no. and -name (M=1:50.000)
1218 I, 1119 II

Deposit name and grid-reference:

Number of pages: 198 Price (NOK): 540
Map enclosures:

Fieldwork carried out:	Date of report:	Project no.:	Person responsible:
June-July 2001	1 September, 2002	293100	

Summary:

This cooperative project, involving NGU, Norsk Hydro ASA, the University of Bergen and Sogn and Fjordane College, aims at documenting past slide/mass movement events recorded in Holocene fjord and lake sediments in western Norway between Sognefjorden and Kristiansund. The assessment of triggering mechanisms of past mass movements is of critical importance for evaluating future risks on coastal infrastructure and offshore installations.

In this report (Phase C) we present the results of laboratory tests and visual descriptions performed on 43 fjord cores and 26 lake cores that have been collected in the frame of the current project. Most of the cores have been profiled using the X-ray inspection system (XRI) and the multi sensor core logger (MSCL). 55 cores were opened and sedimentologically described. Determinations of geotechnical parameters and sediment physical properties were carried out on 27 and 26 fjord cores, respectively. Grain-size distribution has been analysed in 35 samples from 3 fjord cores. Radiocarbon dating of foraminifers and shells in fjord cores and bulk gyttja and shells in lake cores was carried out using both accelerator mass spectrometry (AMS) and conventional radioactive counting methods. The dating samples were typically collected beneath or close to relatively coarse grained sediment intervals that can possibly be linked to mass movement events. 51 samples from 25 cores have been dated and calendar year ages before present (BP) are reported in the text and on figures.

Keywords: Marine Geology	Tsunami	Earthquake
Core	Reflection seismic	Dating
Geological hazard	Turbidite	Slide

CONTENTS

FIGURES

TABLES

APPENDIXES

1. INTRODUCTION

Recent seismic and lithostratigraphic studies in fjords of western Norway, between Sognefjorden and Kristiansund, have suggested a large-scale mass movement event at about ^{14}C-years 7000 BP (Longva et al. 2001, Sejrup et al. 2001), possibly related to the Storegga Slide tsunami (Bondevik et al. 1998, Grøsfjeld et al. 1999). Studies by Longva et al. (2001) and Sejrup et al. (2001) have furthermore provided indications for a mass movement event at about 2000 ^{14}C-years and possibly also at about 9000 ^{14}C-years BP.

The Geological Survey of Norway (NGU) and Norsk Hydro ASA, in cooperation with the University of Bergen and Sogn og Fjordane College, have undertaken a study to track the areal extent and ultimate causes for the suggested 2000 ^{14}C-years BP episode and other such events. This study involves the interpretation of seismic profiles and documentation of 69 sediment cores, obtained from fjords (Fig. 1) and lakes (Fig. 2) between Sognefjorden and Kristiansund.

In this report we present descriptive and analytical results of core samples with the aim to recognize and date sediment intervals that may reflect tsunami / mass movement events. It is assumed that the regular sedimentation pattern was disrupted during these events, and relatively coarse-grained and/or turbiditic sediments accumulated.

2. MATERIALS

The sediment cores described here were collected from 43 fjord locations (Table 1) and from 26 locations in five lakes (Table 2) in the area between Sognefjorden and Kristiansund. Seismic profiles, reported by Longva et al. (2001) and Longva and Olsen (2001) and Sønstegaard et al. (2001), provided the basis for selection of the sampling stations. Sampling was generally undertaken at the planned localities as specified in Longva et al. (2001), Longva and Olsen (2001), although some of the fjord stations are up to 250 m off the planned localities. The exact positions of fjord cores on seismic profiles are shown in Appendix 1.

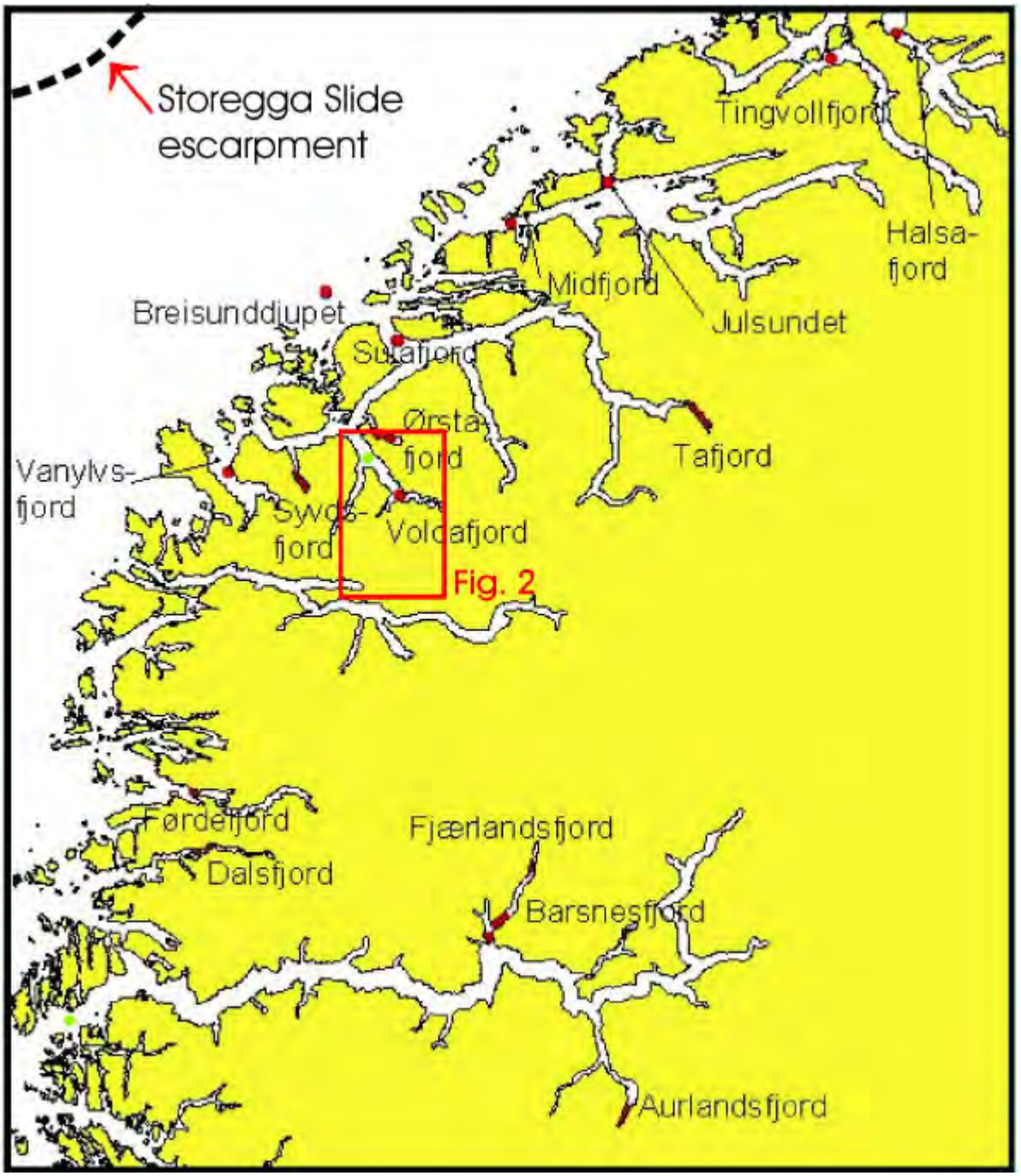

Fig. 1. Map showing core locations (red dots) in fjords investigated in this study. Red box indicates the area shown in Fig.2.

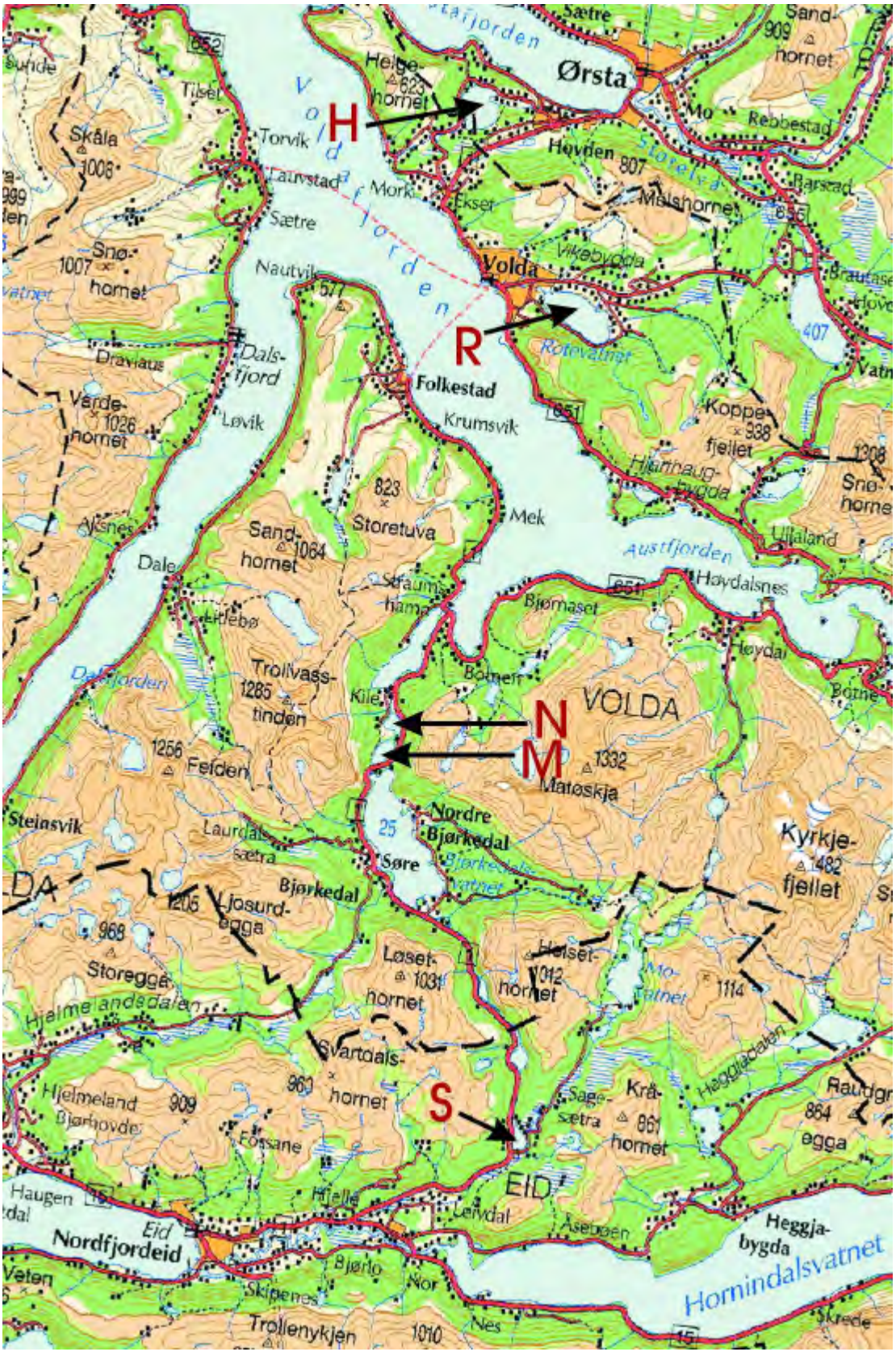

Fig. 2. Locations of investigated lakes: Storsætervatnet (S), Medvatnet (M), Nedstevatnet (N), Rotevatnet (R) and Hovdevatnet (H). For general orientation see Fig. 1.

Table 1. Core inventory, fjords.

Seismic line	Fjord	Core number	X (UTM32)	Y (UTM32)	Latitude WGS84	Longitude WGS84	Water depth (m)	Core length (m)
0002010	Aurlandsfj.	P0103001	399620	6752240	60° 53.5556’	7° 9.008474’	178	1.98
0002011	Aurlandsfj.	P0103002	398844	6750453	60° 52.58125’	7° 8.206415’	73	1.64
0002011	Aurlandsfj.	P0103003	398423	6750180	60° 52.42767’	7° 7.750053’	43	0.78
0002015	Fjærlandsfj.	P0103004	371204	6793299	61° 15.16045’	6° 35.95284’	247	2.30
0002015	Fjærlandsfj.	P0103005	372763	6794625	61° 15.90477’	6° 37.64045’	238	1.93
0002015	Fjærlandsfj.	P0103006	379027	6805562	61° 21.91132’	6° 44.21854’	172	1.60
0102001	Barsnesfj.	P0103007	399035	6791482	61° 14.67339’	7° 7.115135’	82	1.74
0102001	Barsnesfj.	P0103008	399052	6791462	61° 14.66240’	7° 7.134504’	82	1.28
0002015	Fjærlandsfj.	P0103009	369695	6790158	61° 13.43994’	6° 34.39725’	305	1.73
Dalsfj_1B	Dalsfjord	P0103011	305266	6809367	61° 22.15027’	5° 21.35081’	260	0.80
Dalsfj_1B	Dalsfjord	P0103012	308008	6810303	61° 22.74605’	5° 24.36410’	173	1.54
Dalsfj_1B	Dalsfjord	P0103013	308358	6810457	61° 22.83897’	5° 24.74616’	173	1.62
9702003	Førdefj.	P0103014	304986	6822163	61° 29.03091’	5° 20.23141’	340	0.87
0003001	Vanylvsfj.	P0103015	312358	6892247	62° 6.924362’	5° 24.15304’	297	1.64
Syvdfj_1	Syvdsfj.	P0103016	329141	6889338	62° 5.839233’	5° 43.58826’	90	1.35
Syvdfj_1	Syvdsfj.	P0103017	328359	6890251	62° 6.308899’	5° 42.63805’	99	1.44
Syvdfj_1	Syvdsfj.	P0103018	327293	6891540	62° 6.972885’	5° 41.33909’	99	1.49
Syvdfj_1	Syvdsfj.	P0103019	327293	6891555	62° 6.980896’	5° 41.33869’	100	1.58
Syvdfj_1	Syvdsfj.	P0103020	327258	6891591	62° 6.998978’	5° 41.29626’	99	1.14
9909001	Austefj.	P0103021	350294	6887354	62° 5.311890’	6° 7.967291’	317	0.40
0003010	Ørstafj.	P0103022	344780	6901079	62° 12.56035’	6° 9.148121’	172	0.69
9908007	Tafjord	P0103023	416461	6904222	62° 15.62073’	7° 23.47089’	200	0.7
9908008	Tafjord	P0103024	417194	6903270	62° 15.11787’	7° 24.34542’	150	0.95
9908004	Tafjord	P0103025	417187	6903867	62° 15.43922’	7° 24.31981’	190	0.47
9908001	Tafjord	P0103026	416628	6903998	62° 15.50217’	7° 23.67059’	197	1.27
9908009	Tafjord	P0103027	414959	6905842	62° 16.47217’	7° 21.68919’	205	1.00
9908026	Tafjord	P0103028	414892	6905970	62° 16.54015’	7° 21.60833’	207	0.3
9908006	Tafjord	P0103029	414932	6906158	62° 16.64246’	7° 21.64836’	207	1.14
9908006	Tafjord	P0103030	413383	6907603	62° 17.39845’	7° 19.81605’	217	0.83
0003023	Midfjord	P0103031	374839	6947337	62° 38.12500’	6° 33.54000’	253	0.57
SSundalsora	Tingvollfj.	P0103032	444906	6983247	62° 58.48755’	7° 54.79268’	302	0.78
0003010	Ørstafj.	Ørsta-GC1A	348212	6899623	62° 11.8617’	6° 04.9433’	136	1.48
0003010	Ørstafj.	Ørsta-GC1B	348212	6899623	62° 11.8617’	6° 04.9433’	136	1.47
0003010	Ørstafj.	Ørsta-GC2	347897	6900188	62° 12.1583’	6° 04.5517’	137	1.68
0003009	Ørstafj.	Ørsta-GC3	347244	6900268	62° 12.1850’	6° 03.7950’	141	1.92
0003009	Ørstafj.	Ørsta-GC4	346629	6900745	62° 12.4267’	6° 03.0617’	136	1.62
SBreis-Volda	Breisundd.	HM129-03	333849	6931988	62° 28.90’	5° 46.55’	246	2.52
SBreis-Volda	Breisundd.	HM129-04	334074	6931846	62° 28.83’	5° 46.82’	267	2.30
SSt-Breis4	Sulafjord	NGU-2L/SC	349480	6921298	62° 23.5500’	6° 5.2800’	446	4.0
SSt-Breis4	Sulafjord	NGU-3L/SC-1	349646	6921342	62° 23.5783’	6° 5.4700’	443	3.4
SSt-Breis4	Sulafjord	NGU-3L/SC-2	349646	6921342	62° 23.5783’	6° 5.4700’	443	2.0
SHalsafj.	Halsafj.	NGU-4L/SC	459289	6988764	63° 1.5733’	8° 11.7317’	510	7.3
0003025	Julsundet	NGU-6L/SC	395697	6956098	62° 43.2300’	6° 57.6033’	500	6.3

Table 2. Core inventory, lakes.

Lake name	Altitude m a.s.l.	Core number	Latitude (WGS84)	Longitude (WGS84)	Time on seismic data	Water depth (m)	Core length (cm)	X -ray images	Density	Mag. suscept.
Storsetervatnet	277	S1	61 56 481	06 08 312	13:20:25	9	220	x	x	x
Storsetervatnet	277	S2	61 56 740	06 08 328	14:59:53	11	49	x		
Storsetervatnet	277	S3	61 56 778	06 08 282	15:00:47	9	234	x	x	x
Storsetervatnet	277	S4	61 56 772	06 08 302	15:00:23	9	350	x		
Storsetervatnet	277	S5	61 56 778	06 08 213	15:06:55	6	219	x	x	x
Storsetervatnet	277	S6	61 56 758	06 08 315	15:00:07	10	264	x	x	x
Storsetervatnet	277	S7	61 56 776	06 08 292	15:00:33	9	214	x		
Storsetervatnet	277	S8	61 56 798	06 08 218	14:47:50	6	251	x		
Storsetervatnet	277	S9	61 56 615	06 08 525	14:12:35	6	250	x		
Storsetervatnet	277	S10	61 56 800	06 08 249	14:47:00	6	484	x	x	x
Medvatnet	12,5	M1	62 01 929	06 02 923	12:28:58	21	154			
Medvatnet	12,5	M2	62 01 941	06 02 887	12:29:17	22	332	x	x	(x)
Medvatnet	12,5	M3	62 01 740	06 02 726	12:50:45	19	133			
Medvatnet	12,5	M4	62 01 717	06 02 650	12:51:37	19	350	x	x	x
Medvatnet	12,5	M5	62 01 700	06 02 562	12:52:48	21	210	x		
Medvatnet	12,5	M6	62 01 733	06 02 544	12:53:02	22,5	242	x	x	
Nedstevatnet	9	N1	62 02 223	06 02 833	15:50:20	17	540	x	x	x
Nedstevatnet	9	N2	62 02 217	06 02 730	15:49:21	15	383	x	x	x
Nedstevatnet	9	N3	62 02 246	06 02 934	15:51:30	17	330	x	x	x
Nedstevatnet	9	N5	62 02 209	06 02 944	15:36:25	18	313	x	x	(x)
Rotevatnet	47	R1	62 08 517	06 05 831	17:23:52	6	290	x	x	x
Rotevatnet	47	R2	62 08 524	06 05 853	15:12:02	8	231	x		
Rotevatnet	47	R3	62 08 434	06 05 928	13:14:45	12,5	290			
Hovdevatnet	73	H1	62 11 315	06 02 732	13:10:49	15	290	x	x	x
Hovdevatnet	73	H2	62 11 183	06 02 664	12:10:09	14	170	x		
Hovdevatnet	73	H3	62 11 207	06 02 666	12:10:40	14	150	x		

3. METHODS

The laboratory procedures with the sediment cores involved (i) stratigraphic profiling with an X-ray inspection system, (ii) stratigraphic profiling for sediment density and magnetic susceptibility using a multi sensor core logger, (iii) lithostratigraphic description, (iv) subsampling and sample preparation for ^{14}C-dating, (v) grain-size analysis, (vi) determination of geotechnical and physical properties of sediments. More detailed descriptions of methods/procedures are given below.

3.1. X-ray inspection system (XRI)

The images of the XRI system reflect variable X-ray absorption (transparency) of different sediment components. The XRI system consists of an X-ray tube and an image intensifier that converts invisible X-rays into visible light. A CCD camera is used to capture the visible

image. The size of an XRI image depends upon specific settings, typically covering 10-15 cm thick sediment interval. The sediment core is placed between the X-ray tube and the image intensifier; different core sections can be inspected by sliding the assembled X-ray tube and image intensifier along the core. X-ray transparency of a sediment is strongly influenced by the grain-size and the images are generally lighter for the fine-grained sediments and darker for coarse-grained sediments. XRI is a handy, non-destructive method to study the texture and structure of sediments, to characterize the distribution of gas pockets, shells, wood fragments and clasts, and to interpret the disturbances caused by bioturbation, gas escape or shear. The possibility to rotate the core simultaneously with imaging facilitates detailed geometric analyses of specific structural features.

The XRI documentation is given as sequences of digital images where each individual image corresponds to 11-14 cm sediment interval. The scale at the side of the images shows the depth in centimetres from the sediment surface or from the core section top in case of multiple sections. Individual images from all cores have been montaged to provide the complete XRI sequence.

3.2. Multi sensor core logger (MSCL)

The GEOTEK manufactured Multi Sensor Core Logger (MSCL) was used to study physical properties of sediments by means of gamma-ray density, P-wave velocity and magnetic susceptibility. The MSCL consists of a conveyor system, a central unit assembly including three sensors, a microprocessor and a computer. The conveyor system has two track sections, mounted and aligned on either side of the central unit, and a belt driven pusher block which is driven in either direction by a stepper motor and gear box assembly. The central unit assembly incorporates a compressional wave (P-Wave) logger, a gamma ray attenuation logger and a magnetic susceptibility loop. Automation is achieved through the use of an internal processor, interfaced with the rack-mounted computer that controls the entire running process and stores data.

Up to 140 cm long core sections are placed on the right hand track with the top located at the reference position. A conveyor system automatically pushes each core section through the sensor array (incrementally past gamma ray attenuation logger, the p-wave logger and through the magnetic susceptibility coil) with measurements being taken at spatial increments as defined by the user; 0.5 cm and 1 cm step-sizes were used in this study. The computer controlling the conveyor also controls the sensors, so that all data are automatically correlated. Adjacent core sections are loaded on to the conveyor by the user when prompted by the software commands. In this way a complete core can be logged in a continuous process while the raw and processed data are displayed graphically in real time on the monitor. Complete control of the graphic display is provided, both in terms of the presentation and processing protocols. Both raw and processed data are saved in formats suitable for exporting to other software environments for further data manipulation or data presentation.

3.2.1. Gamma ray density

Density is determined by measuring the attenuation of gamma rays through the cores. The gamma ray attenuation unit comprises a 10 millicurie Cesium-137 capsule (housed in a 150 mm diameter primary lead shield) with both 2.5 and a 5.0 mm collimators and a sodium iodide scintillation detector (housed in a 150 mm diameter collimated lead shielding to

minimize any background radiation). A density resolution of better than 1% depending upon counting time used and core condition is normally achieved. The source and detector are mounted diametrically across the diameter of the core.

A narrow (pencil size) beam of gamma rays with energies principally at 0.662 MeV is emitted from the Cesium -137 source and passes through the diameter of the sediment core. At these energy levels Compton scattering is the primary mechanism for the attenuation of the gamma rays in most sedimentary material. The incident photons are scattered by collision with electrons encountered in the core and there is a partial energy loss. This attenuated gamma beam is measured by the Sodium Iodide detector. The Compton scattering of the photons is directly related to the number of electrons in the path of the gamma ray beam. The bulk density of the sediment in each analysed interval is calculated by comparing the attenuation of gamma rays through the sediment core to the attenuation of the gamma rays through a standard of aluminium density calibration billet.

Calibration of the gamma ray attenuation system is performed using aluminium cylinder with 5 different diameters and a section of core liner filled with water. Each diameter slice of aluminium is placed in the liner and the gamma counts are measured over a period of minimum 90 sec. The density x diameter values are plotted vs. ln gamma counts and the resulting slope and intercept are used to calculate bulk density and calibrate the sensor for the liner thickness, type and diameter.

3.2.2. Magnetic susceptibility

The magnetic susceptibility Bartington loop (150 mm) sensor (MS2B) is used in the MSCL system. A low intensity non-saturating alternating magnetic field is produced by an oscillator circuit in the sensor loop. Changes in the oscillator frequency caused by the sediment in the sensor loop are measured and converted into volume specific magnetic susceptibility values (SI units). The magnitude of the magnetic susceptibility values is dependent on the type of sediment, content of magnetic minerals and the volume of sediment within the coil. Identical cores of varying diameters will give different magnetic susceptibility values but will show the same down core profile. The calibration of the magnetic susceptibility loop, performed using a standard of known magnetic susceptibility, gives 5% calibration accuracy.

Density and magnetic susceptibility profiles generally coincide. The main difference is that the magnetic susceptibility signal is collected from 4-6 cm thick sediment intervals whereas the density measurements are obtained from thinner (< 1 cm) sediment intervals. Density logs have therefore proven to be more specific and useful defining stratigraphic boundaries.

3.3. Lithostratigraphic description

Lithostratigraphic description was undertaken on split cores that were obtained by cutting through the tube plastic lengthwise and pulling a steel wire through the sediment. The stratigraphic logging focused upon parameters such as sedimentary structures, texture and colour as well as disturbances caused during core handling or opening. The colour characterisation according to Munsell Soil Colour Charts (Munsell 1954) was performed

immediately after core opening in order to minimize colour changes due to sediment drying or oxidation.

3.4. ^{14}C-dating

Accelerator mass spectrometry (AMS) ^{14}C-dating on foraminifers and shells was performed to determine the age of potential mass movement event(s) in fjords (Table 3). Sub-samples for dating were typically collected from beneath the base of distinct coarse-grained intervals or from above such intervals. Dating samples generally covered 5 cm thick sediment intervals, and consisted of five individual 1 cm thick slices. The idea behind such slicing was to narrow down the window of the dated sediment interval. Only one, closest to the contact, sediment slice was used in case it provided a sufficient amount of foraminifers for dating. Samples preparation for dating was performed at Bergen and Århus universities, and it included concentration of foraminifers by sieving (125 μm sieve), density separation (CCl_4) and hand picking. The ETH laboratory in Zurich was used for ^{14}C age determination of fjord samples.

The age determination of lake samples was performed at the Laboratory for radiological dating, NTNU, Trondheim. Most of the lake samples were dated by the conventional method except 2 that were analysed by AMS. Bulk gyttja and shells were used as a dating material (Table 4). Dating was undertaken at or close to levels that can possibly be linked to mass movement events. The only exception is a sample from the lower part of core S10 (Storsætervatnet) that was dated for deglaciation timing. Dated levels include diamictic zones in the glaciomarine silt (Medvatnet, Nedstevatnet), repeated ash-layer stratigraphy in Storsætervatnet, distinct sedimentary hiatus, and minerogenic silt laminae within gyttja. For age determination of minerogenic laminae, gyttja from both beneath and above the lamina was integrated in the dated material (Table 4). In case of thicker minerogenic layers, separate dating samples were collected from above and/or beneath the layer. Hence these dates give either minimum or maximum age estimates of minerogenic units.

3.5. Grain-size analyses

Grain-size analysis on 35 samples from 3 cores were carried out using sieving for fractions coarser than 2 mm and laser diffraction technique using Coulter LS 200 for fractions finer than 2 mm. The sample suspensions used in Coulter LS 200 were dispersed in ultrasonic bath.

3.6. Determination of geotechnical and physical properties of sediments

3.6.1. Undrained shear strength

The Fall Cone apparatus was used to measure sediment shear strength. The split core was placed underneath the cone holder with the tip of the cone touching the sample. The penetration depth of the cone into the sediment after releasing the cone is proportional to the undrained shear strength (Table 5). Note that the values of undrained shear stress may bear a

systematic error due to compaction and dewatering during transport (14 days upright position) and storage.

3.6.2. Water content, wet density and dry density

These parameters were determined with the aid of a thin-wall steel cylinder with known volume and weight. This cylinder was inserted into the sediment and known volumes of wet, undisturbed sediments were subsampled. Weights of wet and dry (drying at 105 ºC for 24 hours) subsamples, combined with the known volume, allowed calculating water content, wet density and dry density (Table 6) according to the following formulas:

Water content = Weight of pore water / Weight of dry sediment

Wet density = Weight of wet sample / Volume of wet sample

Dry density = Weight of dry sample / Volume of wet sample

Note that the values of water content, wet and dry density may bear a systematic error due to compaction and dewatering during transport (14 days upright position) and storage.

4. RESULTS

4.1. Fjord investigations

Geographic coordinates, fjord affiliations, seismic lines, water depths and lengths of 43 cores from fjords that were collected in the frame of the current study are given in Table 1. All fjord cores were profiled with XRI and MSCL; these profiles are given in Appendix 2. The selection of 29 cores that were opened and lithologically described was made on the basis of XRI and MSCL results. The priority was placed on cores containing relatively coarse-grained, potentially tsunami/mass movement related sediment intervals. 27 sediment intervals from 13 cores were ^{14}C dated (Table 3, Figs 3-10, 12). 10 dating samples from 5 cores were exceedingly poor in foraminifers ("Negative" in Figs. 3-5, 10, 12) hence the age of these samples could not have been determined. The grain size distribution of sediments was analysed on 35 samples from 3 cores (NGU-2L/SC, NGU-4L/SC and NGU-6L/SC). Stratigraphic variations of the mean diameter in NGU-2L/SC, NGU-4L/SC and NGU-6L/SC along with cumulative grain-size distribution plots and statistical characteristics of individual samples are given in Appendix 3. The results of geotechnical tests and sediment physical properties determinations are shown in Tables 5 and 6, respectively.

Table 3. Results of AMS radiocarbon dating performed on hand picked foraminifers from fjord samples. The ^{14}C ages are corrected for reservoir effect (400 ^{14}C-years), and the transformation from ^{14}C age to calendar-year age was done according to Stuiver et al. (1998). In parenthesis, the age ranges include all time intervals contributing to the probability calculations for one standard deviation (1s).

Fjord	Core ID	Depth (m)	Sample No.	Lab. No.	Species	Sample weight (mg)	Uncorrected ^{14}C age (BP)	$\delta^{13}C$ (‰) V-PDB	Reservoir corrected ^{14}C age (BP)	Calendar-year age (BP)
Barsnesfjorden	P0103008	0.18-0.23	2001-6	ETH-25050	*Globobulimina sp., Uvigerina (peregrina) mediterranea*	8,5	1215 ± 65	1.0 ± 1.2	815 ± 65	**736** (824-672)
Barsnesfjorden	P0103008	1.06-1.11	2001-7	ETH-25051	*Nonion labradoricum*	5,2	2030 ± 60	1.6 ± 1.2	1630 ± 60	**1578** (1681-1514)
Dalsfjorden	P0103012	1.37-1.42	2001-10	ETH-25053	*Globobulimina sp., Cibicides*	5,5	8905 ± 90	1.0 ± 1.2	8505 ± 90	**9458** (9765-9108)
Dalsfjorden	P0103013	0.92-1.02	2001-11	ETH-25492	Mixed benthic foraminifers	9.1	2600 ± 55	0.2 ± 1.2	2200 ± 55	**2297** (2331-2182)
Førdefjorden	P0103014	0.55-0.6	2001-13	ETH-25054	*Uvigerina (peregrina) mediterranea, Hyalinea baltica*	11,2	2640 ± 55	-0.7 ± 1.2	2240 ± 55	**2320** (2348-2285)
Vanylvsfjorden	P0103015	1.14-1.19	2001-14	ETH-24864	*Uvigerina (peregrina) mediterranea, Hyalinea baltica*	11	3190 ± 55	1.3 ± 1.2	2790 ± 55	**2962** (3064-2881)
Syvdsfjorden	P0103019	1.5-1.55	2001-15	ETH-24865	*Globobulimina sp.*	14	2665 ± 50	1.1 ± 1.2	2265 ± 50	**2333** (2359-2301)
Tafjorden	P0103026	0.28-0.33	2001-16	ETH-24866	*Globobulimina sp., Bulimina marginata, Uvigerina (peregrina) mediterranea*	8,6	1090 ± 55	2.7 ± 1.2	690 ± 55	**647** (679-616)
Tafjorden	P0103026	0.86-0.91	2001-18	ETH-25055	*Globobulimina sp., Uvigerina (peregrina) mediterranea, Hyalinea baltica*	9,4	3300 ± 70	1.0 ± 1.2	2900 ± 70	**3141** (3239-3021)
Aurlandsfjorden	P0103002	1.5-1.55	2001-21	ETH-25056	*Globobulimina sp., Uvigerina (peregrina) mediterranea*	7,5	3040 ± 70	2.0 ± 1.2	2640 ± 70	**2778** (2866-2736)
Breisunddjupet	HM129-03	1.58-1.63	2001-22	ETH-24867	*Uvigerina (peregrina) mediterranea, Hyalinea baltica*	9,5	3480 ± 60	0.8 ± 1.2	3080 ± 60	**3352** (3419-3297)
Breisunddjupet	HM129-03	1.41-1.46	2001-23	ETH-24868	*Uvigerina (peregrina) mediterranea, Hyalinea baltica*	11	7775 ± 65	-2.1 ± 1.2	7375 ± 65	**8204** (8321-8156)
Ørstafjorden	ØrstaGC1A	0.76-0.81	2001-24	ETH-24869	*Globobulimina sp.*	9,2	2760 ± 60	1.8 ± 1.2	2360 ± 60	**2454** (2605-2345)

Table 3. continued

Fjord	Core ID	Depth (m)	Sample No.	Lab. No.	Species	Sample weight (mg)	Uncorrected ^{14}C age (BP)	δ^{13}C (‰) V-PDB	Reservoir corrected ^{14}C age (BP)	Calendar-year age (BP)
Julsundet	NGU-6L/SC	0.71-0.75	2001-27	ETH-25317	*Hyalinea balthica*		3365 ± 55	0.2 ± 1.2	2965 ± 55	**3222** (3313-3148)
Julsundet	NGU-6L/SC	2.64-2.65	2001-28	ETH-25301	*Astarte sp. (Astarte sulcata)*		8885 ± 65	-0.2 ± 1.2	8485 ± 65	**9447** (9753-9106)
Julsundet	NGU-6L/SC	5.07-5.11	2001-30	ETH-25318	*Melonis barleeanum*		10650 ± 75	1.9 ± 1.2	10250 ± 75	**11900, 11839,11723** (12269-11493)
Halsafjorden	NGU-4L/SC	1.51-1.55	2001-32	ETH-25319	*Hyalinea balthica*		3650 ± 50	2.2 ± 1.2	3250 ± 50	**3548** (3621-3464)
Halsafjorden	NGU-4L/SC	3.71-3.75	2001-33	ETH-25302	Shell fragments		7930 ± 75	0.3 ± 1.2	7530 ± 75	**8374** (8429-8322)
Halsafjorden	NGU-4L/SC	6.51-6.55	2001-36	ETH-25320	*Melonis barleeanum, Nonionellina labradorcia*		12080 ± 80	3.6 ± 1.2	11680 ± 80	**13484** (13806-13413)
Sulafjorden	NGU-2L/SC	3.04-3.08	2001-37	ETH-25321	*Uvigerina (perigrina) mediterrane*		7660 ± 65	1.3 ± 1.2	7260 ± 65	**8111** (8172-8012)
Sulafjorden	NGU-2L/SC	1.82-1.86	2001-38	ETH-25322	*Hyalinea balthica*		4665 ± 55	0.5 ± 1.2	4265 ± 55	**4851** (4949-4819)
Halsafjorden	NGU-4L/SC	4.98-5.02	2001-39	ETH-25493	*Melonis barleeanum, Nonimonellina labradorica, Globobulimina sp.*	31.2	10560 ± 75	-4.0 ± 1.2	10160 ± 75	**11657** (11913-11355)
Julsundet	NGU-6L/SC	0.45-0.50	2001-42	ETH-25667	*Mixed benthic foraminifers and gastropods*		3875 ± 60	2.2 ± 1.2	3475 ± 60	**3828** (3906-3725)
Ørstafjorden	ØrstaGC1A	0.49-0.52	2001-43	ETH-25669	*Globobulimina sp.*		2120 ± 50	0.1 ± 1.2	1720 ± 50	**1695** (1769-1615)
Breisunddjupet	HM129-03	0.25-0.30	2001-45	ETH-25670	*Uvigerina perigrina*		4720 ± 55	0.8 ± 1.2	4320 ± 55	**4940** (5026-4847)
Breisunddjupet	HM129-03	2.29-2.34	2001-46	ETH-25668	Shells (whole with perios)		6530 ± 65	0.1 ± 1.2	6130 ± 65	**7011** (7147-6934)
Syvdsfjorden	P0103019	0.84-0.88	2001-47	ETH-25671	*Globobulimina sp.*		2185 ± 50	-2.6 ± 1.2	1785 ± 50	**1780** (1837-1701)

Table 4. Results of radiocarbon dating performed on samples from lake sediments. The transformation from ^{14}C age to calendar-year age was done according to Stuiver et al. (1998). In parenthesis, the age ranges include all time intervals contributing to the probability calculations for one standard deviation (1s).

Lake	Core ID	Depth (cm)	Sample ID	Lab. No.	Material	Sample weight (g)	Age ^{14}C (BP)	Calendar-year age (BP)	$\delta^{13}C$ (‰)	Remarks
Storsaetervatnet	S1	72-77	S1-72	T-15551A	gyttja	5	4895±70	**5607** (5661-5590)	-29,2	Above and beneath 9 mm silt lamina
Storsaetervatnet	S4	181-183	S4-181	T-15552A	gyttja	7,1	8195±135	**9181** (9416-9008	-27,2	Above hiatus silt/gyttja
Storsaetervatnet	S6	152-157	S6-154	T-15553A	gyttja	4,5	8055±150	**9006** (9243-8649)	-26,8	Above hiatus silt/gyttja
Storsaetervatnet	S9	129-133	S9-133	T-15554A	gyttja	5,6	2585±80	**2744** (2765-2545)	-29	Above gravelly sand layer
Storsaetervatnet	S9	144-147	S9-144	T-15555A	gyttja	5,2	7895±115	**8643** (8996-8544)	-29,8	Below gravelly sand layer
Storsaetervatnet	S9	181-179	S9-180	T-15556A	gyttja	1,9	8285±145	**9366** (9473-9030)	-28,4	Above and beneath 1 cm sand layer
Storsaetervatnet	S10	474	S10-474	TUa-3340A	gyttja	not determined	11345±75	**13254** (13448-13159)	-26,8	Organic laminae below Vedde Ash
Medvatnet	M2	60-64	M2-62	T-15513A	gyttja	2,3	3090±95	**3279** (3389-3167)	-29,9	Above and below 2 cm gravelly silt layer
Medvatnet	M2	160-164	M2-160	T-15557A	gyttja	3,4	4855±120	**5594** (5710-5472)	-29,3	Below pebbles and sand/silt clasts
Medvatnet	M4	90-93	M4-91	T-15514A	gyttja	3,3	3220±105	**3449** (3567-3355)	-28,6	Above and below 2 thin silt lamina
Medvatnet	M6	0-4	M6-02	T-15515A	gyttja	1,6	2505±80	**2619** (2745-2362)	-29,7	Above 9 cm thick sand layer
Nedstevatnet	N2	10-14	N2-12	T-15516A	gyttja	1,9	2880±105	**2979** (3207-2865)	-29,7	Above thick layer containing sand clasts
Nedstevatnet	N2	40-45	N2-42	T-15517A	gyttja	4,9	5780±80	**6600** (6718-6454)	-27,7	Below thick layer containing sand clasts
Nedstevatnet	N2	99-105	N2-103	T-15518A	gyttja	4,3	6430±65	**7367** (7425-7270)	-26,4	Above and below silt/sand lamina
Nedstevatnet	N3	42-45	N3-40	T-15558A	gyttja	3,5	5950±95	**6772** (6889-6667)	-27	Beneath 2 cm thick sand layer
Nedstevatnet	N3	300-306	N3-300	T-15520	shell	not determined	11030±70	**13009** (13146-12907)	-1 (assumed)	diamicton containing Astarte and M. truncata
Nedstevatnet	N3	270	N3-270	T-15519	shell	not determined	10225±120	**11793** (12325-11644)	-1 (assumed)	diamicton containing Mya truncata
Nedstevatnet	N5	14-18	N5-16	T-15521A	gyttja	2,8	2235±75	**2208** (2343-2132)	-29,1	Above tsunami layer
Nedstevatnet	N5	90-91	N5-90	TUa-3322a	gyttja	not determined	8805±80	**9845** (10147-9695)	-28	Above 2 thin sand lamina
Nedstevatnet	N5	96	N5-96	TUa-3341A	gyttja	not determined	9310±65	**10434** (10636-10405)	-26,8	2 mm thick gyttja lamina
Nedstevatnet	N5	105-113	N5-109	T-15522A	brown silt	0,8	9985±190	**11316** (11926-11198)	-24	Above and beneath 2 cm gravelly sand layer
Rotevatnet	R1	171-178	R1-175	T-15525A	gyttja	6,4	5880±130	**6700** (6854-6503)	-29,5	Above and beneath 3 mm silt lamina
Rotevatnet	R1	119-125	R1-121	T-15524A	gyttja	6,2	4605±115	**5314** (5469-5053)	-29,4	Above and beneath 2 mm distinct silt lamina
Rotevatnet	R1	21-28	R1-24	T-15523A	gyttja	5,9	1865±100	**1820** (1921-1633)	-29,5	Above and beneath silt lamina

Table 5. Undrained shear strength determinations.

Core number	Depth in core (cm)	Undrained shear strength (kPa)
P0103002	3	4,9
	50	6,7
	147	11,0
P0103004	10	3,1
	50	3,8
	190	8,9
P0103005	105	4,9
	185	12,0
P0103007	3	5,7
	50	3,8
	100	8,3
	150	7,3
P0103008	3	2,3
	50	4,3
	100	4,9
P0103011	2	9,1
	75	7,6
P0103012	2	9,1
	25	3,4
	70	8,3
	120	7,6
P0103013	2	5,7
	110	12,0
P0103014	2	4,9
	65	6,7
P0103015	2	4,3
	50	4,9
	100	4,3
	125	7,8
P0103017	2	3,0
	50	4,9
	120	6,7
P0103018	10	4,0
	50	4,8
	98	4,4
	144	7,8
P0103019	2	4,3
	50	3,8
	125	7,8
P0103021	28	11
P0103026	45	8,3
	125	19,0
P0103029	50	8,3
	100	5,7
P0103030	35	13,5
	80	5,7
P0103031	55	4,9
P0103032	2	7,8
	80	9,1

Core number	Depth in core (cm)	Undrained shear strength (kPa)
HM129-03	250	15,5
HM129-04	2	4,9
	135	17,0
	185	21,5
	225	27,5
ØrstaGC1A	50	3,0
	100	3,8
ØrstaGC2	10	1,7
	50	3,8
	130	7,8
ØrstaGC3	25	2,5
	50	4,9
	110	4,9
	150	9,2
2L	10	7.8
	60	11.0
	110	12.0
	160	8.3
	210	10.6
	260	10.4
	310	15.5
	340	7.8
4L	20	3.8
	60	7.1
	110	8.3
	145	16.5
	205	12.0
	248	7.1
	300	17.0
	335	12.0
	355	24.5
	400	15.5
	440	24.5
	500	14.5
	540	13.5
	590	12.0
	640	10.0
	690	8.3
6L	30	6.7
	65	15.5
	100	13.5
	270	12.0
	305	10.0
	350	7.0
	405	12.0
	460	10.0
	520	15.5
	555	13.5
	615	8.3

Table 6. Water content, wet density and dry density determinations.

Core number	Depth in core (cm)	Water Content (%)	Wet Density (g/cm^3)	Dry Density (g/cm^3)
P0103004	152	161,96	1,35	0,52
P0103005	137	53,88	1,89	1,23
P0103007	70	69,09	1,77	1,05
P0103008	80	204,38	1,37	0,45
P0103011	60	100,70	1,60	0,80
P0103012	90	49,51	1,95	1,30
P0103013	110	73,31	1,74	1,00
P0103014	60	87,24	1,67	0,89
P0103015	70	134,73	1,49	0,64
P0103017	45	192,06	1,40	0,48
P0103018	44	223,05	1,28	0,40
P0103019	100	107,22	1,57	0,76
P0103021	28	53,71	1,89	1,23
P0103026	60	73,71	1,71	0,98
P0103029	50	95,41	1,62	0,83
P0103030	45	73,57	1,75	1,01
P0103031	32	74,93	1,70	0,97
P0103032	40	93,08	1,64	0,85
HM129-03	60	41,38	2,04	1,44
HM129-03	140	38,15	2,03	1,47
HM129-03	226	42,39	1,96	1,38
HM129-04	50	43,08	1,97	1,38
HM129-04	135	40,99	2,01	1,43
ØrstaGC1A	140	67,37	1,78	1,06
ØrstaGC2	40	161,96	1,35	0,52
ØrstaGC3	135	136,07	1,40	0,59
2L	10	93,20	1,68	0,87
2L	60	82,62	1,64	0,90
2L	110	87,38	1,62	0,86
2L	170	95,63	1,57	0,80
2L	210	72,60	1,69	0,98
2L	270	67,07	1,73	1,04
2L	310	64,97	1,73	1,05
4L	20	132,89	1,46	0,63
4L	60	98,40	1,56	0,79
4L	155	83,20	1,65	0,90
4L	205	83,31	1,61	0,88
4L	250	87,48	1,60	0,85
4L	300	70,49	1,71	1,00
4L	355	53,68	1,85	1,20
4L	400	64,44	1,80	1,10
4L	450	54,82	1,80	1,16
4L	500	76,92	1,65	0,93
4L	550	78,32	1,64	0,92
4L	610	76,45	1,66	0,94
4L	640	68,25	1,75	1,04
4L	690	60,89	1,88	1,17
6L	30	96,59	1,62	0,82
6L	65	65,62	1,70	1,03
6L	115	55,14	1,80	1,16
6L	150	41,36	1,95	1,38
6L	200	32,57	2,03	1,53
6L	270	65,42	1,73	1,05
6L	320	65,33	1,74	1,05
6L	365	60,35	1,80	1,13
6L	415	71,51	1,72	1,00
6L	465	70,63	1,71	1,00
6L	515	51,62	1,83	1,21
6L	555	69,17	1,71	1,01
6L	610	60,25	1,79	1,11

4.1.1. Sogn (Aurlandsfjorden, Fjærlandsfjorden, Barsnesfjorden)

Altogether nine cores were collected from Aurlandsfjorden, Barsnesfjorden and Fjærlandsfjorden (Table 1). Five cores from these three fjords were opened and lithologically described (Fig. 3). Age determination was preformed on three samples from two cores (Fig. 3); three samples from P0103005 could not be dated due to very low yield of foraminifers.

P0103002 (Aurlandsfjorden) This core is stratigraphically monotonous in its entire length (0-1.64 m), and consists of bioturbated dark grey silty clay. Rare isolated clasts occur at ca. 1.2 m sediment depth.

P0103004 (Fjærlandsfjorden) The upper part (0-0.63 m) of the core consists primarily of olive grey silty clay with some gravel clasts at the bottom of the bed. The lower boundary of the bed is erosional. Sediments are bioturbated within the upper portion of this interval (0-0.3 m) but become diffusely banded/laminated in the lower part. Wood fragments occur at ca. 0.18 m depth. Isolated clasts and gravel are common in the lower portion of the interval, and their frequency increases down-core towards the erosional boundary. The lower part of the core (0.63-2.30 m) consists of structureless, dark grey to bluish grey, silty sandy and gravelly clay, rich in sand clasts and isolated gravel clasts. Sand clasts with a diameter up to 5 cm are particularly common in the interval at 2.04-2.10 m.

P0103005 (Fjærlandsfjorden) Bioturbated, olive grey, sandy and clayey silt with isolated clasts at the top of the core (0-0.28 m) is underlain by an interval of upward fining fine sand (0.28-0.32 m). This graded sand interval has an erosional lower boundary. Thin layer (0.32-0.36 m) of sandy and clayey silt is followed down-core by another upward fining fine sand interval occurring at 0.36-0.39 m. The lower boundary of this graded sand interval is sharp, but not erosional.

Bioturbated / diffusely laminated, olive grey, sandy and clayey silt with frequent isolated clasts and shells occurs at 0.39-0.90 m. An upward fining bed at 0.90-1.08 m consists of sand in the upper portion (0.9-0.98 m). The lower part (0.98-1.08 m) of the graded bed consists of poorly sorted gravel containing shells up to1cm, pebbles up to 3 cm and clasts of bluish grey clay. This graded bed has an erosional lower boundary.Bioturbated / diffusely laminated, olive grey, sandy and clayey silt at 1.08-1.78 m contains shells and sand filled burrows that are particularly common near the erosional base of the unit. The lowermost sediment unit (1.78-1.93 m) in P0103005 consists of bluish grey massive clay with isolated clasts.

(P0103007 Barsnesfjorden) An upward fining bed of silty sand forms the top (0-0.04 m) of the core. A bioturbated /diffusely laminated, olive grey interval of silty clay occurs at 0.04-0.89 m. This interval contains shells and isolated clasts, and in places features colour (dark and light) banding of 3-6 cm thick diffuse bands. Strongly bioturbated, dark grey, silty clay at 0.89-1.32 m contains shells and shows patchy colour variations. Dark grey, silty clay at 1.32-1.74 m is generally bioturbated, but displays also diffuse lamination/banding. Shells and isolated clasts are common in this interval.

P0103008 (Barsnesfjorden) The top of the core (0-0.12 m) consists of laminated clayey silt. A bed of upward fining silty and gravelly sand with erosional lower boundary occurs at 0.12-0.18 m. Bioturbated /diffusely layered silty, sandy and gravely clay at 0.18-1.14 m contains shells and isolated clasts. An upward fining interval at 1.14-1.24 m consists of a clayey silt bed at 1.14-1.18 m, organic-rich, silty sand bed at 1.18-1.22 m and gravely sand bed at 1.22-1.24 m. The graded interval has erosional lower boundary, and is underlain by silty clay in the lower part of the core (1.24-1.28 m).

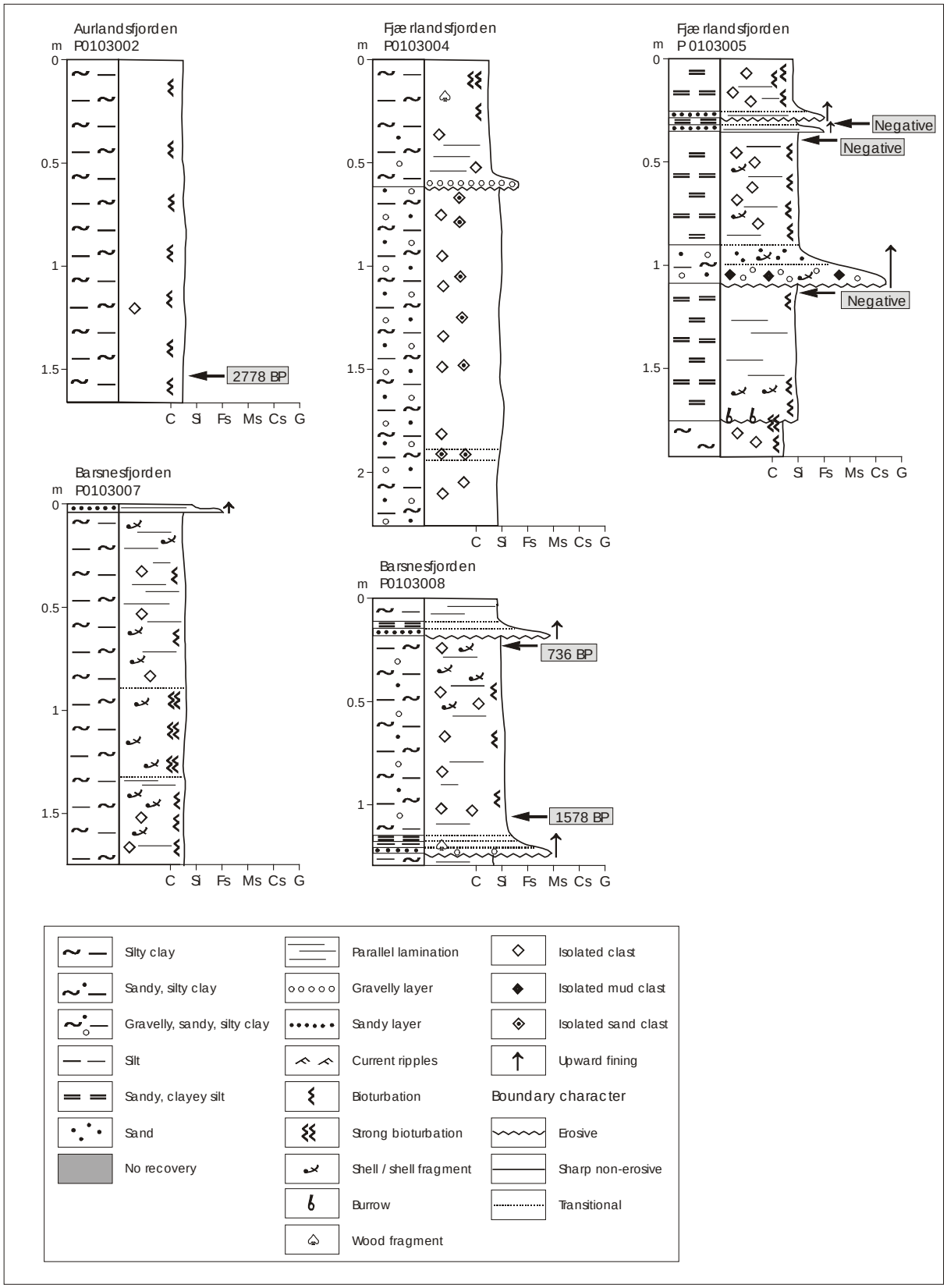

Fig. 3. Cores from Aurlandsfjorden, Fjærlandsfjorden and Barsnesfjorden in Sogn.

4.1.2. Sunnfjord (Dalsfjorden, Førdefjorden)

All four cores collected from Dalsfjorden and Førdefjorden were opened and sedimentologically logged (Fig. 4). Age determination was preformed on three samples from three cores (Fig. 4, Table 3). One sample from P0103012 could not be dated due to very low yield of foraminifers.

P0103011 (Dalsfjorden) The stratigraphic homogeneity of this 0.8 m long core, consisting of dark grey, silty clay, is broken up by a 0.5 cm thick layer of shell sand and gravel at 0.32 m. Sediments are bioturbated throughout the core. Minor diffuse lamination and rare isolated shells occur within the top section (0-0.25 m) of the core.

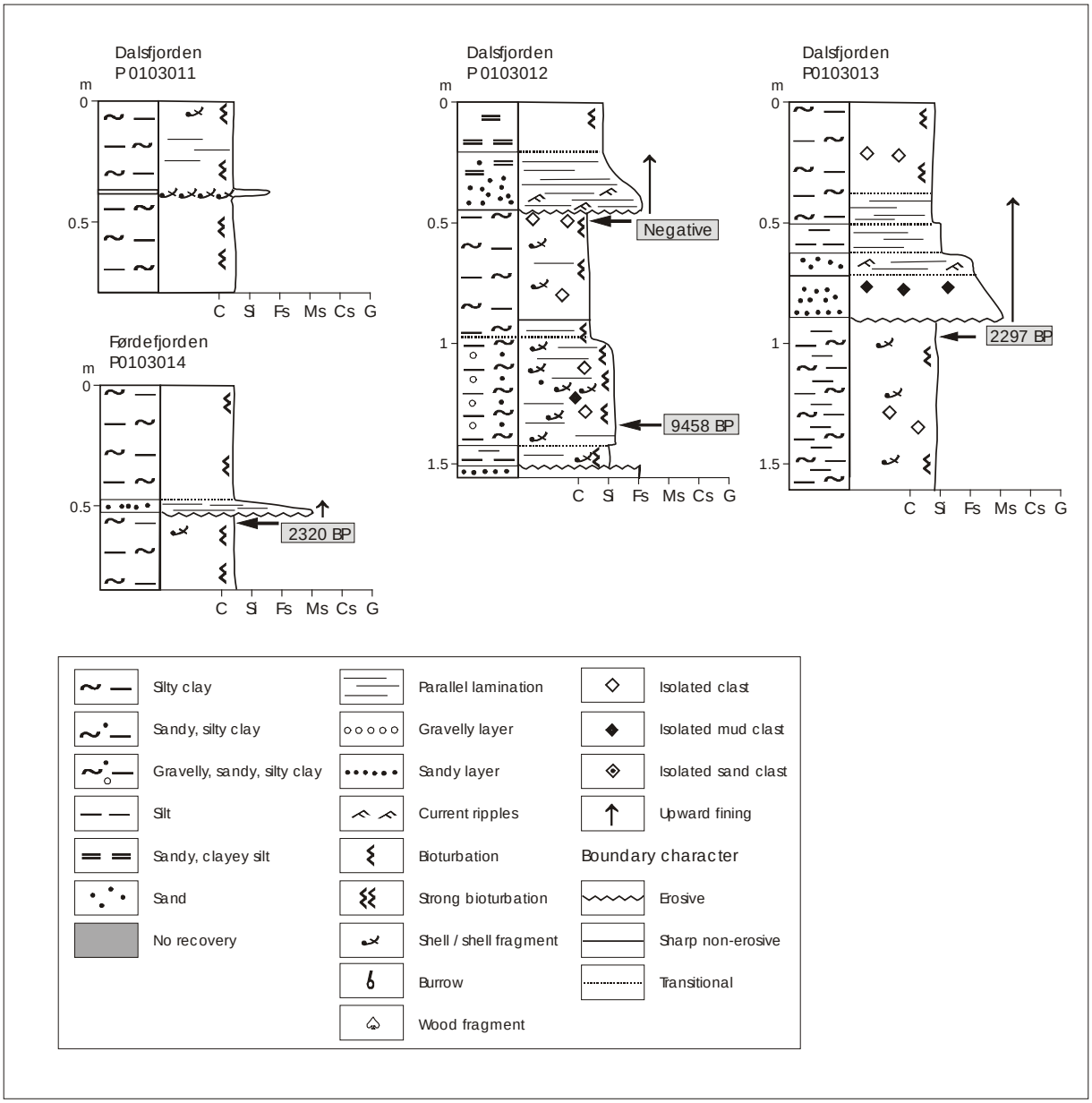

Fig. 4. Cores from Dalsfjorden and Førdefjorden in Sunnfjord.

P01030012 (Dalsfjorden) Bioturbated, dark grey clayey silt in the top of the core (0-0.2 m) is underlain by upward fining bed (0.20-0.43 m) of fine sand and silt. This graded bed is planar laminated, featuring alteration of mm-scale laminae of dark grey and grey sediments. Current ripples were observed in the lower portion of the interval, near the erosional base.

Bioturbated silty clay at 0.43-0.95 m contains shells and isolated clasts. The upper portion (0.43-0.86 m) of this silty clay unit is grey, while the lower portion (0.86-0.95 m) is dark grey. Bioturbated / diffusely laminated, dark grey, gravelly, sandy silt at 0.95-1.43 m is rich in shells and isolated clasts. Brown clast of clayey silt and a 3 cm shell occur at 1.26 m. Bioturbated / diffusely laminated grey silt with an erosional lower boundary occurs at 1.43-1.51 m. The bottom of the core (1.51-1.57 m) consists of grey, massive fine sand.

P0103013 (Dalsfjorden) Bioturbated, dark grey clayey silt forms the upper part (0-0.38 m) of this core. An upward fining sediment unit at 0.38-0.91 m consists of four well defined intervals. Laminated clayey silt in the upper portion (0.38-0.51 m) is followed (0.51-0.63 m) by laminated silt, and then by laminated, grey fine sand (0.63-0.71 m). The lowermost part of the graded unit is massive, grey, medium to fine sand (0.71-0.91 m) that contains brown clay clasts in the interval at 0.75-0.8 m. The boundary between the graded bed and the underlaying clayey silt (0.91-1.63 m) with shells and isolated clasts is marked by an erosional boundary.

P0103014 (Førdefjorden) This 0.85 m long core consists of bioturbated, olive gray clayey silt and an interlayer (0.47-0.54 m) of upward fining medium to fine sand. The graded sand layer has an erosional lower boundary.

4.1.3. Sunnmøre (Vanylvsfjorden, Syvdsfjorden, Voldafjorden, Tafjorden, Ørstafjorden, Breisunddypet, Sulafjorden)

Altogether 22 cores were obtained from fjords in Sunnmøre (Table 1); 13 of these were opened and sedimentologically logged. The sedimentological logs are given in Figs. 5-8. 13 samples from 6 cores were ^{14}C dated (Figs. 5-8; Table 3). One sample from P0103015 could not be dated due to very low yield of foraminifers.

P0103015 (Vanylvsfjorden) Bioturbated, dark grey silty clay with abundant foraminifers at the top (0-0.07 m) of the core is underlain by a layer (0.07-0.96 m) of bioturbated, olive grey silty clay. Diffusely laminated, olive grey silt occurs at 0.96-1.08 m. A layer of laminated silty sand occurs at 1.08-1.13 m. No grading was observed in this sand layer that has an erosional lower boundary. Olive grey, shell-rich silt at 1.13-1.37 m is divided into two units. The upper unit (1.13-1.21 m) is moderately bioturbated whereas the lower unit (1.21-1.37 m) is strongly bioturbated, and contains abundant foraminifers. Clay-filled burrows are common near the base of the lower unit. Bioturbated, dark grey silty clay at 1.37-1.64 m forms the lower part of the core.

P0103017 (Syvdsfjorden) This 1.44 m long core consists of bioturbated, dark grey/brown to black, organic-rich silty clay (gyttja), rich in shells and wood fragments, and has two sandy layers. The upper layer (0.55-0.59 m) consists of fine sand and has an erosional lower boundary with loadcasts. The lower layer (0.78-0.8 m) is made of dark grey, silty and clayey sand and has also an erosional lower boundary. A few sand clasts were observed within the silty clay between the sandy layers.

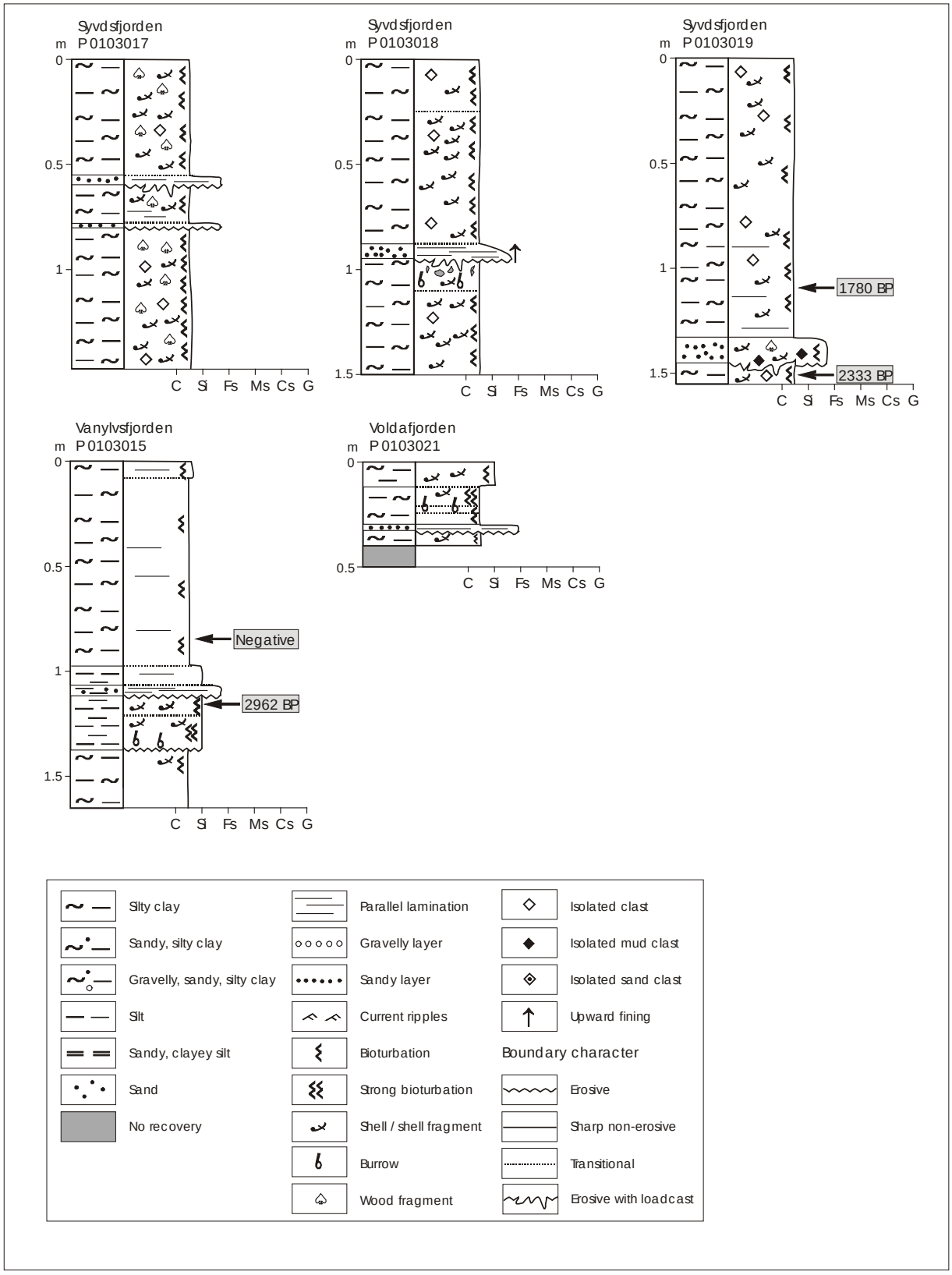

Fig. 5. Cores from Vanylvsfjorden, Syvdsfjorden and Voldafjorden in Sunnmøre.

P0103018 (Syvdsfjorden) The upper interval of the core (0-0.87 m) can be divided in two based on the abundance of shell fragments and colour variations. Shell fragments are present in the black upper part (0-0.23 m), while they are very abundant in the dark brown lower part (0.23-0.87 m). Upward fining bed at 0.87-0.95 m consists of fine sand in the lower portion (0.92-0.95 m) and silty-clayey fine sand in the upper portion (0.87-0.92 m). The lower boundary of the graded bed is erosional. Bioturbated silty clay at 0.95-1.10 m contains abundant shell fragments and clasts (< 2 cm) of fine sand. Bioturbated silty clay at 1.10-1.48 m is rich in shell fragments, particularly between 1.20-1.48 m.

P0103019 (Syvdsfjorden) Bioturbated, dark grey to black silty clay (gyttja) occurs from the surface down to 1.32 m depth. This silty clay contains shells and random isolated clasts and is diffusely laminated between 0.9-1.30 m. Massive, dark grey fine sand containing wood fragments and clasts of the underlaying organic-rich silty clay occurs at 1.32-1.45 m. The lower boundary of this bed features loadcasts. Bioturbated, dark grey to black, organic-rich silty clay (gyttja) forms the bottom of the core (1.45-1.58 m).

P0103021 (Voldafjorden) Bioturbated, dark grey clayey silt occurs at 0-0.12 m. Dark grey silty clay at 0.12-0.29 m is strongly bioturbated at 0.12-0.24 m. Black burrows were found at 0.21-0.24 m. Alteration of silty-clayey sand with silty clay gives rise to lamination in a layer at 0.29-0.32. Bioturbated, dark grey silty clay occurs at the lower part of the core (0.32-0.40 m).

Ørsta-GC1A (Ørstafjorden) Bioturbated, organic-rich, black, silty, sandy clay (gyttja) with wood fragments occurs at 0-0.12 m. Bioturbated, dark grey, organic-rich silty clay (gyttja) at 0.12-0.67 m contains wood fragments, and rare shells and isolated clasts. An upward fining bed at 0.62-0.74 m consists of sandy, silty, organic-rich clay (gyttja) with wood fragments in the upper portion (0.62-0.67 m) and of gravelly sand to fine sand in the lower portion (0.67-0.74 m). Up to 1 cm diameter gravel is particularly abundant near the erosional base of the graded bed. Bioturbated, organic-rich, dark grey, silty clay (gyttja) at 0.74-1,00 m contains wood fragments, isolated clasts and a thin (0.5 cm) poorly sorted sand layer at 0.9 m. Bioturbated, organic-rich, dark grey, silty, sandy clay at 1,00-1.48 m is rich in wood fragments (particularly at 1.37-1.38 m), and contains shells and isolated clasts.

Ørsta-GC2 (Ørstafjorden) Bioturbated, dark grey, organic-rich, silty sandy clay (gyttja) that contains wood fragments, shells and isolated clasts forms the upper part (0-0.73 m) of the core. A thin layer of well sorted, dark grey fine sand with an erosional lower boundary occurs at 0.73-0.75 m. Dark grey, silty clay at 0.75-0.78 m is underlain by another sand layer at 0.78-0.8 m. This dark grey layer is made of fine sand with wood fragments in the top and of medium sand at the erosional base. The abundance of shells and wood fragments allows subdivision of the bioturbated, organic-rich, dark grey, silty clay at 0.80-1.68 m into two units (0.80-1.20 m and 1.20-1.68 m). Biogenic components are relatively common in the upper unit compared to the lower one.

Ørsta-GC3 (Ørstafjorden) Bioturbated, dark grey, organic-rich, silty sandy clay (gyttja) with wood fragments, shells and isolated clasts occurs at 0-0.84 m. The sand content is relatively high in the lower portion of the interval. An upward fining bed at 0.84-0.93 m consists of fine sand, rich in wood fragments in the upper portion (0.84-0.90 m) and well-sorted fine sand in the lower portion (0.9-0.93 m). The lower boundary of this graded bed is erosional. Bioturbated, dark grey, organic-rich, silty sandy clay at 0.90-1.6 m contains a shell rich layer at 1.2 m. The bottom part of the core (1.6-1.92 m) consists of biturbated, grey, silty clay.

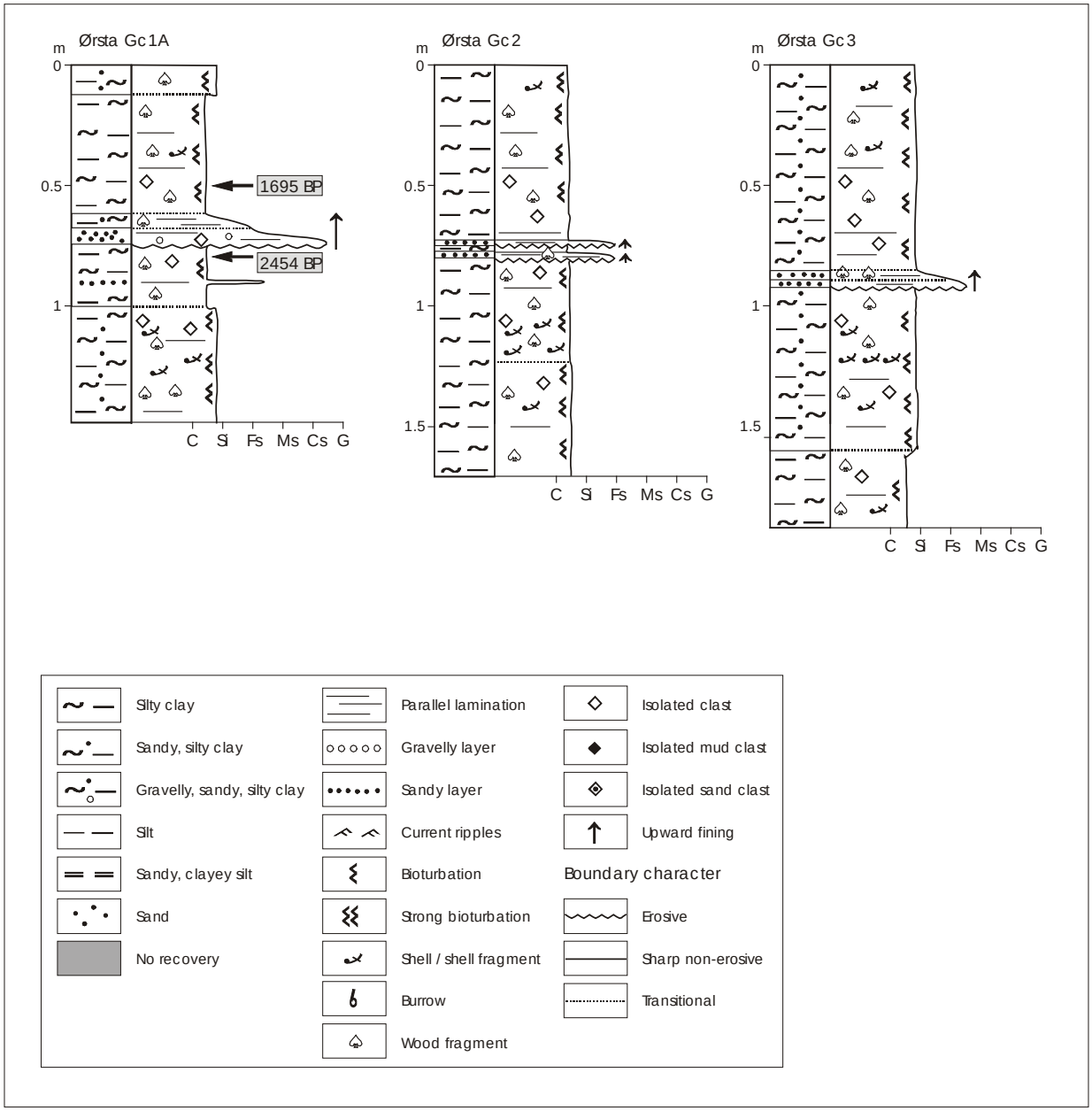

Fig. 6. Cores from Ørstafjorden, Sunnmøre.

GC HM129-03 (Breisunddypet) Dark grey, clayey, silty and gravely (< 1 cm) sand occurs at 0-0.08 m. The sand fraction in this unit consists of lithogenic particles and shell fragments. Bioturbated/diffusely banded, dark grey/olive grey, clayey, silty and gravelly sand at 0.08-1.58 m distinguishes from sediments above by its lower gravel content and by a fader colour, particularly in the interval 0.08-0.40 m. This unit (0.08-1.58 m) has an erosional lower boundary, and near the base there are two thin interlayers (1.49-1.50 m and 1.52-1.56 m) of bioclastic (shells) well-sorted, fine to medium sand. The lower shell sand interlayer (1.52-1.56 m) contains clasts of surrounding clayey, silty and gravely sand. Clay clasts of material resembling the sediment in the lower part of the core (2.37-2.52 m) occur at 1.56-1.58 m. Bioturbated, olive green sandy silt with shells and shell fragments occurs at 1.58-2.37 m. Dark grey, silty clay forms the lower part of the core (2.37-2.52 m).

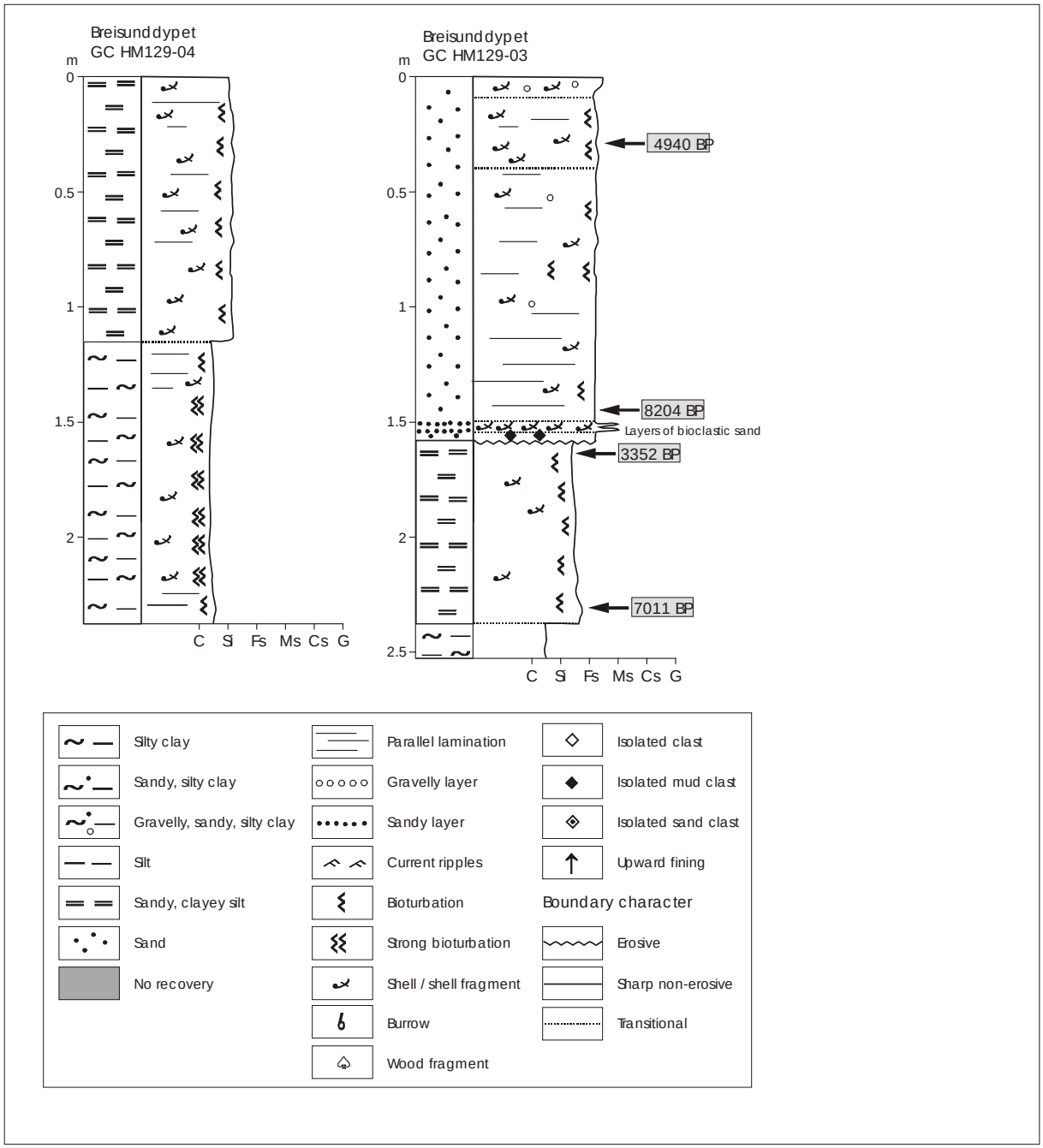

Fig. 7. Cores from Breisunddypet, Sunnmøre.

GC HM129-04 (Breisunddypet) Bioturbated, clayey and sandy silt with numerous shells and shell fragments occurs at 0-1.15 m. The underlaying silty clay at 1.15-2.30 m is strongly bioturbated. Layering that has been disturbed by bioturbation is evident in the upper and lower parts (1.15-1.3 m and 2.2-2.3 m) of the interval.

NGU-2L/SC (Sulafjorden) Strongly bioturbated, olive grey silty clay with numerous shells and shell fragments (up to 1cm) comprises the uppermost 3.15 m of the core. Bioturbeted, homogeneous grey clay occurs at 3.15-3.60 m. An upward fining, dark grey bed at 3.60-3.99 m consists of planar laminated, very fine sand to silt in the upper portion (3.60-3.82 m) and of planar and cross laminated fine to very fine sand in the lower portion (3.82-3.99 m).

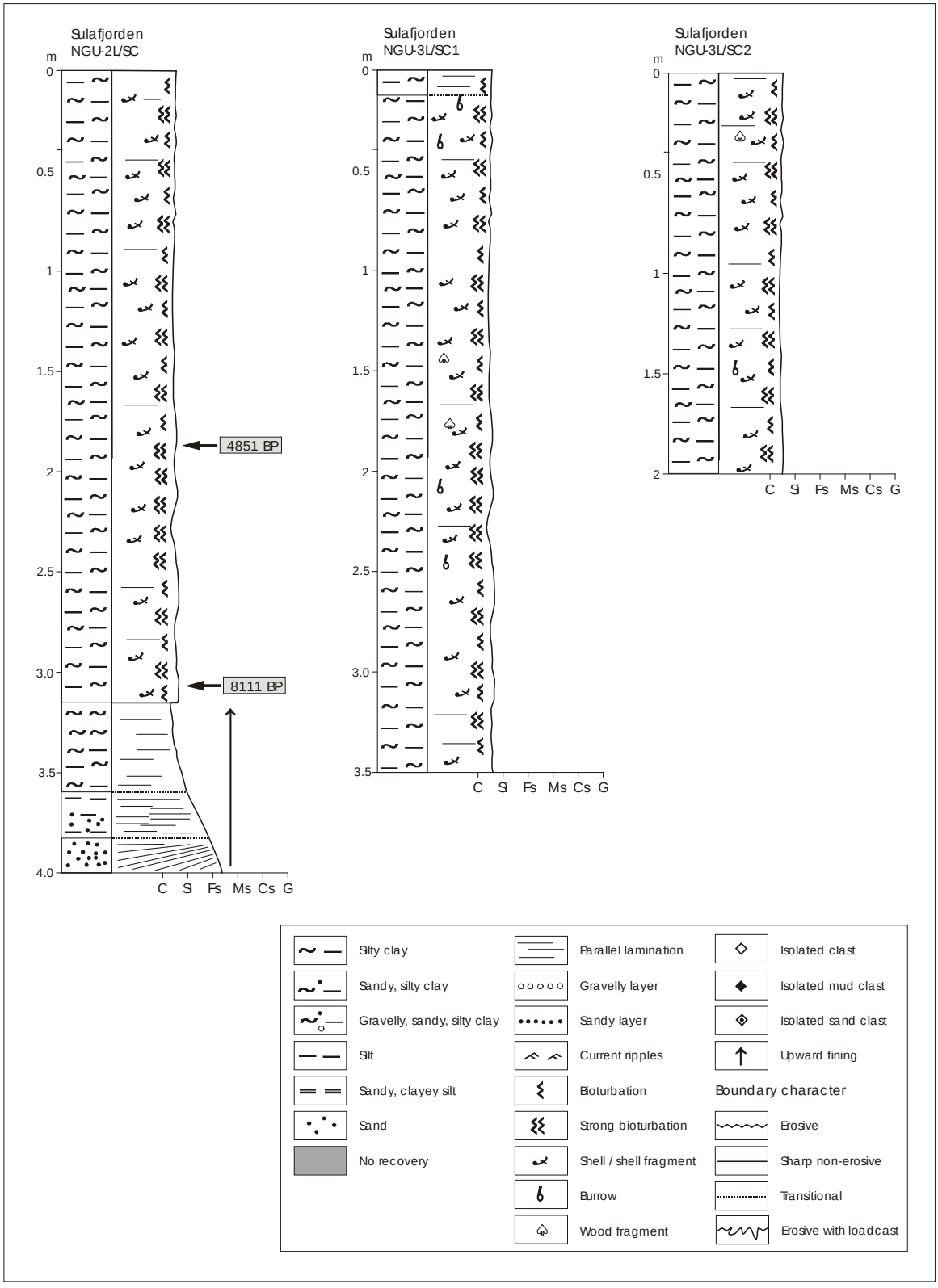

Fig. 8. Cores from Sulafjorden, Sunnmøre.

NGU-3L/SC-1 (Sulafjorden) Diffusely banded / bioturbated clayey silt/silty clay occurs at 0-0.12 m. Alteration of olive and dark grey tones gives rise to diffuse banding in this top bed. Strongly bioturbated, olive grey clayey silt/silty clay at 0.12-3.55 m contains tree fragments and is rich in shells and shell fragments (up to 1 cm).

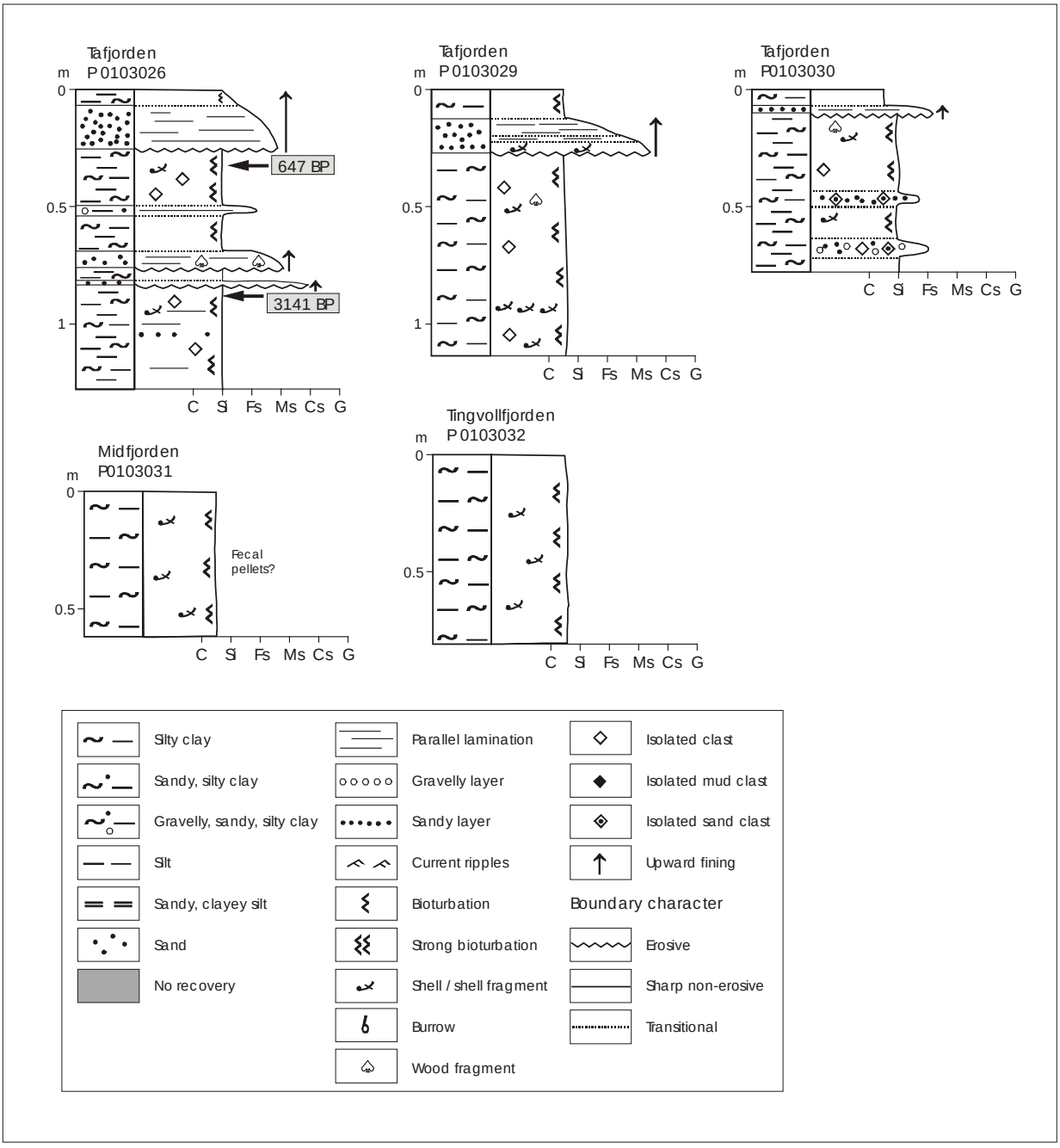

Fig. 9. Cores from Tafjorden, Midfjorden and Tingvollfjorden in Sunnmøre, Romsdal and Nordmøre.

NGU-3L/SC-2 (Sulafjorden) This 2.00 m long core consists in its entire length of bioturbated, olive grey clayey silt/silty clay and contains tree fragments in places. Shells and shell fragments are present throughout the core.

P0103026 (Tafjorden) The bed of upward fining sediments in the upper part of the core (0-0.26 m) consists of clayey silt in the upper portion (0-0.07 m) and laminated, dark grey, coarse to fine sand in the lower portion (0.07-0.26 m). This graded bed has an erosional lower boundary. Bioturbated clayey silt at 0.26-0.49 m contains clasts and shell, and is underlain by

a layer (0.49.0.54 m) of laminated clayey, sandy and gravelly silt. Bioturbated clayey silt occurs at 0.54-0.69 m. Upward fining beds of medium to fine sand with wood fragments at 0.69-0.76 m and coarse to medium sand at 0.82-0.84 m are separated by a layer of bioturbated clayey silt at 0.76-0.82 m. Bioturbated / diffusely laminated clayey and sandy silt occurs in the lower part of the core (0.84-1.27 m). Sandy lamina is evident at 1.06 m.

P0103029: Tafjorden Bioturbated, olive grey, silty clay occurs in the upper part (0-0.12 m) of the core. An upward fining bed at 0.12-0.27 m consists of planar laminated, black, very fine sand (0.12-0.19 m), planar laminated, dark grey, fine sand (0.19-0.22 m), and dark grey, coarse to medium sand, rich in shell fragments (0.22-0.27 m). The graded bed has an erosional lower boundary. Bioturbated, olive grey, silty clay at 0.27-1.14 m contains wood fragments, isolated clasts and shells. Shells and shell fragments are particularly abundant at 0.92-0.95 m.

P0103030 (Tafjorden) Bioturbated, olive grey, silty clay forms the upper part of the core (0-0.07 m). An upward fining, grey, fine to very fine sand with an erosional lower boundary occurs at 0.07-0.10 m. Bioturbated, clayey silt at 0.10.0.83 m contains wood fragments, isolated clasts and sandy lenses. These lenses are particularly common at 0.43-0.50 m and 0.63-0.77 m.

4.1.4. Romsdal (Midfjorden, Julsundet) and Nordmøre (Tingvollfjorden, Halsafjorden)

All four cores collected from Romsdal and Nordmøre were opened and lithologically described (Figs. 9, 10, 12). Radiocarbon dating was attempted on13 samples from Julsundet and Halsafjorden cores. Eight samples were dated whereas five could not be dated due to very low yield of foraminifers (Figs. 10, 12; Table 3).

P0103031 (Midfjorden) This 0.57 m long core consists in its entire length of bioturbated, olive silty clay. Shell fragments are present throughout the core, and appear as fecal pellets in places.

P0103032 (Tingvollfjorden) Sediments in this 0.81 m long core are stratigraphically homogeneous, consisting of bioturbated, olive grey, silty clay with shell fragments.

NGU-4L/SC (Halsafjorden) The stratigraphy of strongly bioturbated, olive grey, homogeneous silty clay/clayey silt, rich in shells and shell fragments (< 1 mm) at 0-6.91 m is broken up by five upward fining thin beds at 3.61-3.70 m, 5.02-5.13 m, 5.68-5.74 m, 6.08-6.11 m and 6.68-6.91 m. Homogeneous silty clay/clayey silt is stained by numerous black (FeS) spots at 6.11-6.36 m. The uppermost of the upward fining beds (3.61-3.70 m) has erosional lower boundary and it comprises laminated, dark grey medium sand grades into silt. The bed at 5.02-5.13 m consists of grey, laminated silt in the upper portion (5.02-5.08 m) The lower portion (5.08-5.13 m) of this bed comprises dark grey, laminated fine to very fine sand that is strongly influenced by loading/soft sediment deformation. The graded bed at 5.68-5.74 m is made of light grey silt (5.74-5.73 m) and clayey silt (5.73-5.68 m), and the bed at 6.08-6.11 m consists of light grey silt fining upwards into clayey silt. These both beds (5.68-5.74 m and 6.08-6.11 m) have erosional lower boundaries. Relatively thick graded bed at 6.68-6.91 m consists of laminated, grey, fine sand to silt, strongly influenced by loading/soft sediment deformation at the base.

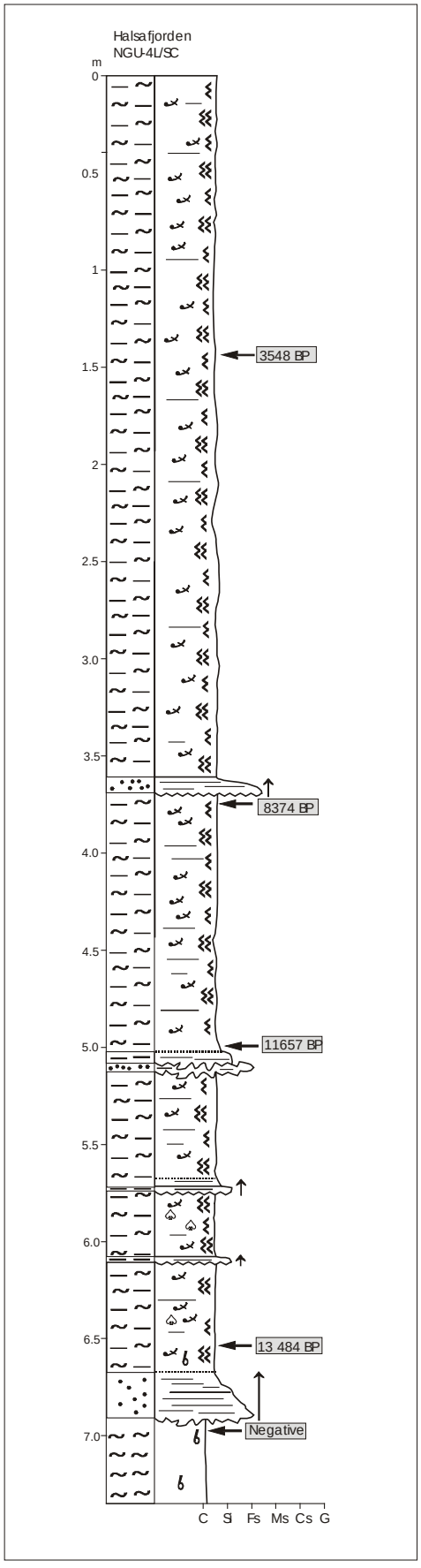

Fig. 10. Core from Halsafjorden, Nordmøre.

Homogeneous, light grey clay occurs at the bottom of the core at 6.91-7.36 m. This interval as well as homogeneous silty clay/clayey silt at 5.74-6.08 m and 6.11-6.68 m contain numerous, sub-horizontal chimneys and rods of clusters of framboidal pyrite, up to 5 mm in diameter (Fig. 11). The framboid surfaces display variety of morphologies, including crystalline appearance, and secondary overgrowths and infillings of different dagree (Fig. 11). These authigenic pyrite accumulations appear as dark, distinct stripes on XRI images (Appendix 1). The process responsible for precipitation of pyrite chimneys and rods is yet to be studied; possible explanations may include mineralisation of burrows and/or precipitation at reactant (dissolved ferrous Fe, H_2S) diffusion pathways.

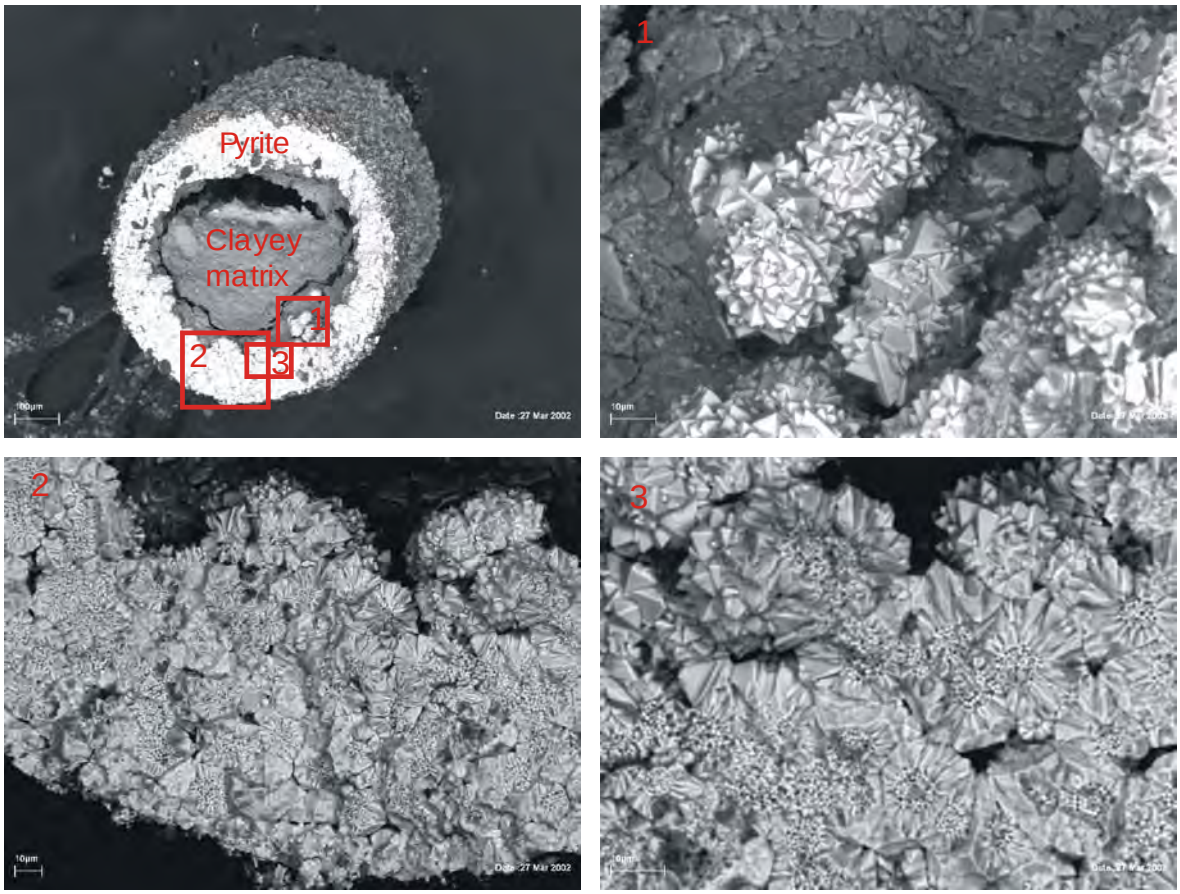

Fig. 11. SEM-BSE (Scanning Electron Microscope BackScattered Electron) images of accumulations of authigenic framboidal pyrite in the lower part NGU-4L/SC. Clusters of framboidal pyrite commonly form subvertical rods and chimneys. Pyrite chimneys are occasionally filled with clayey sediment matrix. Close-ups of pyrite framboids demonstrate different morphologies including crystalline surfaces as well as relatively smooth infilling appearances (next page).

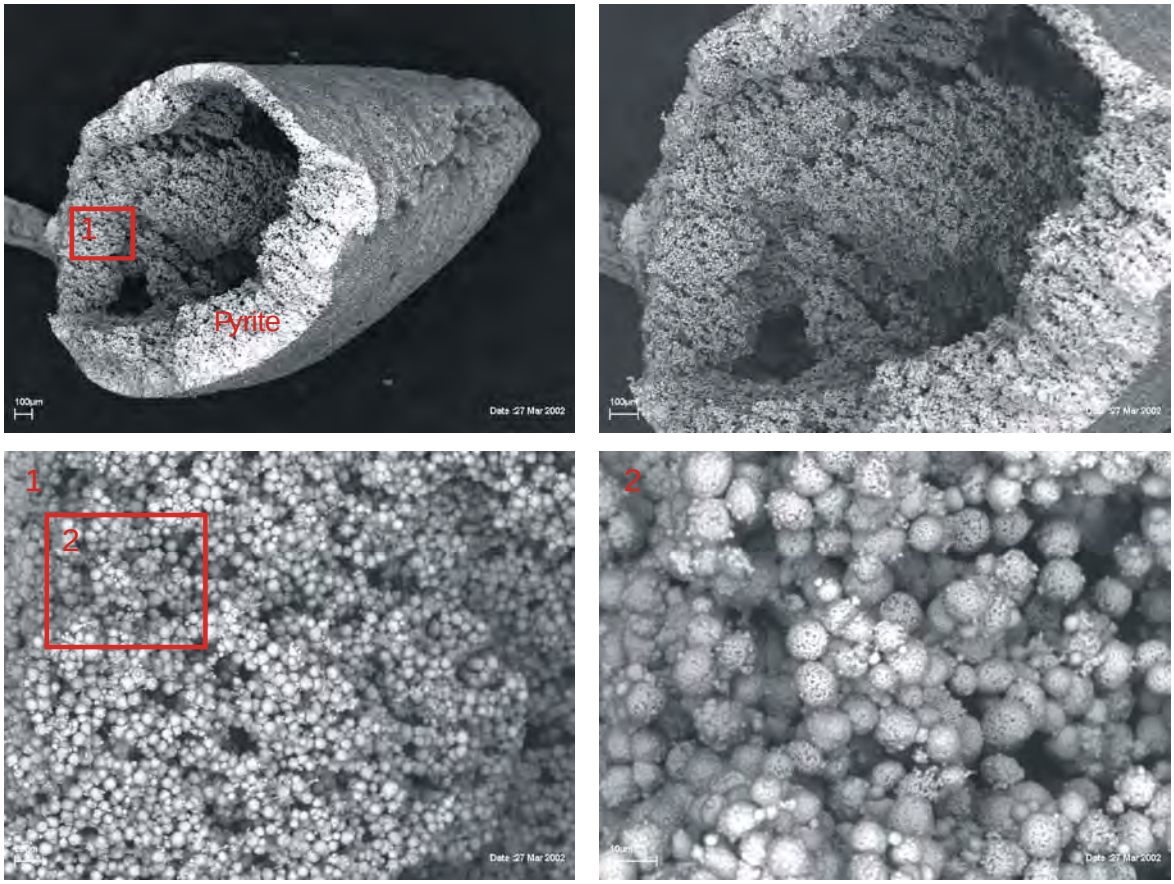

Fig. 11. (continued).

NGU-6L/SC (Julsundet) The uppermost 0.11 m of the core consists of very dark grey, poorly sorted, normally graded sand, rich in shells and shell fragments (up to 1 cm). Base of this top bed is erosional. Olive grey, normally graded silty clay/clayey silt occurs at 0.11-0.77 m. The uppermost part (0.11-0.29 m) of this interval is laminated. Olive grey laminated/banded, clayey and silty fine sand with medium sand size shell fragments occurs at 0.77-0.88 m. This laminated/layered bed has a sharp, planar upper boundary and a sharp, undulating (load structures) lower boundary.

An upward fining unit with an erosive lower boundary occurs at 0.88-2.67 m. Bioturbated, upward fining clayey silt to silty clay with large burrows at 0.88-1.30 m forms the uppermost part of the unit. Planar laminated, upward fining, very fine sand to silt occurs at 1.30-1.90 m., Cross-laminated and planar laminated, upward fining, fine to very fine sand at 1.90-2.50 m has non-erosional, but well defined boundary to underlain planar laminated, upward fining, very coarse to fine sand at 2.62-2.50 m. At the base of the upward fining unit there is a 5 cm thick bed (2.62-2.67 m) consisting of gravel (up to 1 cm) and clay clasts (up to 2 cm; from the underlying unit).

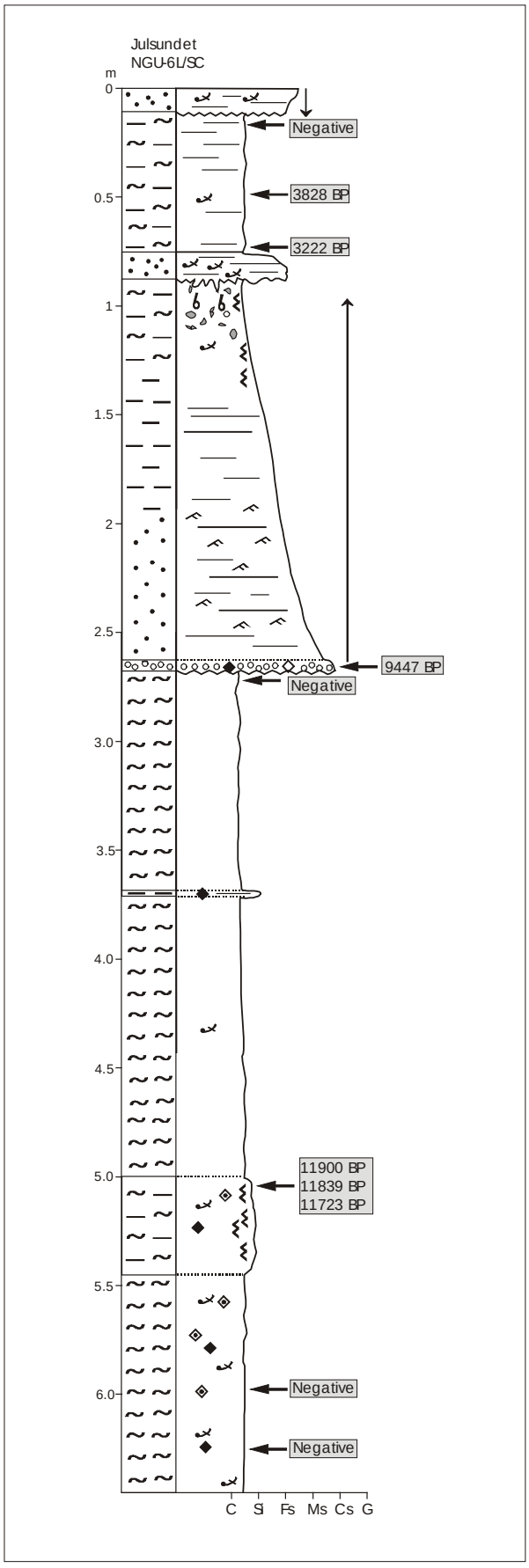

Fig. 12. Core from Julsundet, Romsdal.

Homogeneous, light grey to grey clay occurs at 2.67-5.02 m. This clay interval includes a band of laminated and partly cemented silt at 3.70-3.72; black staining was observed at 2.67-2.82 m and 3.77-3.87 m. Thin layer of laminated and partly cemented silt occurs at 5.02-5.09 m. Homogeneous, olive grey silty clay/clayey silt at 5.09-6.47 m is bioturbated in the upper portion (5.09-5.47 m) and contains numerous small and large (up to 15 cm length) sand clasts. These sand clasts are rich in shells and shell fragments, and are consolidated/partly cemented.

4.2. Lake investigations

The locations of the five investigated lakes - Storsætervatnet, Medvatnet, Nedstevatnet, Rotevatnet and Hovdevatnet - investigated are shown in Fig. 2. The geographic coordinates, water depths and lengths of all 26 lake cores along with the specification laboratory tests are indicated in Table 2. XRI profiles were obtained on 23 cores, density and magnetic susceptibility logging using MSCL was performed on 14 and 13 cores respectively (Table 2). XRI and MSCL analyses were carried out at NGU in week 29, 2001. A general lithostratigraphical description and core correlation for each lake is given in the text body. The interpretative terms such as "Holocene gyttja", "glaciomarine/glaciolacustrine silt" and "Vedde Ash" are used in the description because this is common praxis characterising lake sediments with well known regional stratigraphy. Lithostratigraphical, XRI and MSCL logs are shown in Appendix 4. The variations of magnetic susceptibility are for most cores shown in logarithmic scale, but in case of magnetic mineral deficient sediments (cores M2, M4, R1 and H1) a linear scale is used.

4.2.1. Storsætervatnet

Ten cores were collected from Storsætervatnet (Figs. 13-14). Seven samples from five cores were submitted for radiocarbon dating (Table 4).

S1 The faintly laminated Holocene gyttja sequence in the upper part of the core (0-1.40 m) contains three distinct silt laminae at 0.40 m, 0.72 m and 1.40 m. The glaciolacustrine silt in the lower part of the core (1.40-2.20 m) includes a 10 cm thick Vedde Ash layer at 1.55-1.65 m. The boundary between Holocene gyttja and glaciolacustrine silt is transitional.

S2 This 0.49 m long core consists entirely of glaciolacustrine silt and sand. The Vedde Ash occurs at 0.28-0.40 m.

S3 Six distinct silt laminae at 0.45 m, 1.40 m, 1.45 m, 1.82 m, 1.85 m and 1.88 m were recognized in the faintly laminated Holocene gyttja (0-2.24 m). The 1 cm thick lamina at 1.45 m is upward fining. An erosional boundary separates the Holocene gyttja from underlying glaciolalcustrine silt (2.24-2.34 m).

S4 An erosional boundary at 1.82 m divides upward darkening Holocene gyttja (0-1.82 m) from underlying glaciolacustrine silt and sand (1.82-3.50 m). An 8 mm thick silt lamina occurs at 1.16 m.

S5 The Holocene gyttja (0-1.85 m) has a brownish colour in its upper part (0-0.1 m), and contains four distinct silt lamina at 0.35 m, 0.88 m, 1.20 m and 1.45 m. The boundary between gyttja and underlying glaciolacustrine silt (1.85-2.64 m) is transitional. The Vedde Ash occurs at 2.00-2.08 m.

S6 An erosional boundary separates faintly laminated Holocene gyttja (0-1.57 m) and glaciolacustrine sediments (1.57-2.64 m). The gyttja is rich in plant fragments in the interval 0.91-0.99 m; wood fragments are common at 1.13-1.24 m. The interval 0.84-0.91 m comprises two upward fining sand-silt layers. The silt in the upper part of the glaciolacustrine unit (1.57-2.34 m) in underlain by fine sand in the lower part (2.34-2.64 m).

S7 The stratigraphy of Holocene gyttja in this 2.14 m long core is broken up by 1-5 mm thick silt laminae occurring at 0.87 m, 1.34 m and 1.64 m, and by a sand layer at 1.91-2.02 m. The sand layer contains gyttja clasts, and has a sharp, non-erosional upper boundary and an erosional lower boundary.

S8 The Holocene gyttja (0-2.34 m) contains six silt laminae (0.58 m, 1.13 m, 1.37 m, 1.46 m, 1.50 m and 1.89 m) of which the one at 1.50 m is 1 cm thick, the rest being 1 mm thick. The glaciolacustrine silt in the lower part of the core (2.34-2.45 m) contains a 6 cm thick layer of the Vedde Ash (2.34-2.40 m). The boundary between silt and gyttja is sharp, but probably not erosional.

S9 Faintly laminated Holocene gyttja (0-2.09 m) contains frequent wood fragments and moss (?) fibres. Two gravelly silt/sand beds at 1.34-1.43 m are separated by a 2 mm thick gyttja lamina. The uppermost gravelly silt/sand bed exhibits upward coarsening while the lower shows upward fining. A light brown sand layer occurs at 1.81-1.82 m. A distinct silt layer at 2.10-2.11 m occurs within the transitional zone (2.09-2.19 m) between the Holocene gyttja and the glaciolacustrine silt (2.19-2.50 m). The Vedde Ash occurs at 2.26-2.43 m and is distinctly laminated.

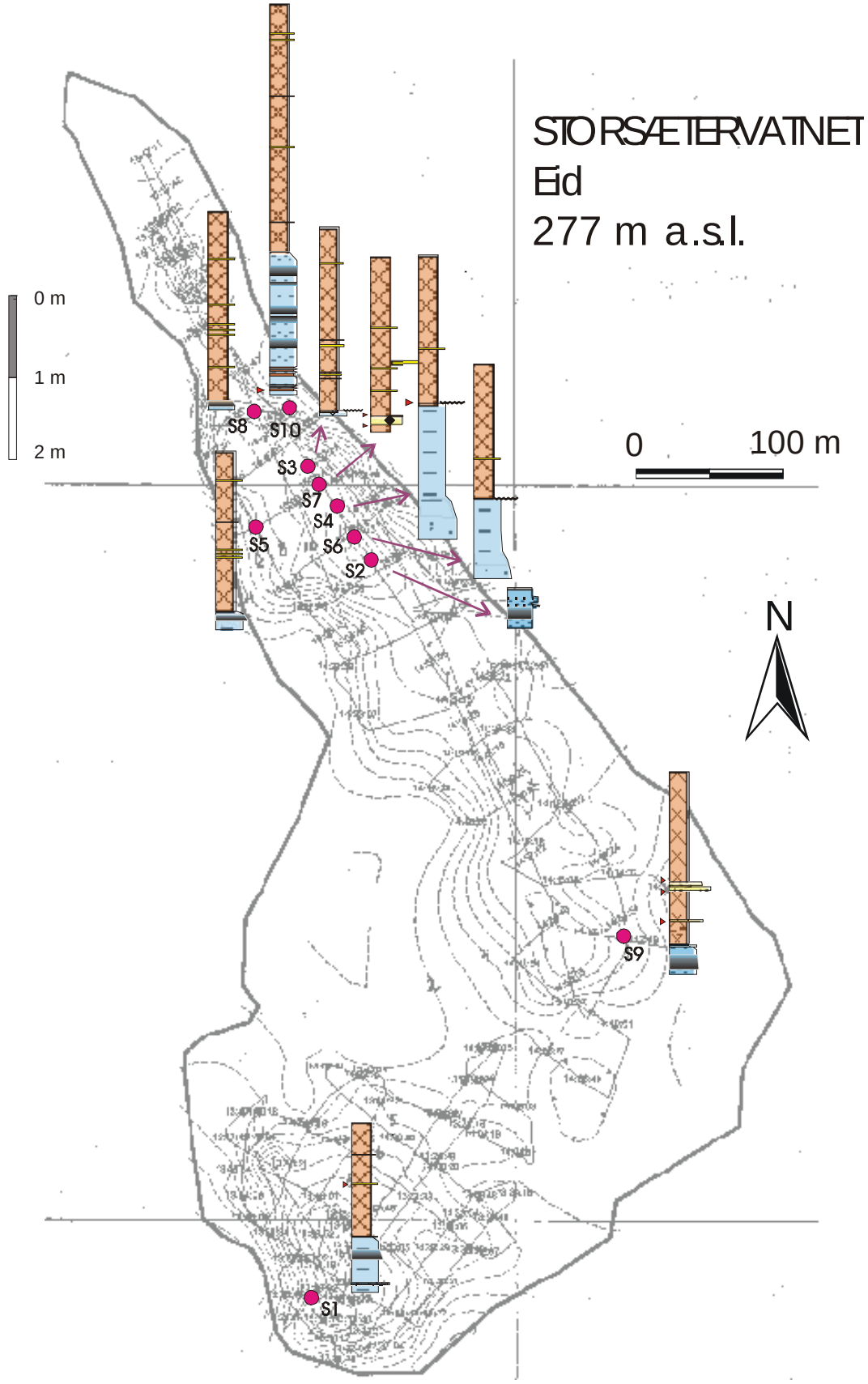

Fig. 13. Map showing core localities in Storsætervatnet. For core descriptions see Fig. 14 and Appendix 4.

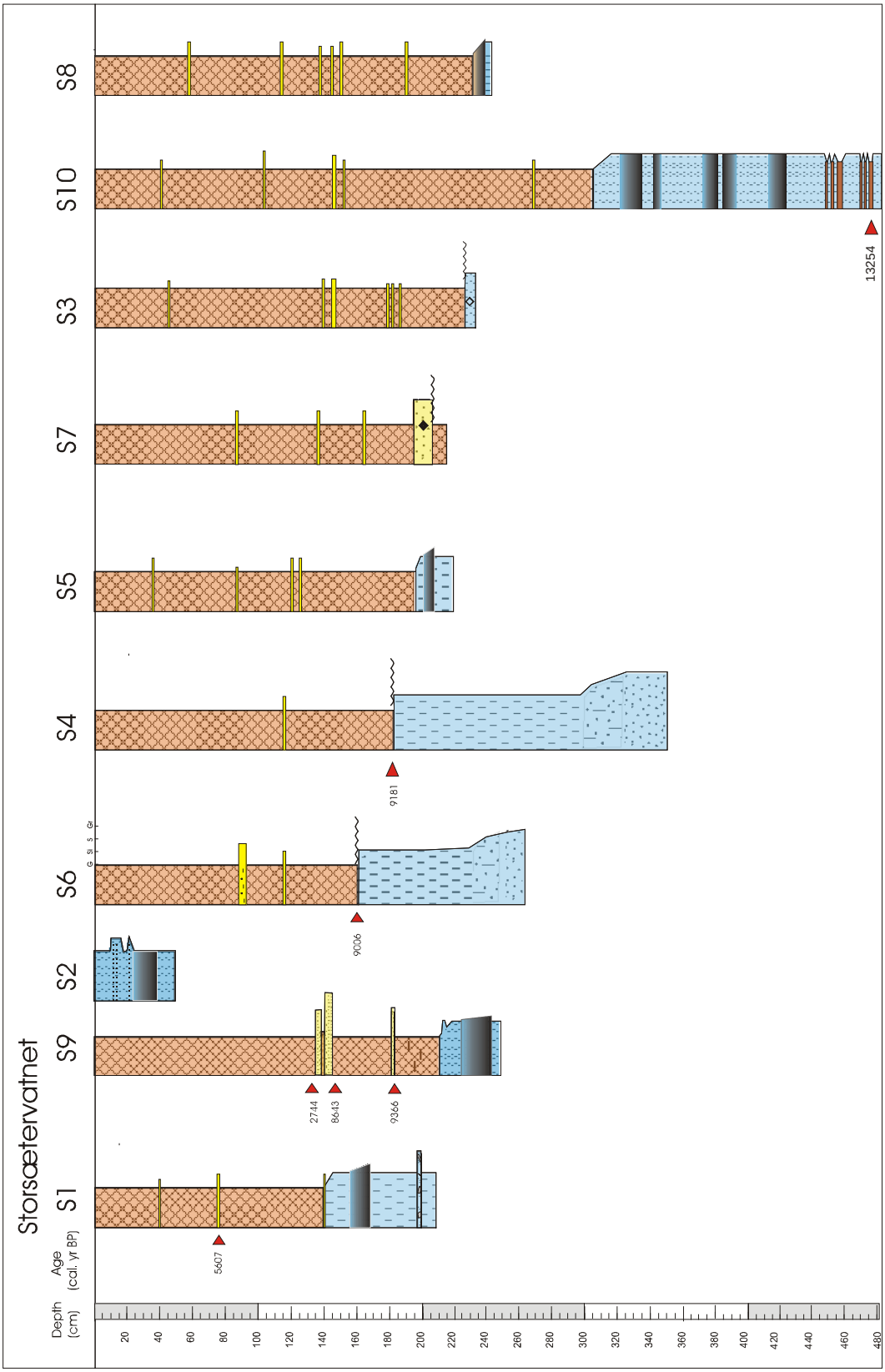

Fig. 14. Lithological logs of cores from Storsætervatnet. Cores are aligned in a general direction from south (left) to north (right). For legend see Fig. 16.

S10 Faintly laminated Holocene gyttja in the upper part of the core (0-3.05 m) contains five distinct silt laminae at 0.42 m, 1.03 m, 1.46 m, 1.49 m and 2.66 m. The glaciolacustrine silt in the lower part of the core (3.05-4.84 m) contains five ash layers (3.23-3.37 m, 3.41-3.44 m, 3.73-3.81 m, 3.83- 3.92 m and 4.13-4.23 m) that are interpreted to be repeated Vedde Ash layers. Organic-rich layers occur at 4.48-4.57 m and 4.71-4.76 m.

4.2.2. Medvatnet

Six cores were collected from Medvatnet (Figs. 15-16). Four samples from three cores were radiocarbon dated (Table 4).

M1 The boundary between faintly laminated Holocene gyttja (0-1.48 m) and glaciomarine silt with shells (1.48-1.54 m) is transitional. Silt layers occur within the Holocene gyttja at 0.60 m and 1.00 m, and a 7 cm thick gravely sand layer occurs at 1.20-1.27 m.

M2 Holocene gyttja (0-2.60 m) contains three distinct coarse grained beds. A silty layer at 0.61-0.63 m is rich in gravel and coarse plant fragments. A disturbed layer at 1.58-1.60 m comprises sandy silt (or clasts of sandy silt) and contains pebbles up to 3 cm diameter near its base. A layer of gravelly sand occurs at 2.05-2.35 m. The boundary between Holocene gyttja and underlying glaciomarine silt with shells (2.60-3.32 m) is transitional. A sandy-gravelly diamicton occurs at 2.76-2.96 m.

M3 Three distinct interlayers were found in the faintly laminated Holocene gyttja (0-1.22 m). These interlayers are made of sand (0.25-0.27 m), gravely sand (0.87-0.95 m) and silt (5 mm thick at 1.13 m). A large wood fragment (diameter 10 cm) was located at 0.30-0.40 m. The boundary between Holocene gyttja and underlying glaciomarine silt (1.22-1.33 m) is transitional.

M4 Holocene gyttja in the upper part of the core (0-2.70 m) contains four silt lamina (0.70 m, 0.91 m, 0.92 m and 2.53 m), a gravelly silt lamina (1.15 m) and a gravelly sand layer (1.74-1.95 m). The glaciomarine sediments in the lower part of the core (2.70-3.50 m) consist of silt (2.70-2.78 m and 2.98-3.13 m), sandy and gravely diamicton (2.78-2.98 m) and gravelly sand (3.13-3.50 m). All these glaciomarine units contain shells.

M5 Faintly laminated Holocene gyttja (0-1.50 m) contains a layer of gravelly sand at 1.05-1.22 m. A 3 cm diameter pebble occurs at 150 cm and a 7 cm diameter wood fragment was located at 143 cm. The boundary from gyttja to underlying brown, upward darkening glaciomarine silt (1.50-2.10 m) is transitional. Shells and barnacles are common in the lower part (1.90-2.10 m) of the glaciomarine silt.

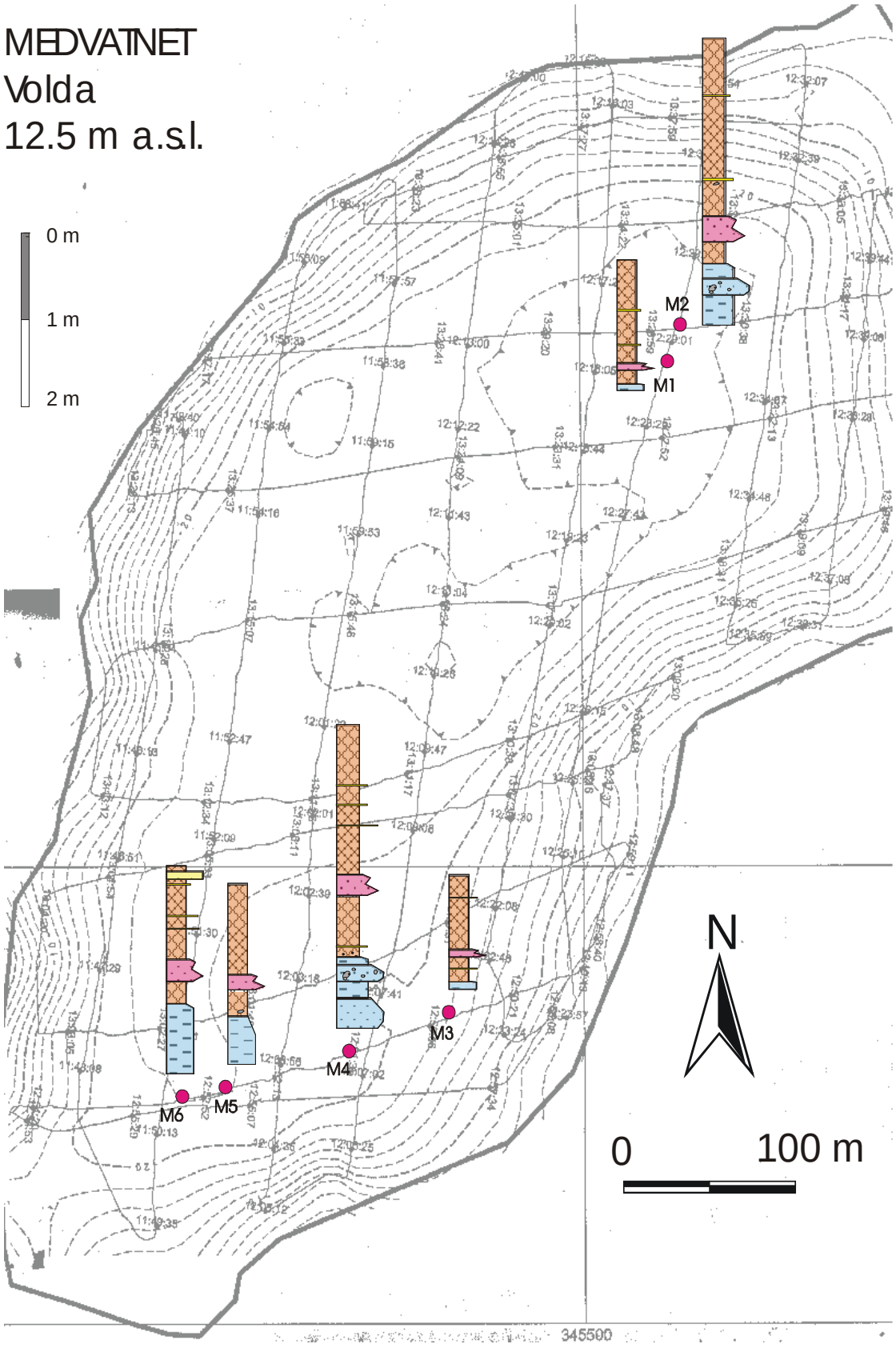

Fig. 15. Map showing core localities in Medvatnet. For core descriptions see Fig. 16 and Appendix 4.

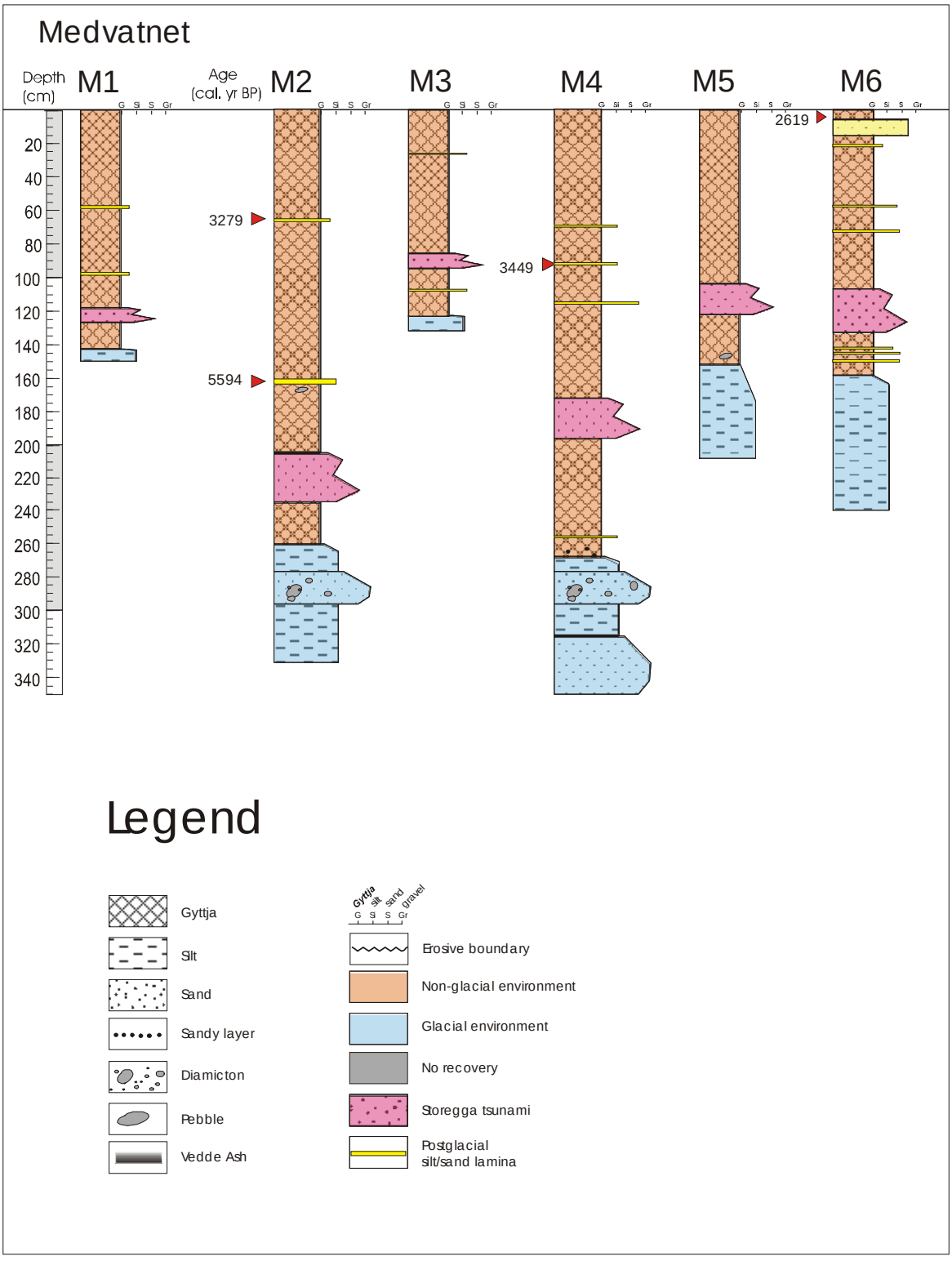

Fig. 16. Lithological logs of cores from Medvatnet.

M6 Laminated Holocene gyttja (0-1.60 m) contains laminae of silt (0.58 m and 0.72 m), sand (1.42 m, 1.45 m, 1.50 m), and layers of sand and gravelly sand at 0.09-0.18 m and 1.05-1.30 m, respectively. Wood fragments are comparatively abundant throughout the Holocene gyttja, particularly in the upper part of the sequence. A transitional boundary separates Holocene gyttja from underlying glaciolacustrine silt (1.60-2.42 m) that becomes gradually darker upwards and contains shells in the lower part (2.10-2.42 m).

4.2.3. Nedstevatnet

Four cores were collected from Nedstevatnet (Figs. 17-18). Ten samples from three cores were submitted for radiocarbon dating (Table 4).

N1 Laminated Holocene gyttja in the upper part of the core (0-3.65 m) contains a layer of gravelly sand (2.95-3.30 m) and laminae of silt (0.35 m) and sand (3.50 m and 3.58 m). The gyttja is slightly coarser, and more silty at 3.30-3.65 m. The boundary between Holocene gyttja and underlying glaciomarine sediments (3.65-5.40 m) is transitional.

Silt in the upper part of the glaciomarine sequence (3.65-4.00 m) is followed downcore by shell-rich diamicton (4.00- 4.13 m), silt (4.13-4.47 m), another layer of diamicton with shells (4.47-4.70 m) and pebbly clayey silt (4.70-5.40 m). The sequence of glaciomarine sediments darkens gradually upward.

N2 Holocene gyttja (0-2.90 m) contains a horizon of distorted sand (sand clasts) in a gyttja matrix (0.20-0.40 m), laminae of sand (1.02 m) and silt (2.85 m), a layer of gravelly sand (2.10-2.36 m) and a layer of upward coarsening sand (2.79-2.82 m). Small twigs are common at 0.15-0.20 m, and a shell (*Buccinum undatum*) was found at 1.45 m. The boundary between Holocene gyttja and underlying shell-rich, brown glaciomarine sediments (2.90-3.83 m) is transitional. Two layers of sandy and gravelly diamicton (3.23-3.33 m and 3.67-3.73 m) occur within otherwise silty glaciomarine sediments.

N3 Holocene gyttja in the upper part of the core (0-2.10 m) contains a layer of gravelly sand at 1.50-1.75 m and 6 sand layers/laminae (up to 2 cm thick) at 0.09 m, 0.42-0.44 m, 1.82-1.84 m, 1.87 m, 1.92 m and 2.04 m. A transitional boundary separates Holocene gyttja from underlying glaciomarine sediments (2.10-3.30 m) consisting of silt interlayerd by three beds of shell-rich, sandy and gravelly diamicton (2.52-2.64 m, 2.73-2.82 m, 2.97-3.10 m).

N5 Two sand laminae (0.90 m and 0.96 m) and a gravelly sand layer (0.18-0.48 m) occur in Holocene gyttja (0-1.02 m). The boundary from gyttja to underlying glaciomarine sediments (1.02-3.13 m) is transitional. Glaciomarine sediments consist predominantly of silt with shells. The silt is interlayered by three beds of sandy and gravelly diamicton (1.39-1.64 m, 1.88-2.03 m and 2.24-2.36 m) and 5 layers/laminae of gravelly sand (1.08-1.10 m, 2.67 m, 2.74 m, 2.78 m, 2.86 m.

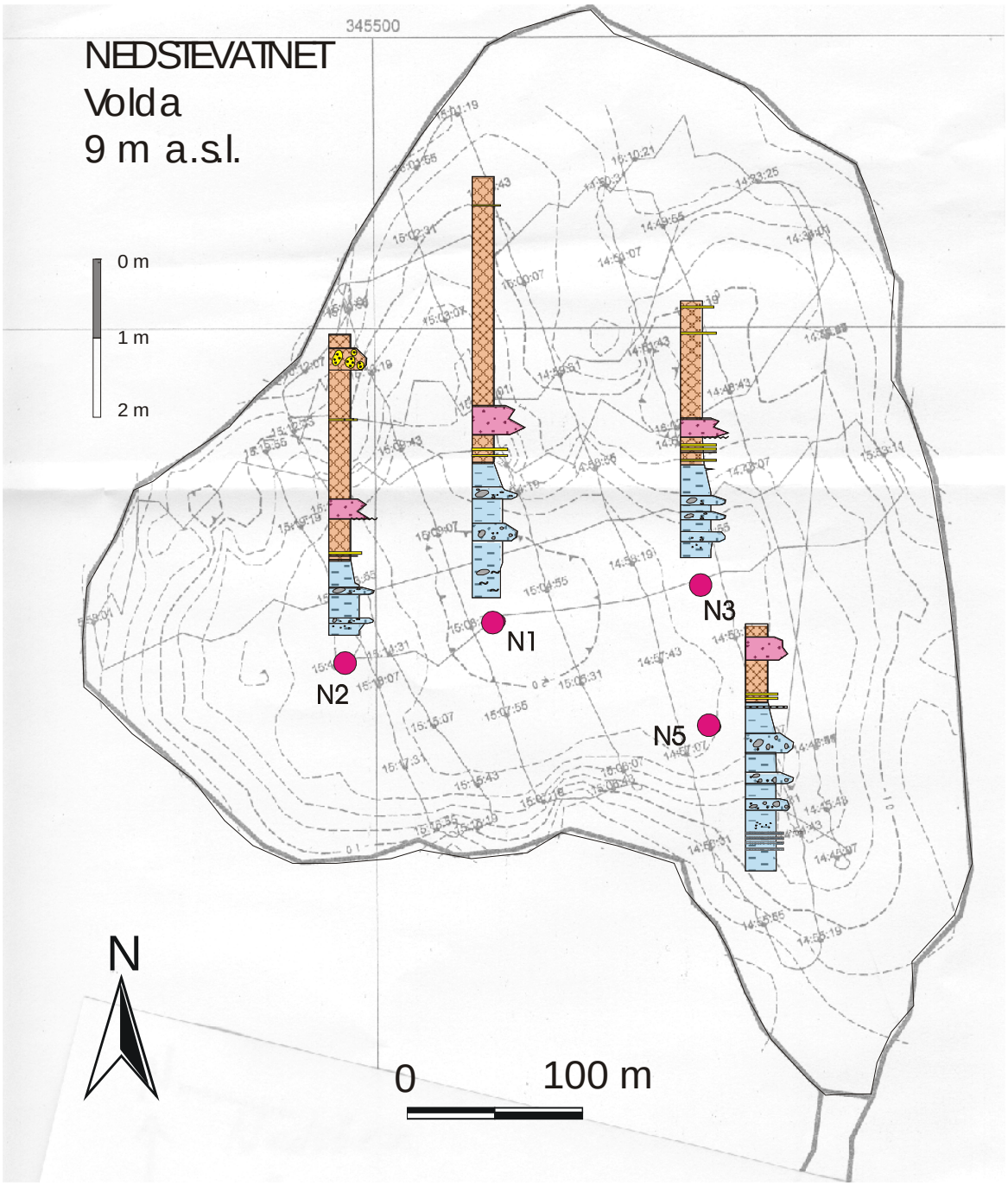

Fig. 17. Map showing core localities in Nedstevatnet. For core descriptions see Fig. 18 and Appendix 4.

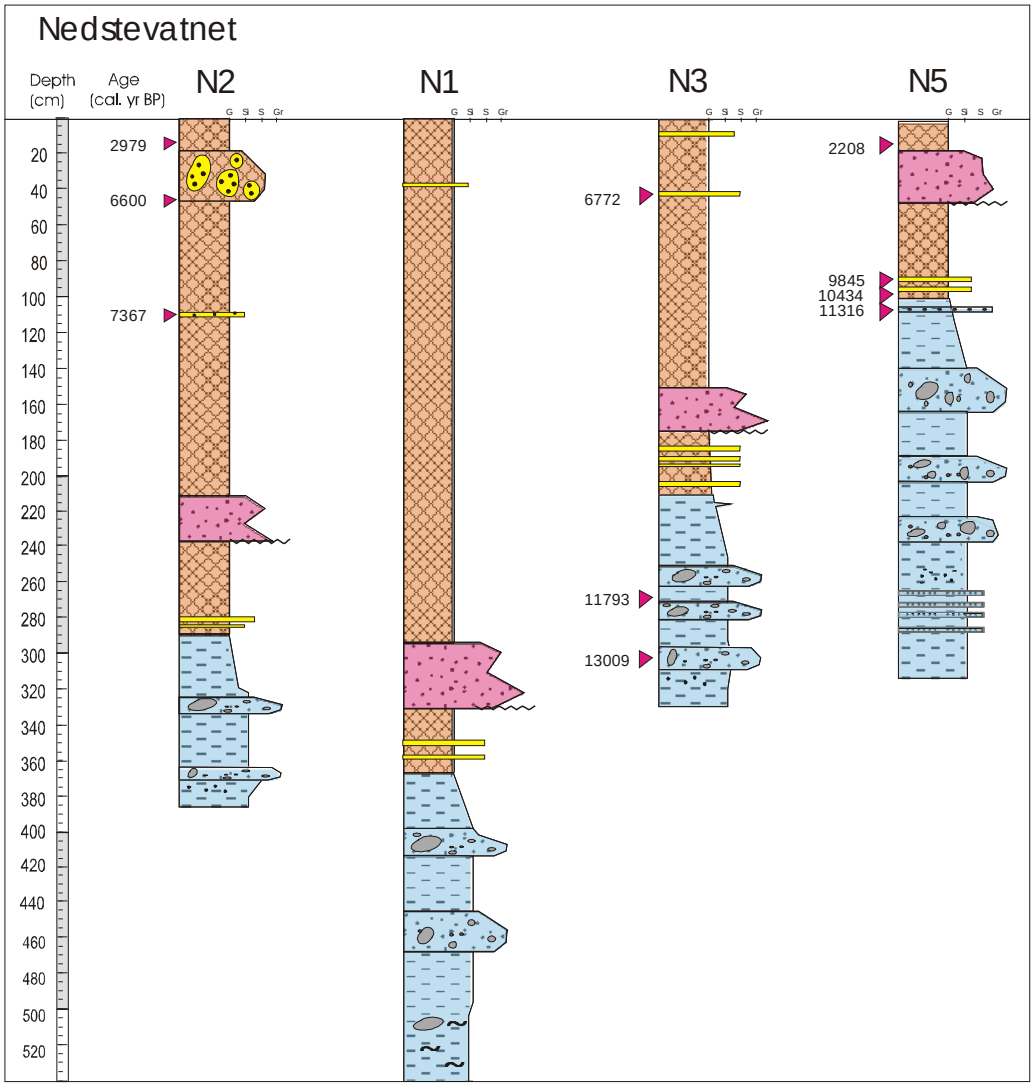

Fig. 18. Lithological logs of cores from Nedstevatnet. Cores are aligned in a general direction from west (left) to east (right). For legend see Fig. 16.

4.2.4. Rotevatnet

Six cores were collected from Rotevatnet (Figs. 19-20). Three samples from one core were radiocarbon dated (Table 4).

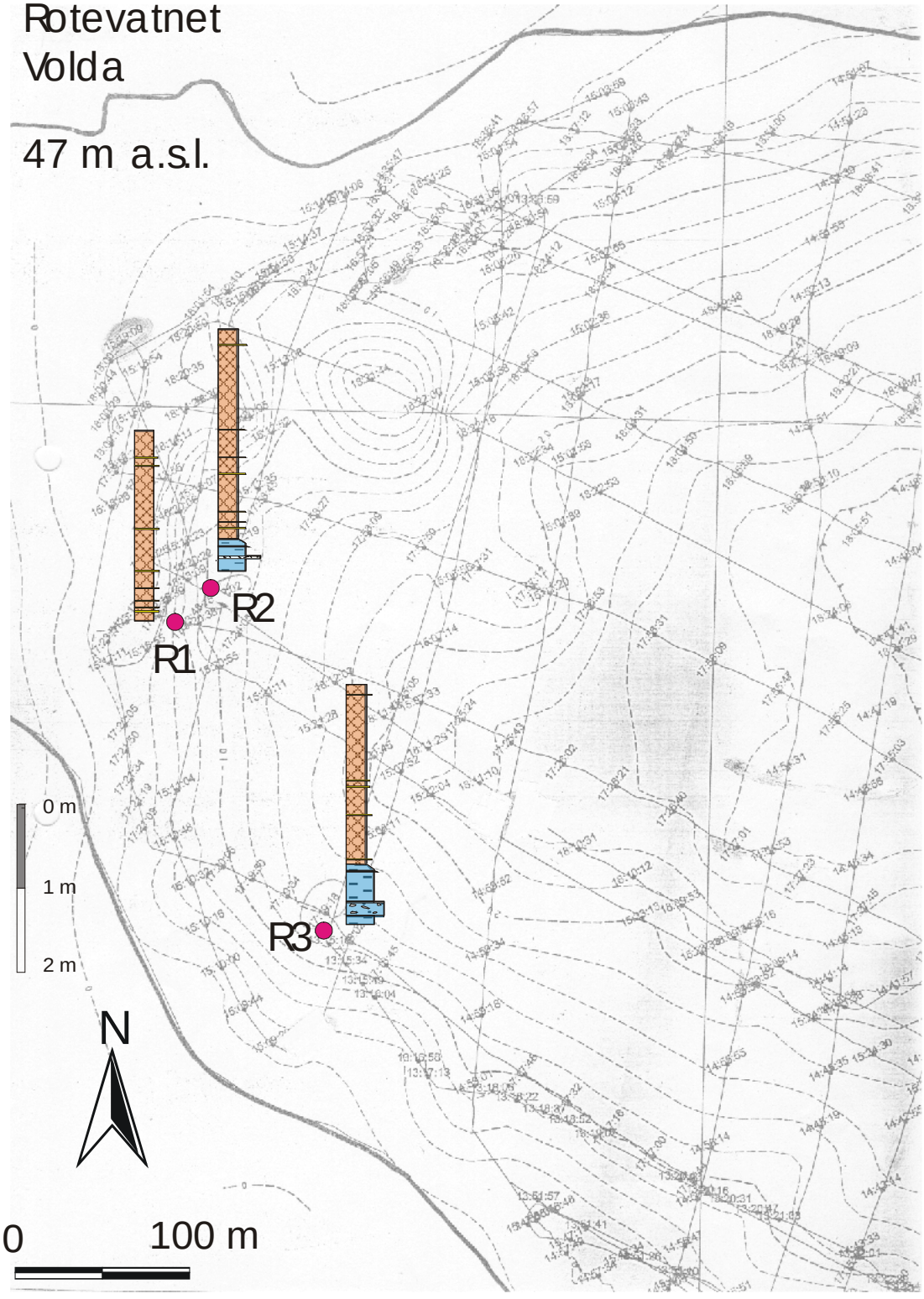

Fig. 19. Map showing core localities in Rotevatnet. For core descriptions see Fig. 20 and Appendix 4.

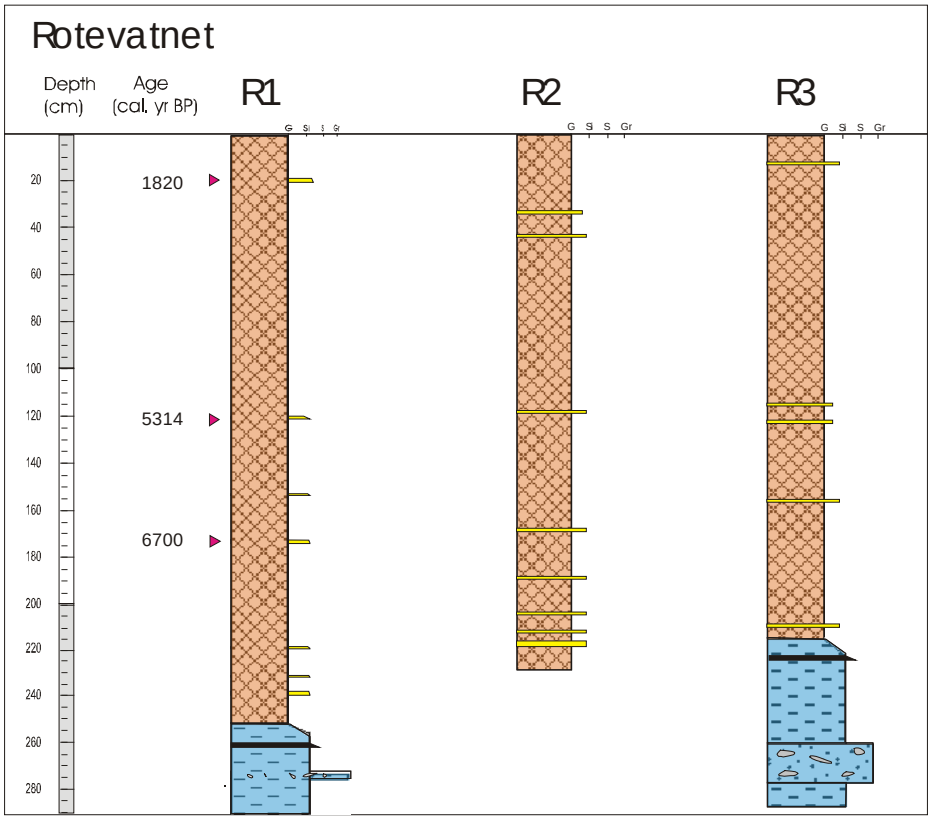

Fig. 20. Lithological logs of cores from Rotevatnet. For legend see Fig. 16.

R1 Holocene gyttja (0-2.50 m) contains 7 upward fining, up to 10 mm thick silt laminae (0.24 m, 1.21 m, 1.53 m, 1.75 m, 2.20 m, 2.32 m, 2.40 m). The Holocene gyttja is light brown and diffusely laminated in the upper part (0-2.00 m) while the laminated lower part (2.00-2.50) is dark brown. The boundary from gyttja to underlying glaciolacustrine silt (2.50-2.90) is transitional. The Vedde Ash occurs at 2.59-2.61 m and a layer of gravelly sandy diamicton occurs at 2.70-2.75 m.

R2 This 2.31 m long core consists entirely of Holocene gyttja. Thin silt laminae occur at 0.34 m, 0.44 m, 1.19 m, 1.69 m, 1.90 m, 2.04 m, 2.12 m and 2.18 m.

R3 Holocene gyttja (0-2.15 m) contains 5 silt laminae at 0.12 m, 1.14 m, 1.21 m, 1.55 m and 2.08 m. Glaciolacustrine sediments, below a transitional boundary, consist predominantly of silt, and include Vedde Ash at 2.22-2.24 m and a sandy gravelly diamicton at 2.60-2.75 m. Shell fragments occur above the diamicton.

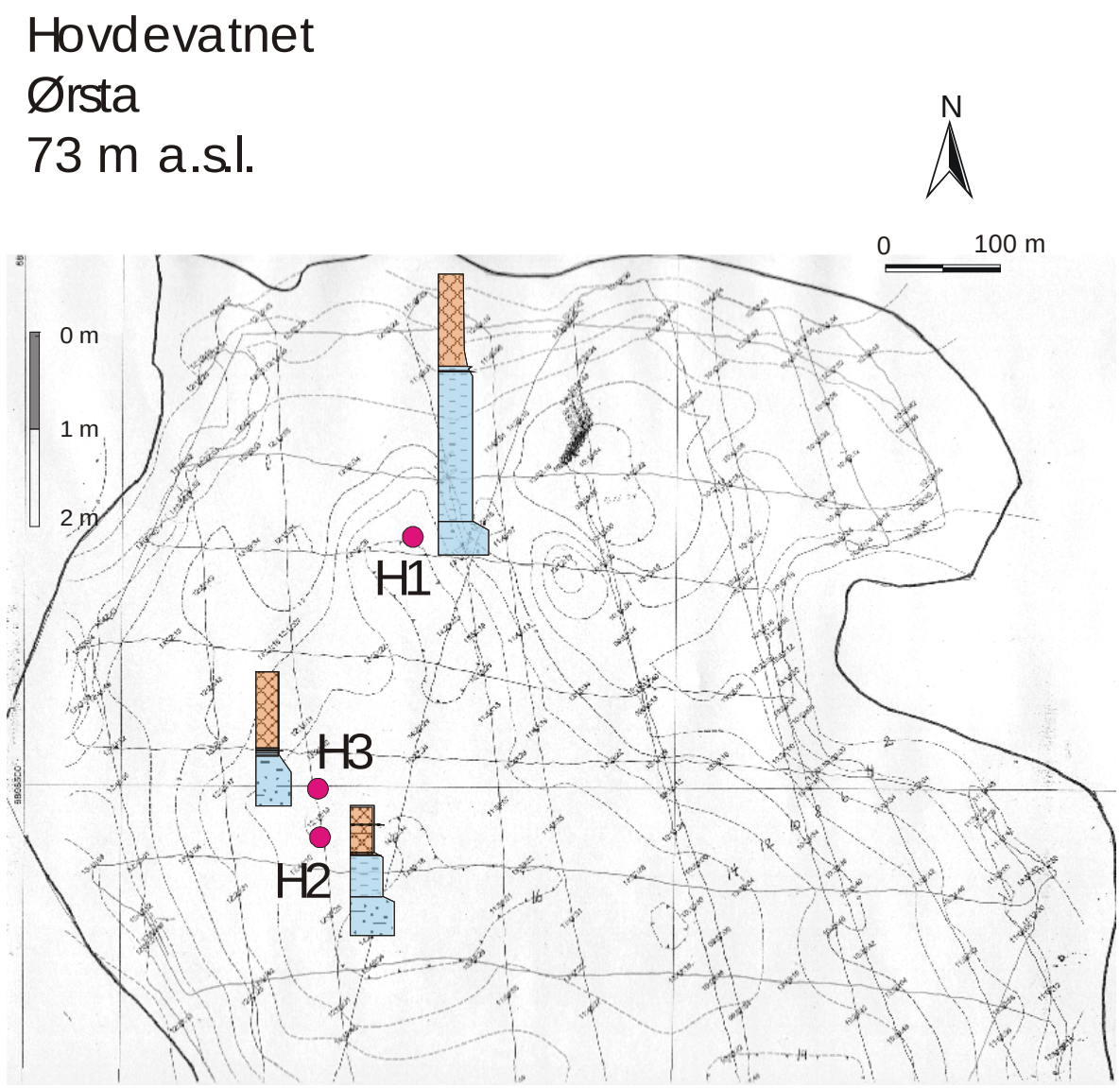

Fig. 21. Map showing core localities in Hovdevatnet. For core descriptions see Fig. 22 and Appendix 4.

4.2.5. Hovdevatnet

Six cores were collected from Hovdevatnet (Figs. 21-22). No dating was done on these cores.

H1 Faintly laminated Holocene gyttja (0-0.95 m) is dark brown at 0-0.70 m and light brown at 0.70-0.95 m. The gyttja is underlain by glaciolacustrine sediments consisting of silt (0.95-2.60 m) and sand (2.60-2.90 m). The boundary between Holocene and glaciolacustrine sediments is transitional. The Vedde Ash occurs at 0.99-1.01 m.

H2 Faintly laminated Holocene gyttja (0-0.50 m) contains a sand lamina at 0.14 m. The gyttja has dark brown colour at 0-0.20 m and is light brown at 0.20-0.50 m. The gyttja is

underlain by glaciolacustrine sediments consisting of silt (0.50-0.95 m) and sand (0.95-1.27 m). The boundary between Holocene and glaciolacustrine sediments is transitional. A thin, discontinuous Vedde Ash layer occurs at 0.48-0.49 m.

H3 Faintly laminated Holocene gyttja (0-0.67 m) is dark brown at 0-0.37 m and light brown at 0.37-0.67 m. The gyttja is underlain by glaciolacustrine sediments consisting of silt (0.67-0.92 m) and sand (0.92-1.24 m). The transition from Holocene to glaciolacustrine sediments is gradual. The Vedde Ash occurs at 0.69-0.71 m.

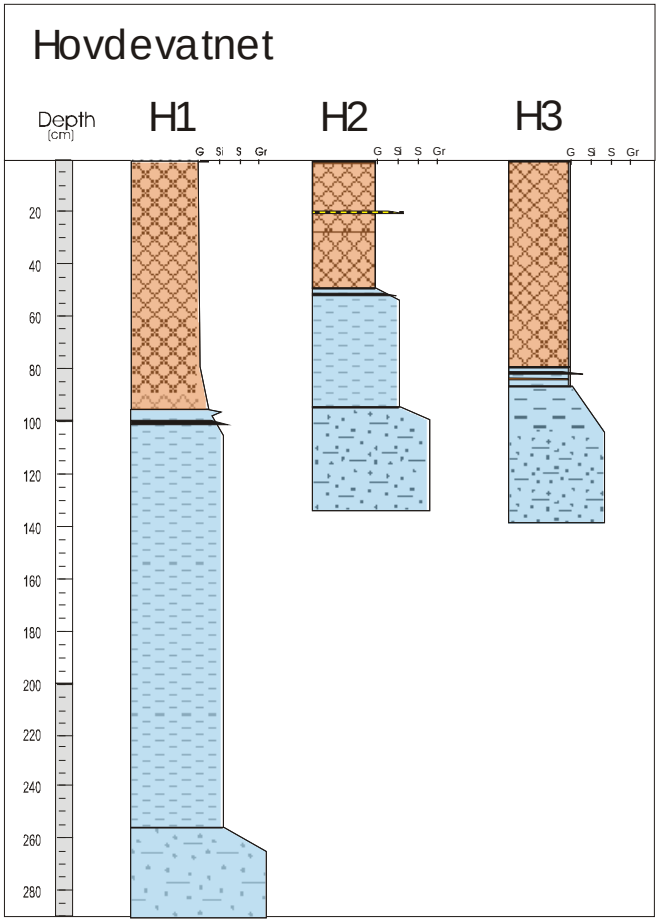

Fig. 22. Lithological logs of cores from Hovdevatnet. For legend see Fig. 16.

5. REFERENCES

Bondevik, S., Svendsen, J. I. and Mangerud, J. 1998: Distinction between the Storegga Tsunami and the Holocene marine transgression in coastal basin deposits of western Norway. *Journal of Quaternary Science 13*, 529-537.

Grøsfjeld, K., Larsen, E., Sejrup, H. P., de-Vernal, A., Flatebø, T., Vestbø, M., Haflidason, H. and Aarseth, I. 1999: Dinoflagellate cysts reflecting surface-water conditions in Voldafjorden, western Norway during the last 11 300 years. *Boreas 28*, 403-415.

Longva, O. and Olsen, H.A. 2001: Regional landslide occurrences and possible post-glacial earthquake acitivity in northwest Western Norway: Phase A2; Penetration echosounding in 5 lakes in Sunnmøre and Nordfjord. *NGU Report 2001.049*, 23 pp.

Longva, O., Blikra, L.H., Olsen, H.A. and Stalsberg, K. 2001a: Regional landslide occurrences and possible post-glacial earthquake activiy in northwest Western Norway: Phase A1: interpretation of seismic data and proposal of core-locations in fjords and along the coast. *NGU Report 2001.048*, 46 pp.

Longva, O., Bøe, R. and Howe, J. 2001b: Cruise 0103 with R/V Seisma to fjords in Sogn og Fjordane and Møre og Romsdal - cruise report (Phase B1). *NGU Report 2001.100*, 22 pp.

Munsell 1954: Munsell Colour Chart. Munsell Soil Company Inc., Baltimore, Maryland, USA.

Sejrup, H.P., Haflidason, H., Flatebø, T., Klitgaards Kristensen, D., Grøsfjeld, K. and Larsen, E. 2001: Late-glacial to Holocene environmental changes and climate variability: evidence from Voldafjorden, western Norway. *Journal of Quaternary Science 16*, 181-198.

Stuiver, M., Reimer, P.J., Bard, E., Beck, J.W., Burr, G.S., Hughen, K.A., Kromer, B., McCormac, F.G., v.d. Plicht, J., and Spurk, M. 1998. INTCAL98 Radiocarbon Age Calibration, 24,000-0 cal BP. *Radiocarbon 40*:1041-1083

Sønstegaard, E., Sandnes, R., Hovland, C. and Bøe, R. 2001: Regional landslide occurrences and possible post-glacial earthquake activity in northwest Western Norway: sediment cores from five lakes in Nordfjord and Sunnmøre (Phase B2). *NGU Report 2001.101*, 42 pp.

APPENDIX 1

Locations of fjord cores on seismic profiles

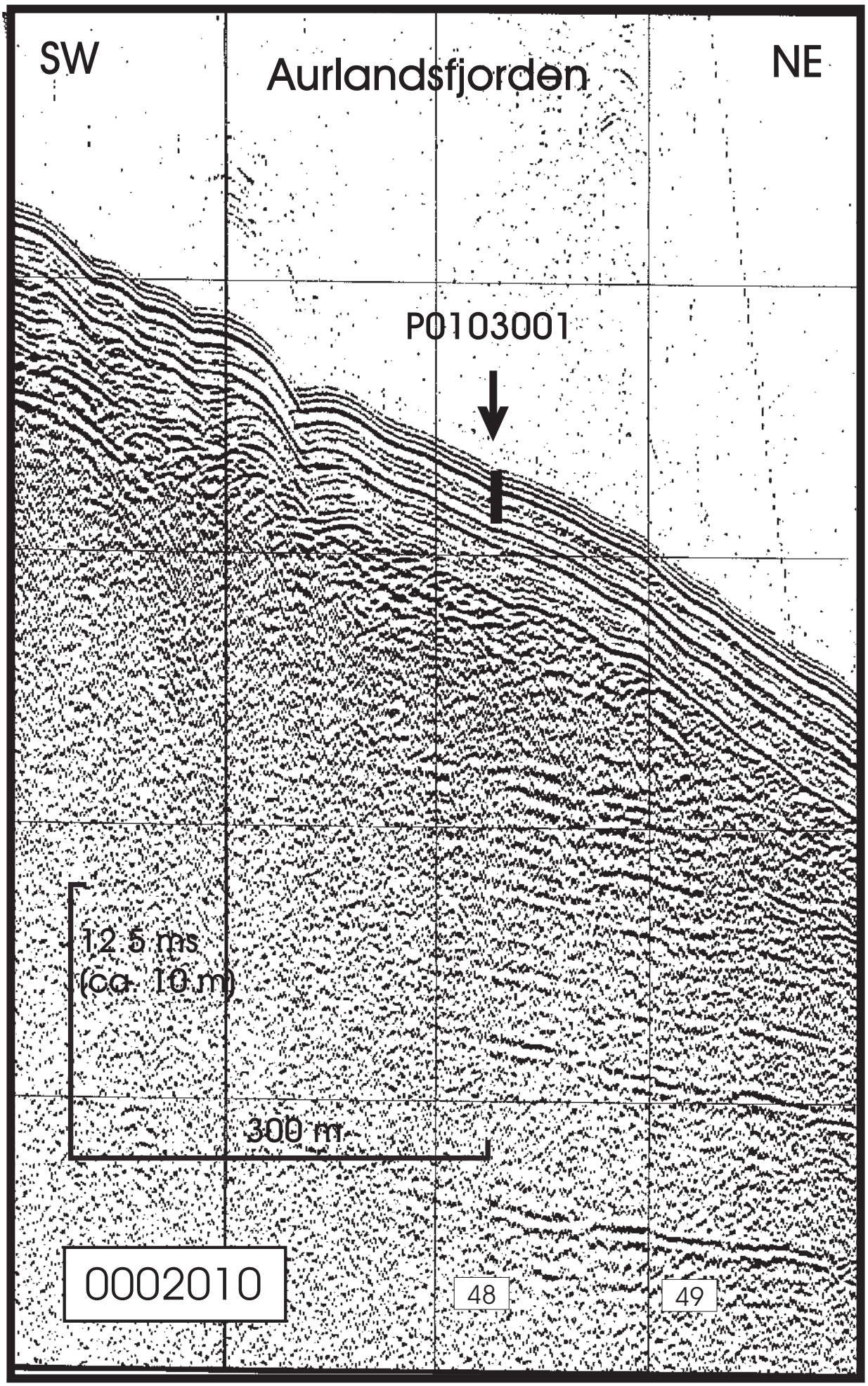
SW
Aurlandsfjorden
NE
P0103001
12.5 ms
(ca. 10 m)
300 m
0002010
48
49

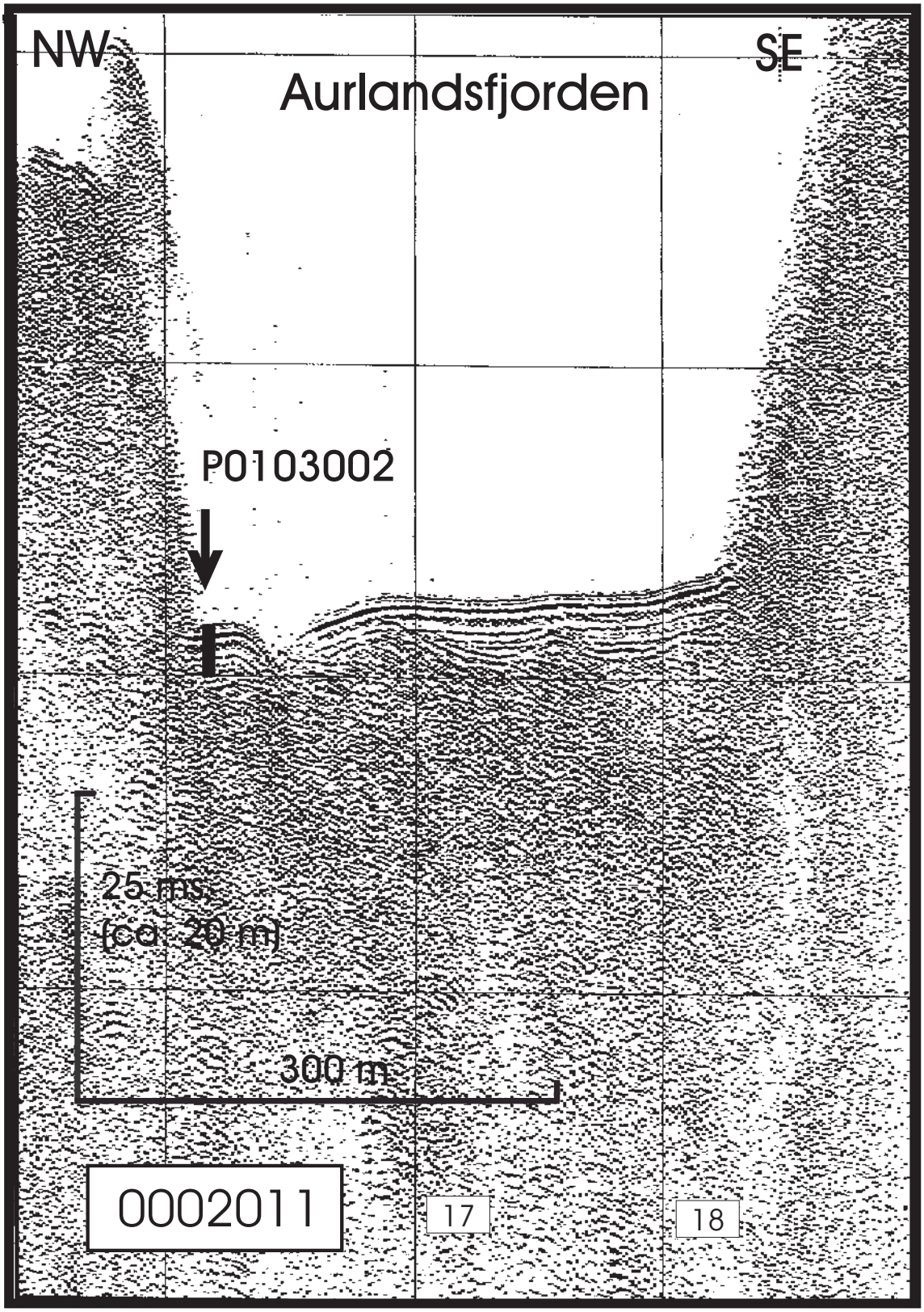
NW
SE
Aurlandsfjorden
P0103002
25 ms
(ca 20 m)
300 m
0002011
17
18

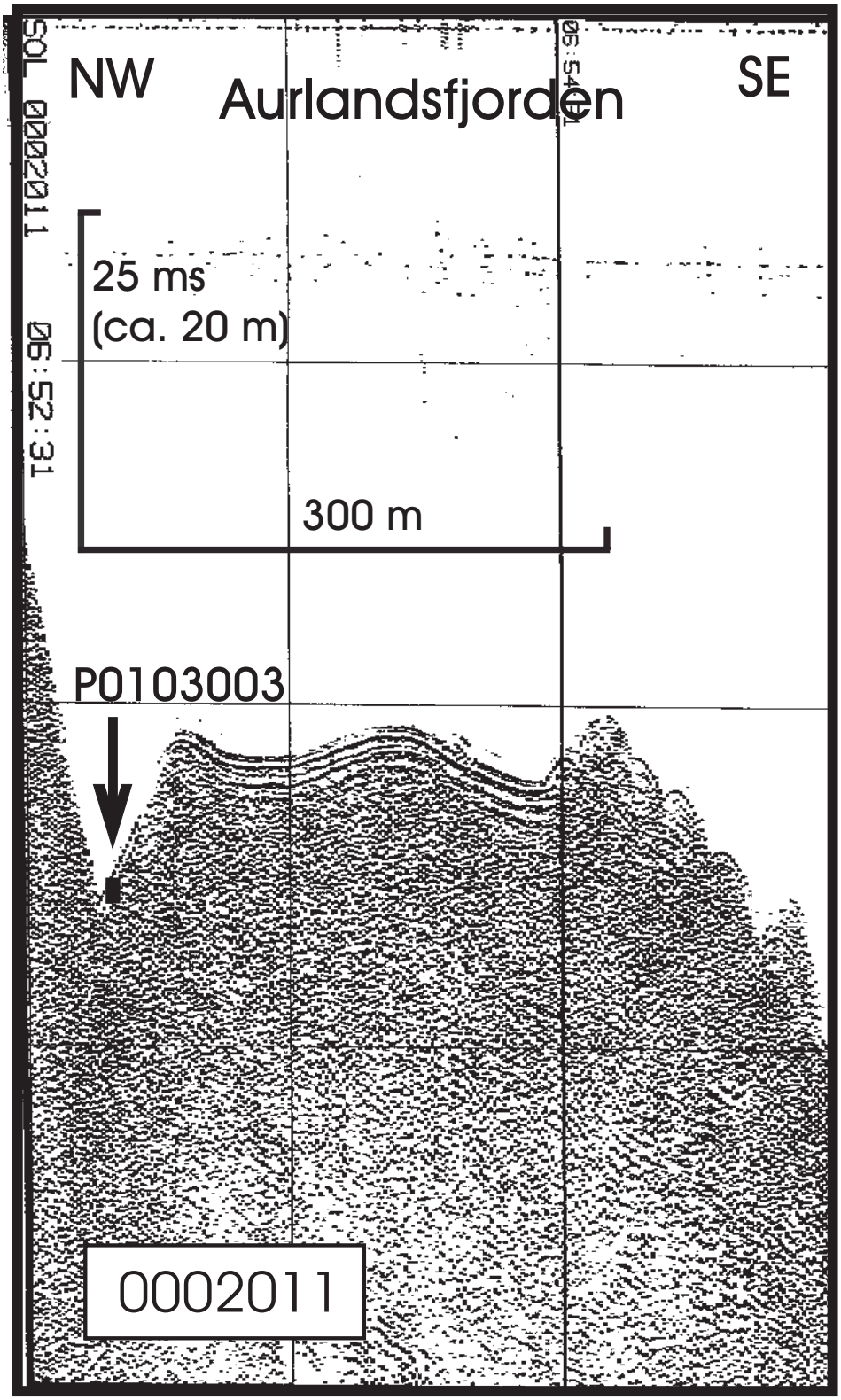
NW
Aurlandsfjorden
SE
SOL 0002011
06:52:31
06:54:01
25 ms
(ca. 20 m)
300 m
P0103003
0002011

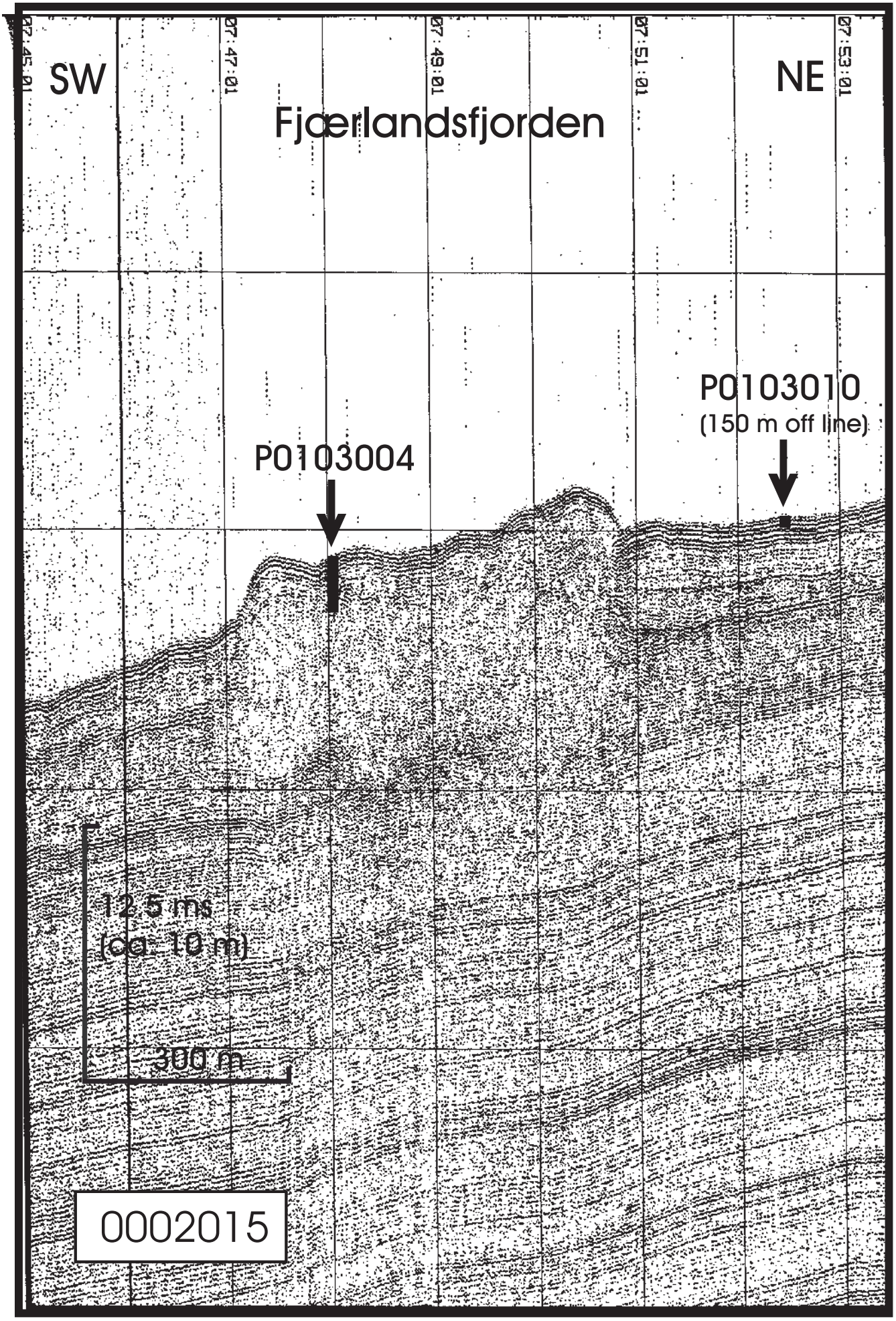
SW
NE
Fjærlandsfjorden
P0103004
P0103010
(150 m off line)
12.5 ms
(ca. 10 m)
300 m
0002015

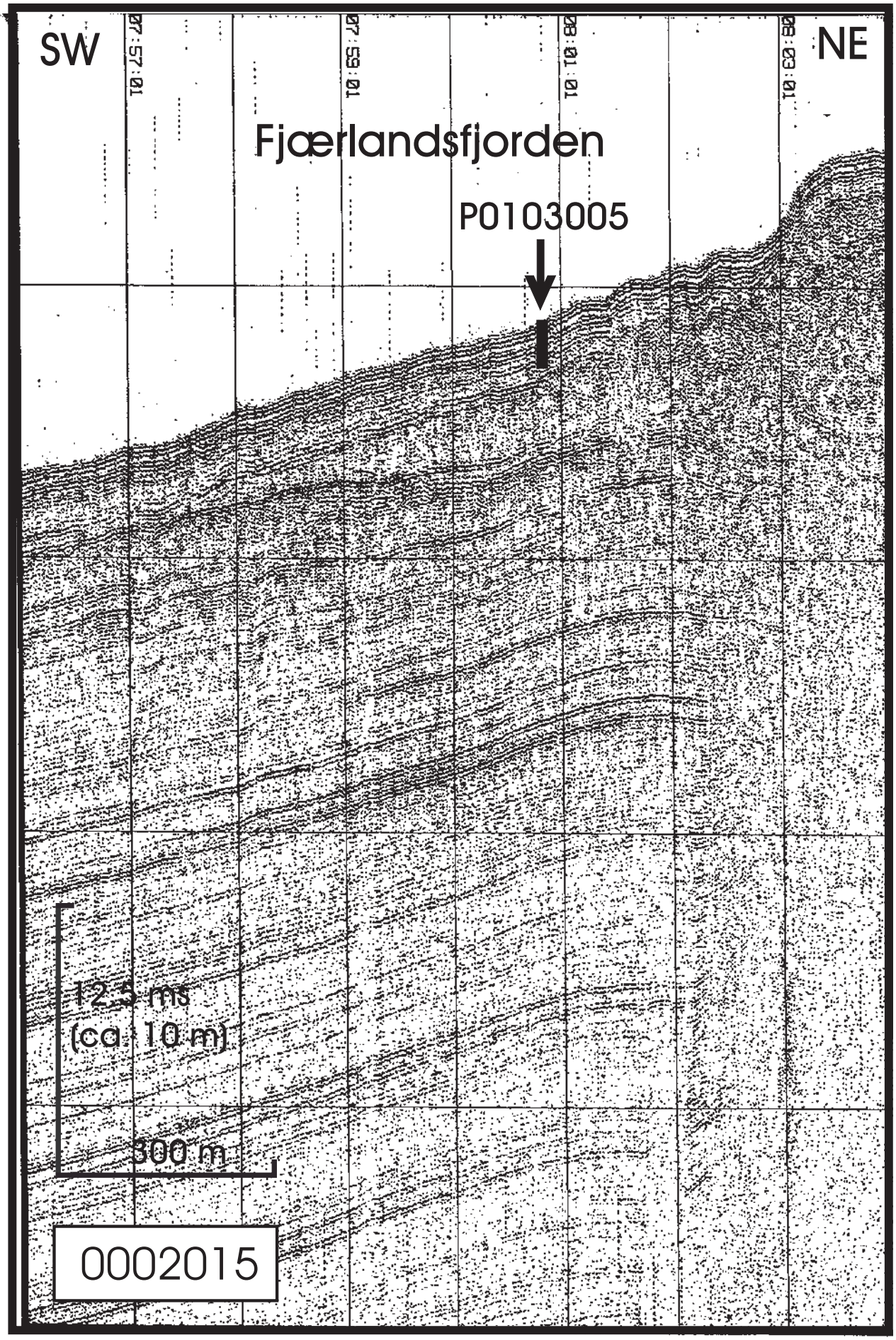
SW
NE
07:57:01
07:59:01
08:01:01
08:03:01
Fjærlandsfjorden
P0103005
12.5 ms
(ca. 10 m)
300 m
0002015

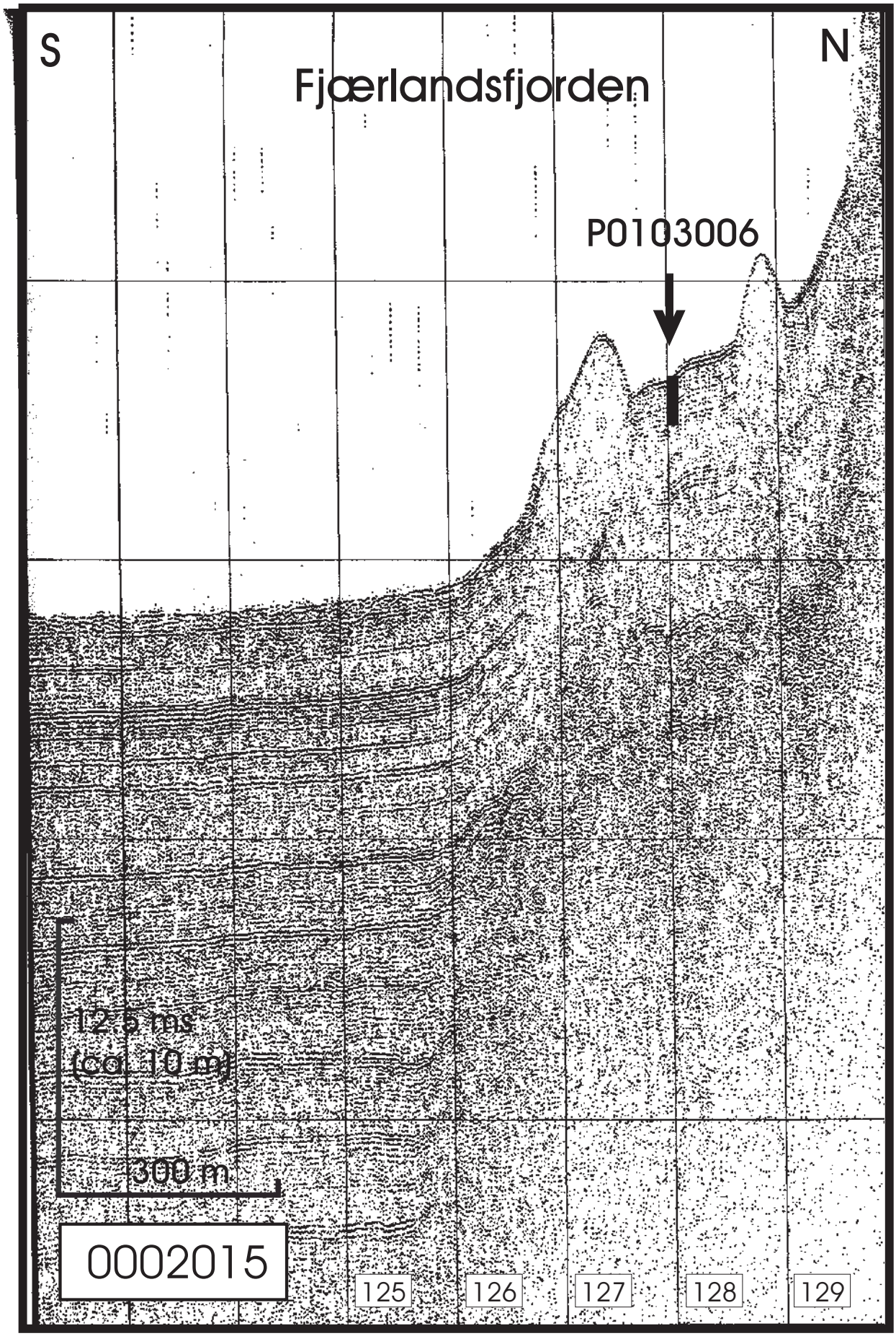
S
N
Fjærlandsfjorden
P0103006
12.5 ms
(ca. 10 m)
300 m
0002015
125
126
127
128
129

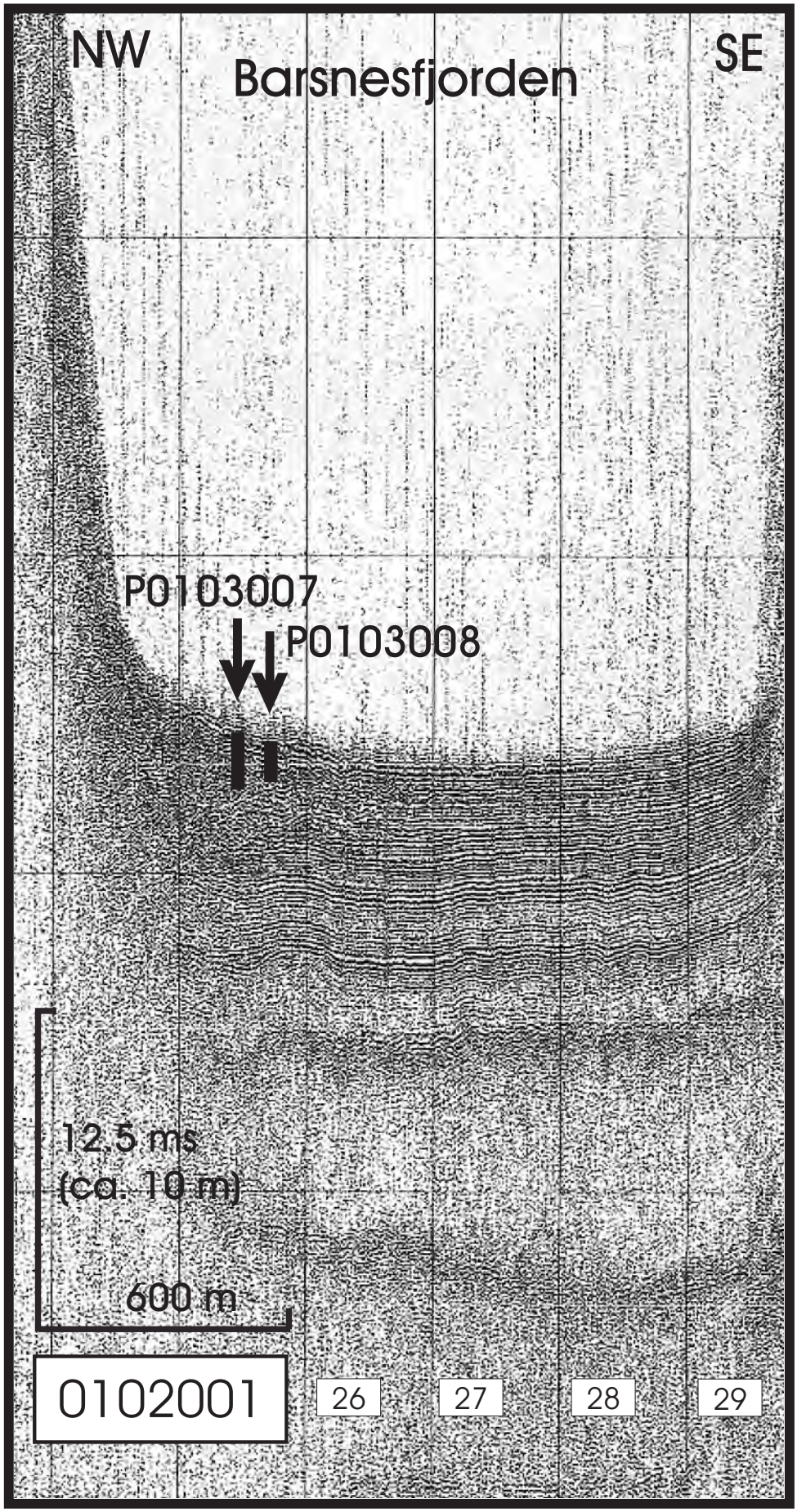
NW
Barsnesfjorden
SE
P0103007
P0103008
12,5 ms
(ca. 10 m)
600 m
0102001
26
27
28
29

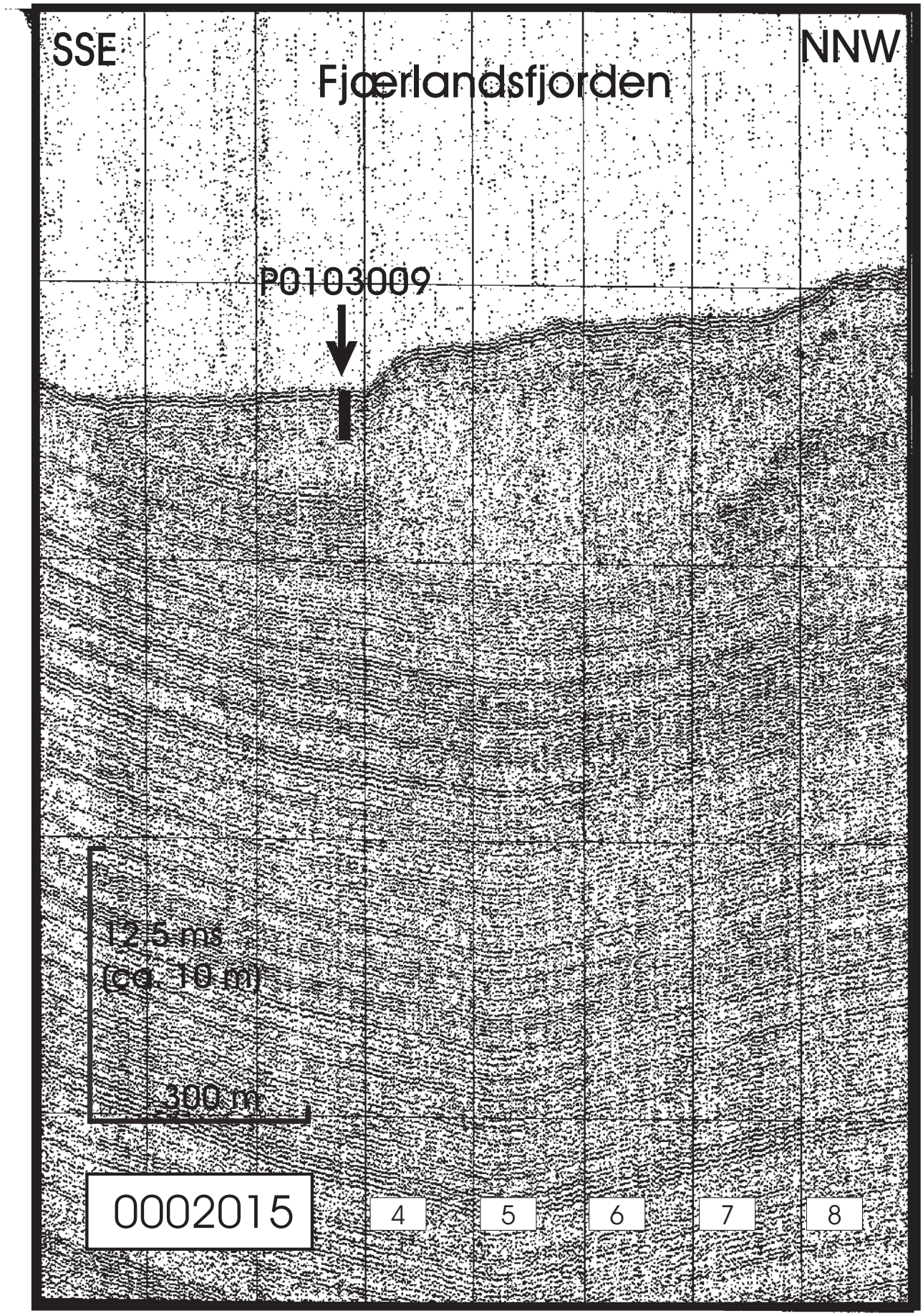
SSE
Fjærlandsfjorden
NNW
P0103009
12.5 ms
(ca. 10 m)
300 m
0002015
4
5
6
7
8

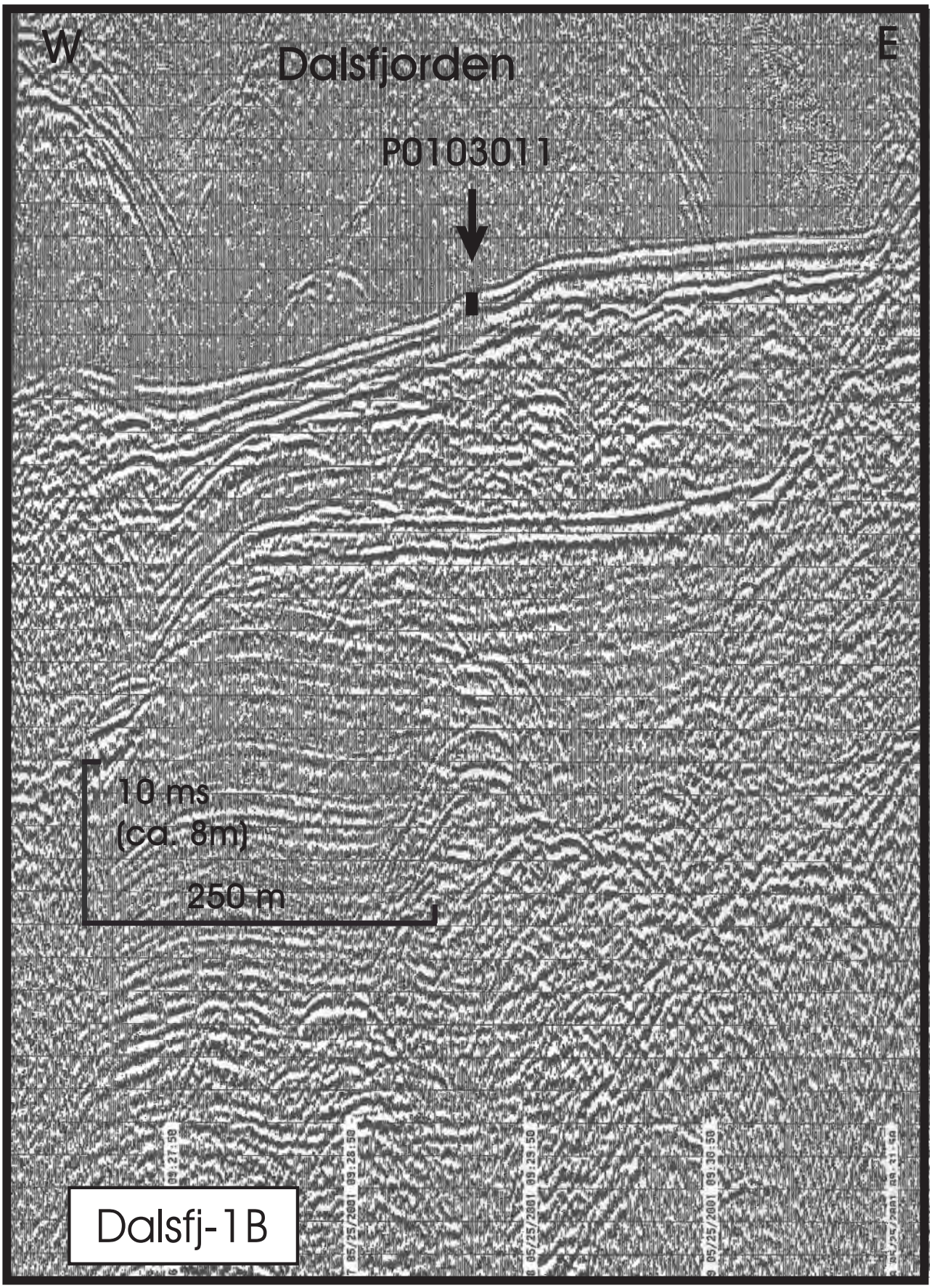
W
Dalsfjorden
E
P0103011
10 ms
(ca. 8m)
250 m
Dalsfj-1B

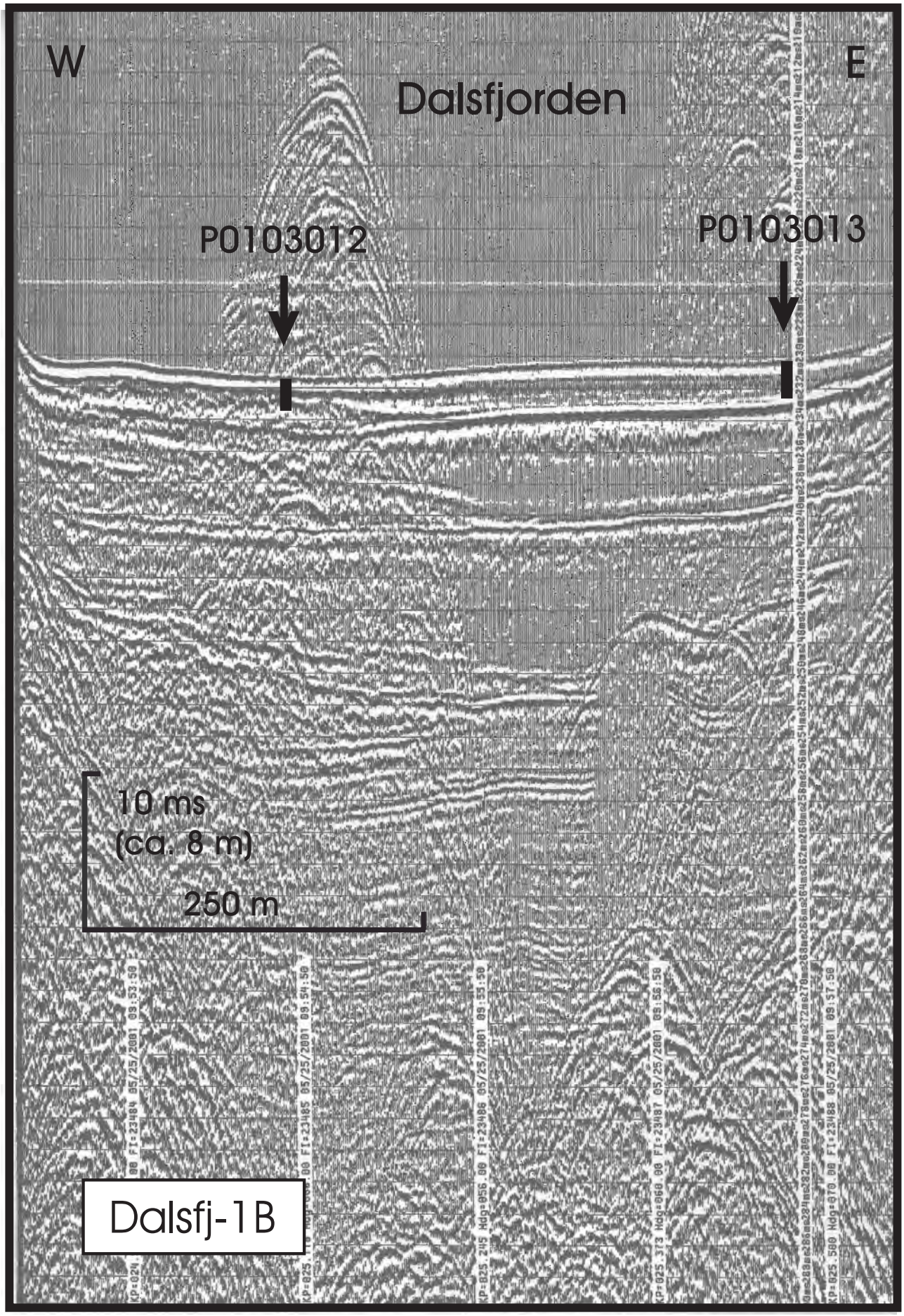
W
E
Dalsfjorden
P0103012
P0103013
10 ms
(ca. 8 m)
250 m
Dalsfj-1B

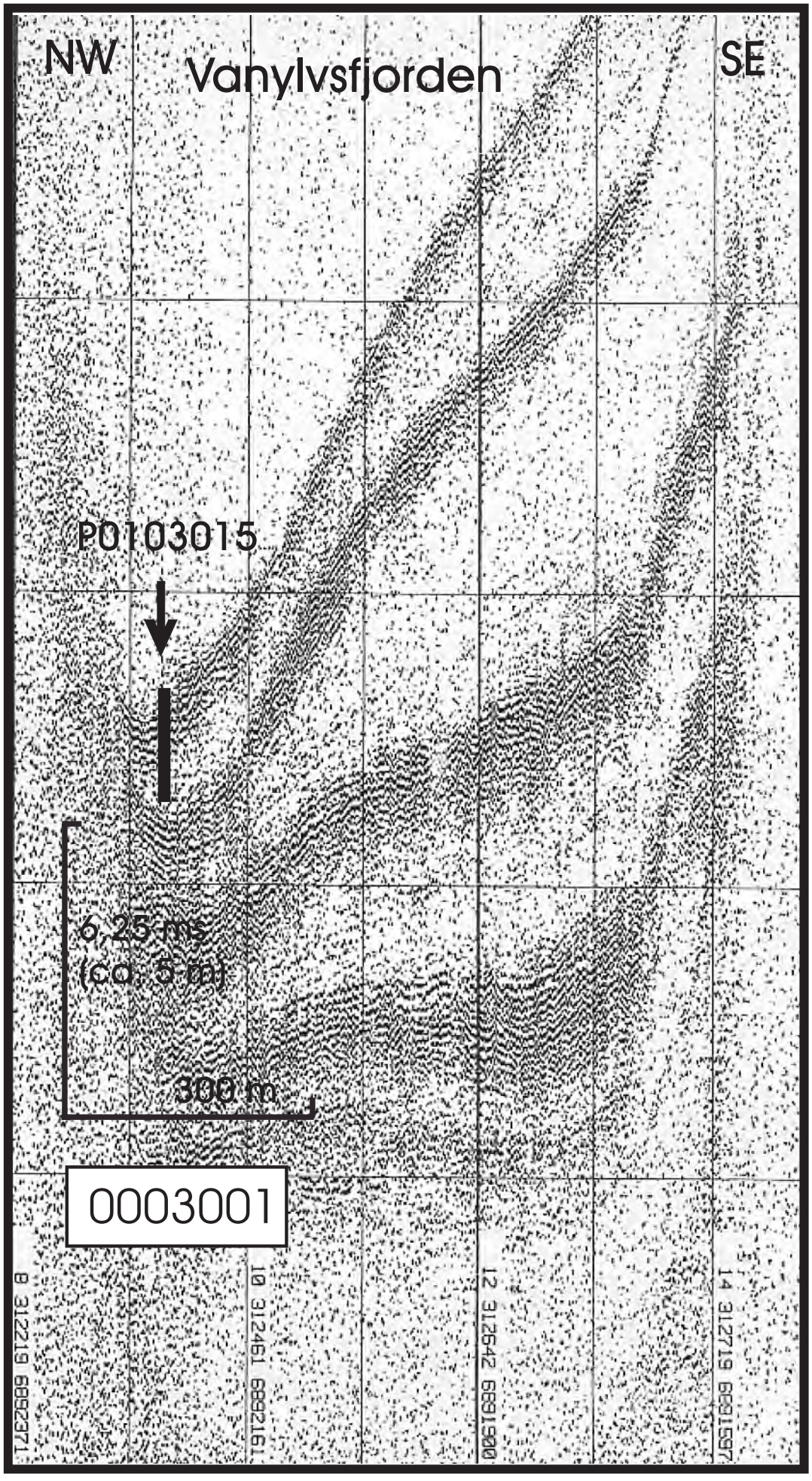
NW
Vanylvsfjorden
SE
P0103015
6,25 ms
(ca. 5 m)
300 m
0003001
8 312219 6892371
10 312461 6892161
12 312542 6891900
14 312719 6891597

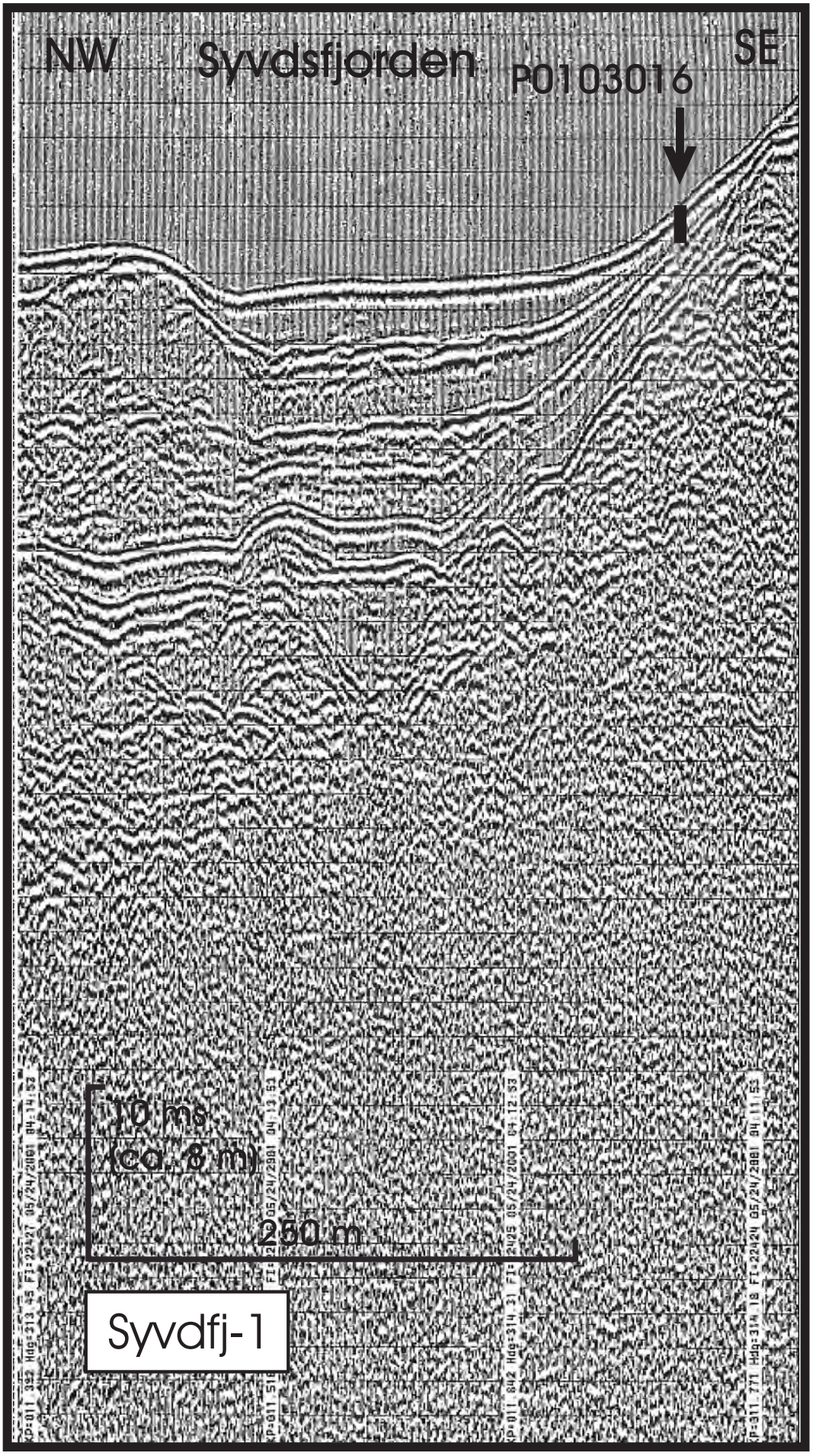
NW
Syvdsfjorden
P0103016
SE
10 ms
(ca. 8 m)
250 m
Syvdfj-1

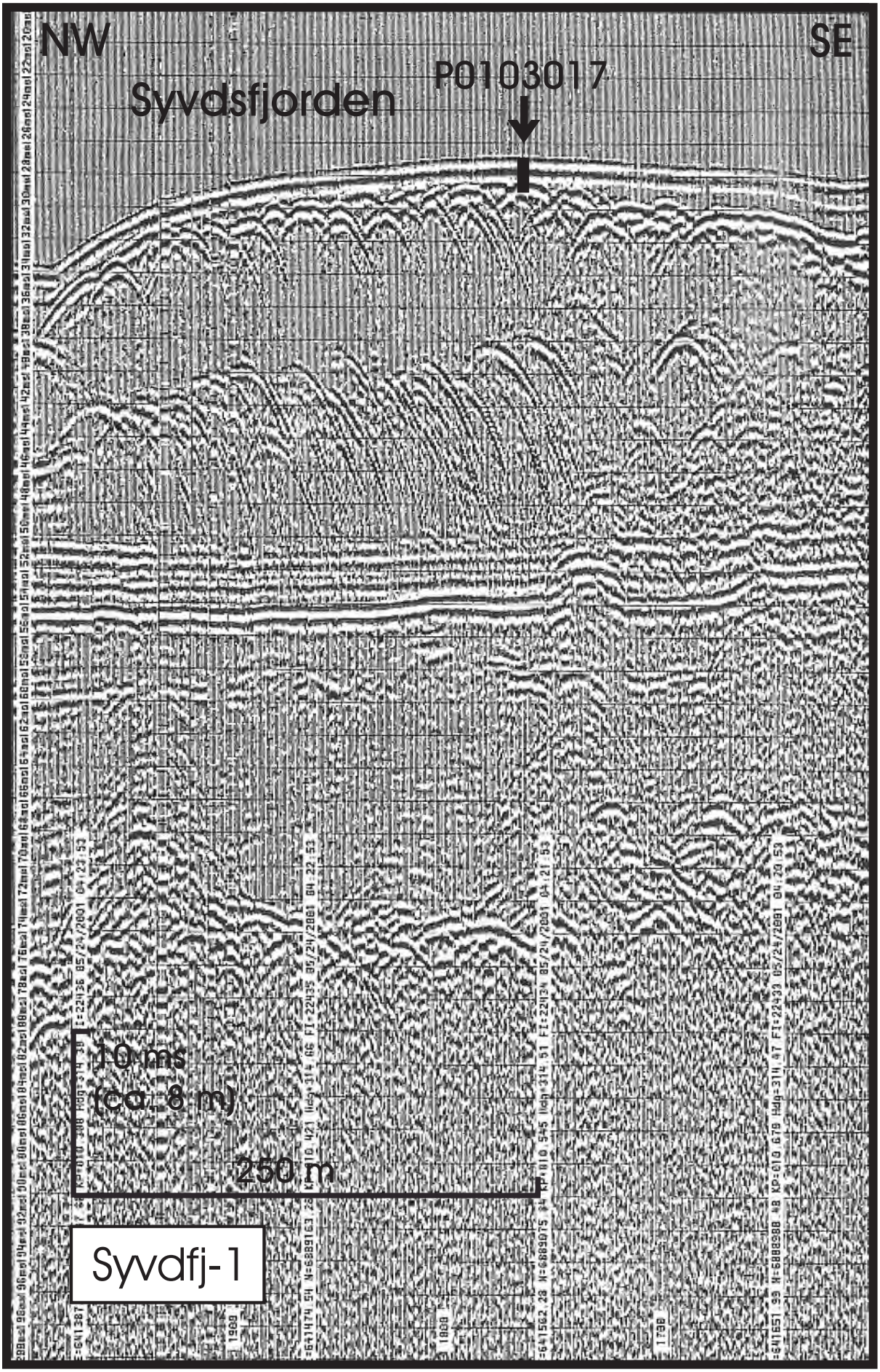
NW
SE
Syvdsfjorden
P0103017
10 ms
(ca. 8 m)
250 m
Syvdfj-1

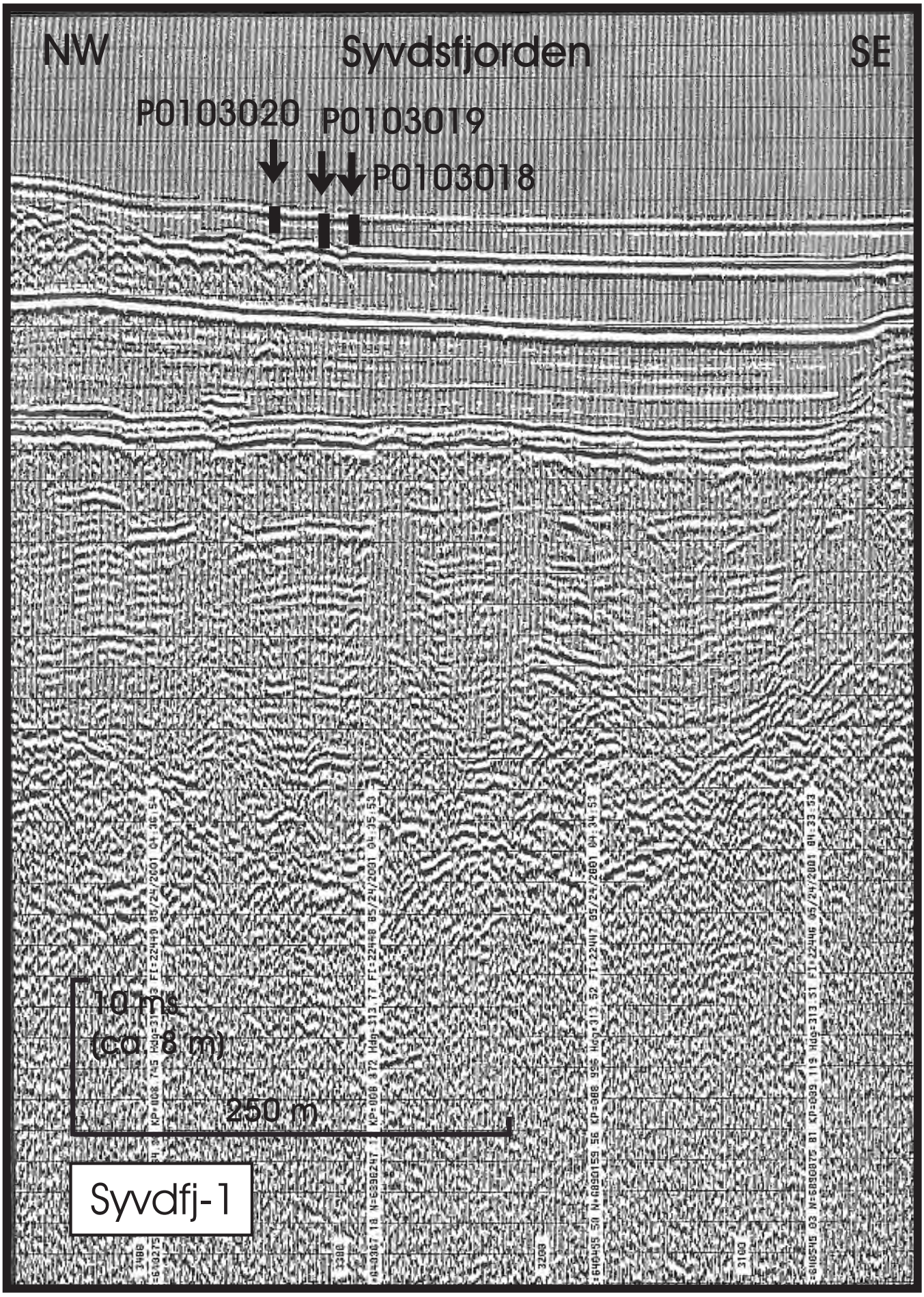
NW
Syvdsfjorden
SE
P0103020
P0103019
P0103018
10 ms
(ca. 8 m)
250 m
Syvdfj-1

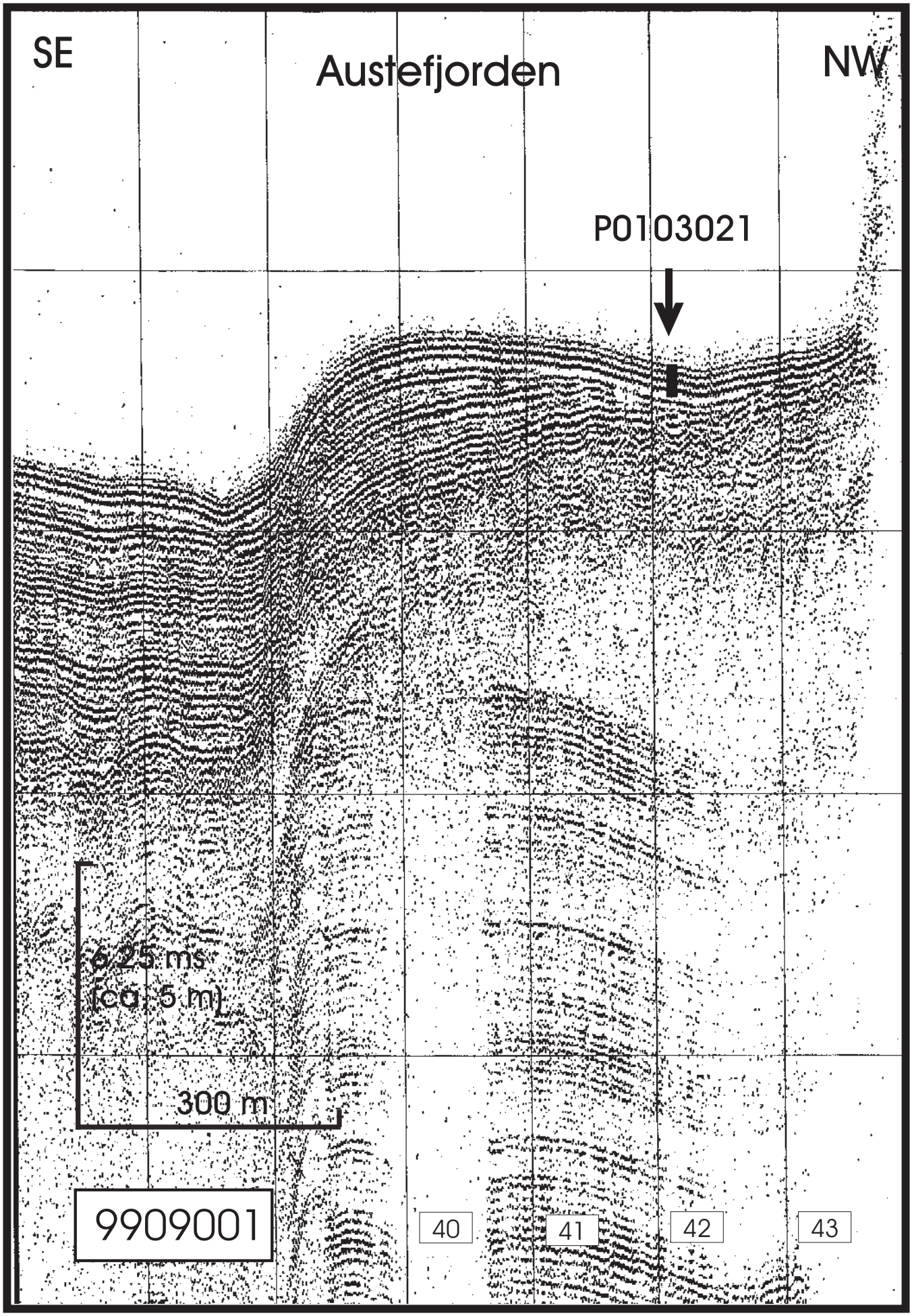
SE
Austefjorden
NW
P0103021
6.25 ms
(ca. 5 m)
300 m
9909001
40
41
42
43

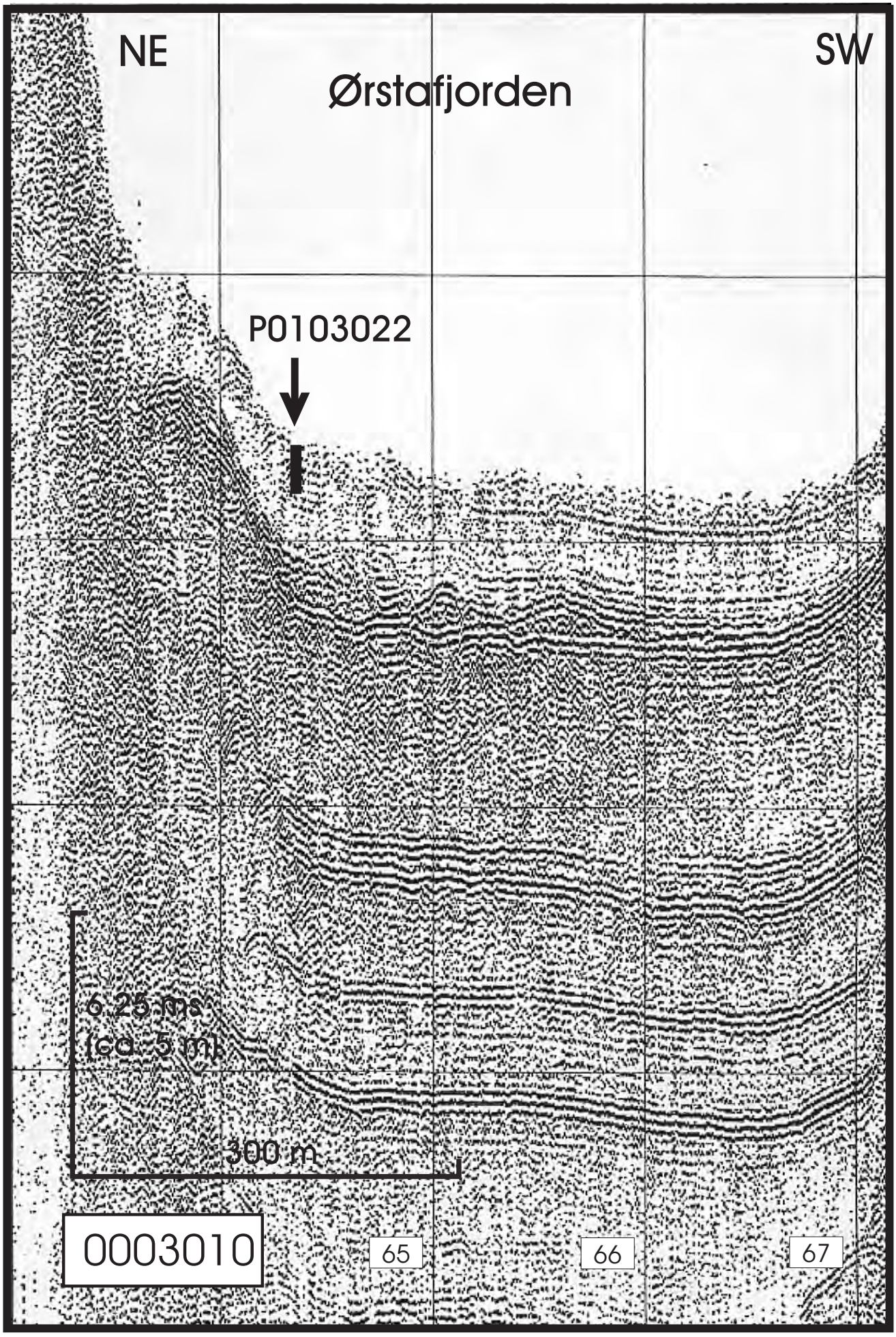
NE
SW
Ørstafjorden
P0103022
6.25 ms
(ca. 5 m)
300 m
0003010
65
66
67

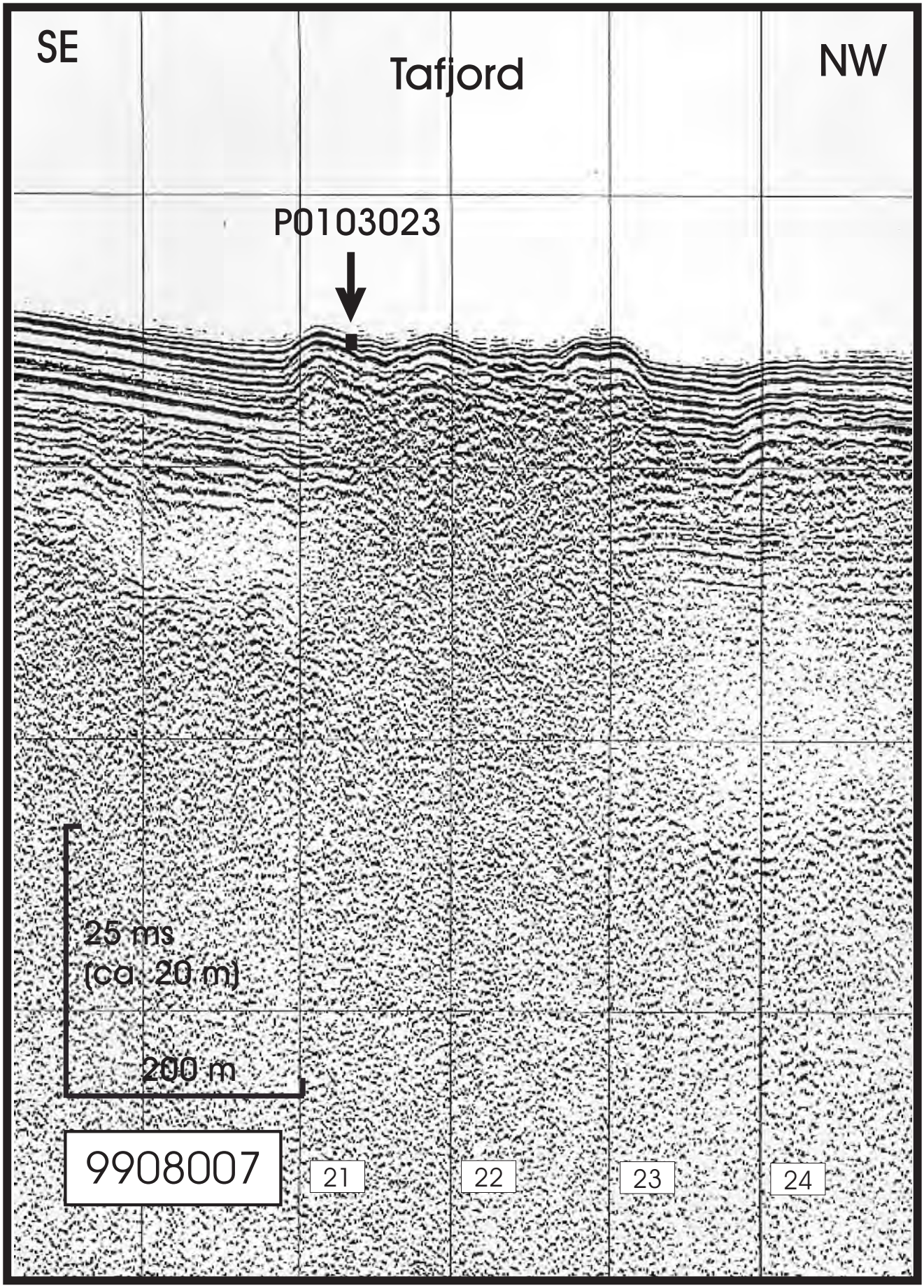
SE
Tafjord
NW
P0103023
25 ms
(ca 20 m)
200 m
9908007
21
22
23
24

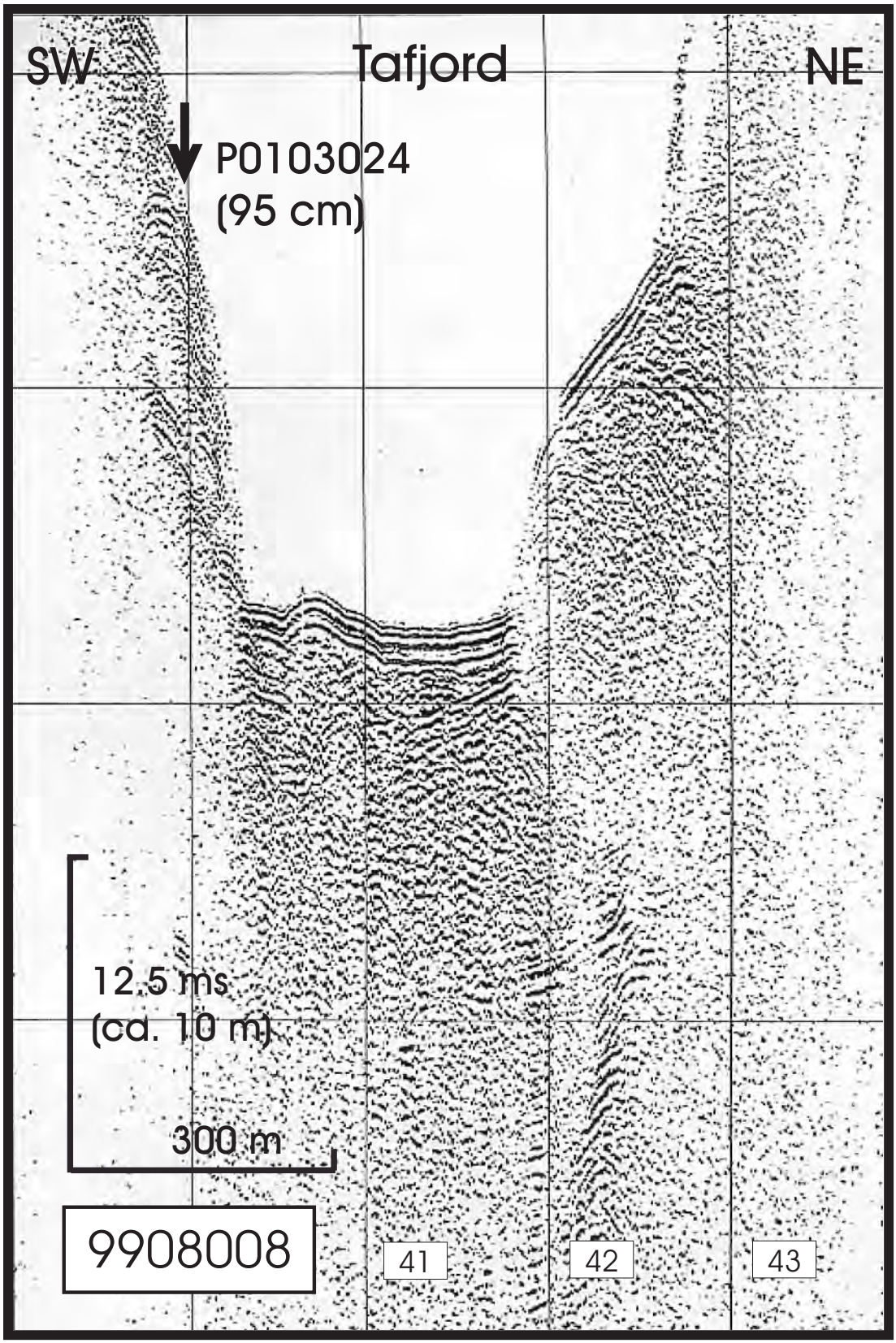
SW
Tafjord
NE
P0103024
(95 cm)
12.5 ms
(ca. 10 m)
300 m
9908008
41
42
43

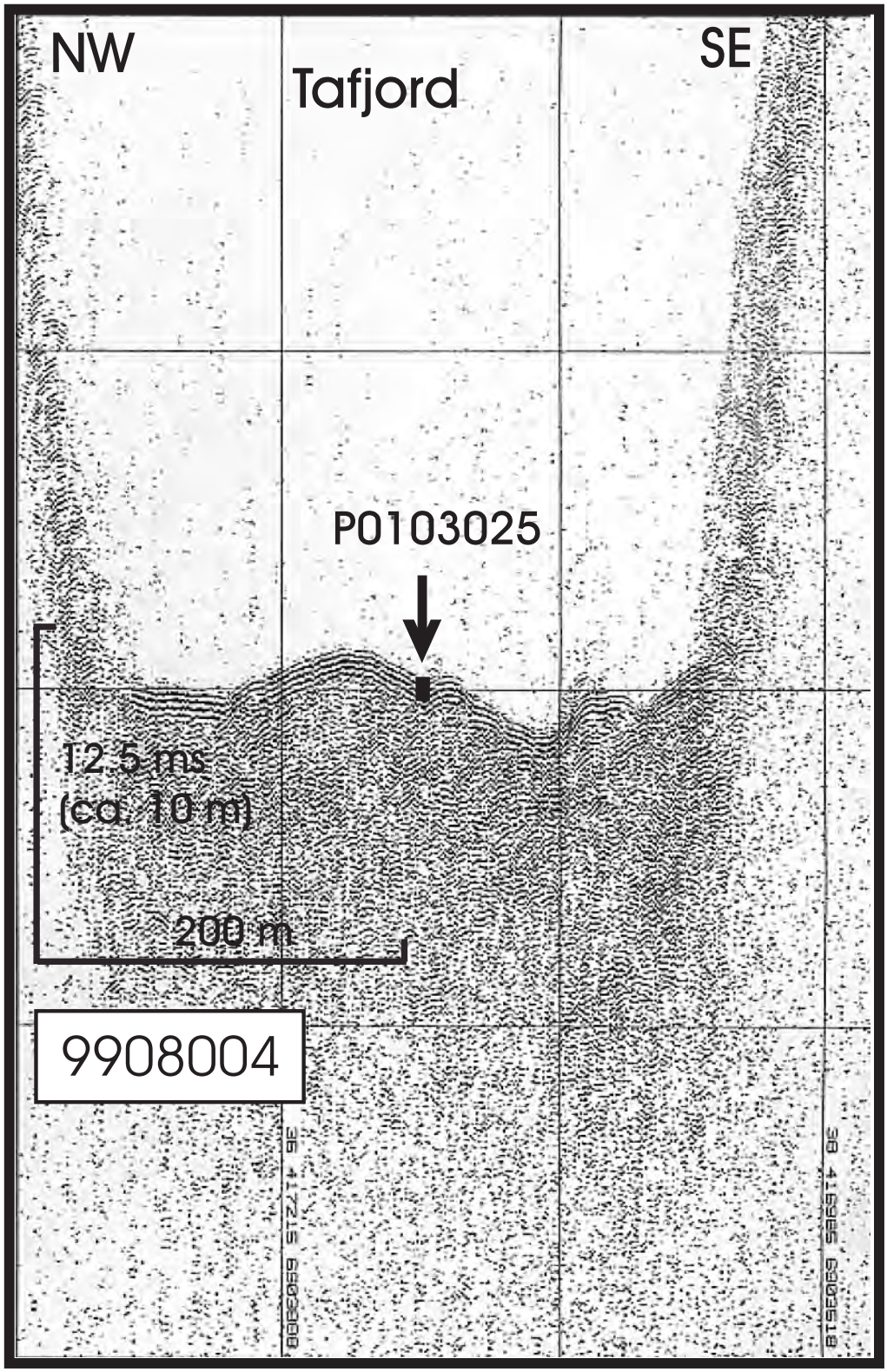
NW
Tafjord
SE
P0103025
T2.5 ms
(ca. 10 m)
200 m
9908004

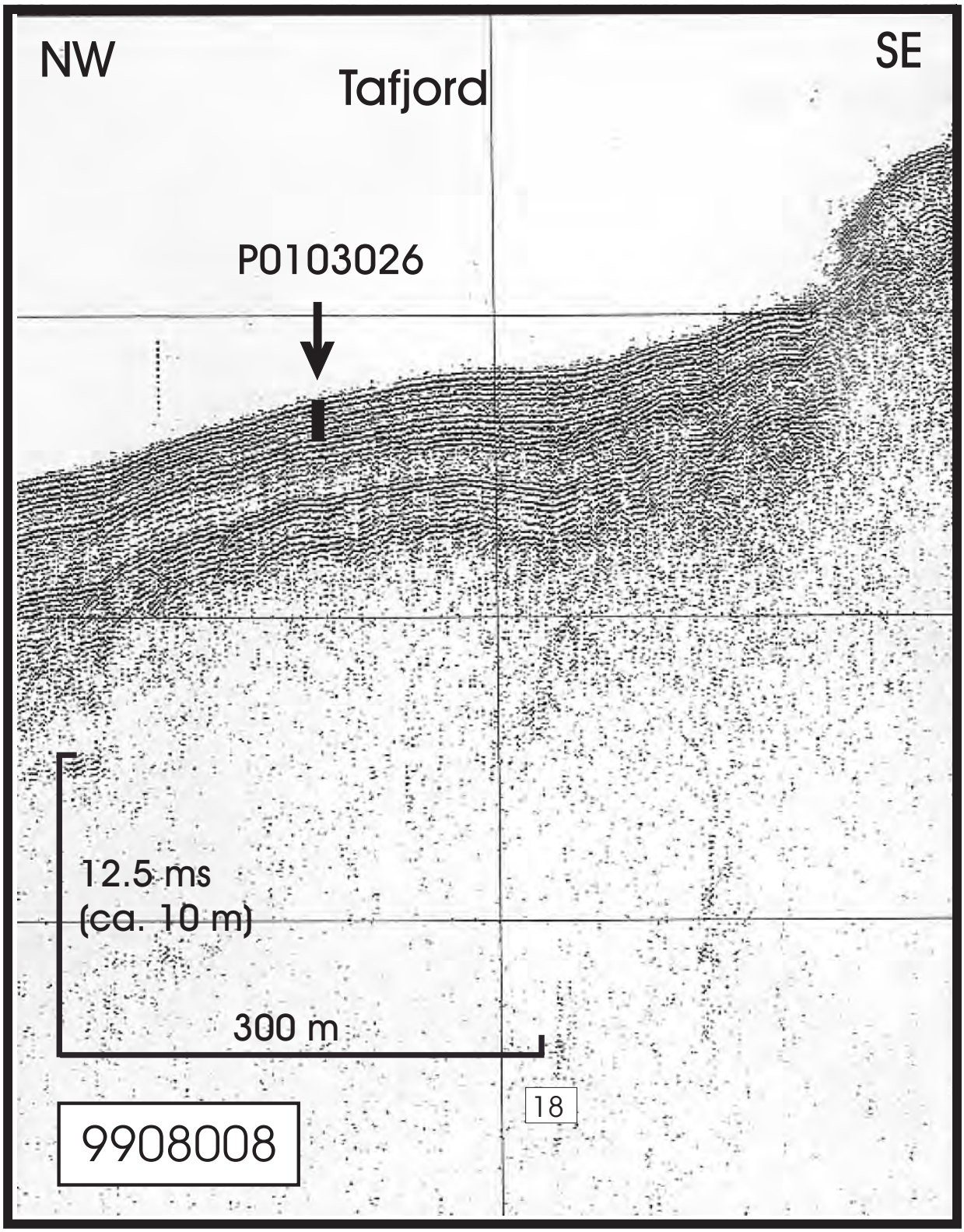
NW
Tafjord
SE
P0103026
12.5 ms
(ca. 10 m)
300 m
18
9908008

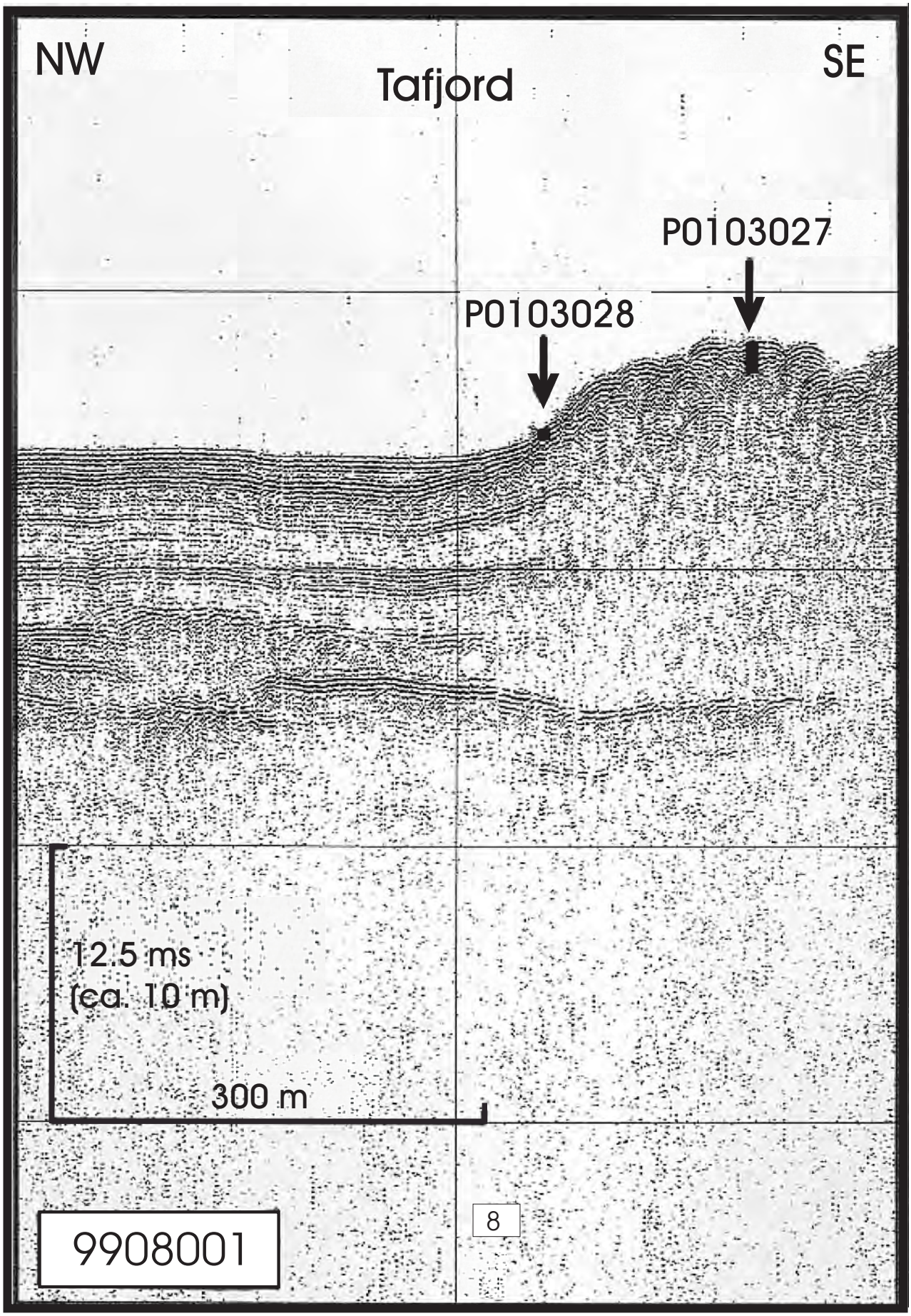
NW
Tafjord
SE
P0103027
P0103028
12.5 ms
(ca. 10 m)
300 m
8
9908001

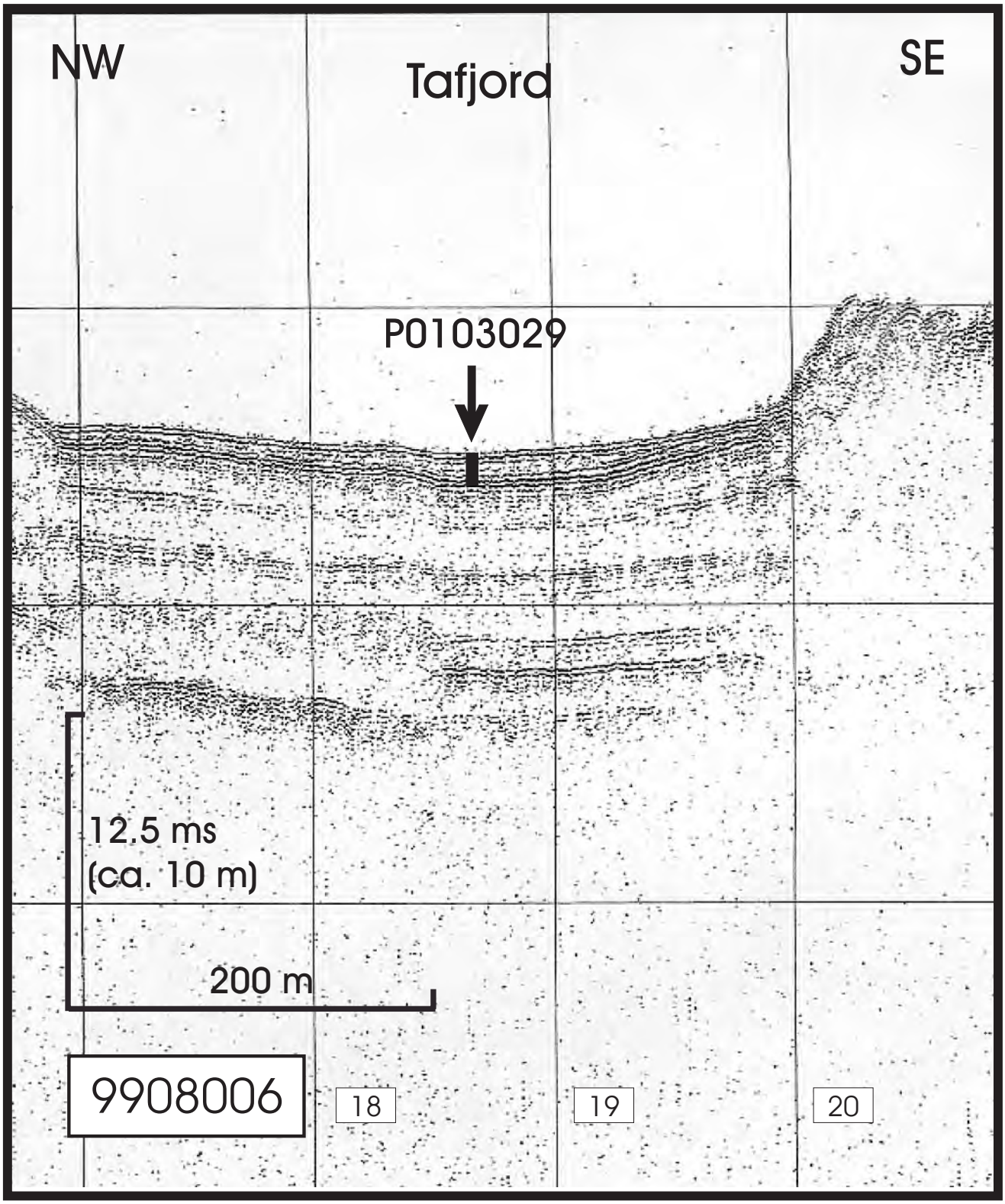
NW
Tafjord
SE
P0103029
12,5 ms
(ca. 10 m)
200 m
9908006
18
19
20

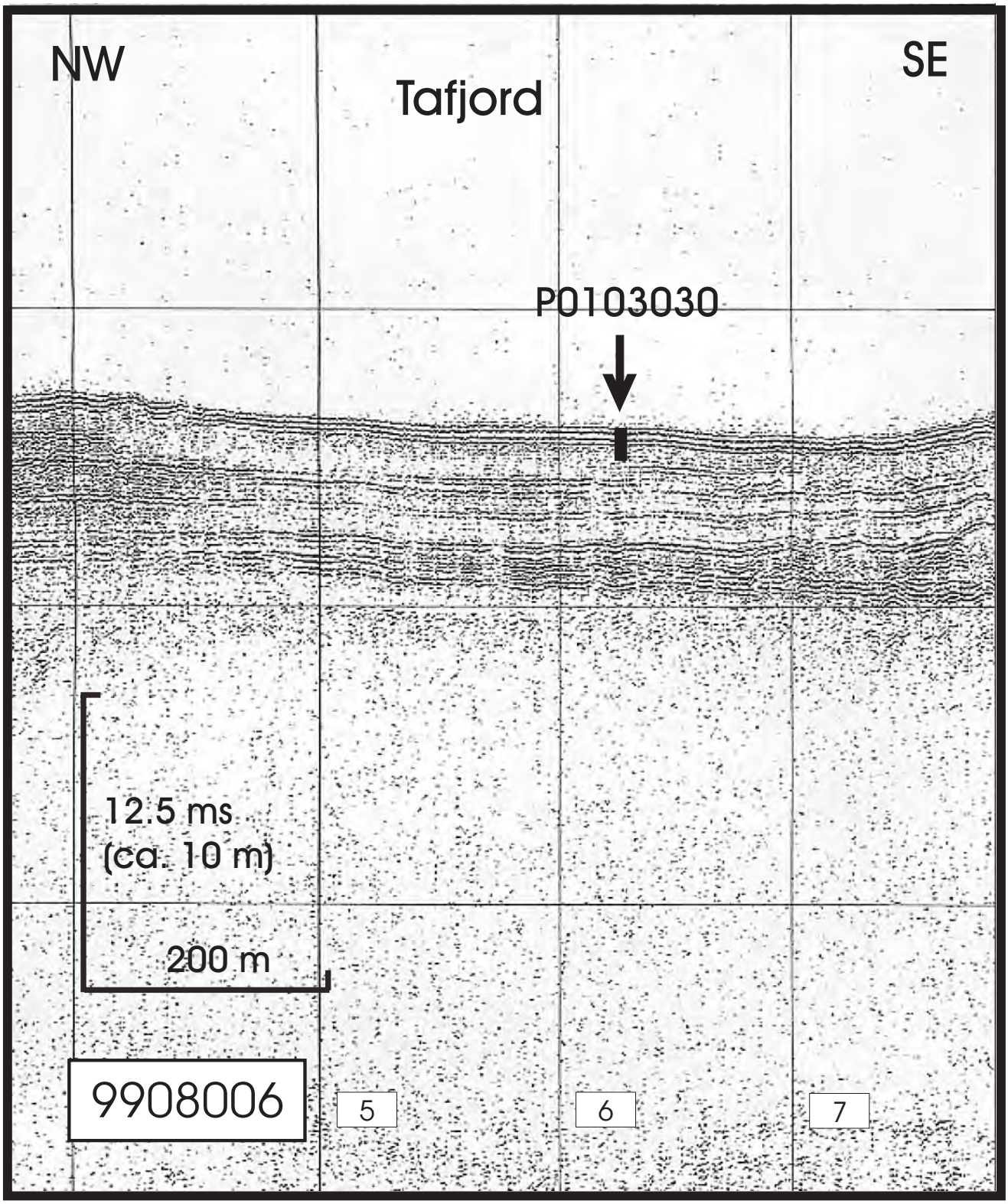
NW
Tafjord
SE
P0103030
12.5 ms
(ca. 10 m)
200 m
9908006
5
6
7

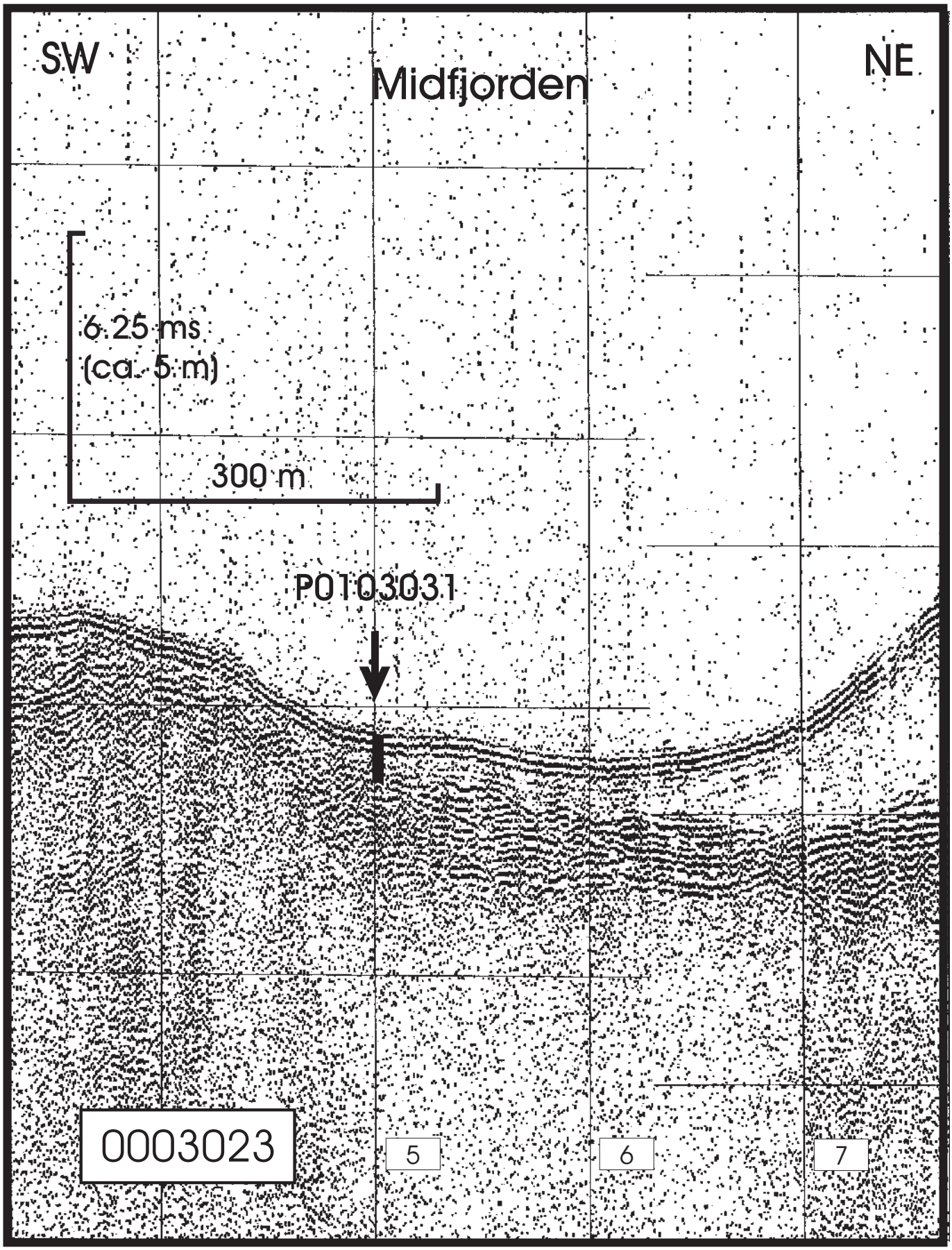
SW
Midfjorden
NE
6.25 ms
(ca. 5 m)
300 m
P0103031
0003023
5
6
7

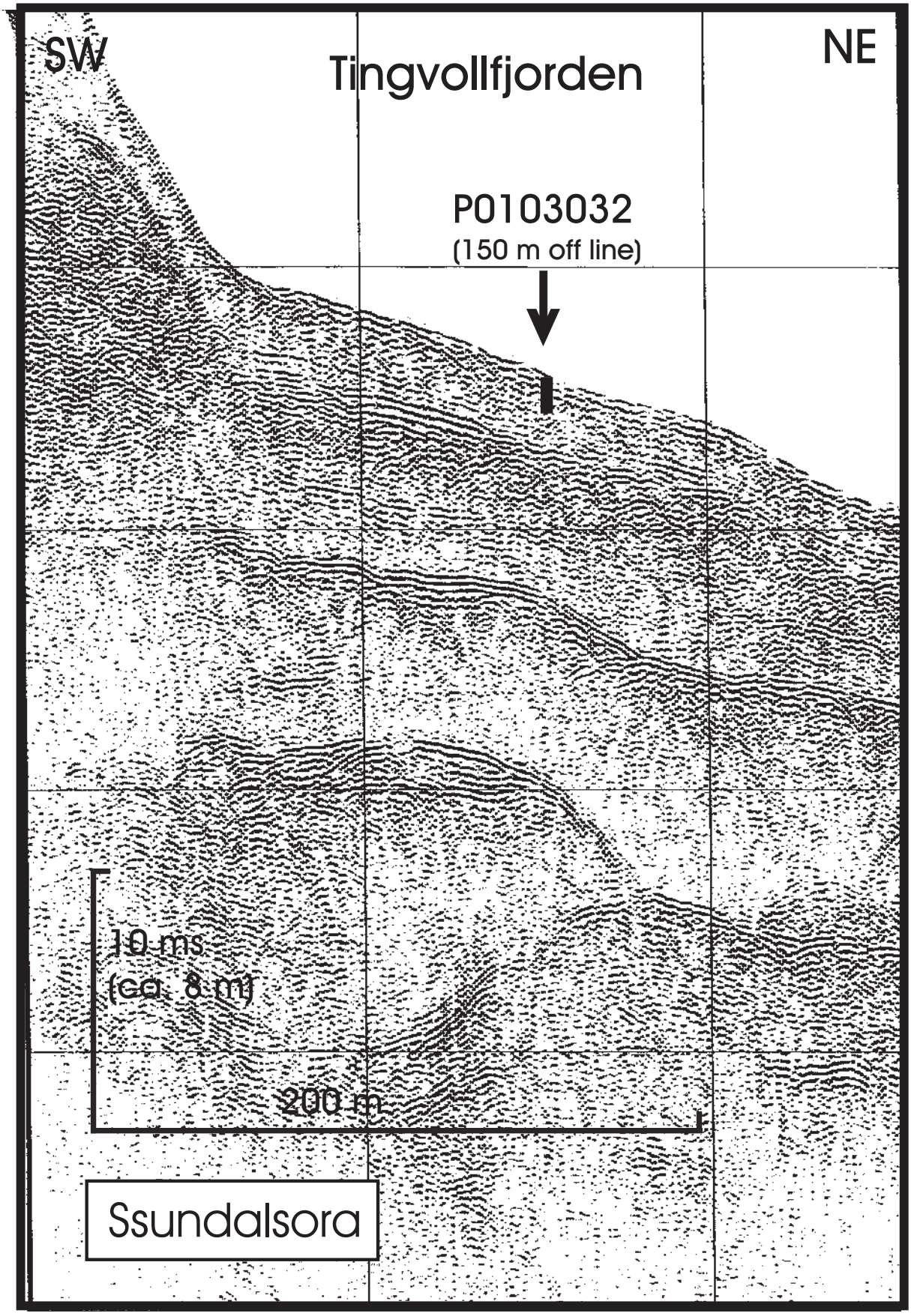
SW
Tingvollfjorden
NE
P0103032
(150 m off line)
10 ms
(ca. 8 m)
200 m
Ssundalsora

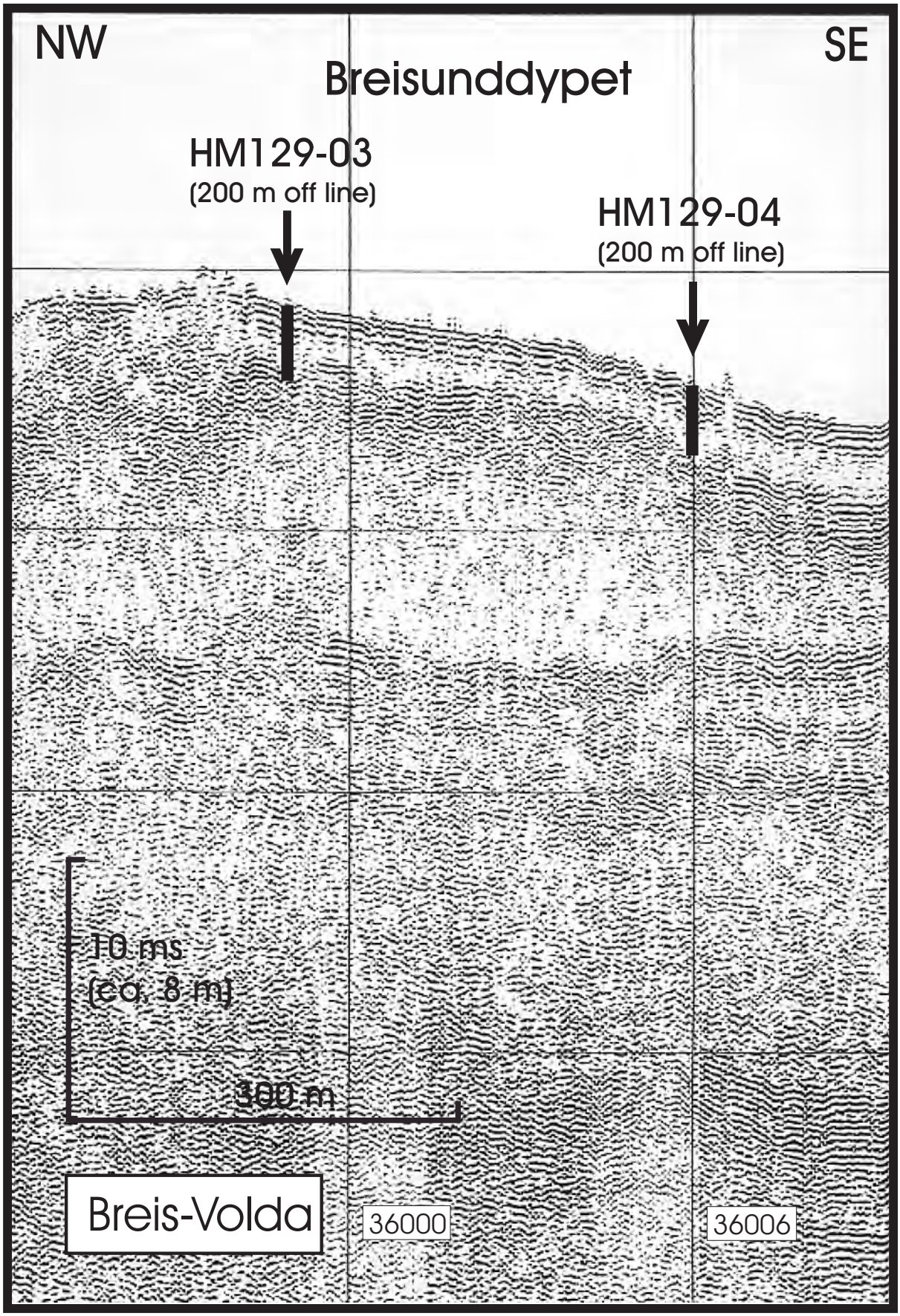
NW
SE
Breisunddypet
HM129-03
(200 m off line)
HM129-04
(200 m off line)
10 ms
(ca. 8 m)
300 m
Breis-Volda
36000
36006

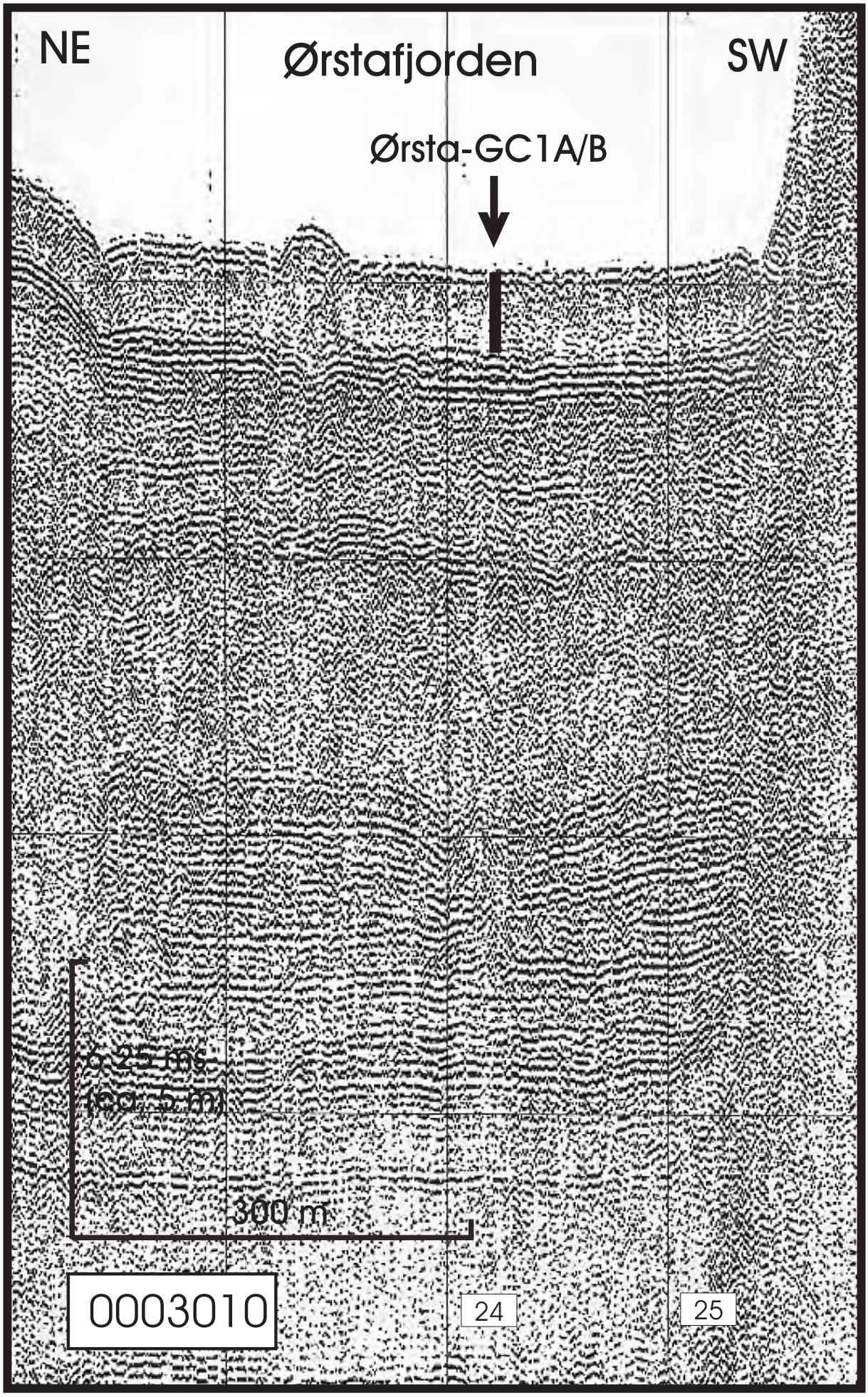
NE
Ørstafjorden
SW
Ørsta-GC1A/B
6.25 ms
(ca. 5 m)
300 m
0003010
24
25

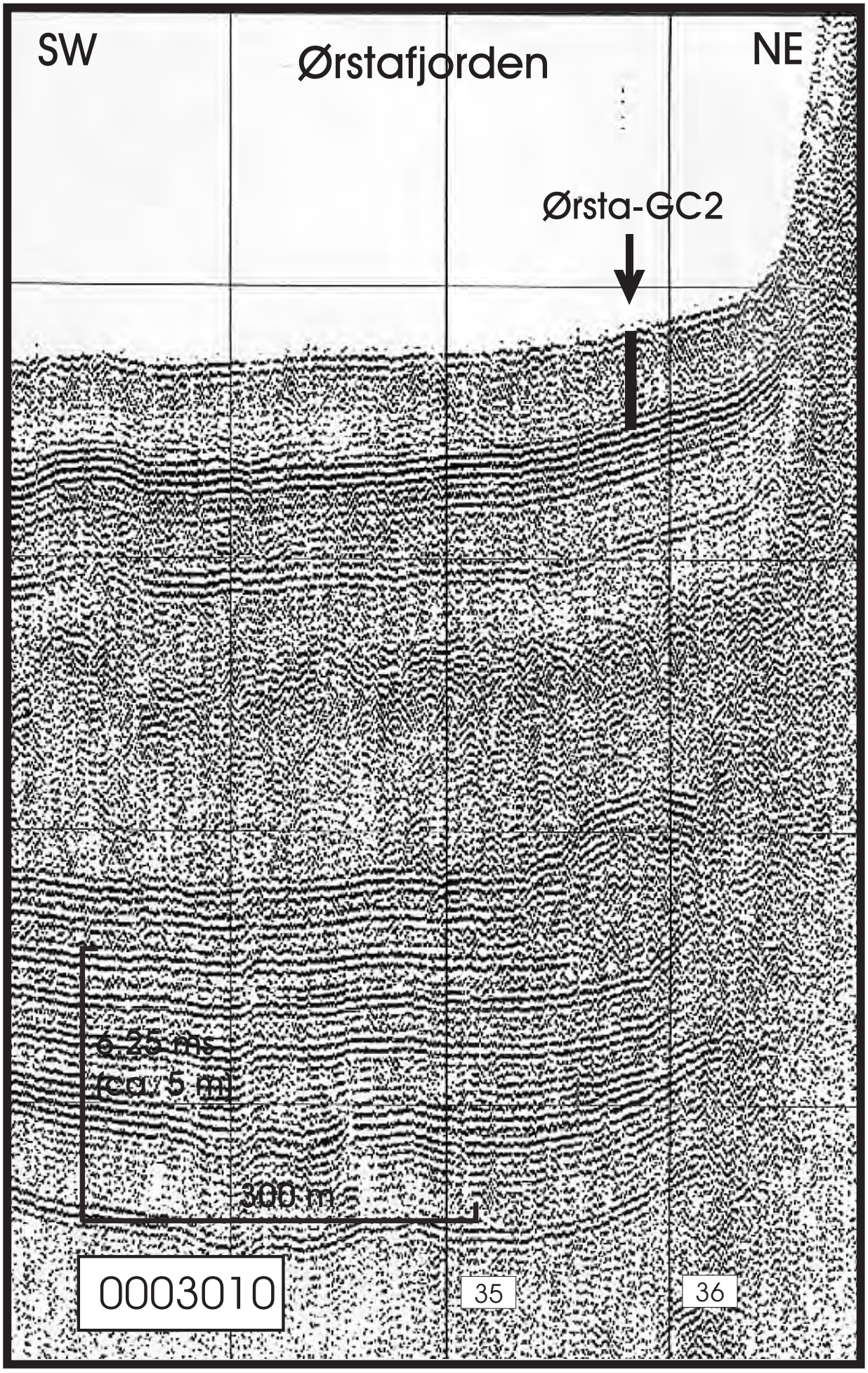
SW
Ørstafjorden
NE
Ørsta-GC2
ó 25 ms
(ca. 5 m)
300 m
0003010
35
36

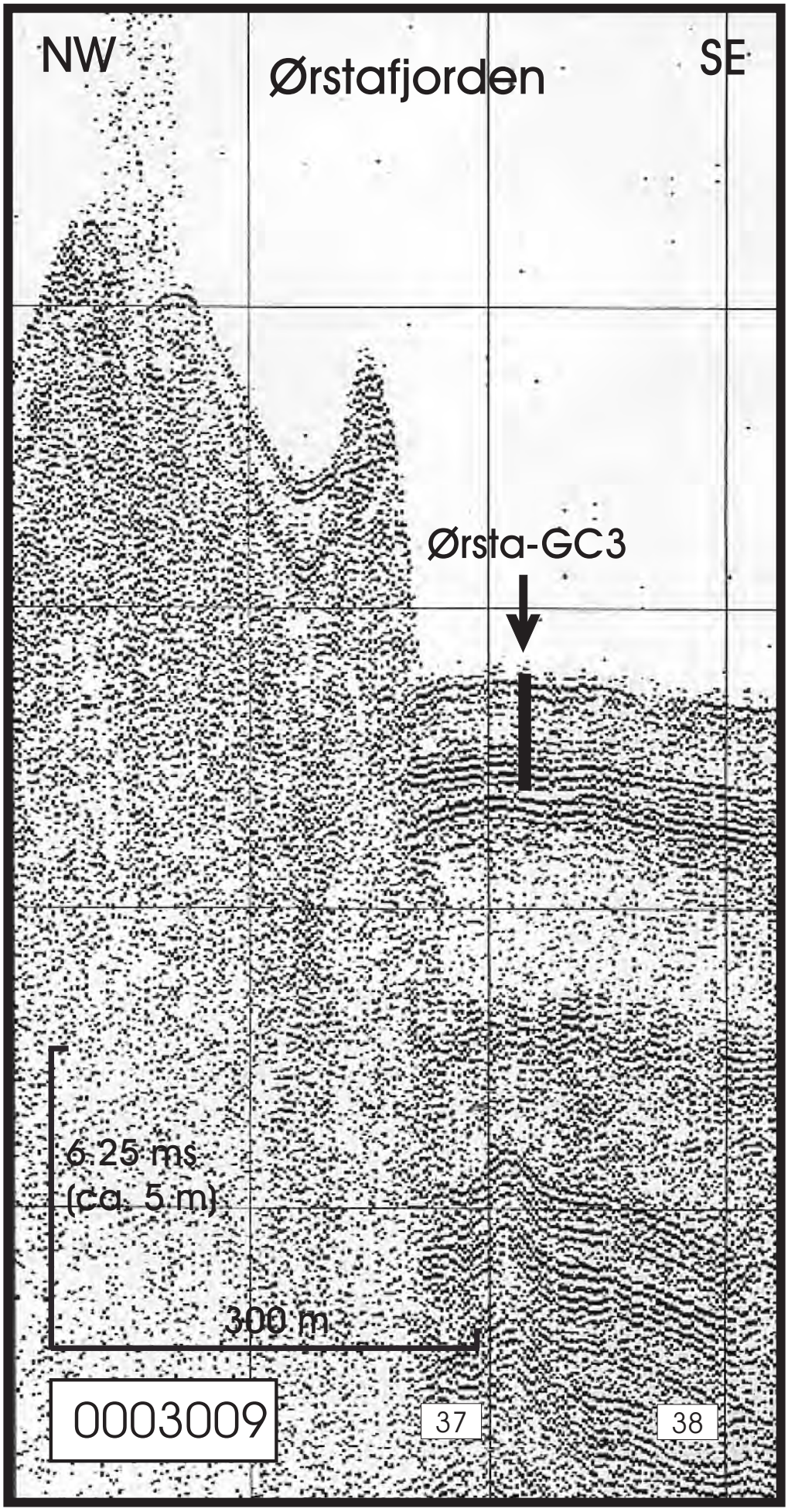
NW
Ørstafjorden
SE
Ørsta-GC3
6.25 ms
(ca. 5 m)
300 m
0003009
37
38

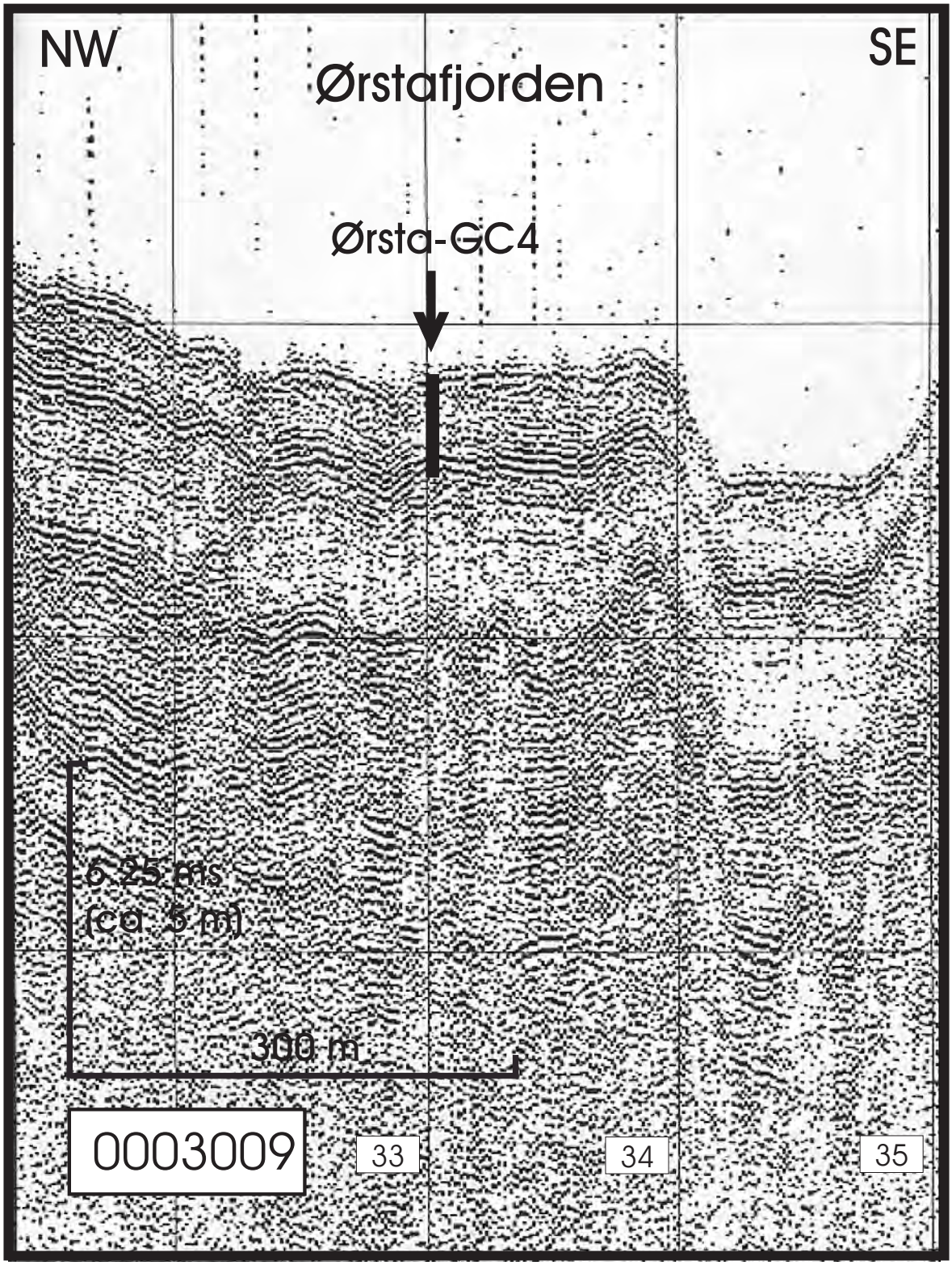
NW
SE
Ørstafjorden
Ørsta-GC4
6.25 ms
(ca. 5 m)
300 m
0003009
33
34
35

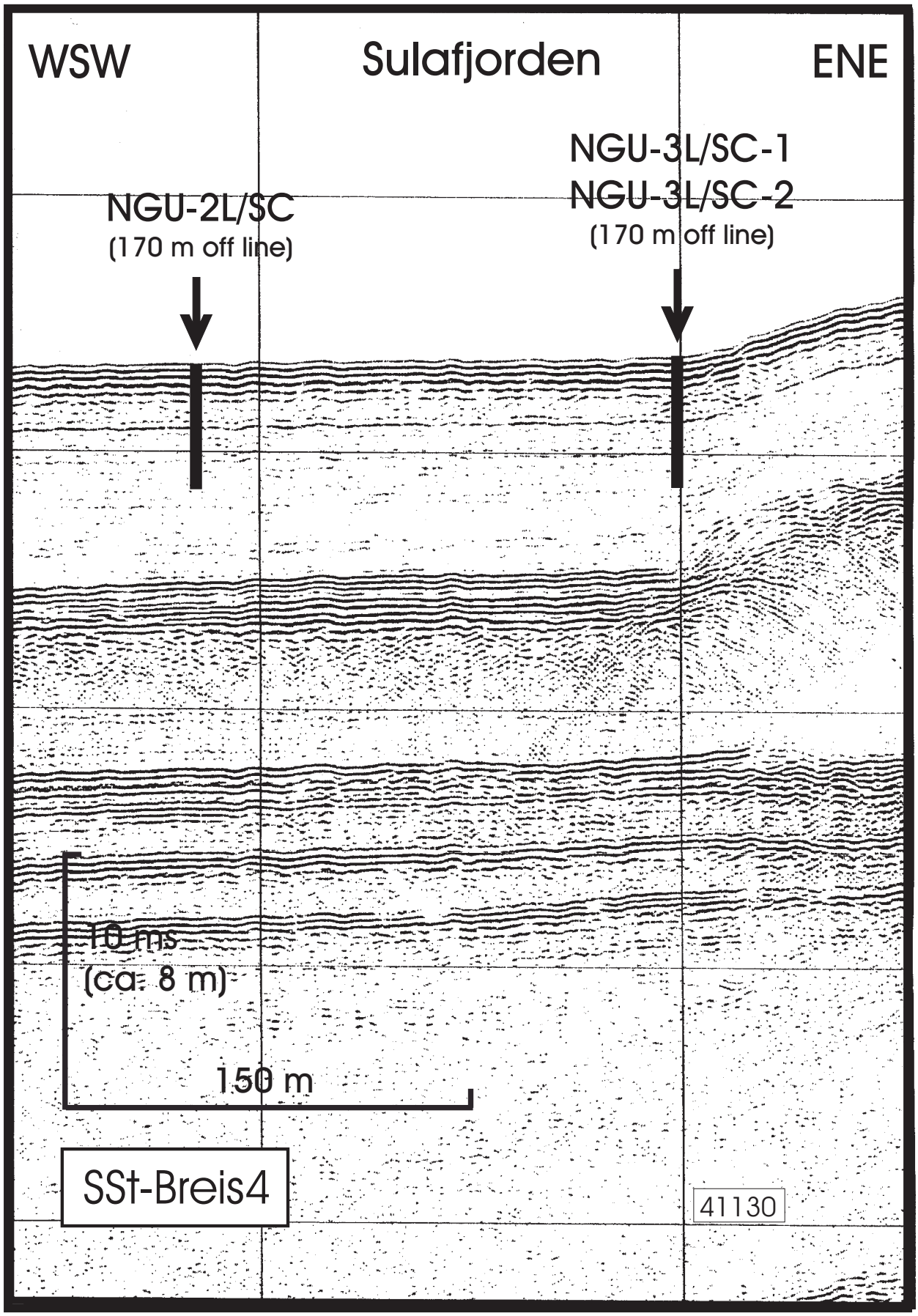
WSW
Sulafjorden
ENE
NGU-3L/SC-1
NGU-3L/SC-2
(170 m off line)
NGU-2L/SC
(170 m off line)
10 ms
(ca. 8 m)
150 m
SSt-Breis4
41130

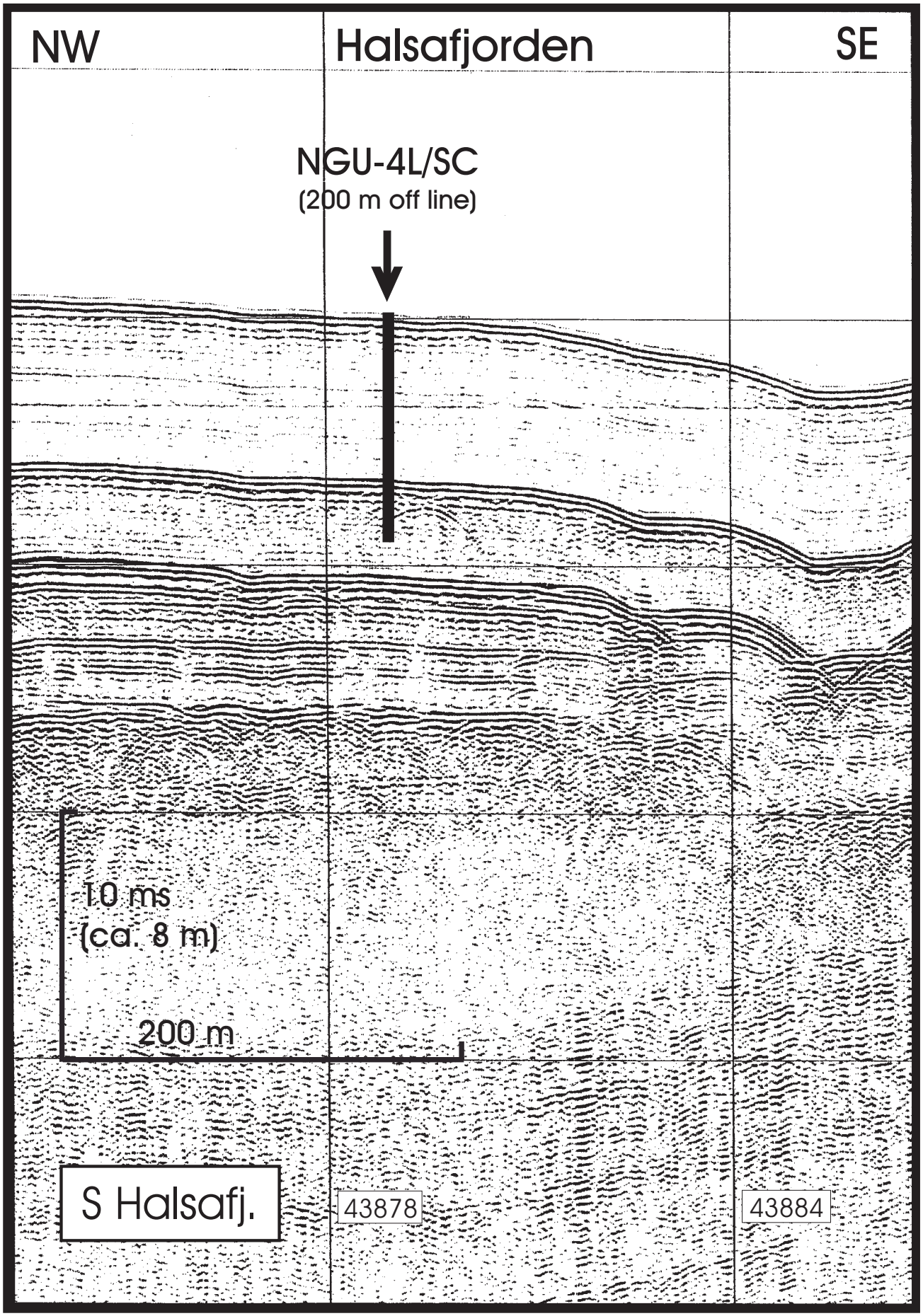
NW
Halsafjorden
SE
NGU-4L/SC
(200 m off line)
10 ms
(ca. 8 m)
200 m
S Halsafj.
43878
43884

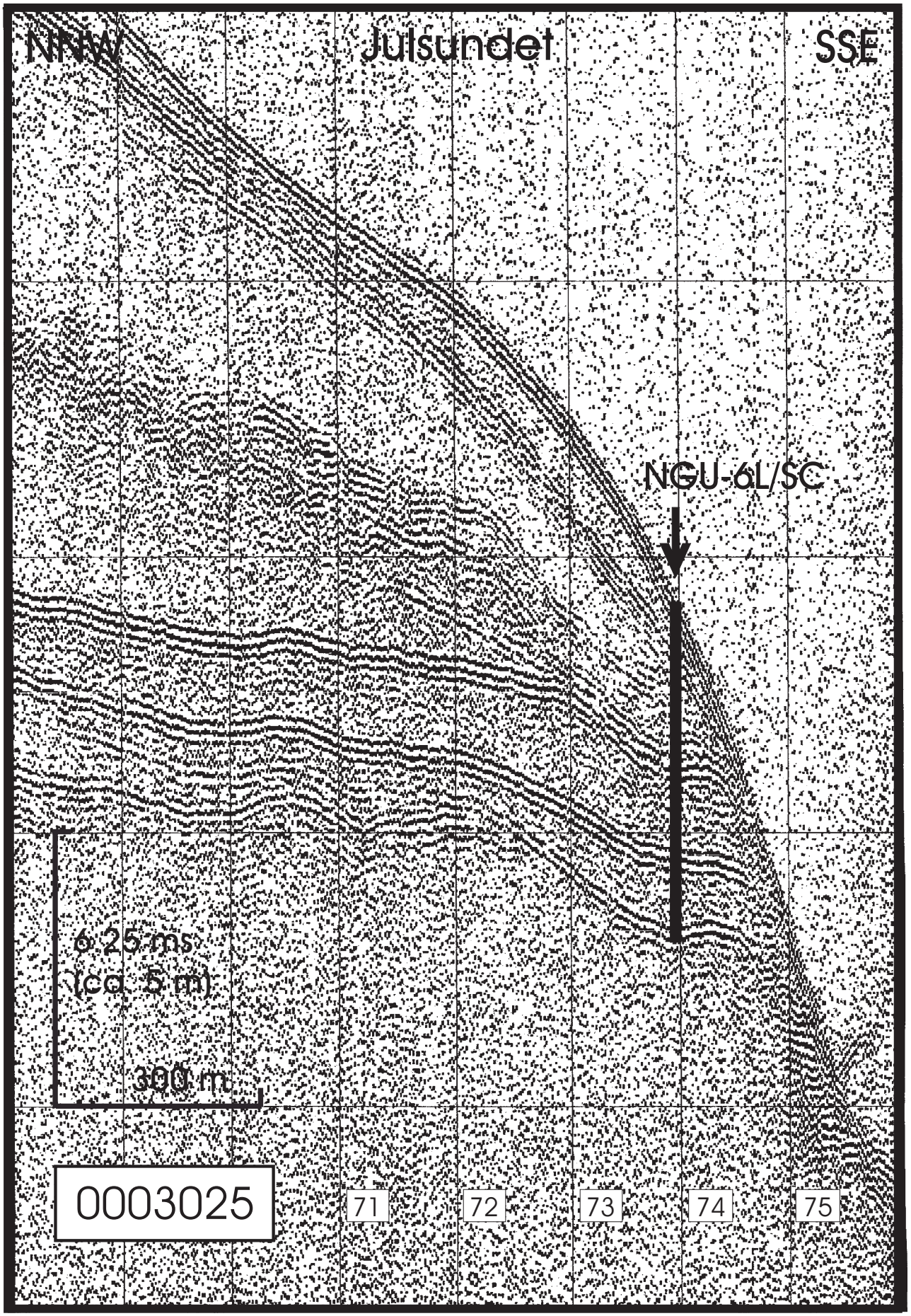
NNW
Julsundet
SSE
NGU-6L/SC
6.25 ms
(ca. 5 m)
300 m
0003025
71
72
73
74
75

APPENDIX 2

Stratigraphic profiles of sediment density, magnetic susceptibility and X-ray images (XRI) of fjord cores

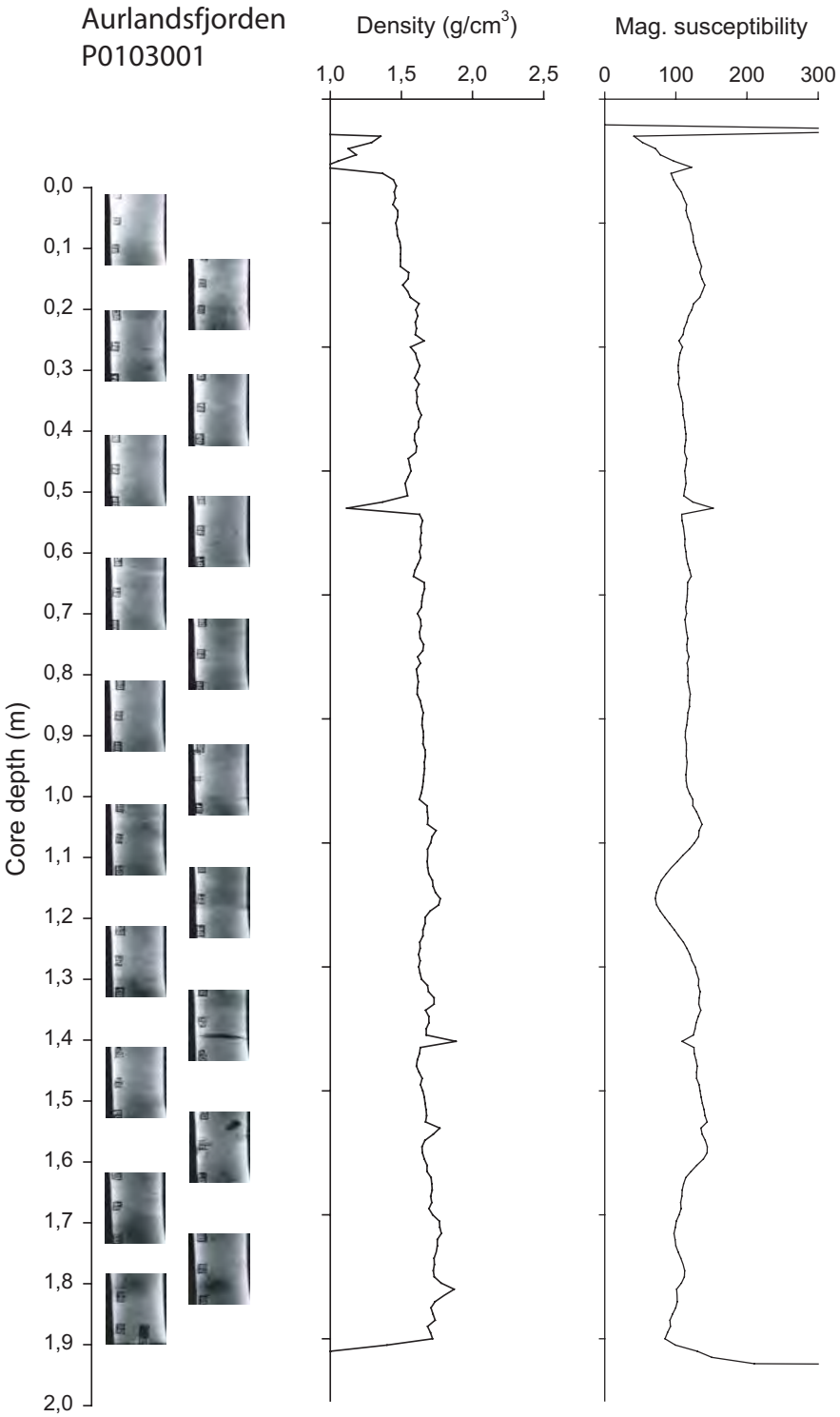
Aurlandsfjorden
P0103001
Density (g/cm3)
Mag. susceptibility
1,0
1,5
2,0
2,5
0
100
200
300
Core depth (m)
0,0
0,1
0,2
0,3
0,4
0,5
0,6
0,7
0,8
0,9
1,0
1,1
1,2
1,3
1,4
1,5
1,6
1,7
1,8
1,9
2,0

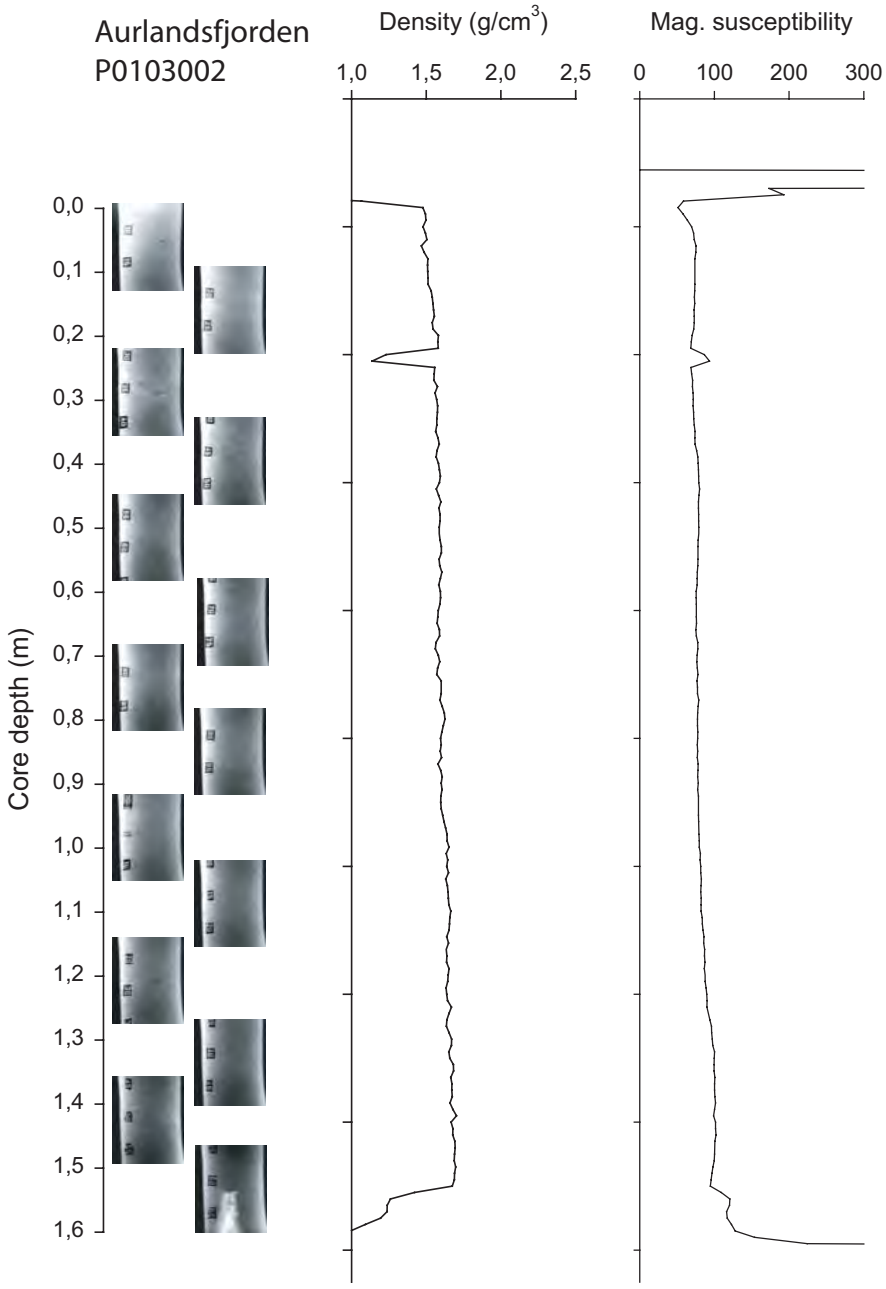
Aurlandsfjorden
P0103002
Density (g/cm3)
1,0
1,5
2,0
2,5
Mag. susceptibility
0
100
200
300
Core depth (m)
0,0
0,1
0,2
0,3
0,4
0,5
0,6
0,7
0,8
0,9
1,0
1,1
1,2
1,3
1,4
1,5
1,6

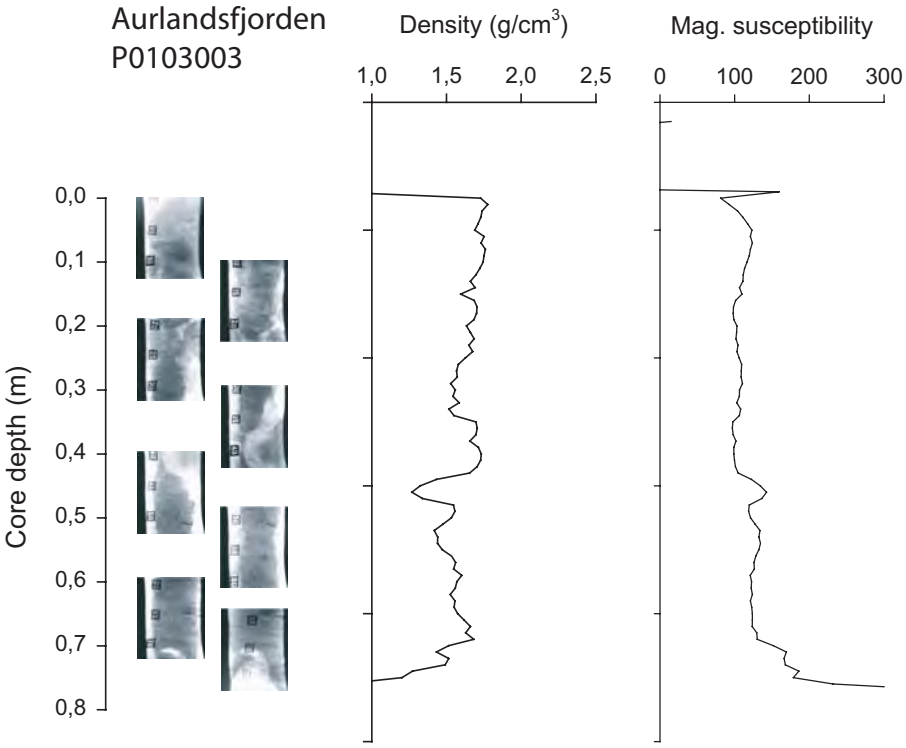
Aurlandsfjorden
P0103003
Density (g/cm3)
Mag. susceptibility
1,0
1,5
2,0
2,5
0
100
200
300
Core depth (m)
0,0
0,1
0,2
0,3
0,4
0,5
0,6
0,7
0,8

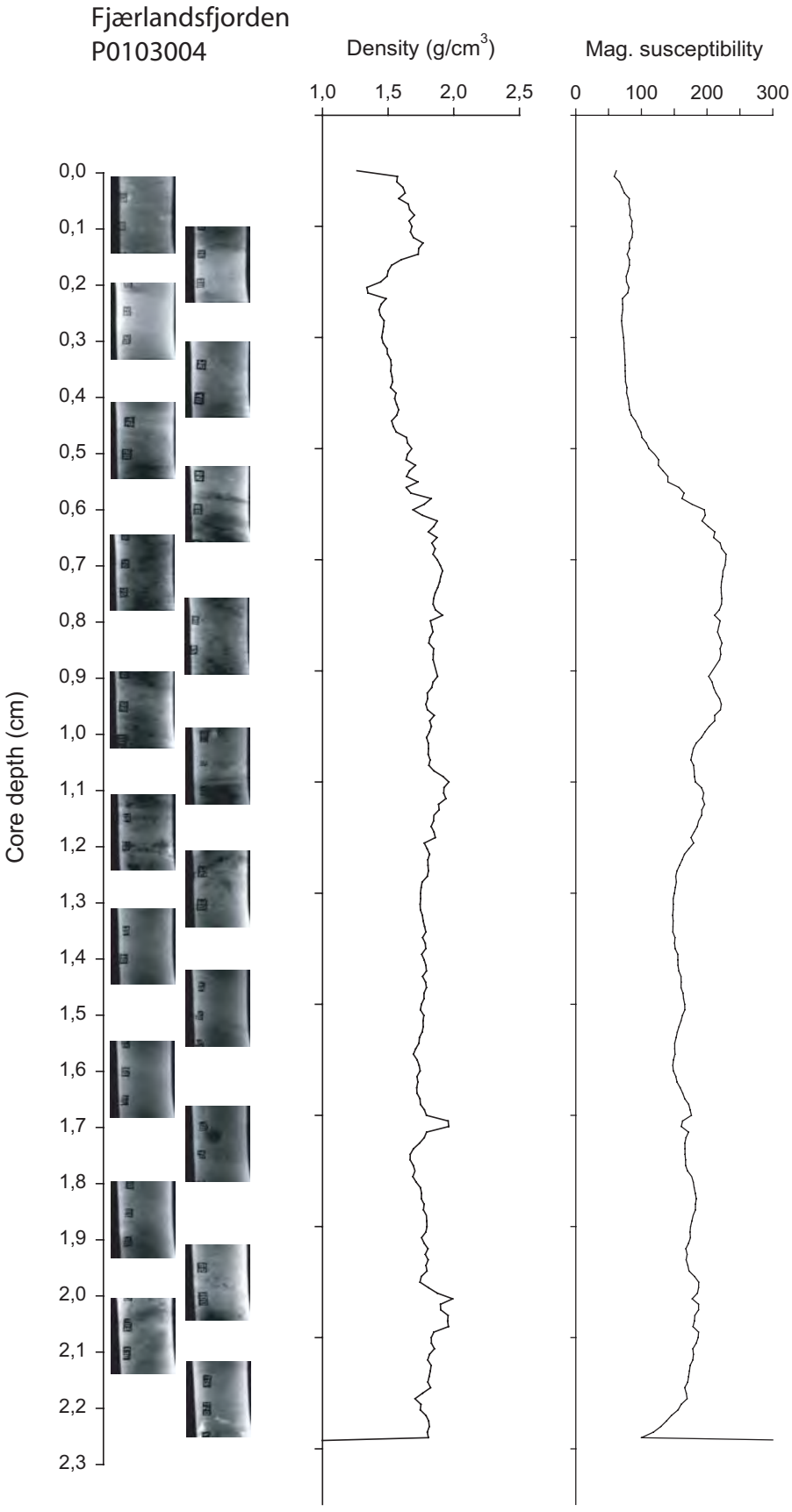
Fjærlandsfjorden
P0103004
Density (g/cm3)
Mag. susceptibility
1,0
1,5
2,0
2,5
0
100
200
300
Core depth (cm)
0,0
0,1
0,2
0,3
0,4
0,5
0,6
0,7
0,8
0,9
1,0
1,1
1,2
1,3
1,4
1,5
1,6
1,7
1,8
1,9
2,0
2,1
2,2
2,3

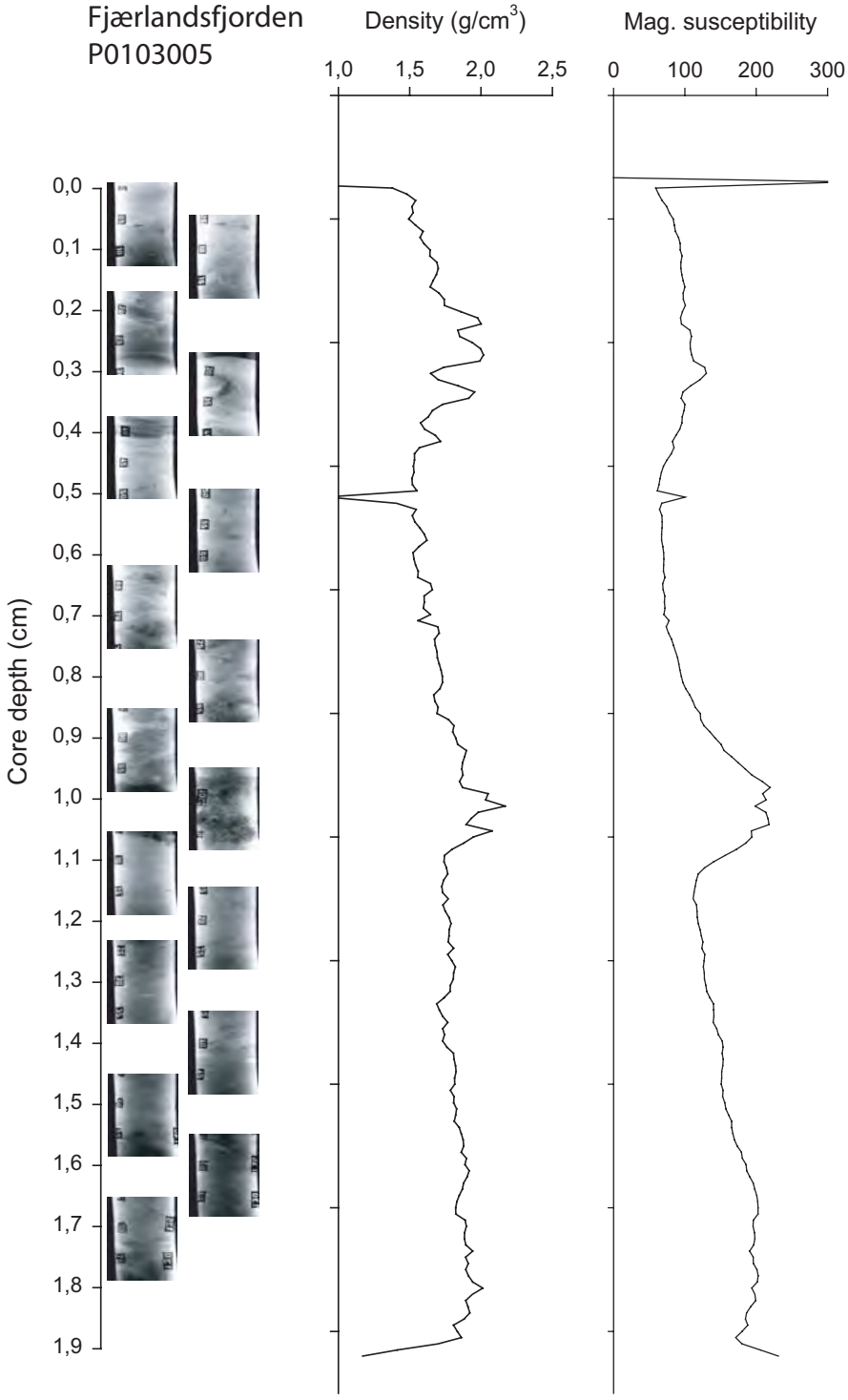
Fjærlandsfjorden
P0103005
Density (g/cm3)
1,0
1,5
2,0
2,5
Mag. susceptibility
0
100
200
300
Core depth (cm)
0,0
0,1
0,2
0,3
0,4
0,5
0,6
0,7
0,8
0,9
1,0
1,1
1,2
1,3
1,4
1,5
1,6
1,7
1,8
1,9

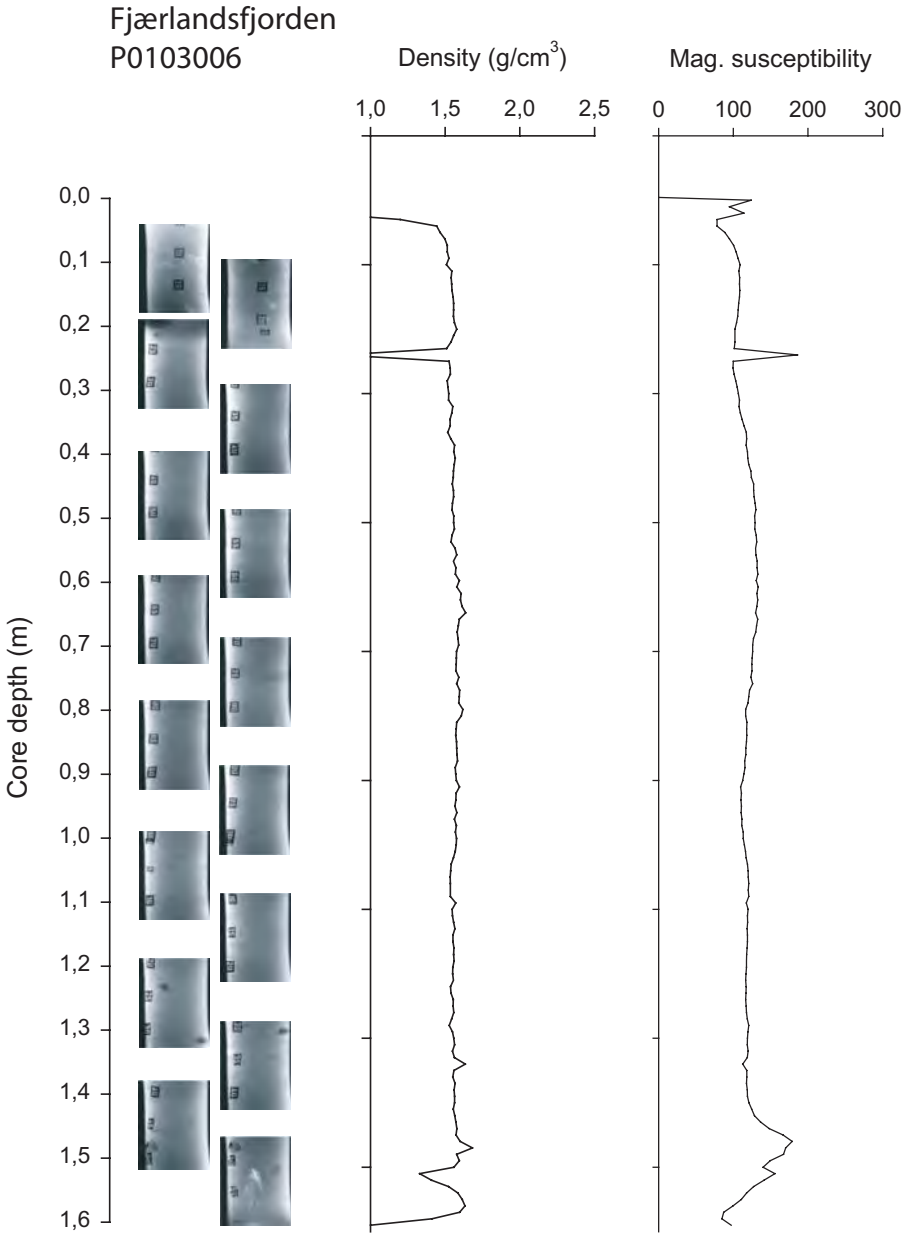
Fjærlandsfjorden
P0103006
Density (g/cm3)
Mag. susceptibility
1,0
1,5
2,0
2,5
0
100
200
300
Core depth (m)
0,0
0,1
0,2
0,3
0,4
0,5
0,6
0,7
0,8
0,9
1,0
1,1
1,2
1,3
1,4
1,5
1,6

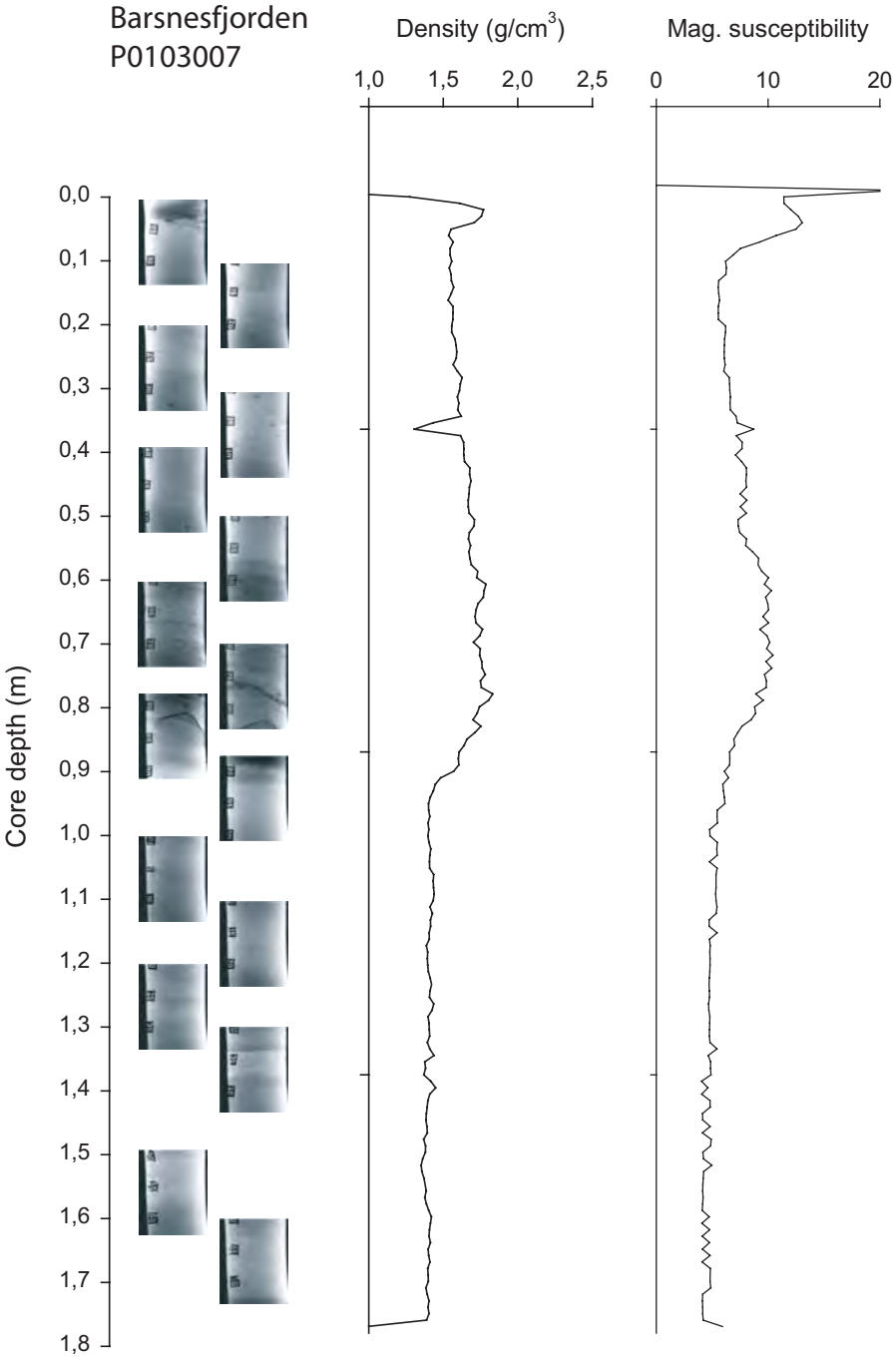
Barsnesfjorden
P0103007
Density (g/cm3)
Mag. susceptibility
1,0
1,5
2,0
2,5
0
10
20
Core depth (m)
0,0
0,1
0,2
0,3
0,4
0,5
0,6
0,7
0,8
0,9
1,0
1,1
1,2
1,3
1,4
1,5
1,6
1,7
1,8

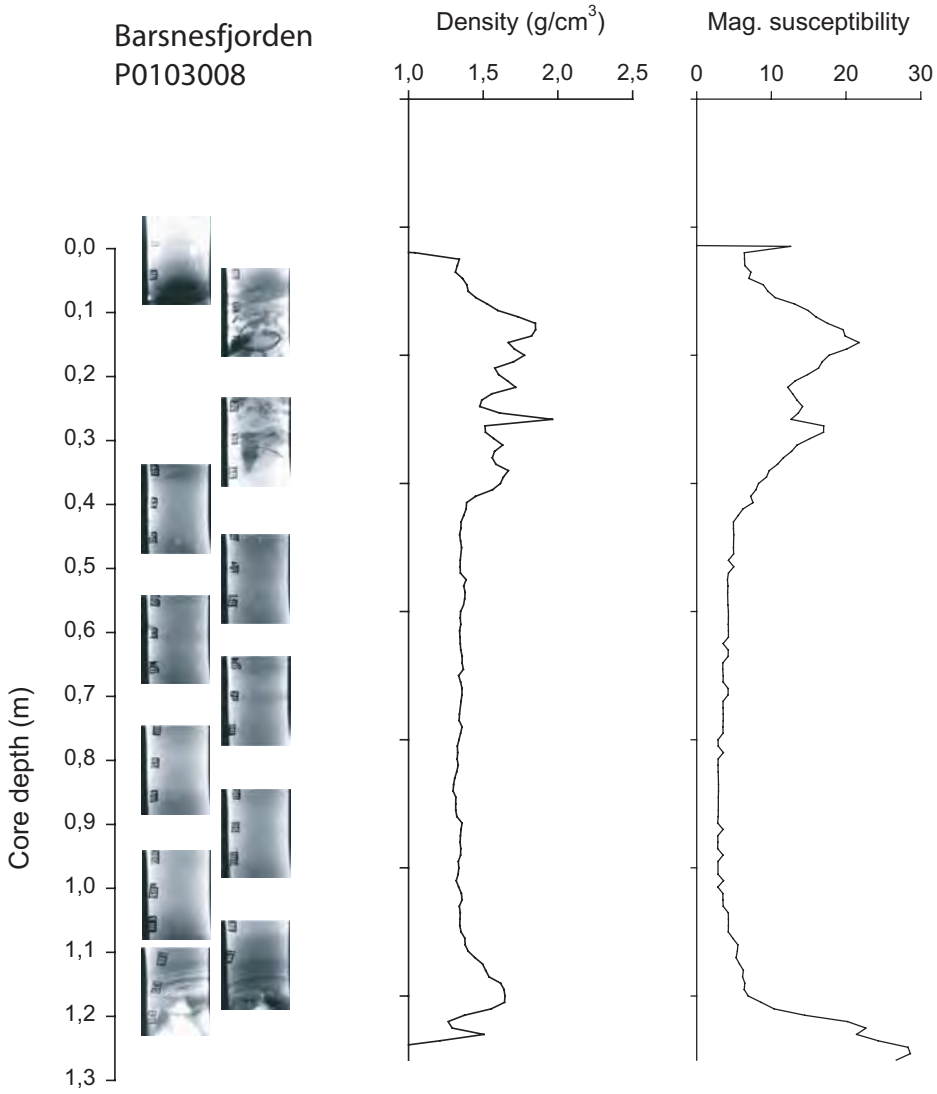
Barsnesfjorden
P0103008
Density (g/cm3)
Mag. susceptibility
1,0
1,5
2,0
2,5
0
10
20
30
Core depth (m)
0,0
0,1
0,2
0,3
0,4
0,5
0,6
0,7
0,8
0,9
1,0
1,1
1,2
1,3

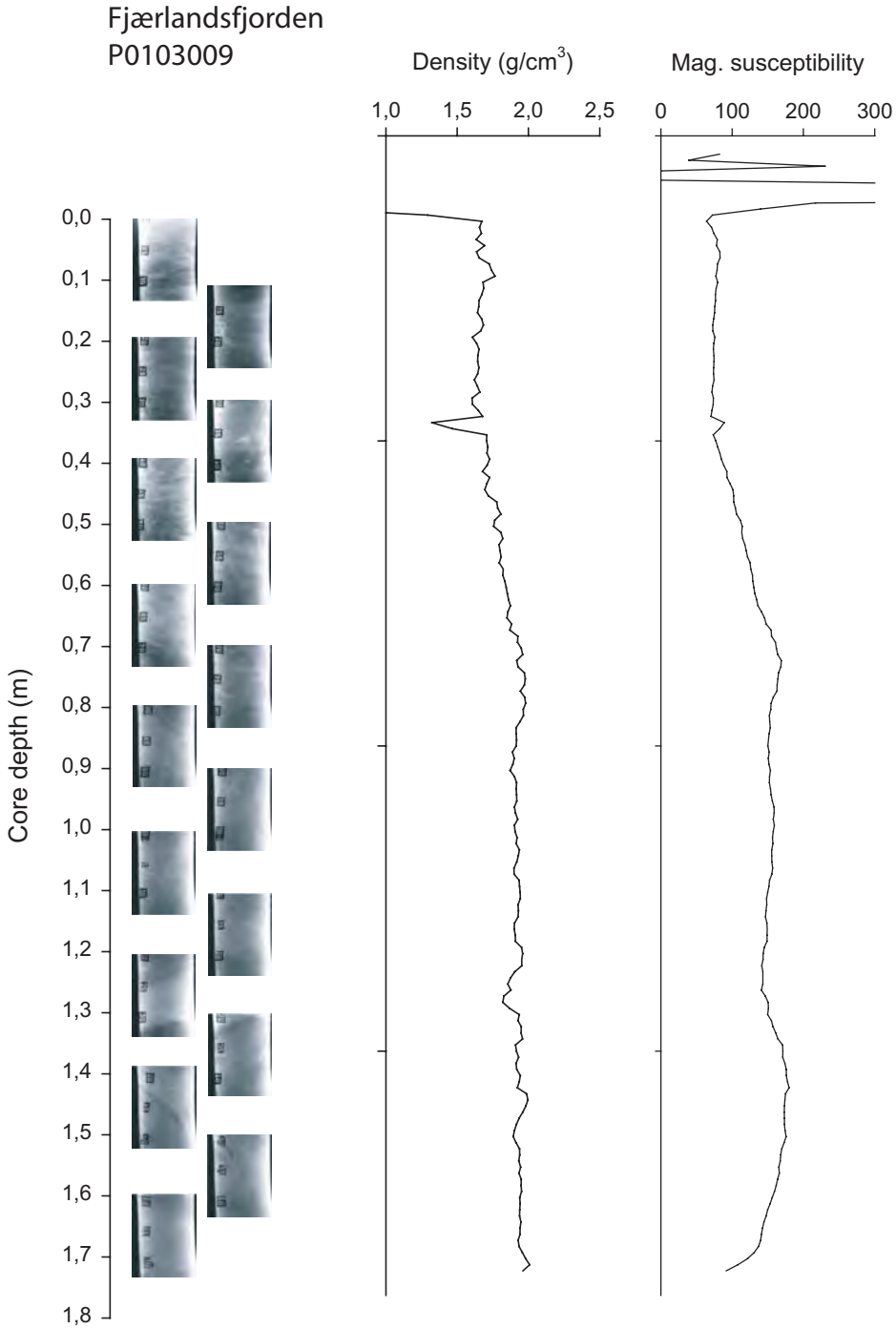
Fjærlandsfjorden
P0103009
Density (g/cm3)
Mag. susceptibility
1,0
1,5
2,0
2,5
0
100
200
300
Core depth (m)
0,0
0,1
0,2
0,3
0,4
0,5
0,6
0,7
0,8
0,9
1,0
1,1
1,2
1,3
1,4
1,5
1,6
1,7
1,8

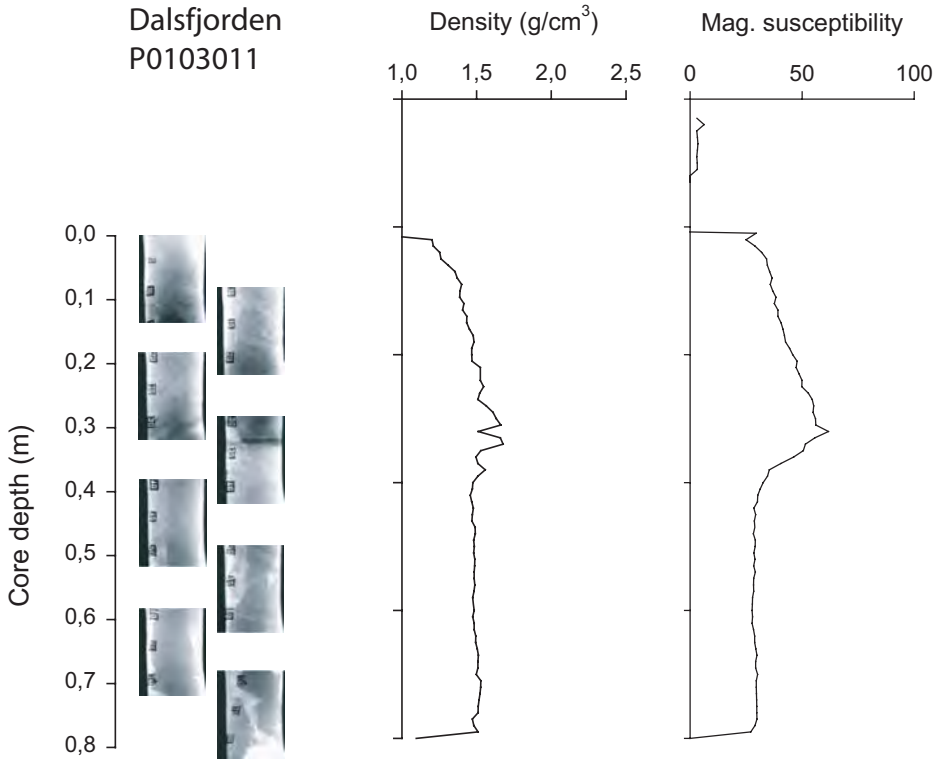
Dalsfjorden
P0103011
Density (g/cm3)
Mag. susceptibility
1,0
1,5
2,0
2,5
0
50
100
Core depth (m)
0,0
0,1
0,2
0,3
0,4
0,5
0,6
0,7
0,8

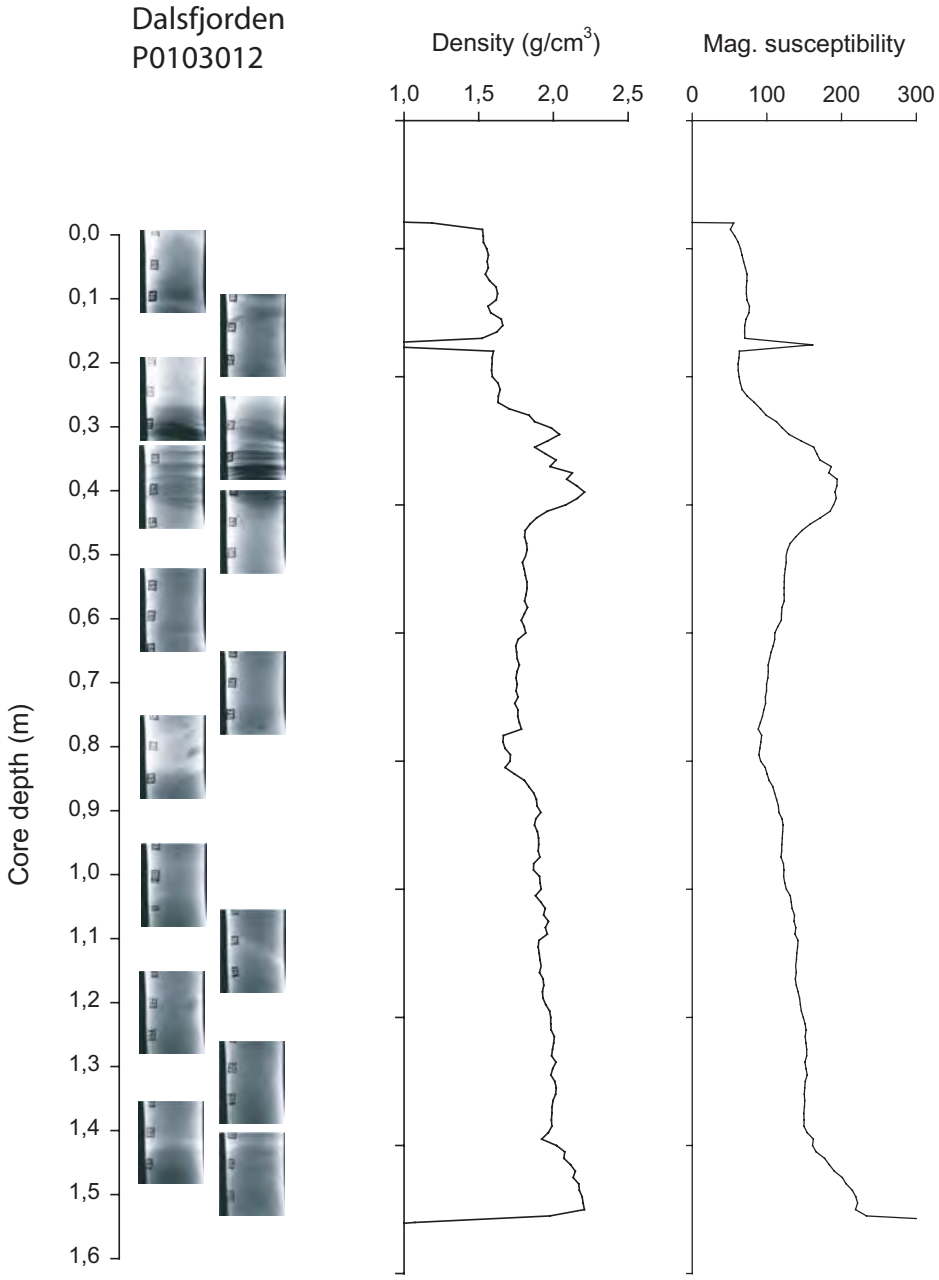
Dalsfjorden
P0103012
Density (g/cm3)
Mag. susceptibility
1,0
1,5
2,0
2,5
0
100
200
300
Core depth (m)
0,0
0,1
0,2
0,3
0,4
0,5
0,6
0,7
0,8
0,9
1,0
1,1
1,2
1,3
1,4
1,5
1,6

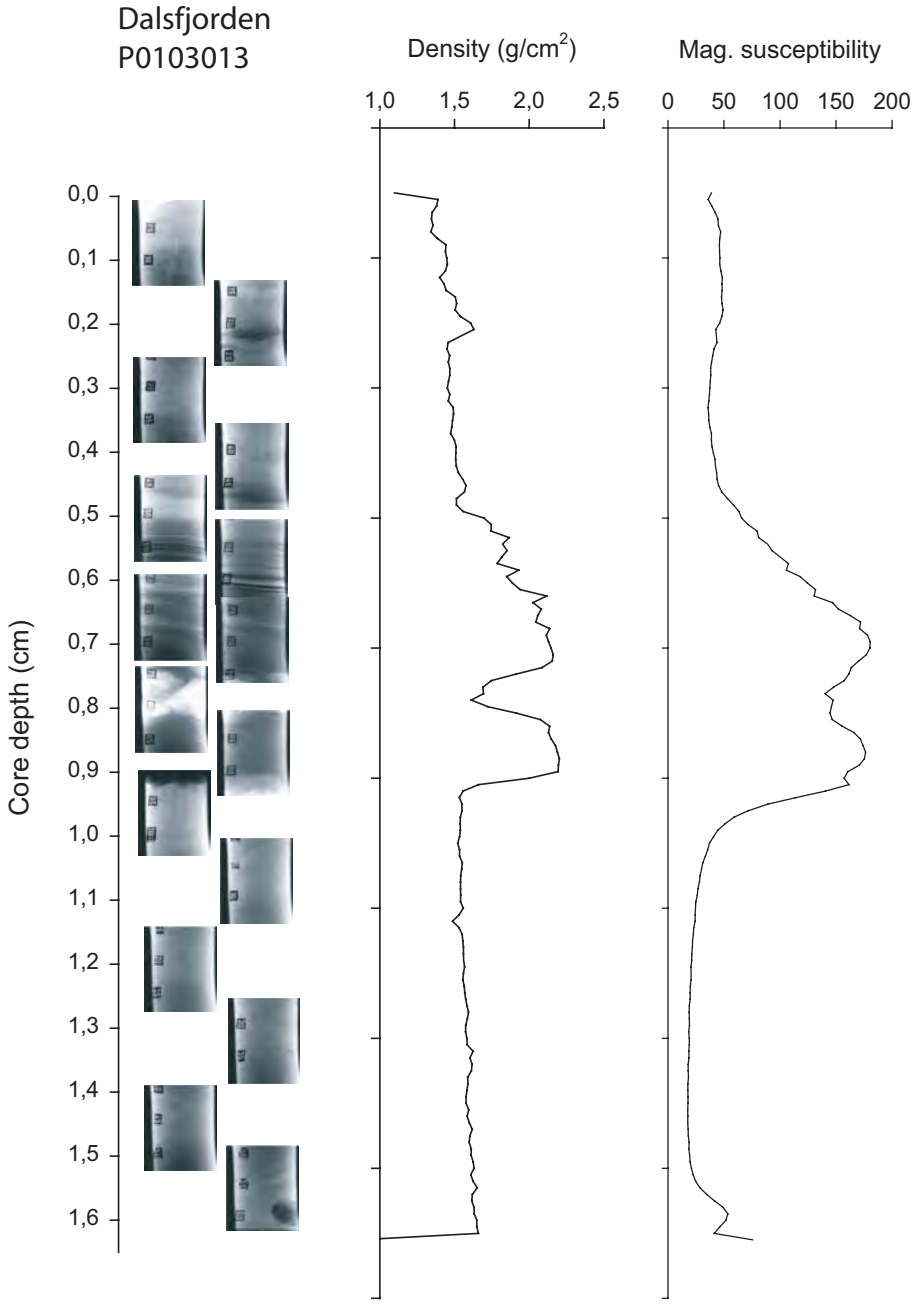
Dalsfjorden
P0103013
Density (g/cm2)
Mag. susceptibility
1,0
1,5
2,0
2,5
0
50
100
150
200
Core depth (cm)
0,0
0,1
0,2
0,3
0,4
0,5
0,6
0,7
0,8
0,9
1,0
1,1
1,2
1,3
1,4
1,5
1,6

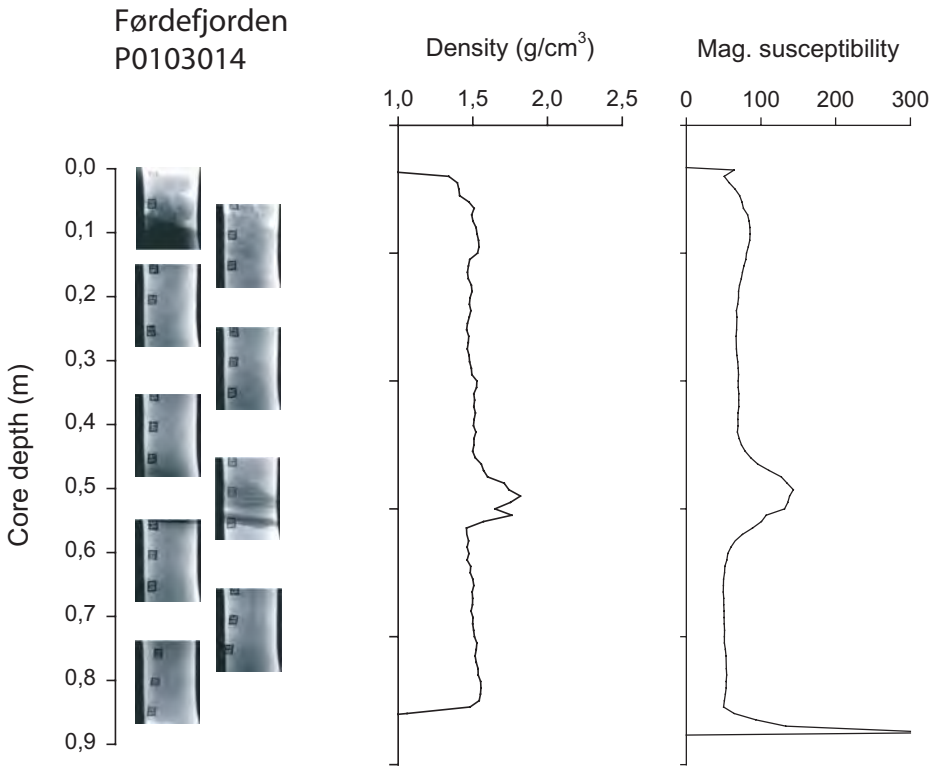
Førdefjorden
P0103014
Density (g/cm3)
Mag. susceptibility
1,0
1,5
2,0
2,5
0
100
200
300
Core depth (m)
0,0
0,1
0,2
0,3
0,4
0,5
0,6
0,7
0,8
0,9

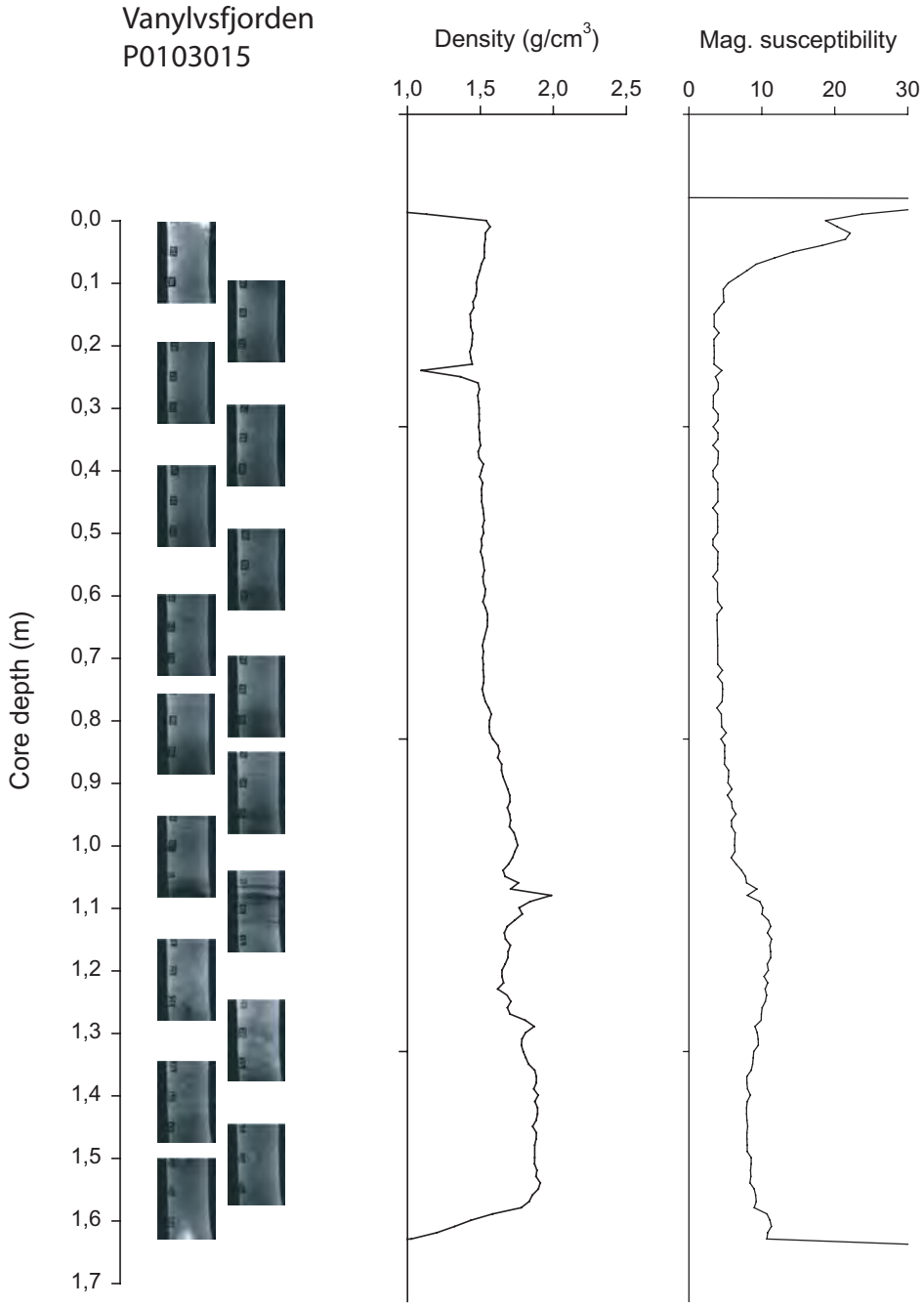
Vanylvsfjorden
P0103015
Density (g/cm3)
Mag. susceptibility
1,0
1,5
2,0
2,5
0
10
20
30
Core depth (m)
0,0
0,1
0,2
0,3
0,4
0,5
0,6
0,7
0,8
0,9
1,0
1,1
1,2
1,3
1,4
1,5
1,6
1,7

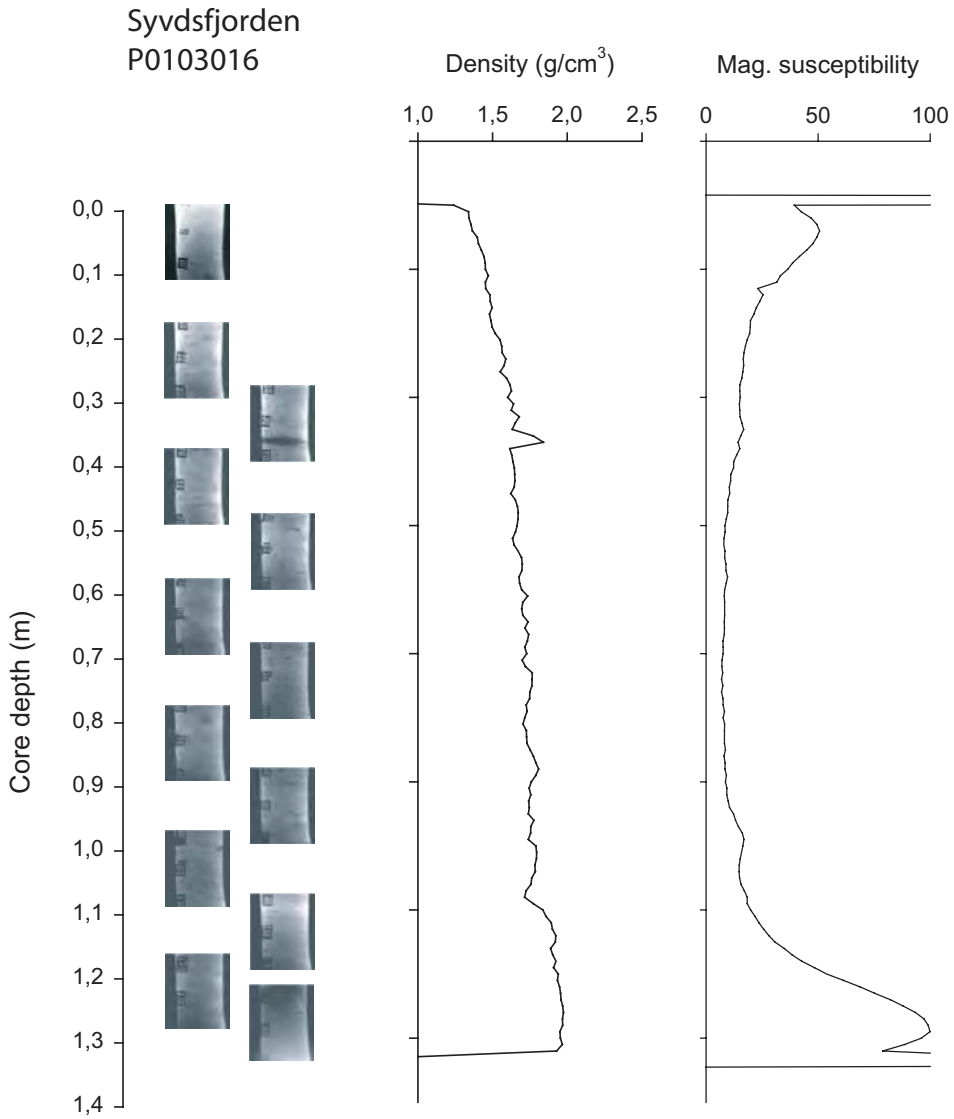
Syvdsfjorden
P0103016
Density (g/cm3)
Mag. susceptibility
1,0
1,5
2,0
2,5
0
50
100
Core depth (m)
0,0
0,1
0,2
0,3
0,4
0,5
0,6
0,7
0,8
0,9
1,0
1,1
1,2
1,3
1,4

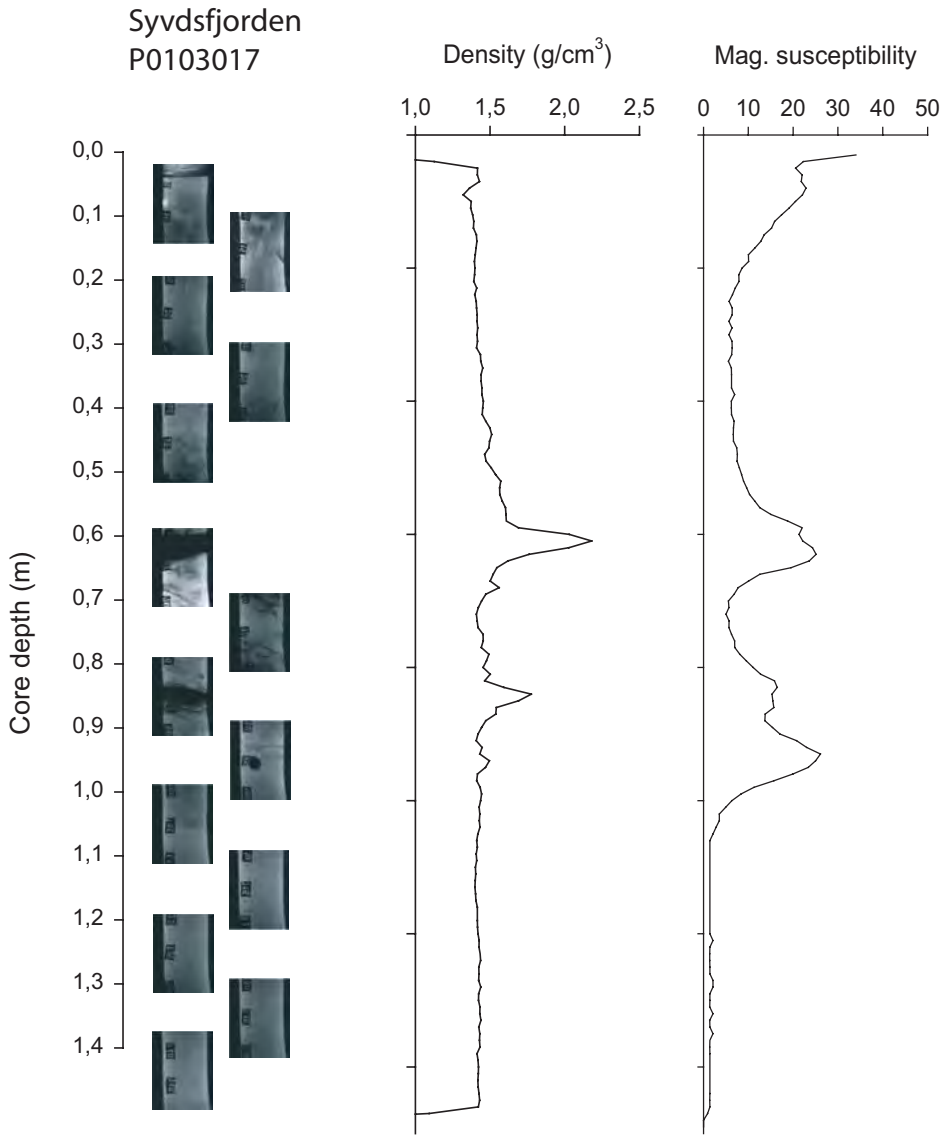
Syvdsfjorden
P0103017
Density (g/cm3)
Mag. susceptibility
1,0
1,5
2,0
2,5
0
10
20
30
40
50
0,0
0,1
0,2
0,3
0,4
0,5
0,6
0,7
0,8
0,9
1,0
1,1
1,2
1,3
1,4
Core depth (m)

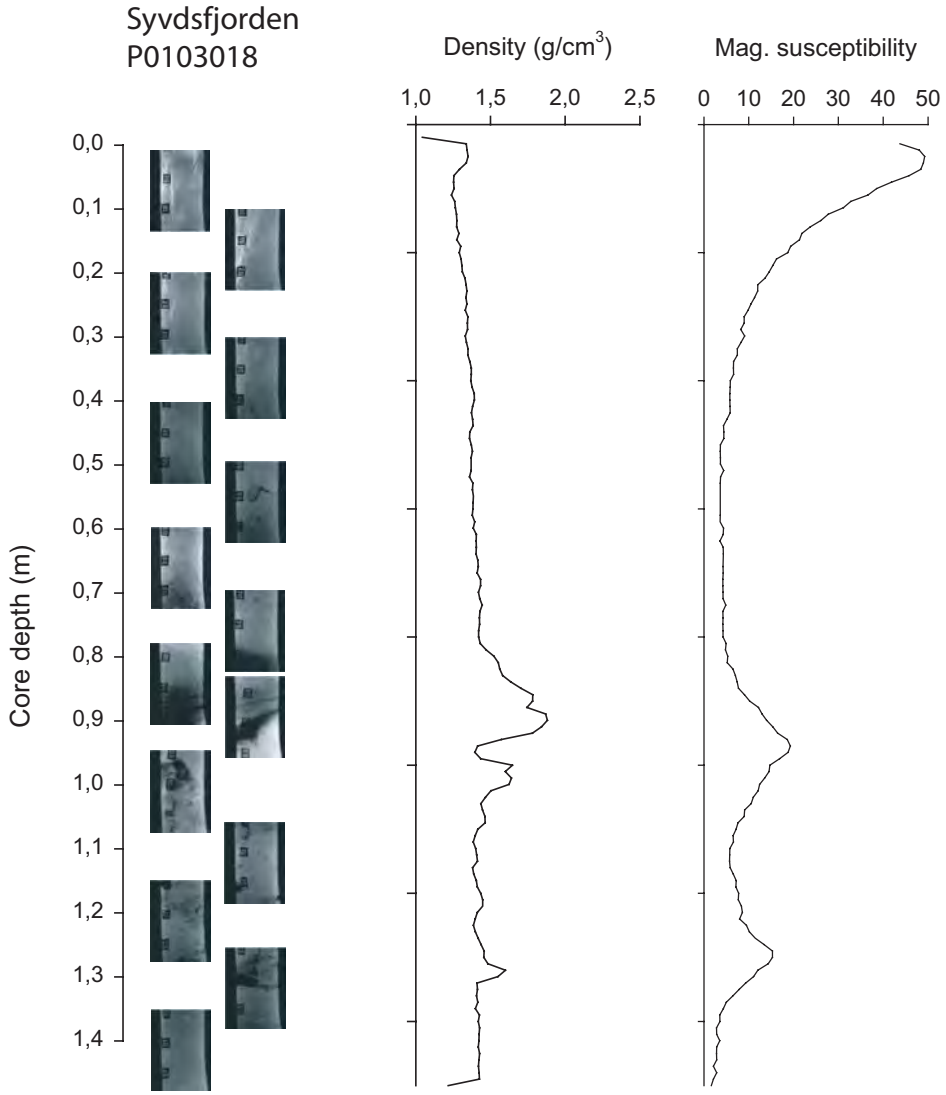
Syvdsfjorden
P0103018
Density (g/cm3)
Mag. susceptibility
1,0
1,5
2,0
2,5
0
10
20
30
40
50
Core depth (m)
0,0
0,1
0,2
0,3
0,4
0,5
0,6
0,7
0,8
0,9
1,0
1,1
1,2
1,3
1,4

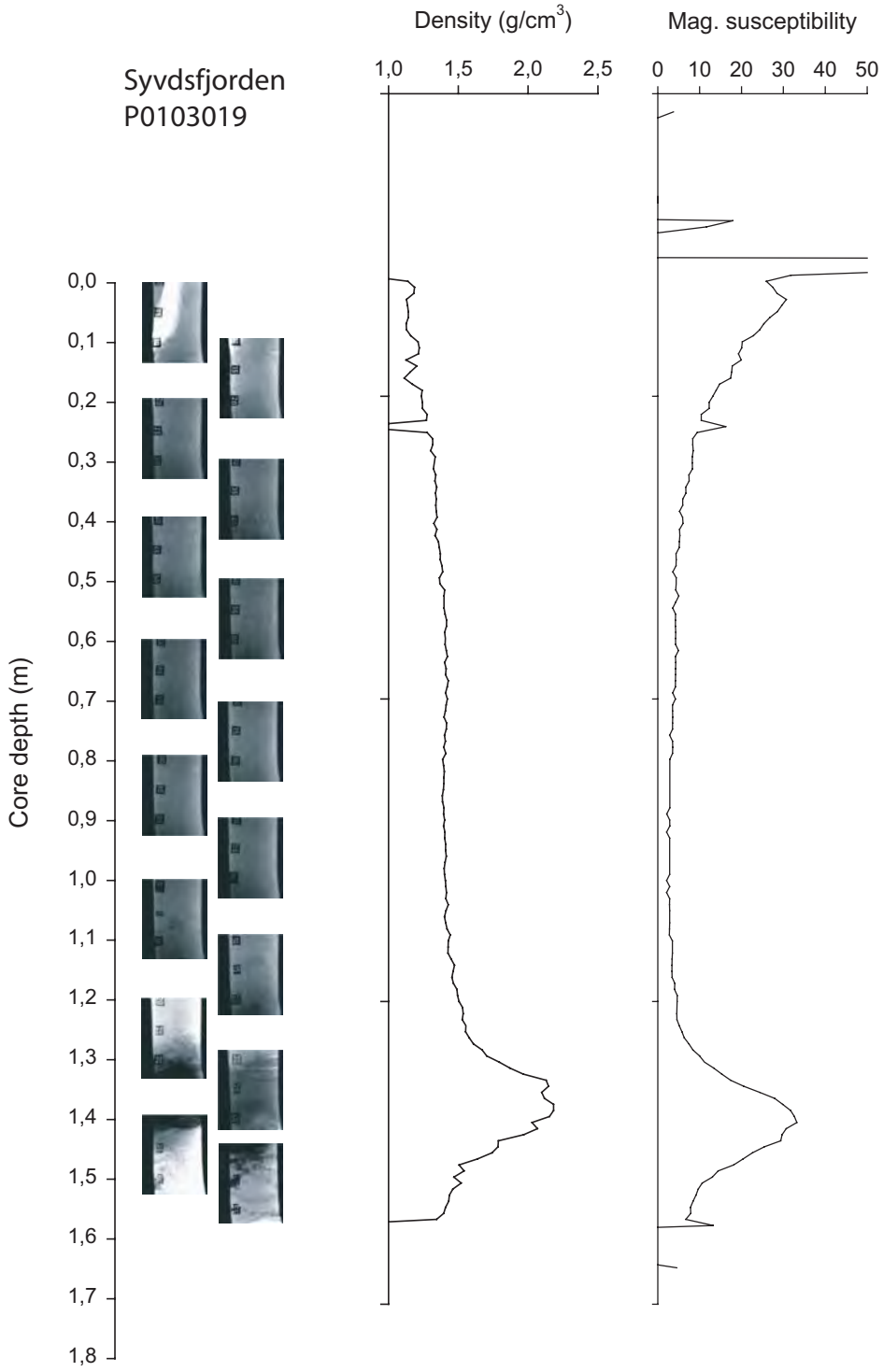
Syvdsfjorden
P0103019
Density (g/cm3)
Mag. susceptibility
1,0 1,5 2,0 2,5
0 10 20 30 40 50
Core depth (m)
0,0 0,1 0,2 0,3 0,4 0,5 0,6 0,7 0,8 0,9 1,0 1,1 1,2 1,3 1,4 1,5 1,6 1,7 1,8

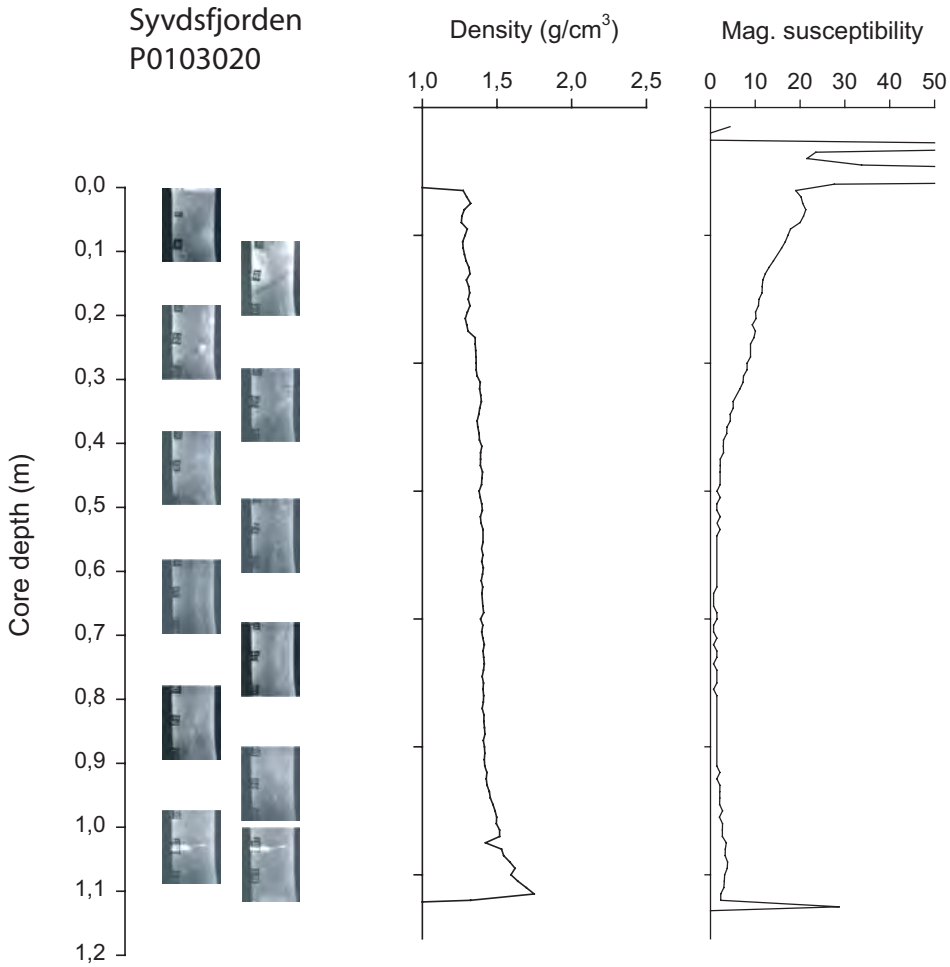
Syvdsfjorden
P0103020
Density (g/cm3)
Mag. susceptibility
1,0
1,5
2,0
2,5
0
10
20
30
40
50
Core depth (m)
0,0
0,1
0,2
0,3
0,4
0,5
0,6
0,7
0,8
0,9
1,0
1,1
1,2

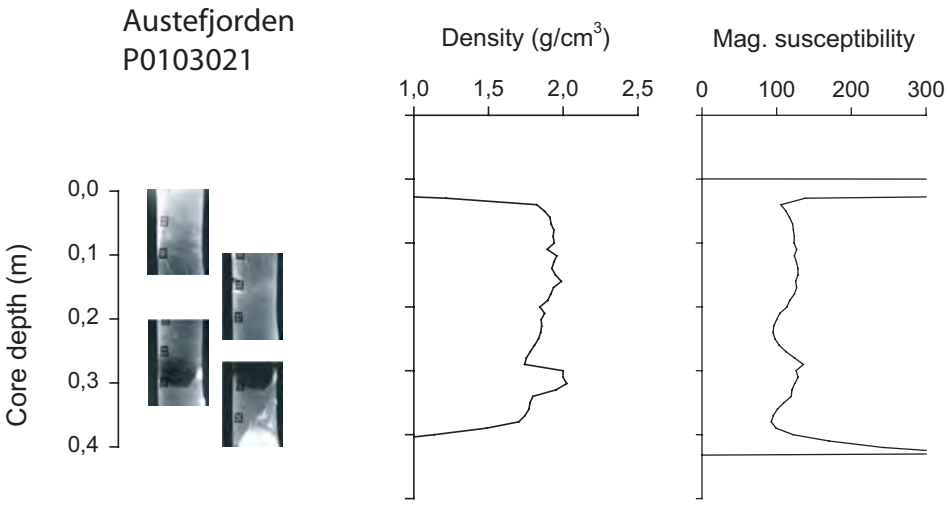
Austefjorden
P0103021
Density (g/cm3)
Mag. susceptibility
1,0
1,5
2,0
2,5
0
100
200
300
Core depth (m)
0,0
0,1
0,2
0,3
0,4

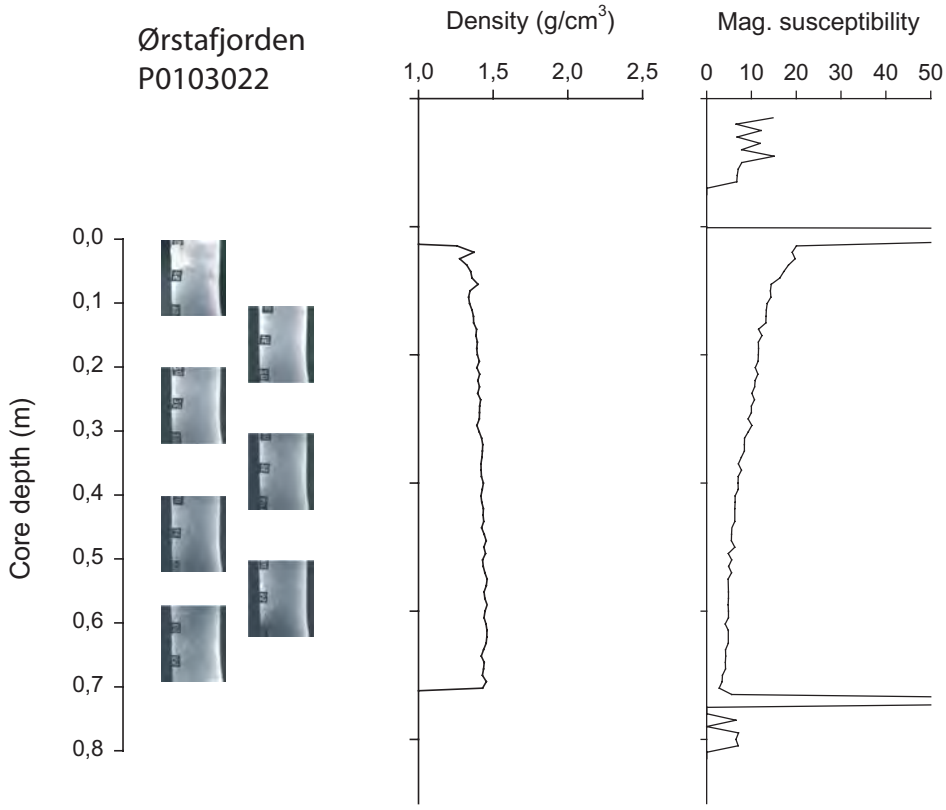
Ørstafjorden
P0103022
Density (g/cm3)
Mag. susceptibility
1,0
1,5
2,0
2,5
0
10
20
30
40
50
Core depth (m)
0,0
0,1
0,2
0,3
0,4
0,5
0,6
0,7
0,8

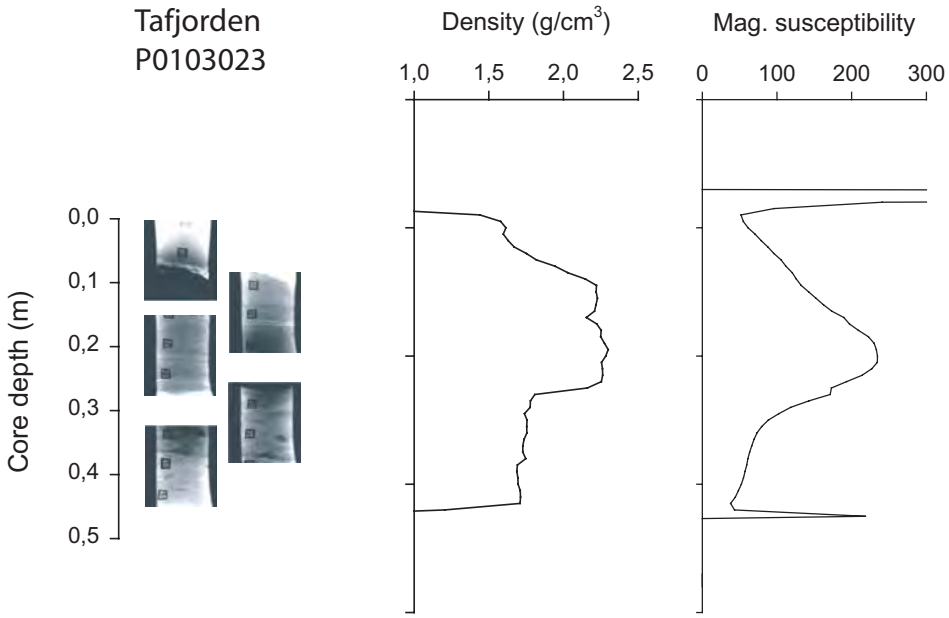
Tafjorden
P0103023
Density (g/cm3)
Mag. susceptibility
1,0
1,5
2,0
2,5
0
100
200
300
Core depth (m)
0,0
0,1
0,2
0,3
0,4
0,5

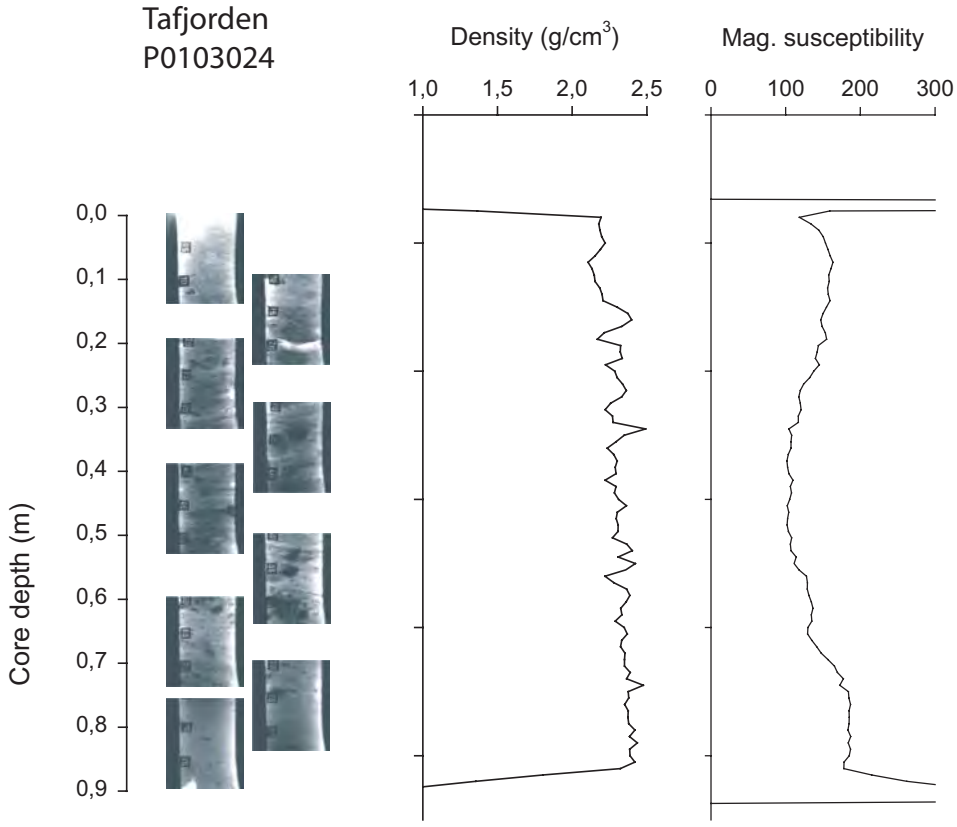
Tafjorden
P0103024
Density (g/cm3)
Mag. susceptibility
1,0
1,5
2,0
2,5
0
100
200
300
Core depth (m)
0,0
0,1
0,2
0,3
0,4
0,5
0,6
0,7
0,8
0,9

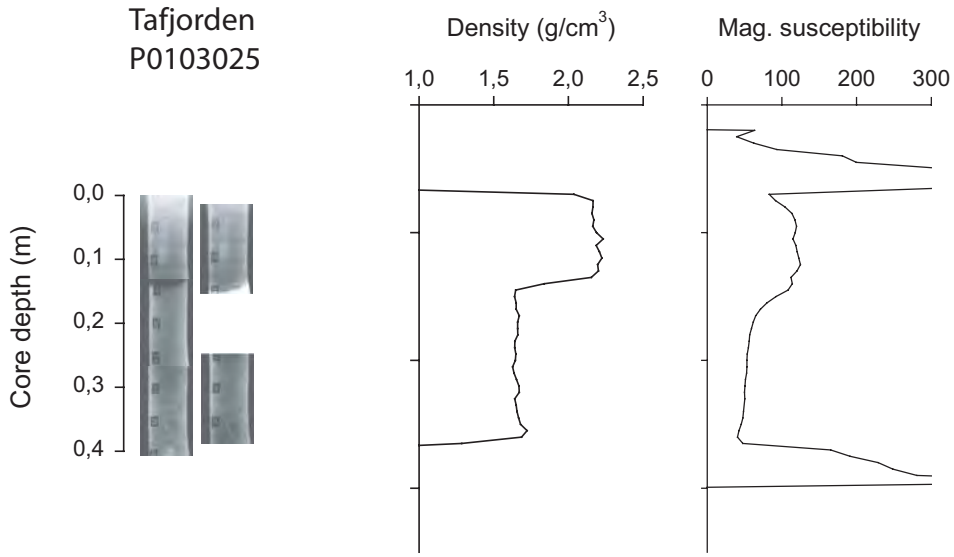
Tafjorden
P0103025
Density (g/cm3)
Mag. susceptibility
1,0
1,5
2,0
2,5
0
100
200
300
Core depth (m)
0,0
0,1
0,2
0,3
0,4

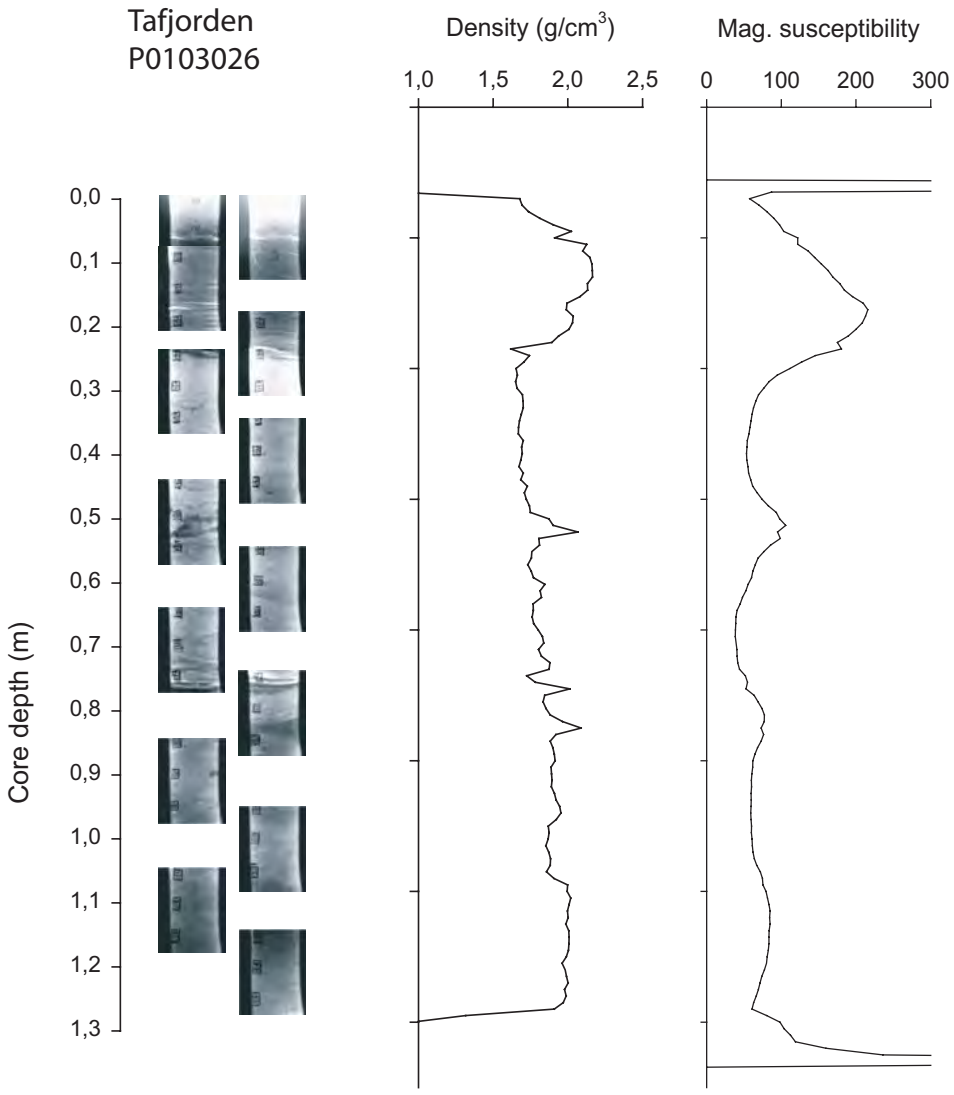
Tafjorden
P0103026
Density (g/cm3)
Mag. susceptibility
1,0
1,5
2,0
2,5
0
100
200
300
Core depth (m)
0,0
0,1
0,2
0,3
0,4
0,5
0,6
0,7
0,8
0,9
1,0
1,1
1,2
1,3

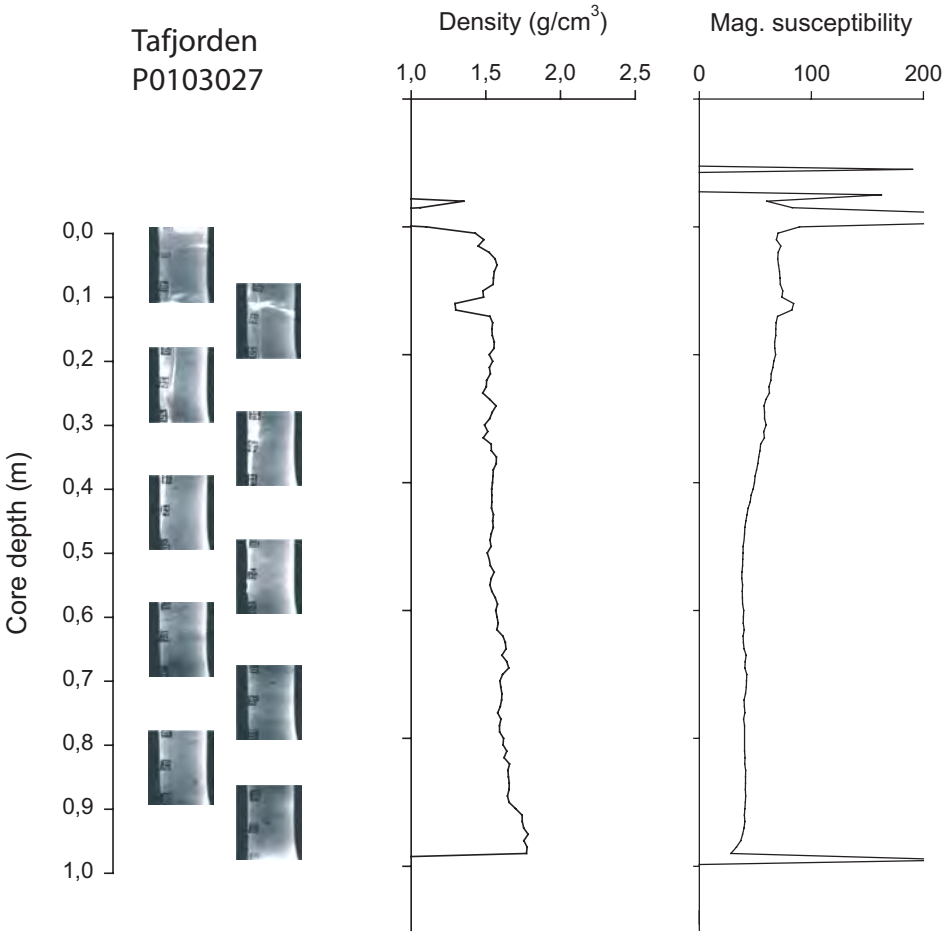
Tafjorden
P0103027
Density (g/cm3)
1,0
1,5
2,0
2,5
Mag. susceptibility
0
100
200
Core depth (m)
0,0
0,1
0,2
0,3
0,4
0,5
0,6
0,7
0,8
0,9
1,0

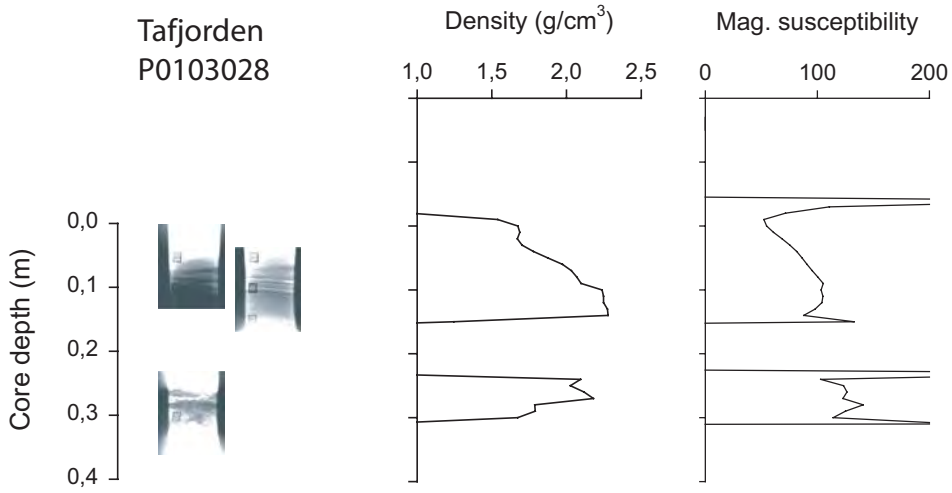
Tafjorden
P0103028
Density (g/cm3)
Mag. susceptibility
1,0
1,5
2,0
2,5
0
100
200
Core depth (m)
0,0
0,1
0,2
0,3
0,4

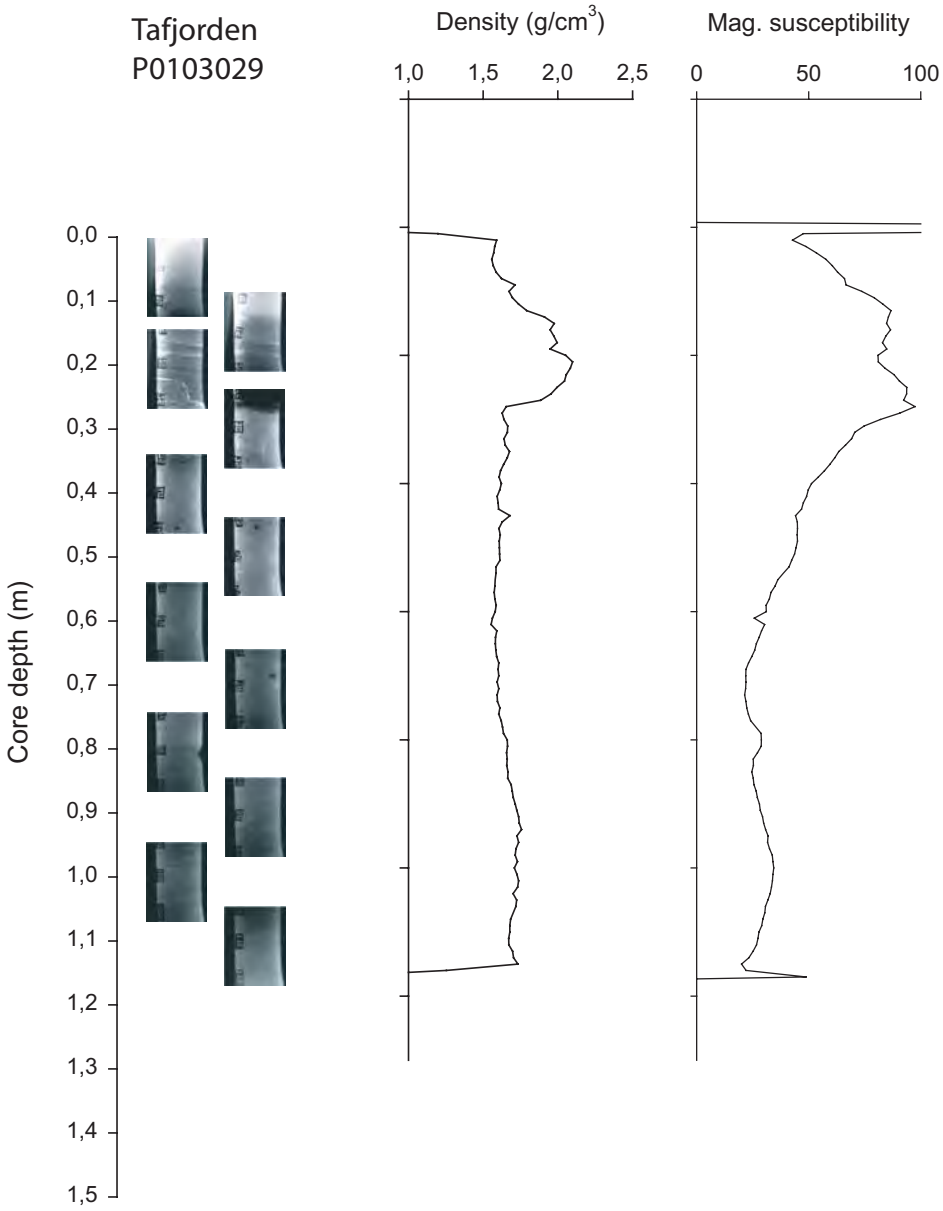
Tafjorden
P0103029
Density (g/cm3)
1,0
1,5
2,0
2,5
Mag. susceptibility
0
50
100
Core depth (m)
0,0
0,1
0,2
0,3
0,4
0,5
0,6
0,7
0,8
0,9
1,0
1,1
1,2
1,3
1,4
1,5

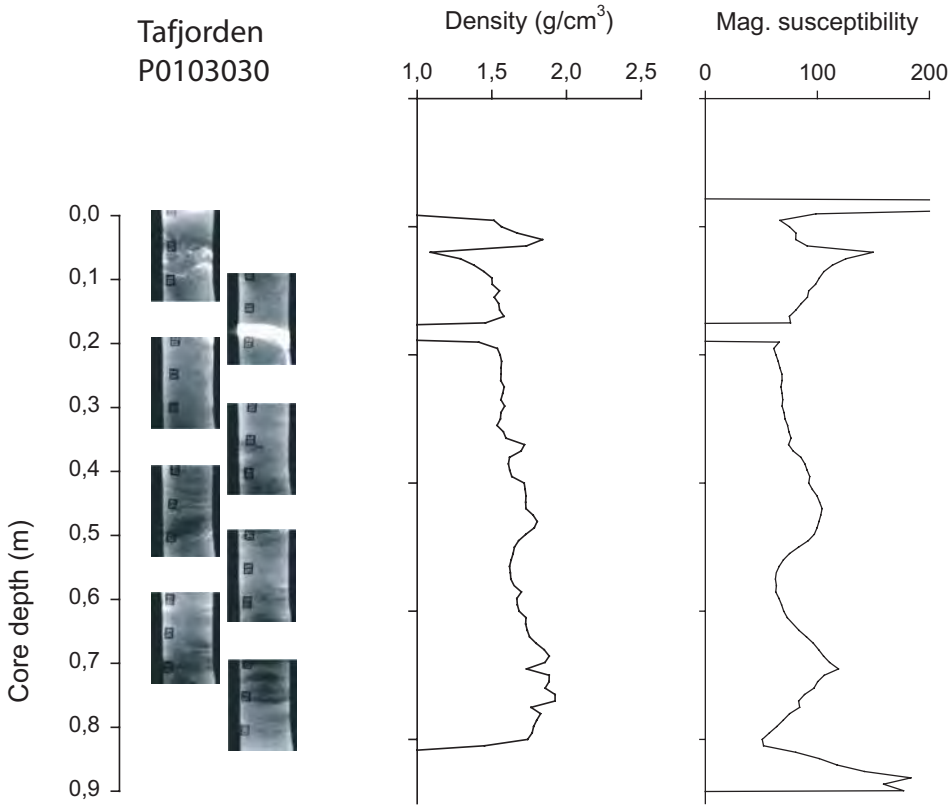
Tafjorden
P0103030
Density (g/cm3)
Mag. susceptibility
1,0
1,5
2,0
2,5
0
100
200
Core depth (m)
0,0
0,1
0,2
0,3
0,4
0,5
0,6
0,7
0,8
0,9

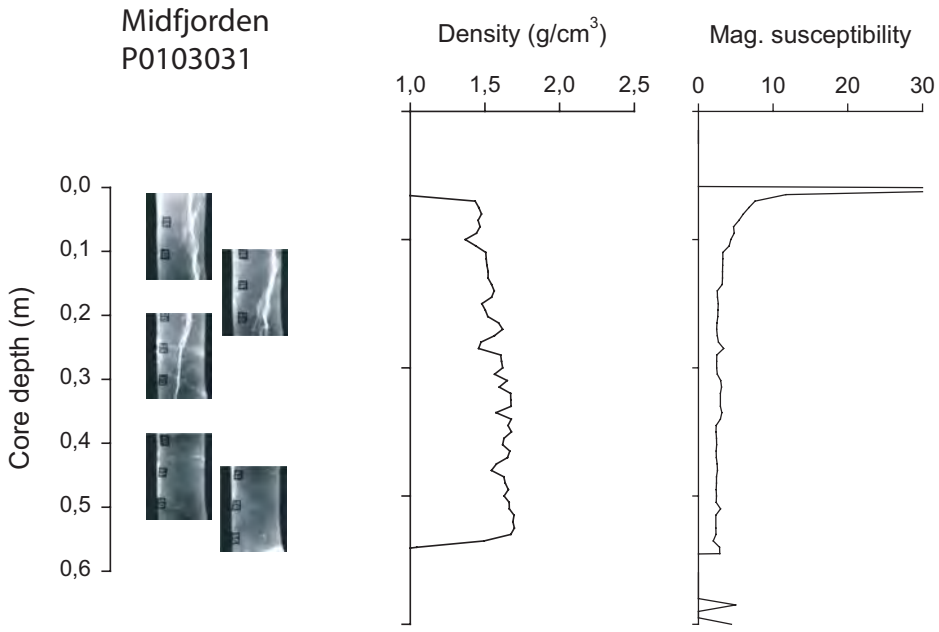
Midfjorden
P0103031
Density (g/cm3)
Mag. susceptibility
1,0
1,5
2,0
2,5
0
10
20
30
Core depth (m)
0,0
0,1
0,2
0,3
0,4
0,5
0,6

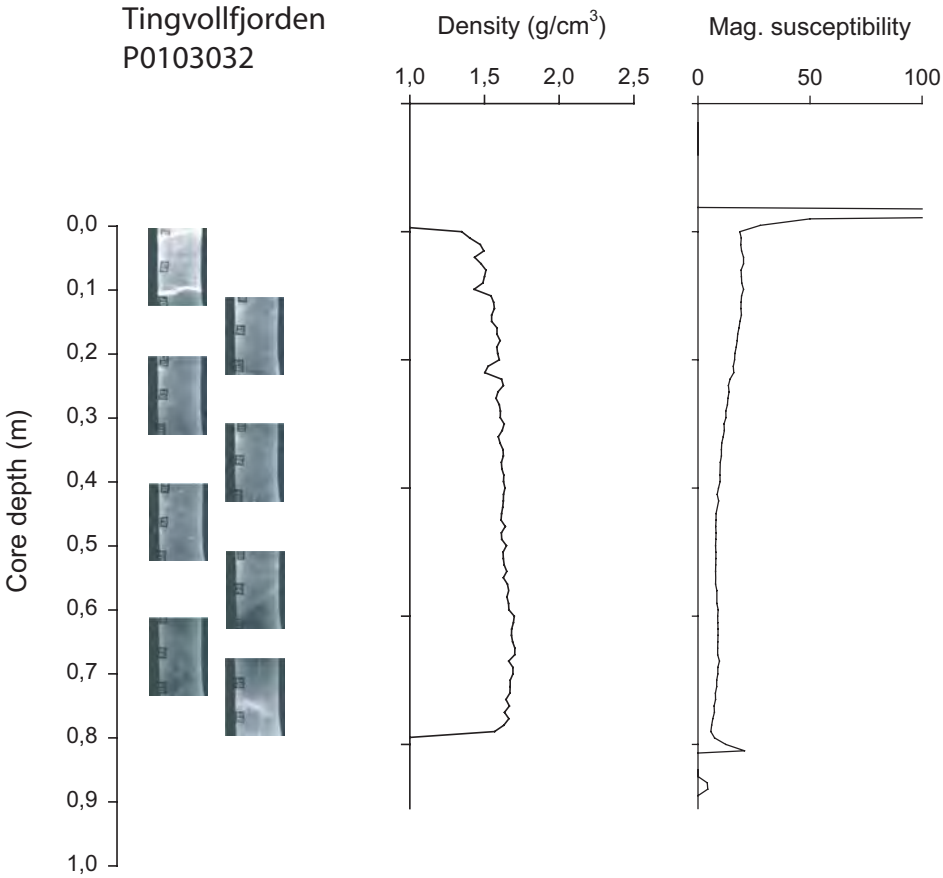
Tingvollfjorden
P0103032
Density (g/cm3)
Mag. susceptibility
1,0
1,5
2,0
2,5
0
50
100
Core depth (m)
0,0
0,1
0,2
0,3
0,4
0,5
0,6
0,7
0,8
0,9
1,0

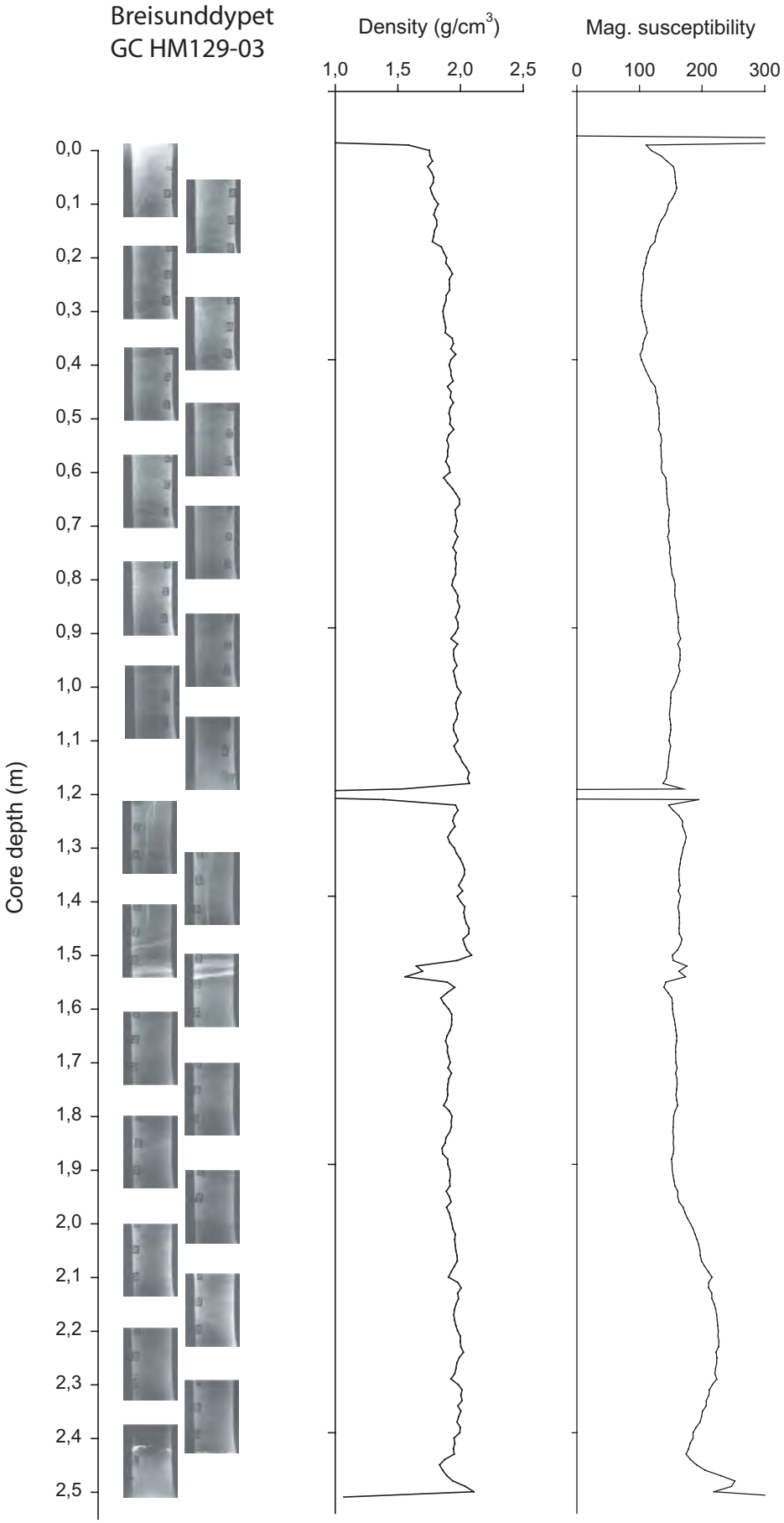
Breisunddypet
GC HM129-03
Density (g/cm3)
1,0
1,5
2,0
2,5
Mag. susceptibility
0
100
200
300
Core depth (m)
0,0
0,1
0,2
0,3
0,4
0,5
0,6
0,7
0,8
0,9
1,0
1,1
1,2
1,3
1,4
1,5
1,6
1,7
1,8
1,9
2,0
2,1
2,2
2,3
2,4
2,5

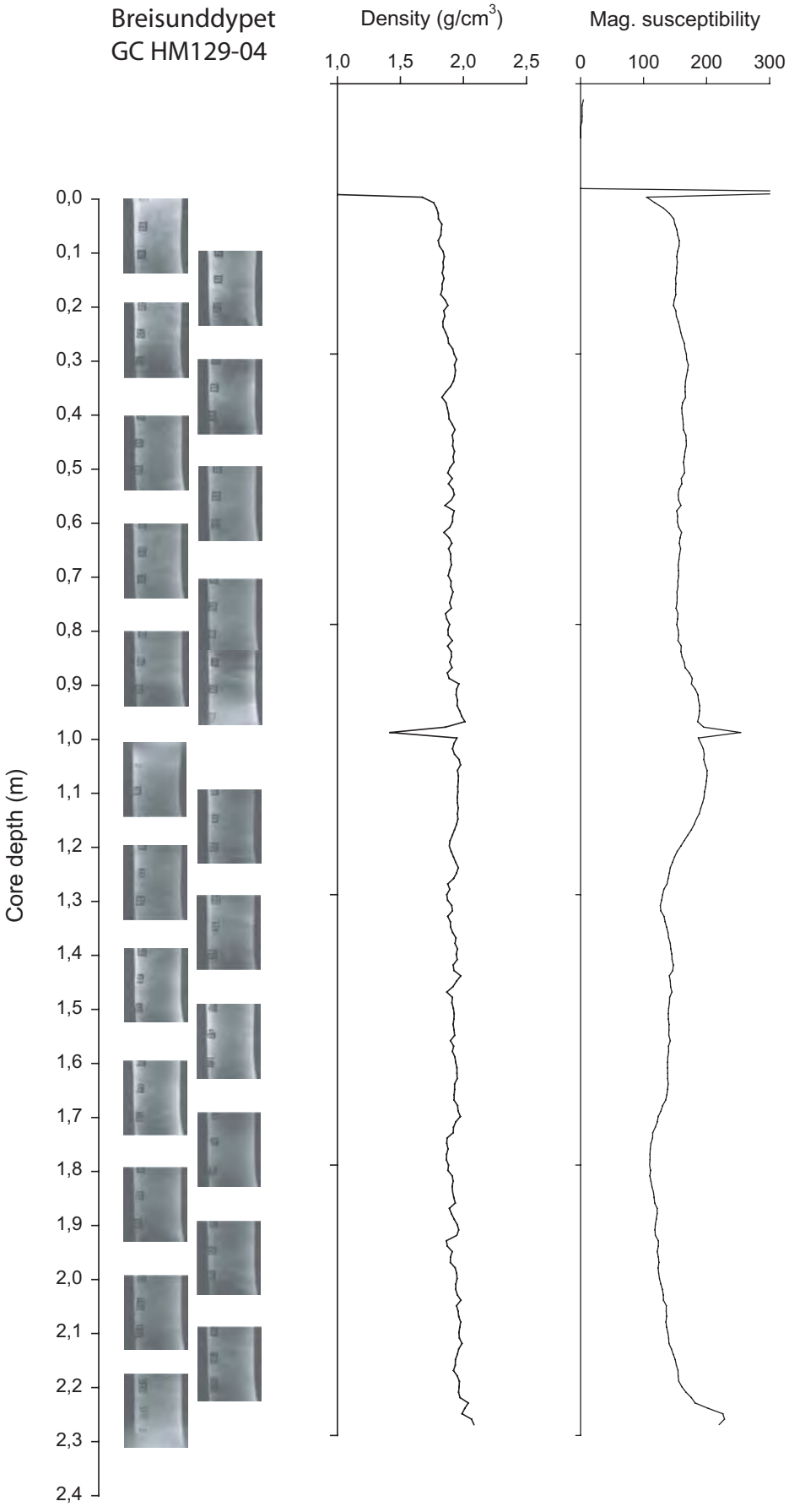
Breisunddypet
GC HM129-04
Density (g/cm3)
1,0
1,5
2,0
2,5
Mag. susceptibility
0
100
200
300
Core depth (m)
0,0
0,1
0,2
0,3
0,4
0,5
0,6
0,7
0,8
0,9
1,0
1,1
1,2
1,3
1,4
1,5
1,6
1,7
1,8
1,9
2,0
2,1
2,2
2,3
2,4

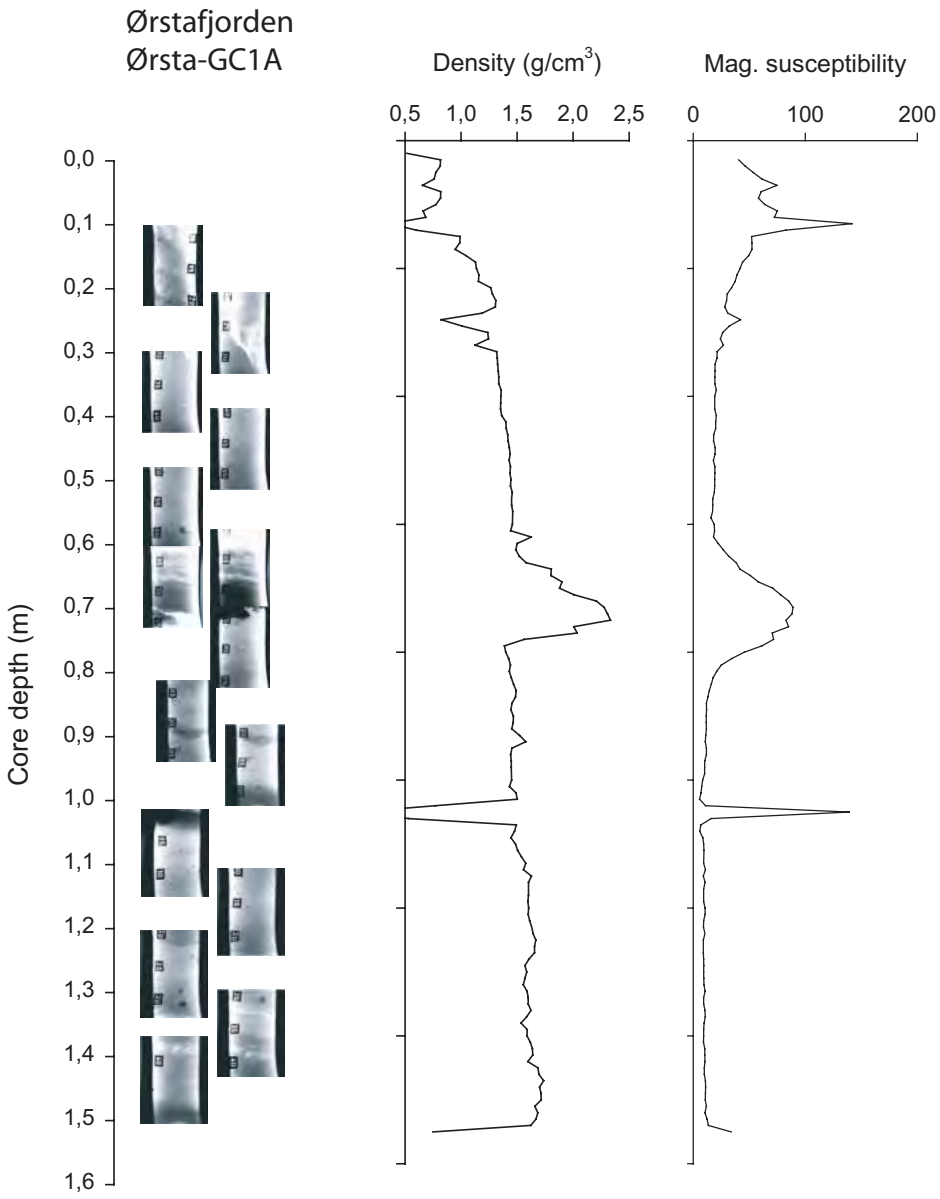
Ørstafjorden
Ørsta-GC1A
Density (g/cm3)
Mag. susceptibility
0,5 1,0 1,5 2,0 2,5
0 100 200
Core depth (m)
0,0 0,1 0,2 0,3 0,4 0,5 0,6 0,7 0,8 0,9 1,0 1,1 1,2 1,3 1,4 1,5 1,6

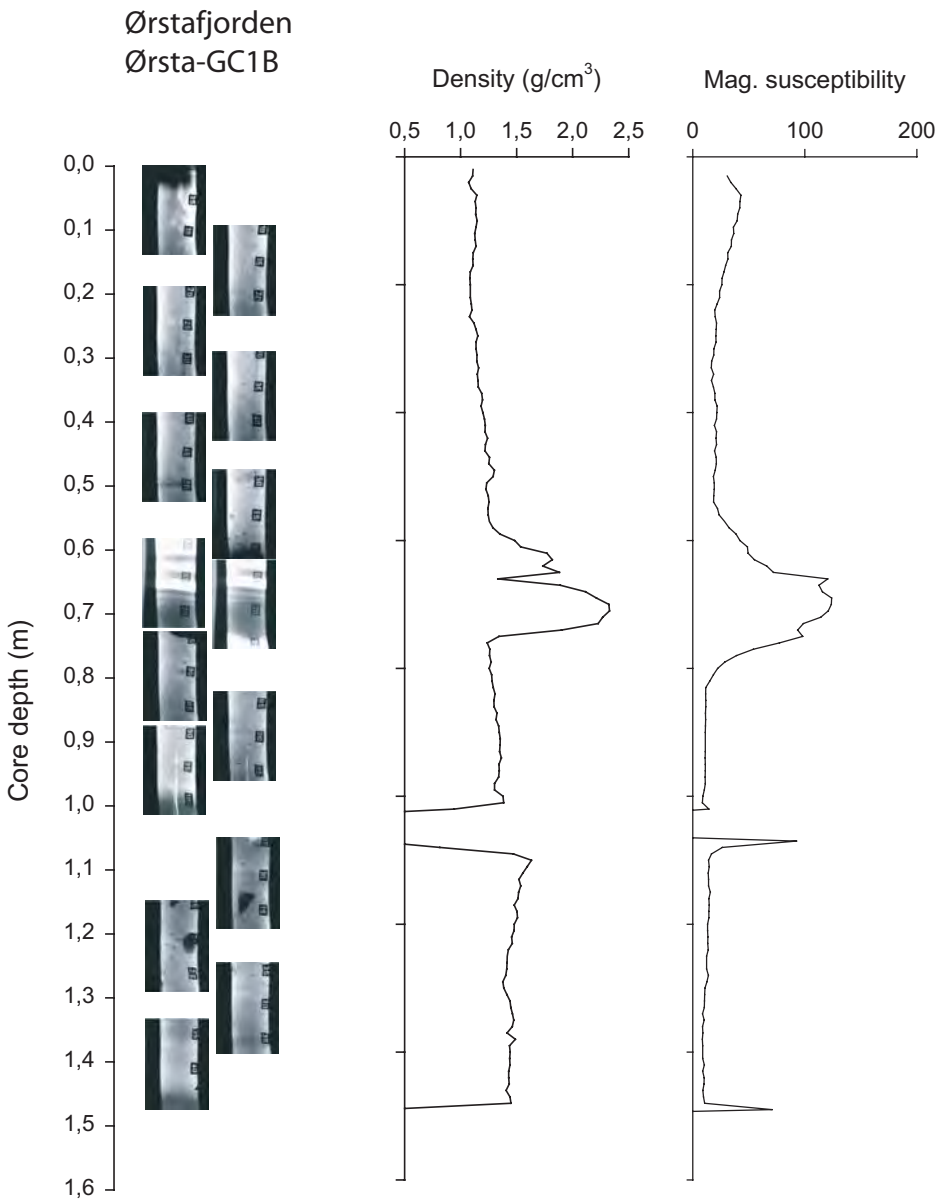
Ørstafjorden
Ørsta-GC1B
Density (g/cm3)
Mag. susceptibility
0,5 1,0 1,5 2,0 2,5
0 100 200
Core depth (m)
0,0 0,1 0,2 0,3 0,4 0,5 0,6 0,7 0,8 0,9 1,0 1,1 1,2 1,3 1,4 1,5 1,6

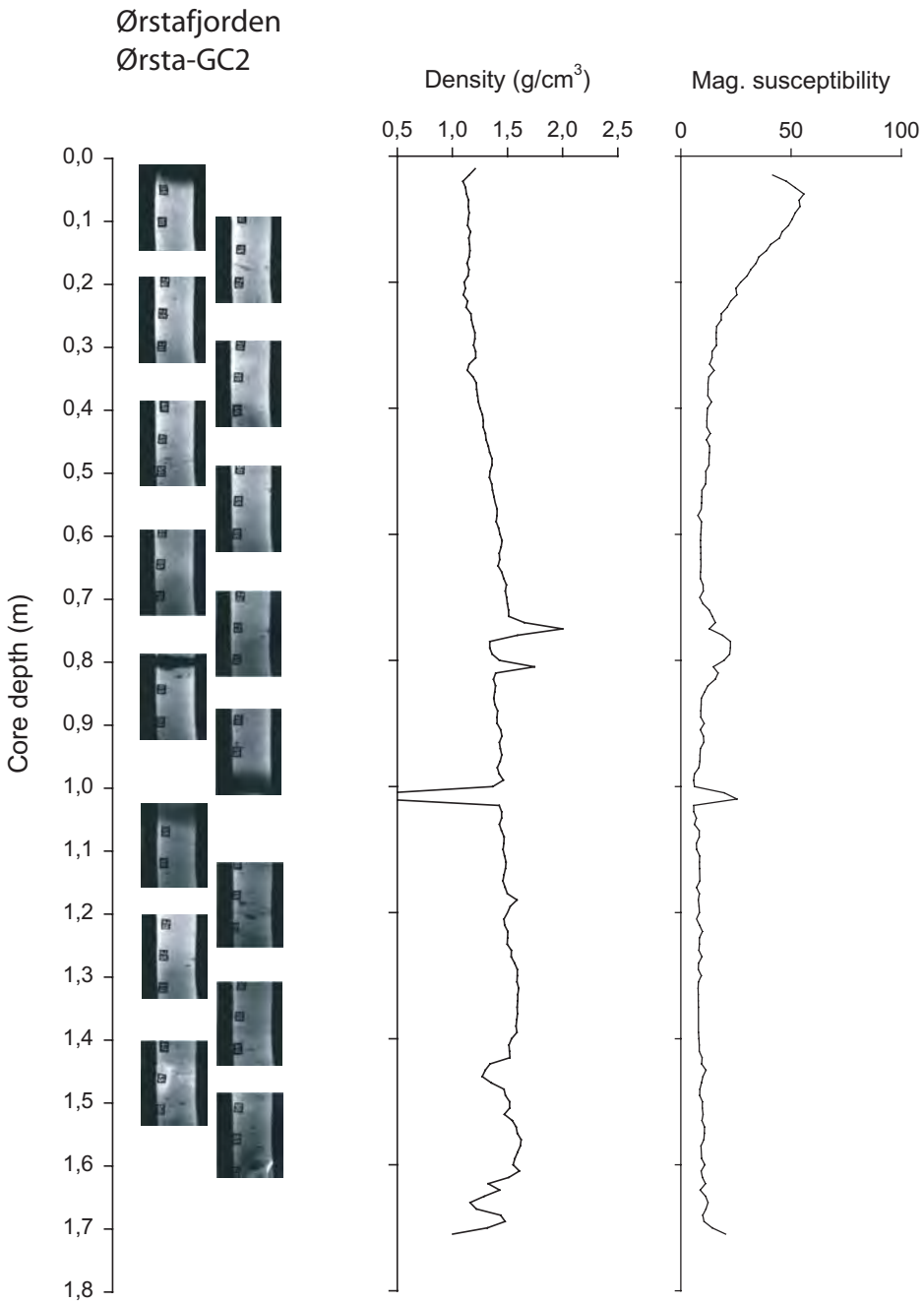
Ørstafjorden
Ørsta-GC2
Density (g/cm3)
Mag. susceptibility
0,5 1,0 1,5 2,0 2,5
0 50 100
Core depth (m)
0,0 0,1 0,2 0,3 0,4 0,5 0,6 0,7 0,8 0,9 1,0 1,1 1,2 1,3 1,4 1,5 1,6 1,7 1,8

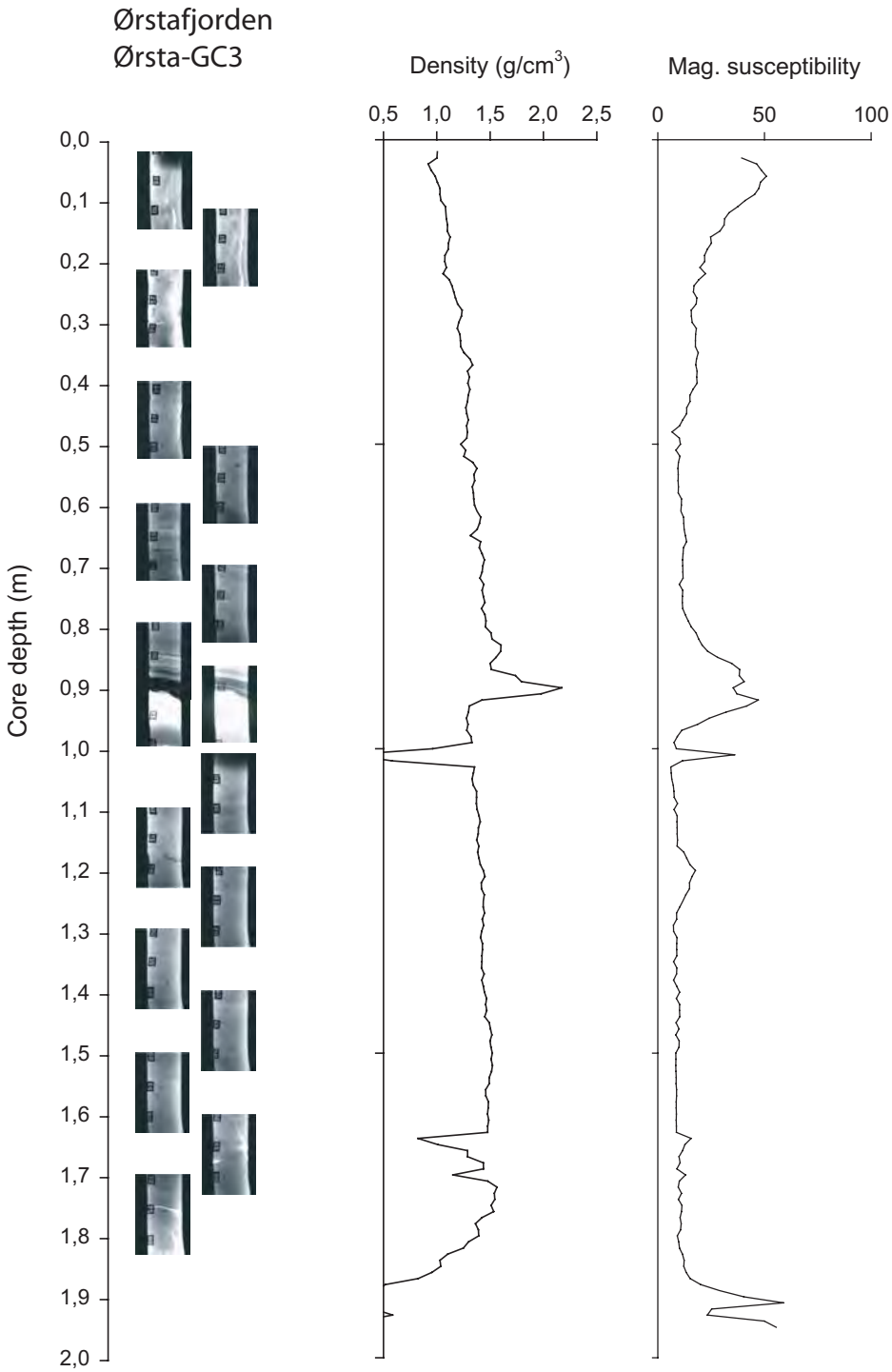
Ørstafjorden
Ørsta-GC3
Density (g/cm3)
Mag. susceptibility
0,5 1,0 1,5 2,0 2,5
0 50 100
Core depth (m)
0,0 0,1 0,2 0,3 0,4 0,5 0,6 0,7 0,8 0,9 1,0 1,1 1,2 1,3 1,4 1,5 1,6 1,7 1,8 1,9 2,0

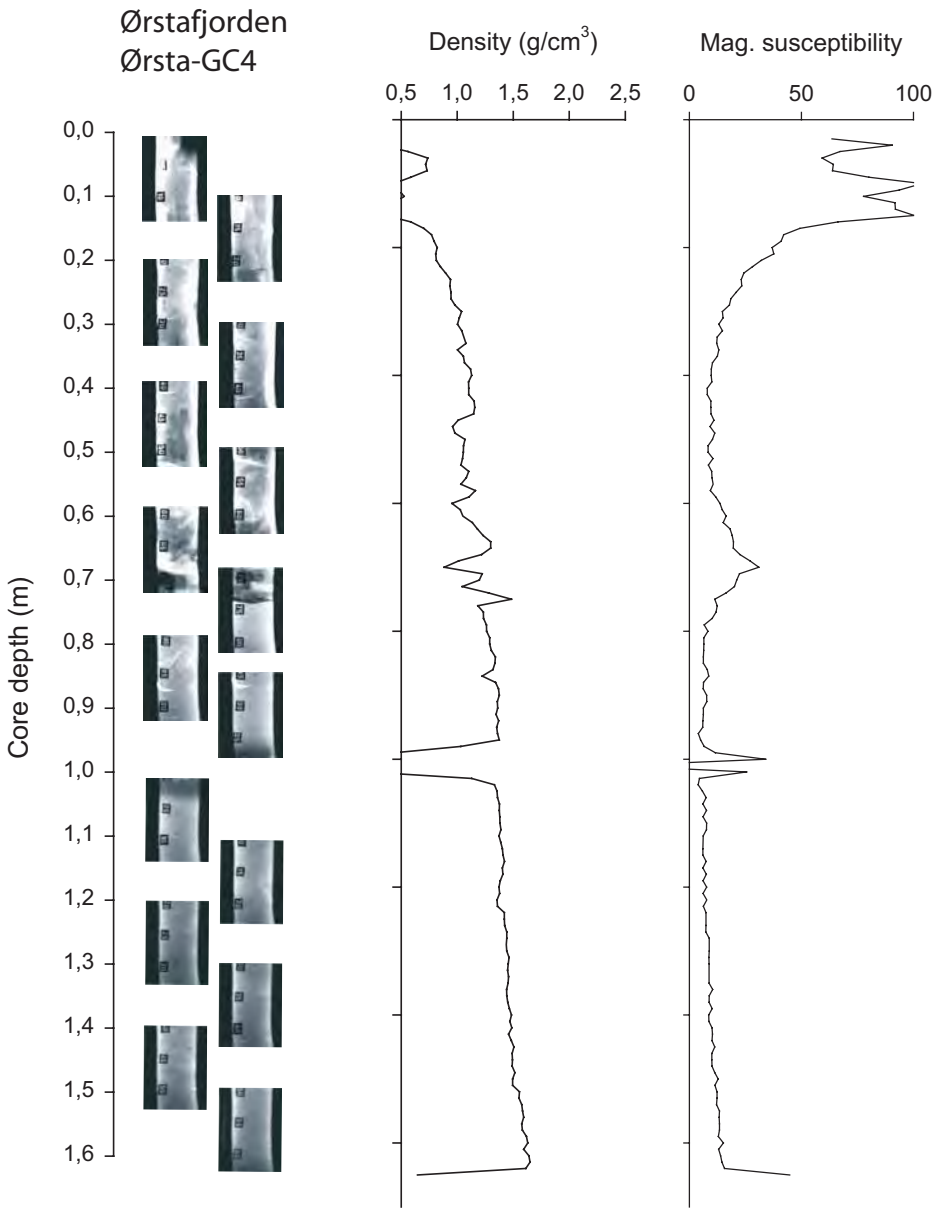
Ørstafjorden
Ørsta-GC4
Density (g/cm3)
Mag. susceptibility
0,5 1,0 1,5 2,0 2,5
0 50 100
Core depth (m)
0,0 0,1 0,2 0,3 0,4 0,5 0,6 0,7 0,8 0,9 1,0 1,1 1,2 1,3 1,4 1,5 1,6

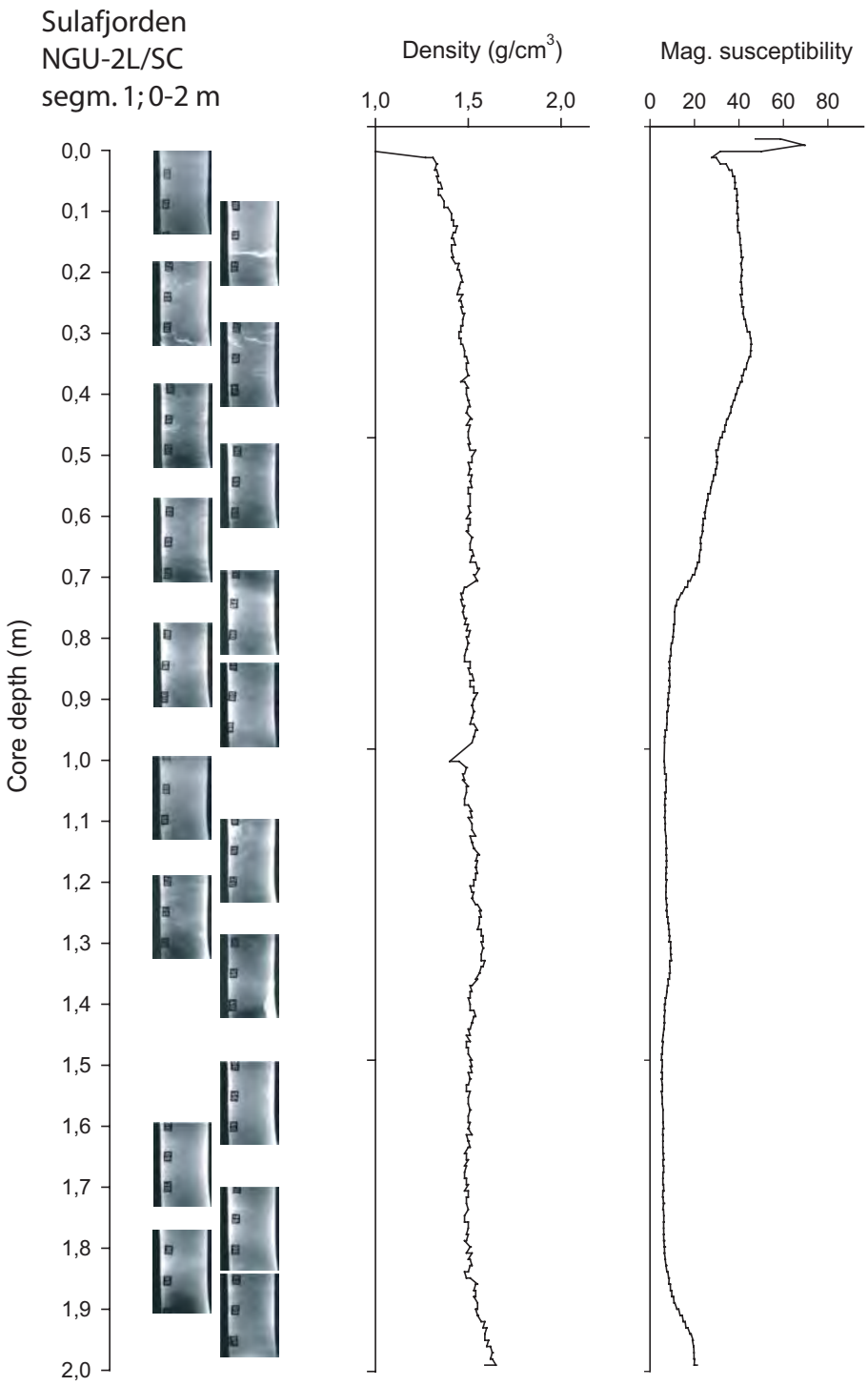
Sulafjorden
NGU-2L/SC
segm. 1; 0-2 m
Density (g/cm3)
Mag. susceptibility
1,0
1,5
2,0
0
20
40
60
80
Core depth (m)
0,0
0,1
0,2
0,3
0,4
0,5
0,6
0,7
0,8
0,9
1,0
1,1
1,2
1,3
1,4
1,5
1,6
1,7
1,8
1,9
2,0

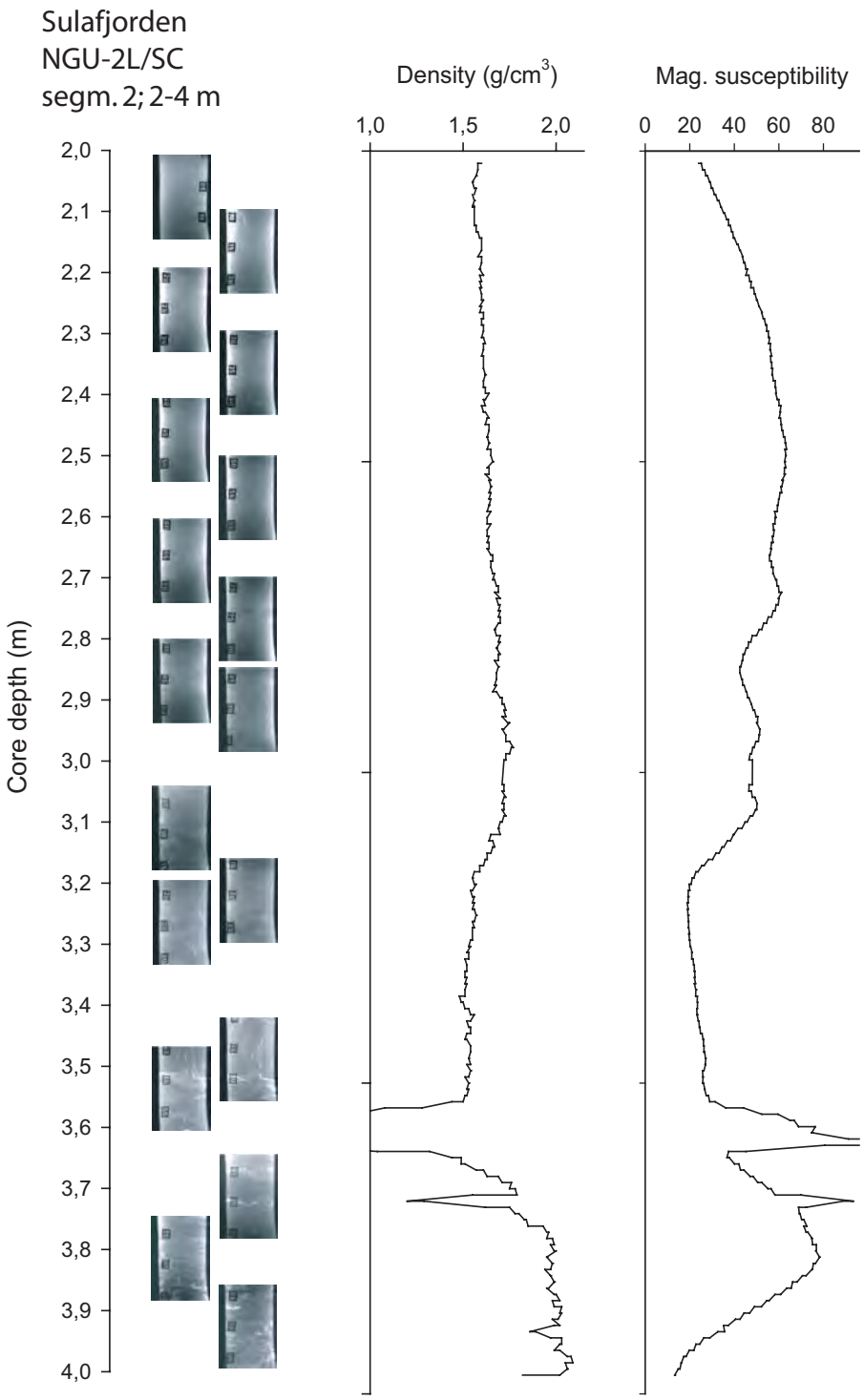
Sulafjorden
NGU-2L/SC
segm. 2; 2-4 m
Density (g/cm3)
Mag. susceptibility
1,0
1,5
2,0
0
20
40
60
80
Core depth (m)
2,0
2,1
2,2
2,3
2,4
2,5
2,6
2,7
2,8
2,9
3,0
3,1
3,2
3,3
3,4
3,5
3,6
3,7
3,8
3,9
4,0

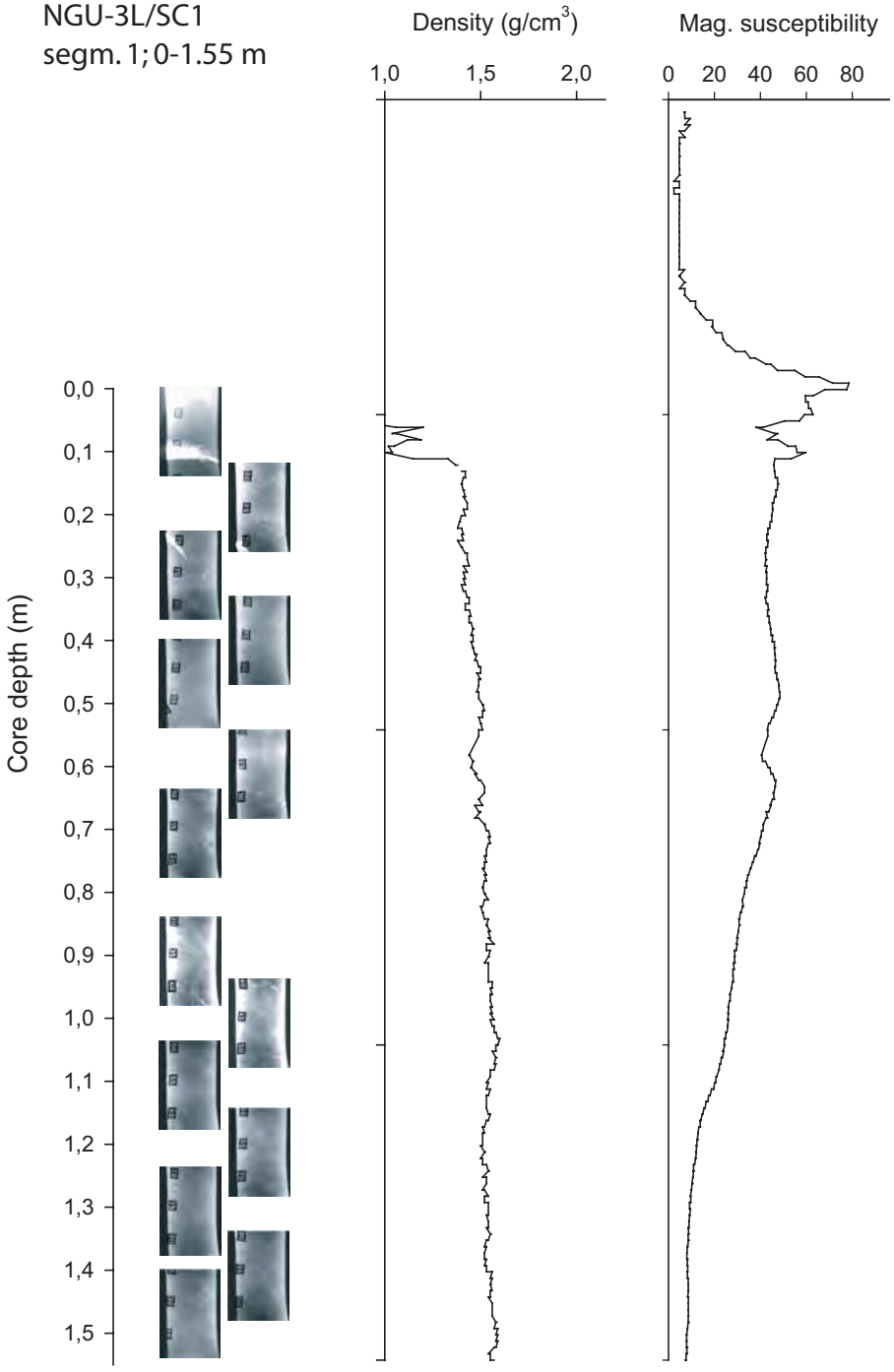
Sulafjorden
NGU-3L/SC1
segm. 1; 0-1.55 m
Density (g/cm3)
1,0
1,5
2,0
Mag. susceptibility
0
20
40
60
80
Core depth (m)
0,0
0,1
0,2
0,3
0,4
0,5
0,6
0,7
0,8
0,9
1,0
1,1
1,2
1,3
1,4
1,5

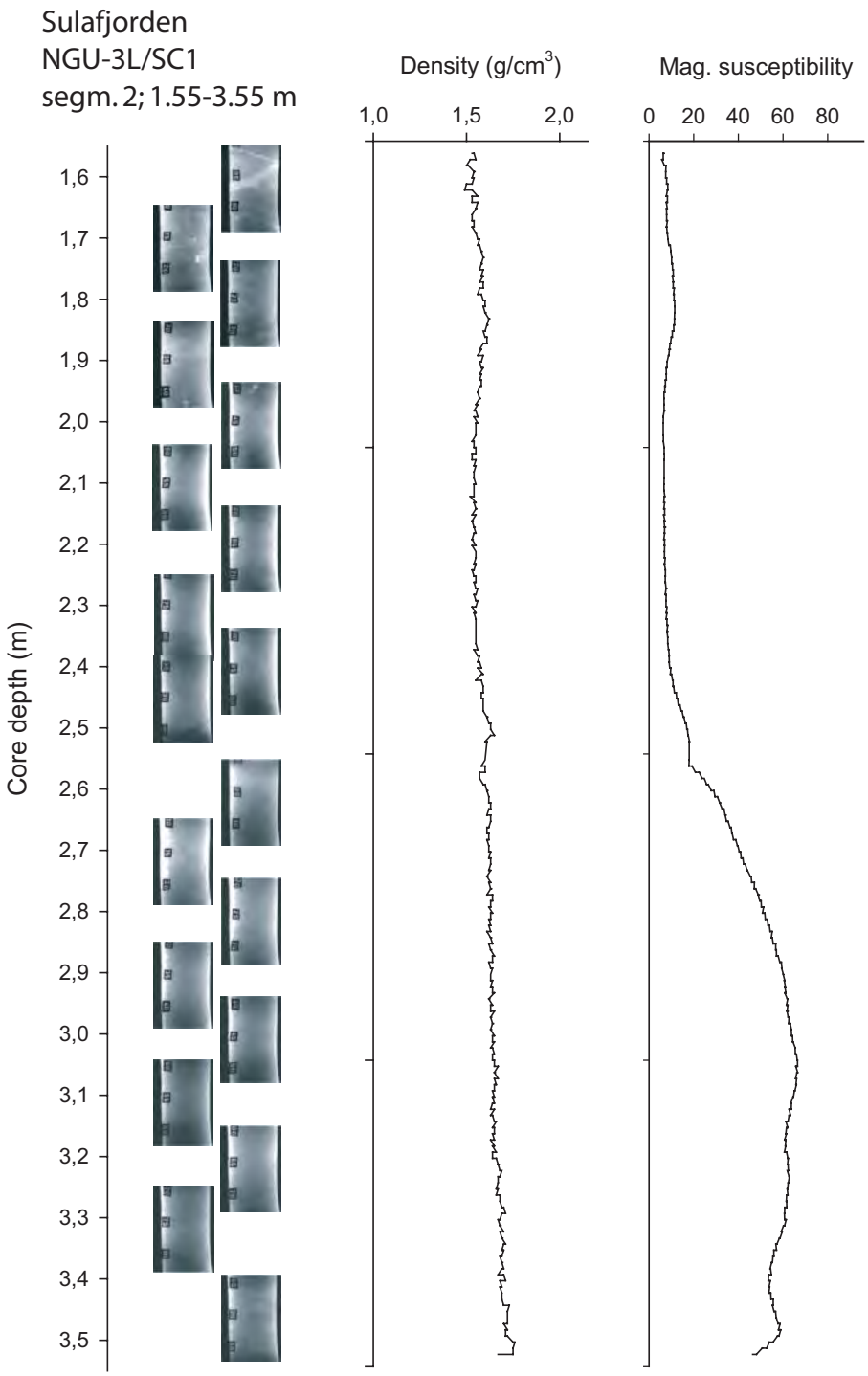
Sulafjorden
NGU-3L/SC1
segm. 2; 1.55-3.55 m
Density (g/cm3)
1,0
1,5
2,0
Mag. susceptibility
0
20
40
60
80
Core depth (m)
1,6
1,7
1,8
1,9
2,0
2,1
2,2
2,3
2,4
2,5
2,6
2,7
2,8
2,9
3,0
3,1
3,2
3,3
3,4
3,5

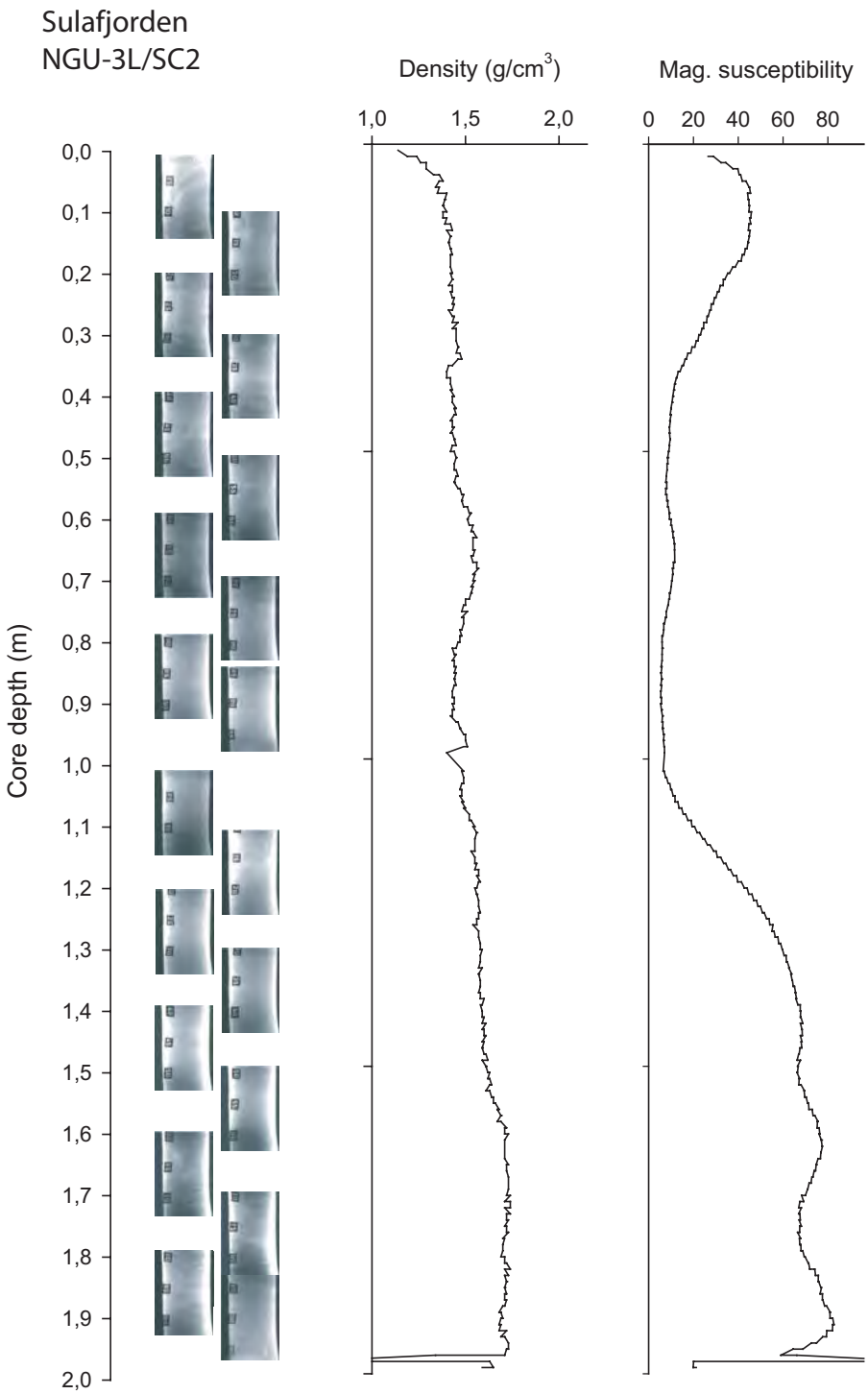
Sulafjorden
NGU-3L/SC2
Density (g/cm3)
Mag. susceptibility
1,0
1,5
2,0
0
20
40
60
80
Core depth (m)
0,0
0,1
0,2
0,3
0,4
0,5
0,6
0,7
0,8
0,9
1,0
1,1
1,2
1,3
1,4
1,5
1,6
1,7
1,8
1,9
2,0

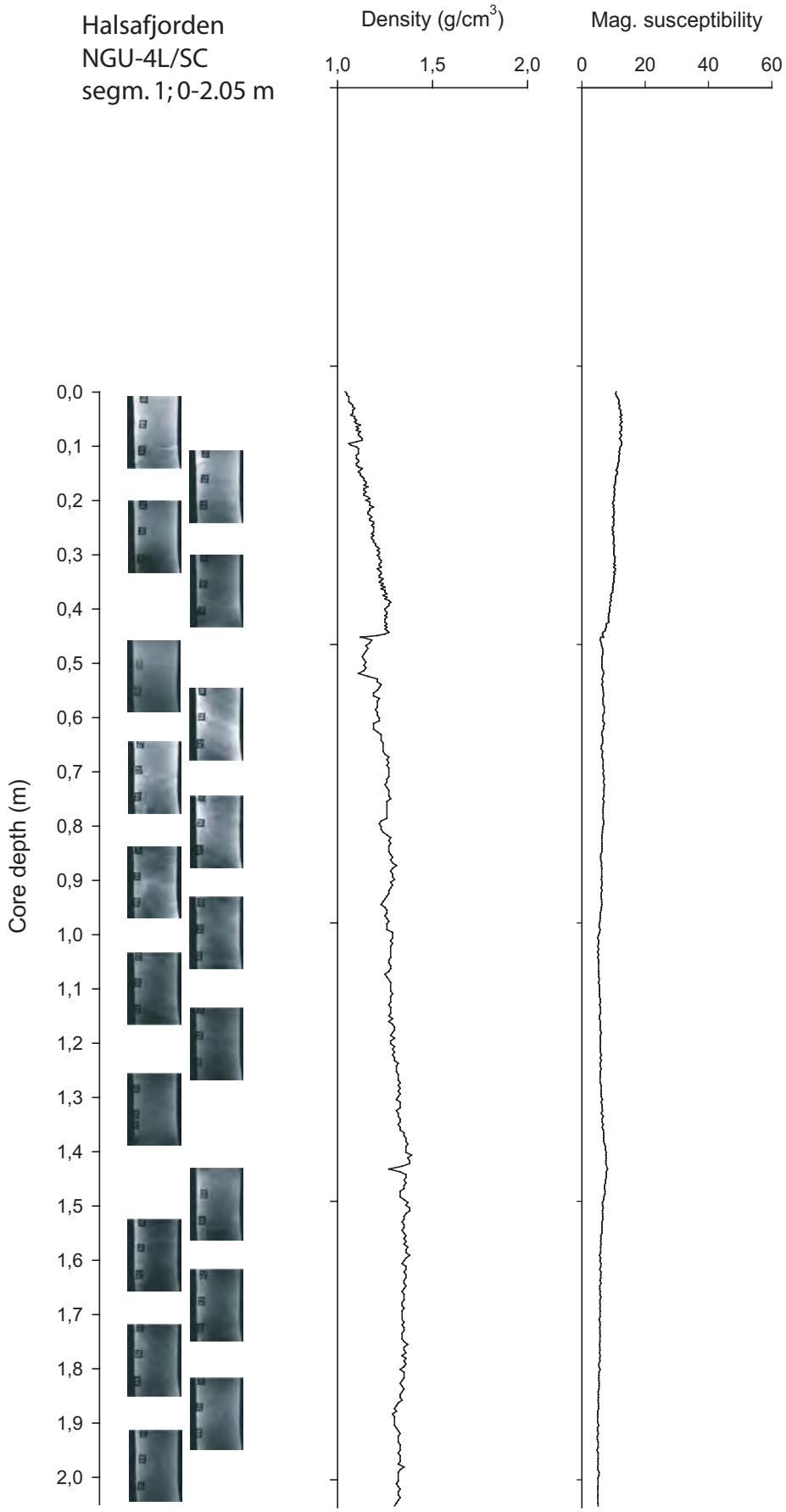
Halsafjorden
NGU-4L/SC
segm. 1; 0-2.05 m
Density (g/cm3)
1,0
1,5
2,0
Mag. susceptibility
0
20
40
60
Core depth (m)
0,0
0,1
0,2
0,3
0,4
0,5
0,6
0,7
0,8
0,9
1,0
1,1
1,2
1,3
1,4
1,5
1,6
1,7
1,8
1,9
2,0

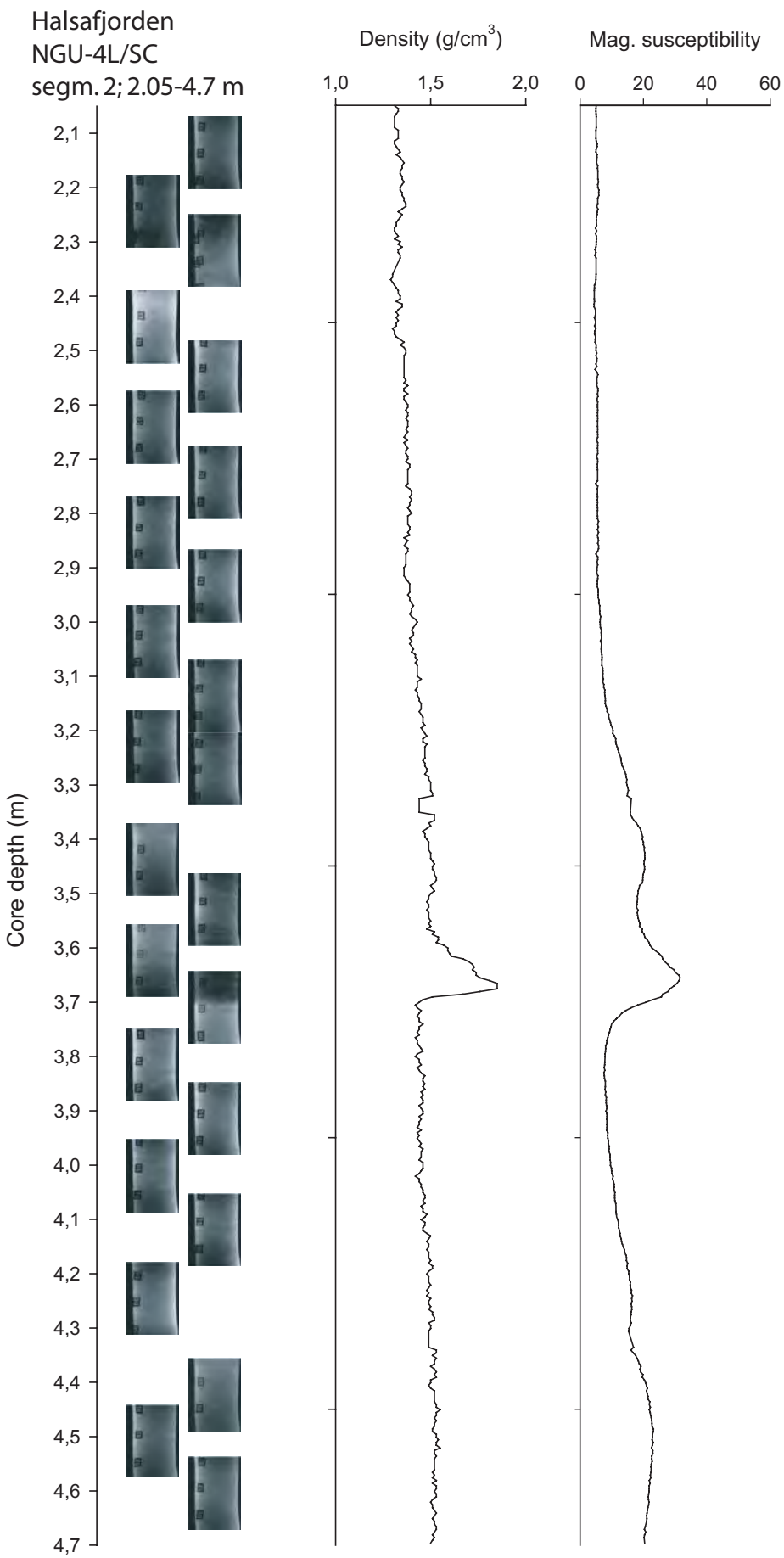
Halsafjorden
NGU-4L/SC
segm. 2; 2.05-4.7 m
Density (g/cm3)
Mag. susceptibility
1,0
1,5
2,0
0
20
40
60
Core depth (m)
2,1
2,2
2,3
2,4
2,5
2,6
2,7
2,8
2,9
3,0
3,1
3,2
3,3
3,4
3,5
3,6
3,7
3,8
3,9
4,0
4,1
4,2
4,3
4,4
4,5
4,6
4,7

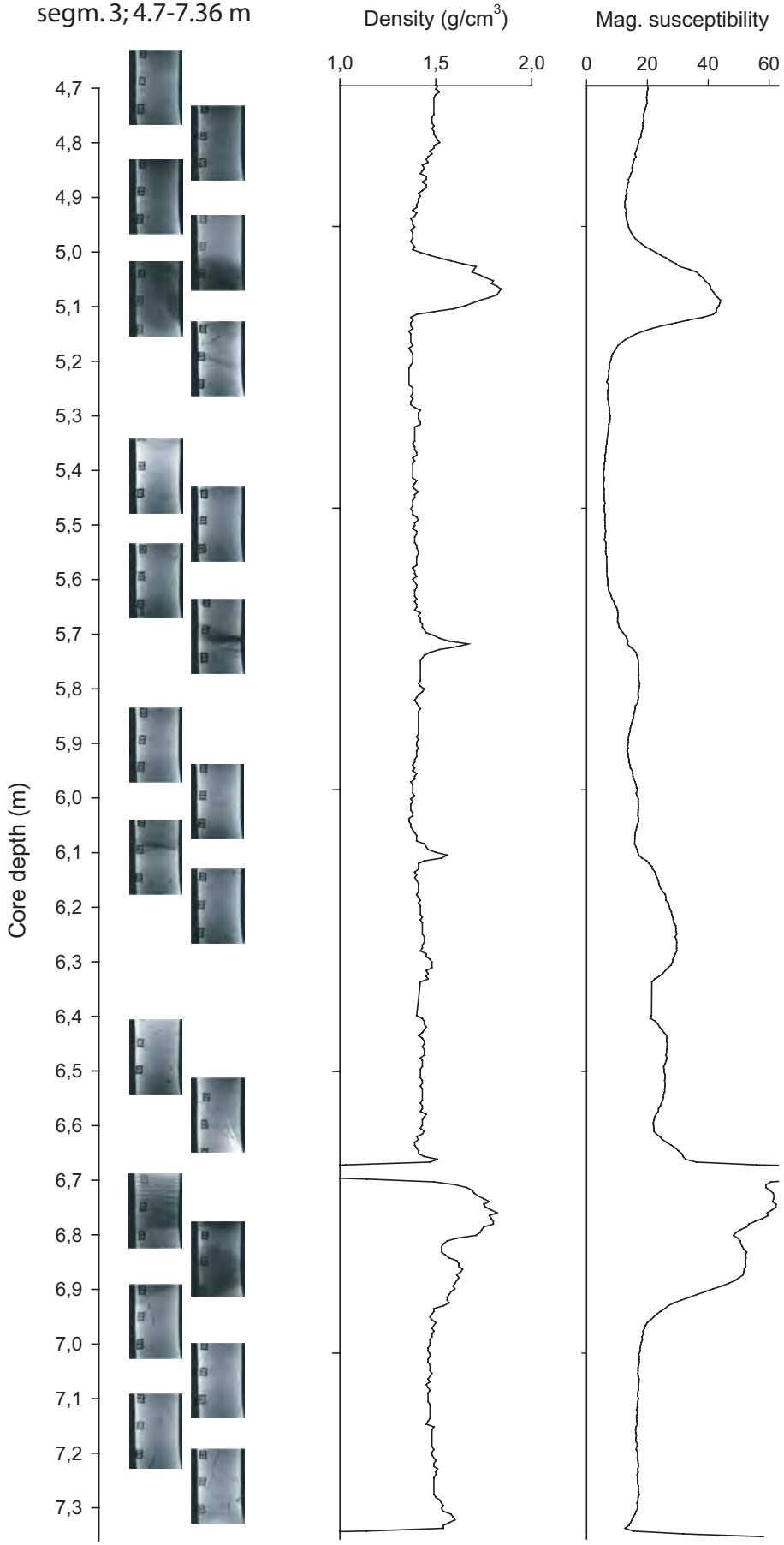
Halsafjorden
NGU-4L/SC
segm. 3; 4.7-7.36 m
Density (g/cm3)
Mag. susceptibility
1,0
1,5
2,0
0
20
40
60
Core depth (m)
4,7
4,8
4,9
5,0
5,1
5,2
5,3
5,4
5,5
5,6
5,7
5,8
5,9
6,0
6,1
6,2
6,3
6,4
6,5
6,6
6,7
6,8
6,9
7,0
7,1
7,2
7,3

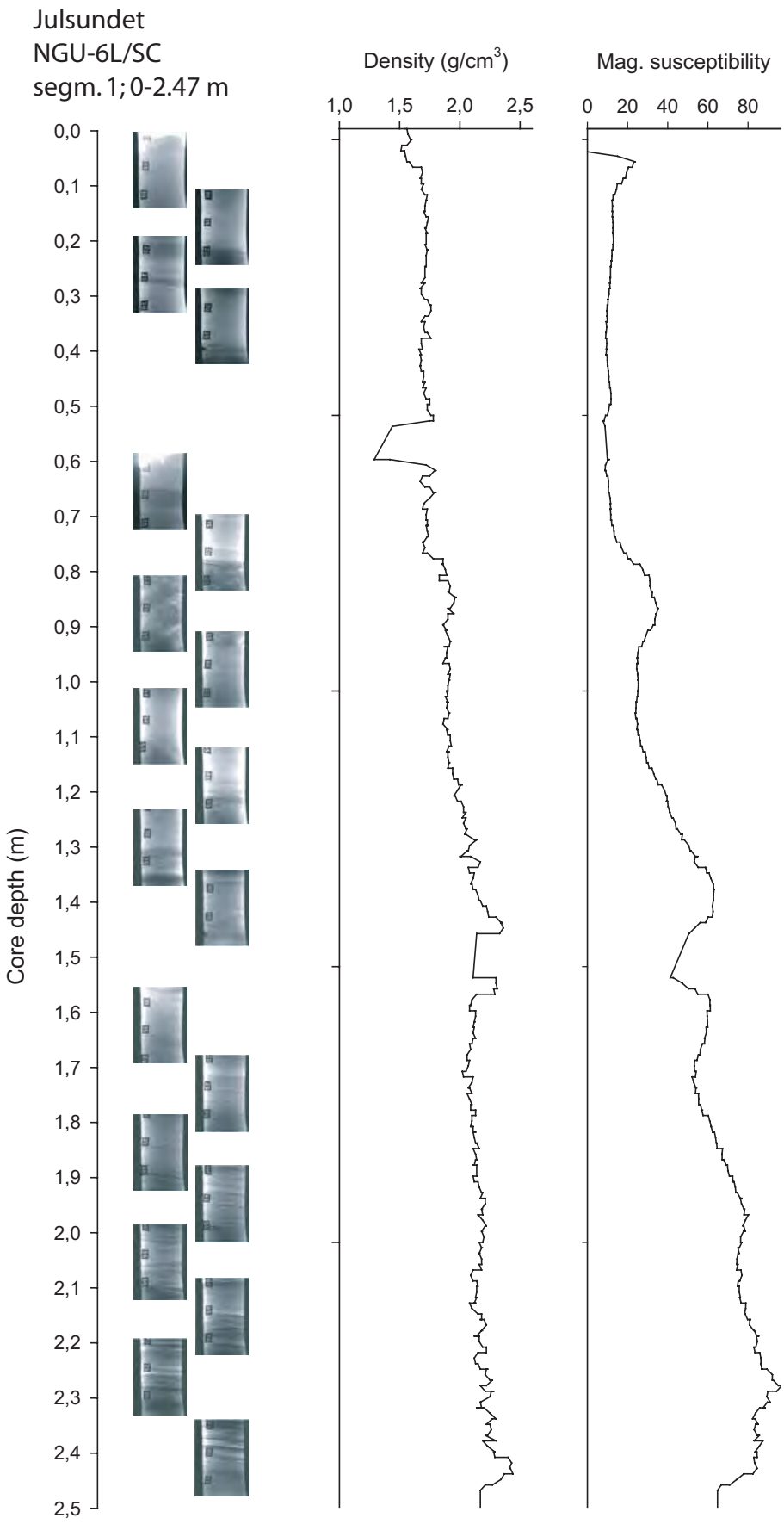
Julsundet
NGU-6L/SC
segm. 1; 0-2.47 m
Density (g/cm3)
Mag. susceptibility
Core depth (m)
1,0
1,5
2,0
2,5
0
20
40
60
80
0,0
0,1
0,2
0,3
0,4
0,5
0,6
0,7
0,8
0,9
1,0
1,1
1,2
1,3
1,4
1,5
1,6
1,7
1,8
1,9
2,0
2,1
2,2
2,3
2,4
2,5

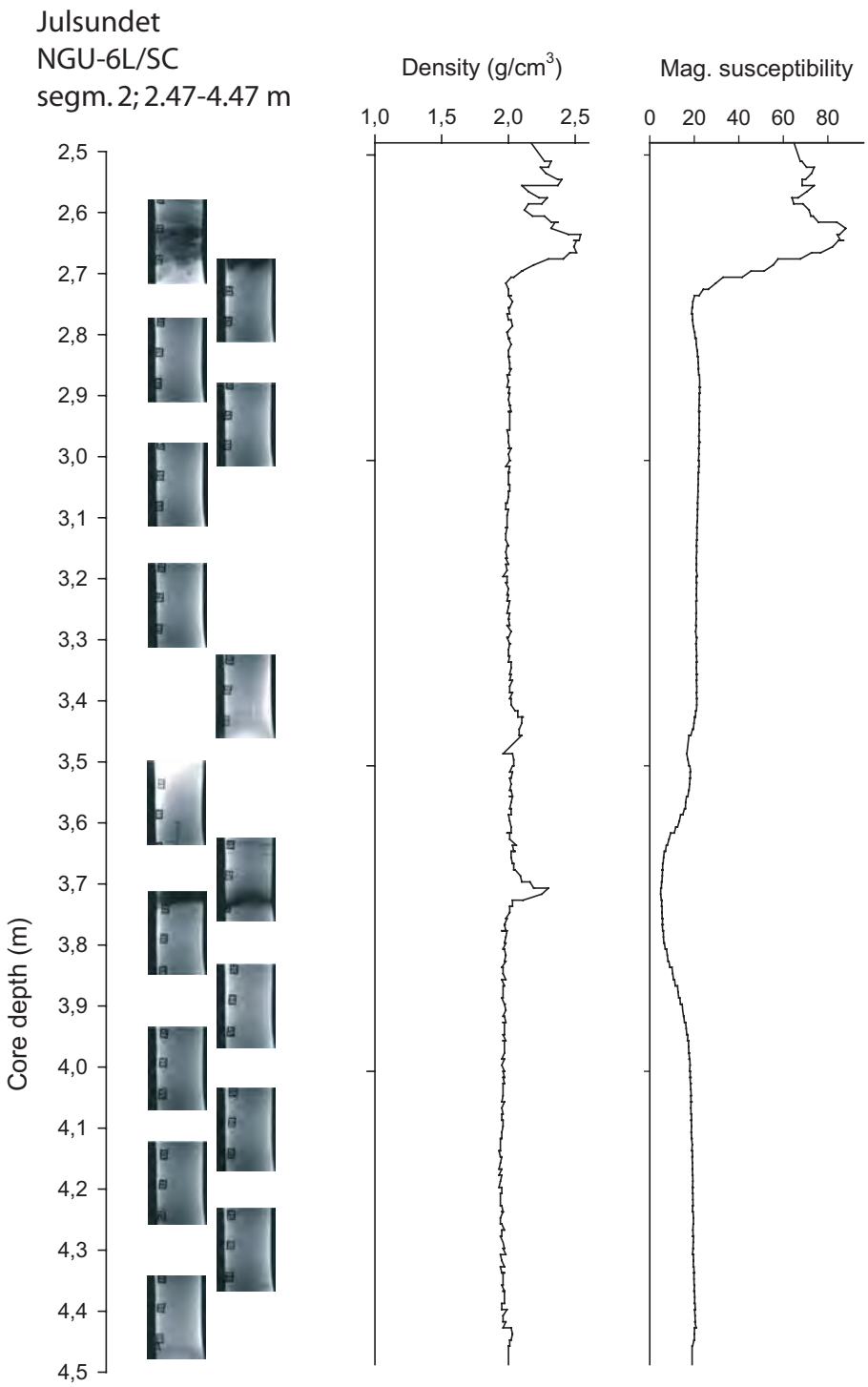
Julsundet
NGU-6L/SC
segm. 2; 2.47-4.47 m
Density (g/cm3)
1,0
1,5
2,0
2,5
Mag. susceptibility
0
20
40
60
80
Core depth (m)
2,5
2,6
2,7
2,8
2,9
3,0
3,1
3,2
3,3
3,4
3,5
3,6
3,7
3,8
3,9
4,0
4,1
4,2
4,3
4,4
4,5

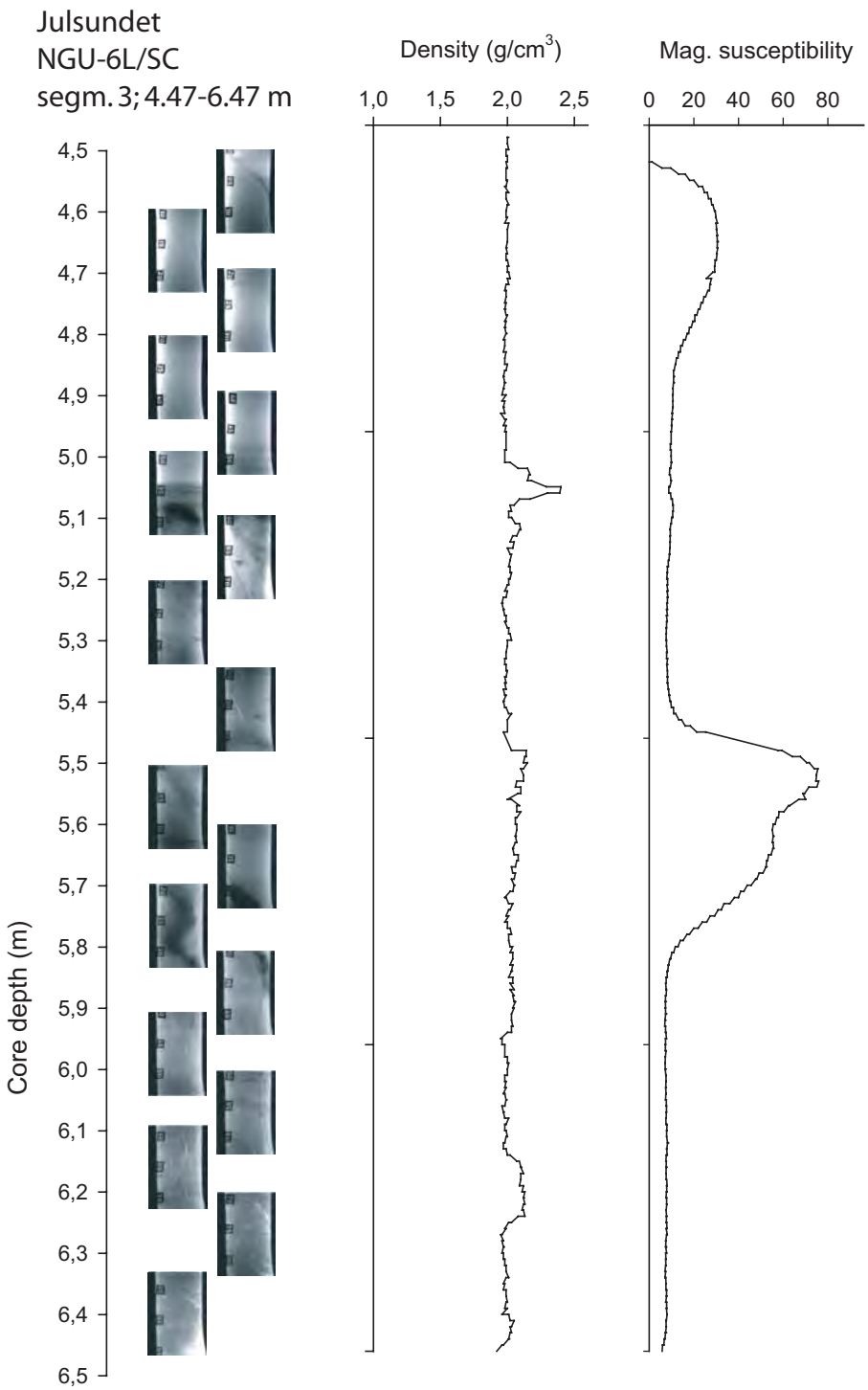
Julsundet
NGU-6L/SC
segm. 3; 4.47-6.47 m
Density (g/cm3)
Mag. susceptibility
1,0
1,5
2,0
2,5
0
20
40
60
80
Core depth (m)
4,5
4,6
4,7
4,8
4,9
5,0
5,1
5,2
5,3
5,4
5,5
5,6
5,7
5,8
5,9
6,0
6,1
6,2
6,3
6,4
6,5

APPENDIX 3

Stratigraphic profiles of the mean diameter in NGU-2L/SC, NGU-4L/SC and NGU-6L/SC and cumulative grain-size distribution plots and statistical characteristics of individual samples

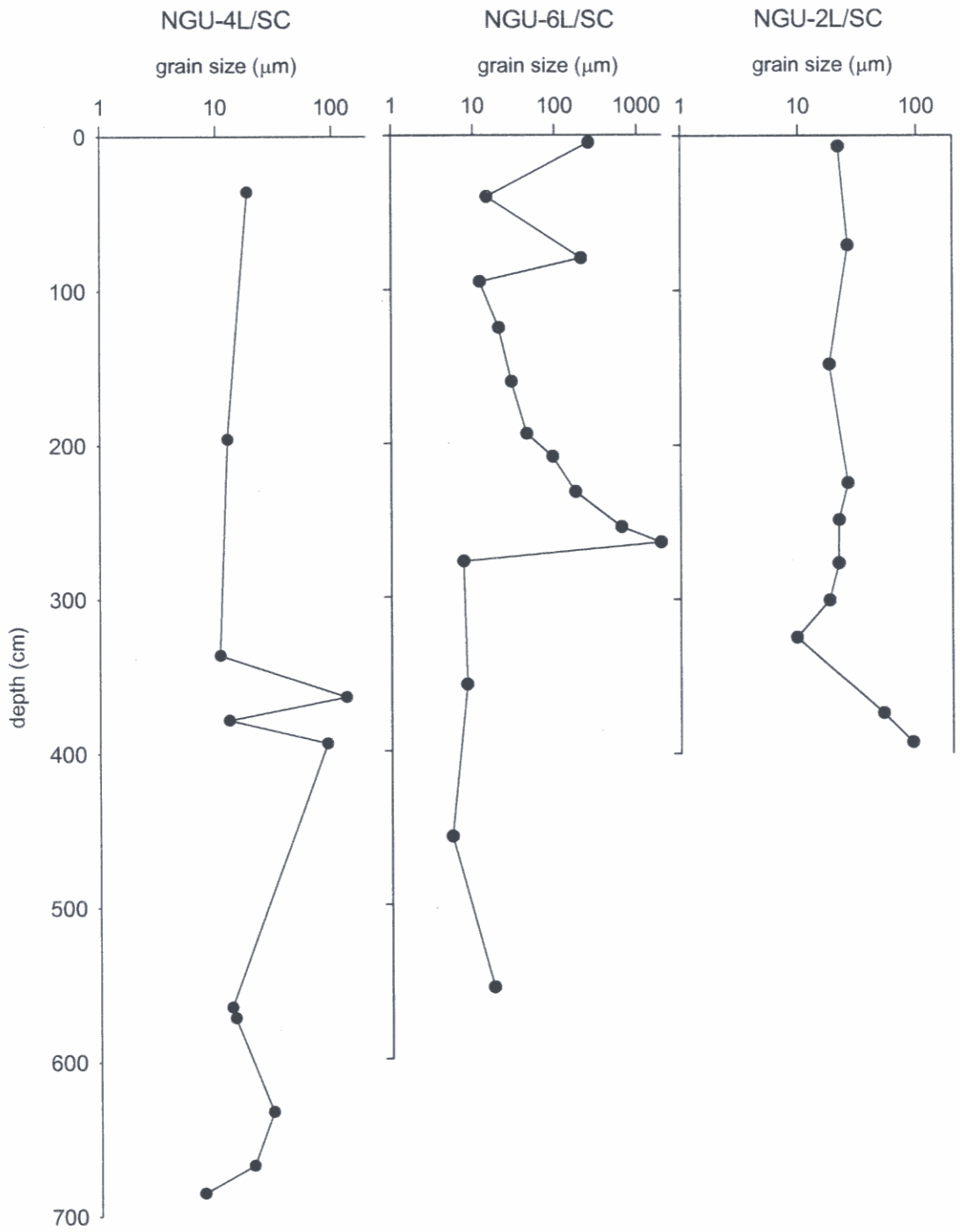
NGU-4L/SC
grain size (μm)
1
10
100
NGU-6L/SC
grain size (μm)
1
10
100
1000
NGU-2L/SC
grain size (μm)
1
10
100
depth (cm)
0
100
200
300
400
500
600
700

NGU-6L/SC:454-458

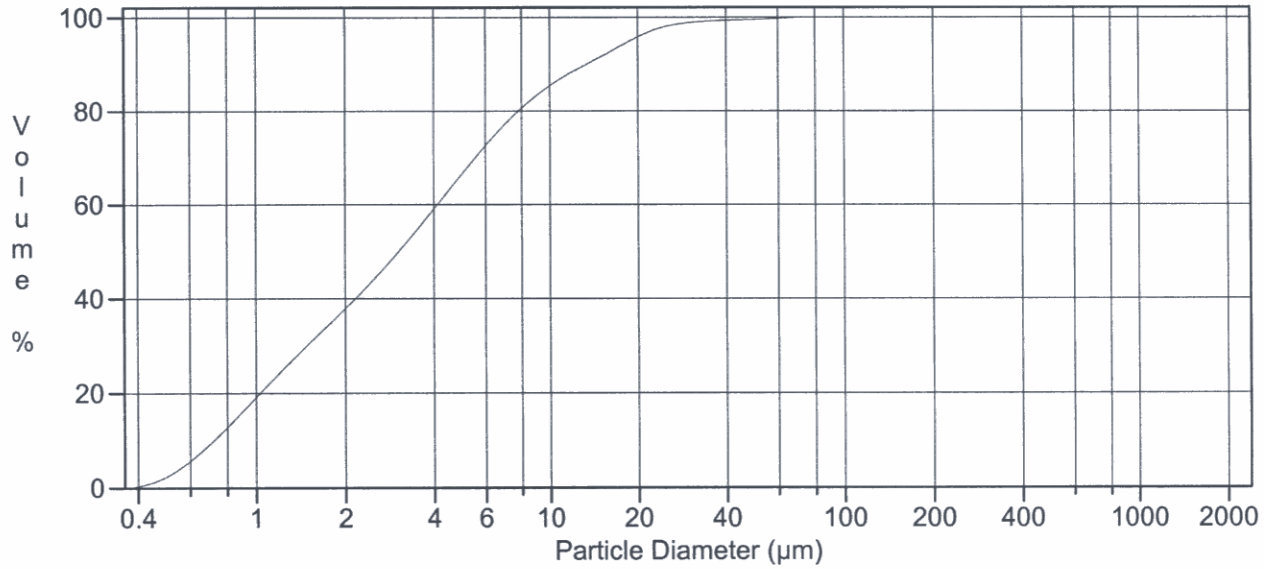

Volume Statistics (Arithmetic) 34.$02

Calculations from 0.375 µm to 2000 µm

Volume	100.0%		
Mean:	5.453 µm	95% Conf. Limits:	0-19.78 µm
Median:	3.048 µm	S.D.:	7.312 µm
D(3,2):	1.817 µm	Variance:	53.46 µm^2
Mean/Median Ratio:	1.789	C.V.:	134%
Mode:	4.444 µm	Skewness:	4.003 Right skewed
d_{10}:	0.722 µm	Kurtosis:	24.94 Leptokurtic
d_{50}:	3.048 µm		
d_{90}:	13.42 µm		
Specific Surf. Area	33022 cm^2/ml		

% <	10	25	60	75	90
Size µm	0.722	1.239	4.130	6.525	13.42

34.$02

Particle Diameter µm	Volume %
1.000	18.8
2.000	28.7
5.000	18.9
10.00	6.20
15.00	4.15
20.00	2.28
25.00	1.27
40.00	0.21
50.00	0.21
60.00	0.20
70.00	0.059
75.00	0.033
80.00	0.023
90.00	0.0022

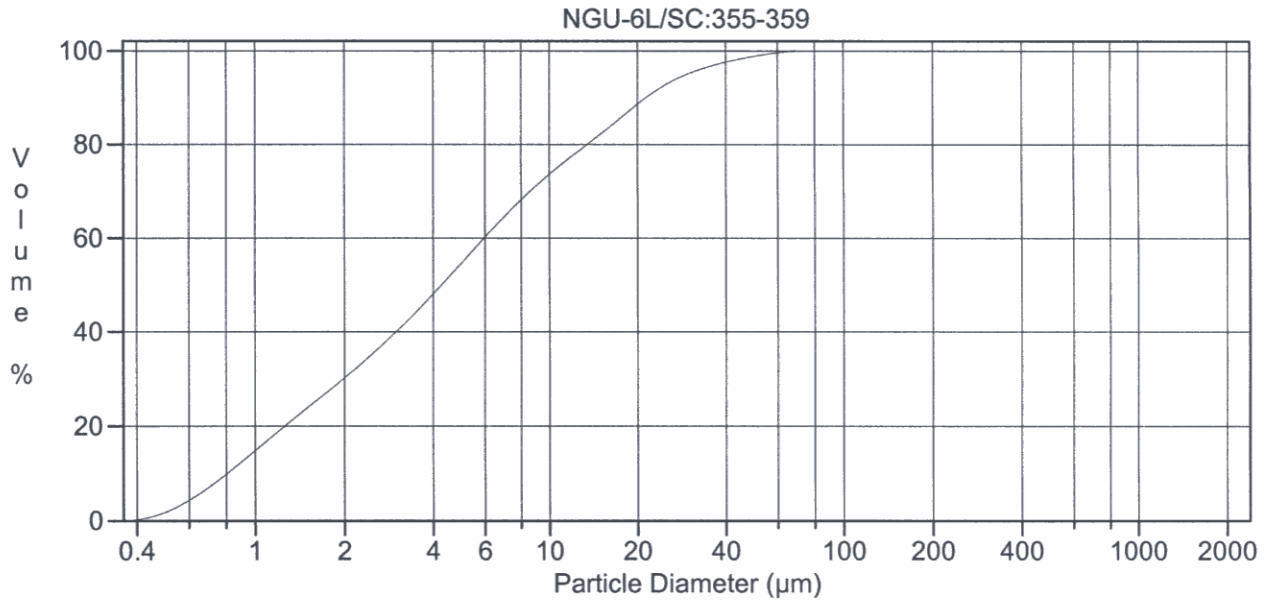

Volume Statistics (Arithmetic) 33#.$02

Calculations from 0.375 µm to 2000 µm

Volume	100.0%		
Mean:	8.340 µm	95% Conf. Limits:	0-29.02 µm
Median:	4.281 µm	S.D.:	10.55 µm
D(3,2):	2.212 µm	Variance:	111.3 µm^2
Mean/Median Ratio:	1.948	C.V.:	127%
Mode:	4.878 µm	Skewness:	2.478 Right skewed
d_{10}:	0.809 µm	Kurtosis:	7.604 Leptokurtic
d_{50}:	4.281 µm		
d_{90}:	21.52 µm		
Specific Surf. Area	27123 cm^2/ml		

% <	10	25	60	75	90
Size µm	0.809	1.586	5.981	10.64	21.52

33#.$02

Particle Diameter µm	Volume %
1.000	15.4
2.000	24.5
5.000	19.0
10.00	8.54
15.00	6.33
20.00	4.29
25.00	4.77
40.00	1.26
50.00	0.74
60.00	0.36
70.00	0.063
75.00	0.030
80.00	0.016
90.00	0.0011

NGU-6L/SC:275-279

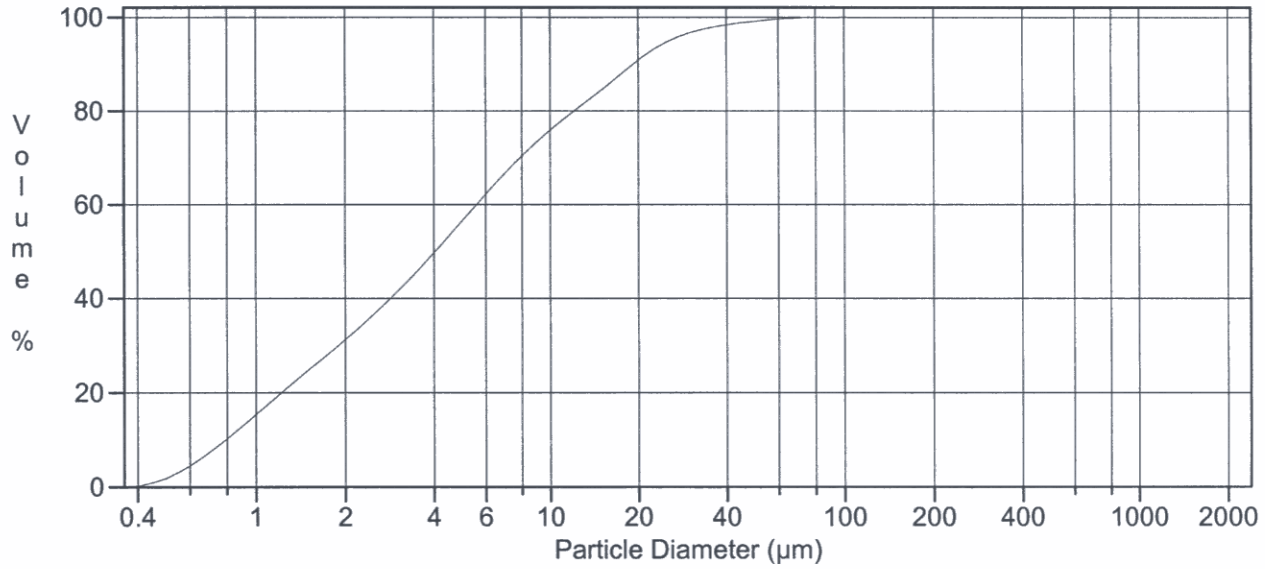

Volume Statistics (Arithmetic) 32.$02

Calculations from 0.375 µm to 2000 µm

Volume	100.0%		
Mean:	7.591 µm	95% Conf. Limits:	0-26.37 µm
Median:	4.056 µm	S.D.:	9.579 µm
D(3,2):	2.143 µm	Variance:	91.76 µm^2
Mean/Median Ratio:	1.871	C.V.:	126%
Mode:	4.878 µm	Skewness:	2.774 Right skewed
d_{10}:	0.794 µm	Kurtosis:	10.64 Leptokurtic
d_{50}:	4.056 µm		
d_{90}:	19.35 µm		
Specific Surf. Area	28004 cm^2/ml		

% <	10	25	60	75	90
Size µm	0.794	1.523	5.602	9.656	19.35

32.$02

Particle Diameter µm	Volume %
1.000	15.9
2.000	25.3
5.000	19.4
10.00	8.60
15.00	6.28
20.00	3.97
25.00	3.67
40.00	0.77
50.00	0.47
60.00	0.29
70.00	0.070
75.00	0.039
80.00	0.026
90.00	0.0026

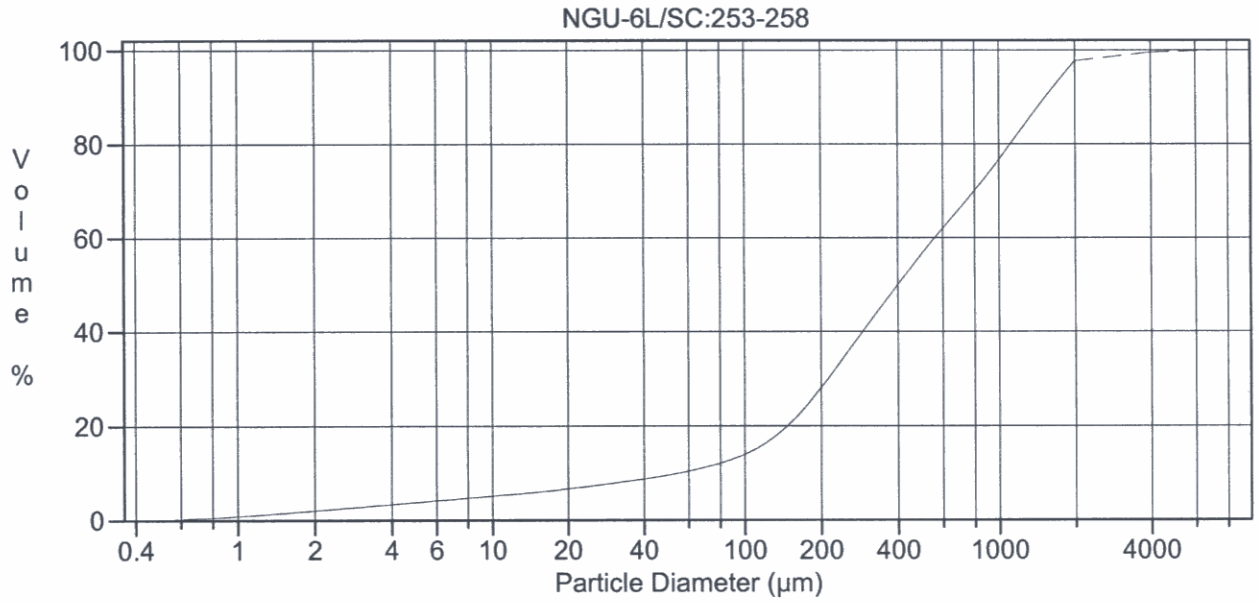

Volume Statistics (Arithmetic) 31a.$02

Calculations from 0.375 µm to 8000 µm

Volume	100.0%		
Mean:	644.9 µm	95% Conf. Limits:	0-2000 µm
Median:	402.0 µm	S.D.:	691.6 µm
D(3,2):	30.73 µm	Variance:	478302 µm^2
Mean/Median Ratio:	1.604	C.V.:	107%
Mode:	269.2 µm	Skewness:	2.663 Right skewed
d_{10}:	56.20 µm	Kurtosis:	12.87 Leptokurtic
d_{50}:	402.0 µm		
d_{90}:	1533 µm		
Specific Surf. Area	1952 cm^2/ml		

% <	10	25	60	75	90
Size µm	56.20	180.2	561.6	949.9	1533

31a.$02

Particle Diameter µm	Volume %
1.000	1.20
2.000	1.77
5.000	1.33
10.00	0.83
15.00	0.71
20.00	0.62
25.00	1.44
40.00	0.81
50.00	0.82
60.00	0.84
70.00	0.42
75.00	0.43
80.00	0.90
90.00	87.1

NGU-6L/SC:263-268

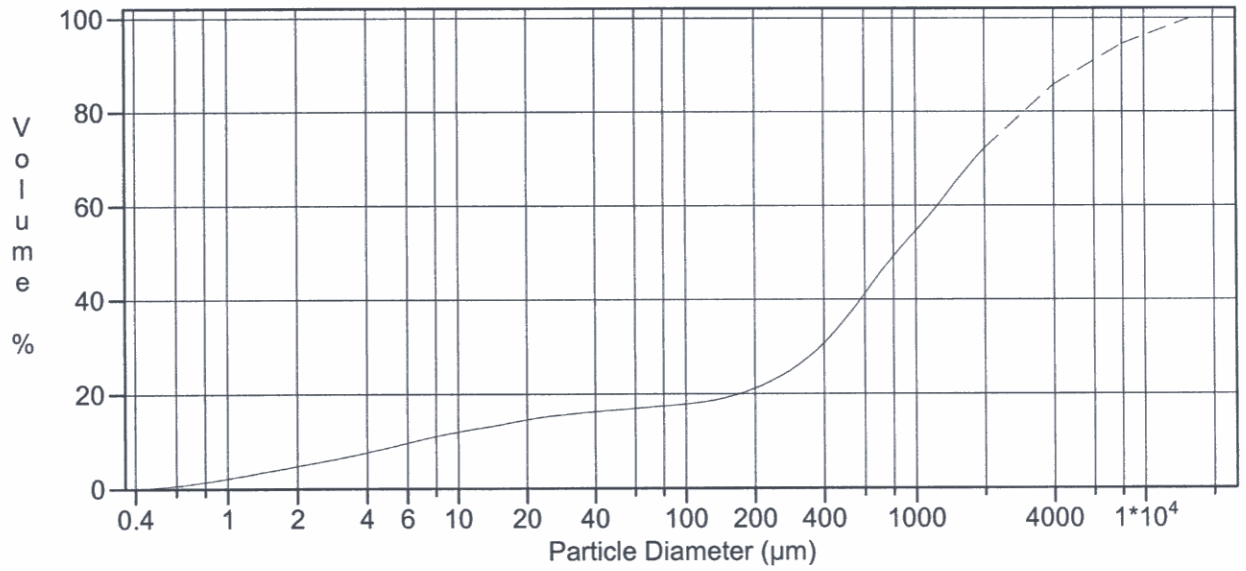

Volume Statistics (Arithmetic) 30#a.$02

Calculations from 0.375 µm to 16000 µm

Volume	100.0%		
Mean:	1954 µm	95% Conf. Limits:	0-7387 µm
Median:	831.1 µm	S.D.:	2772 µm
D(3,2):	14.05 µm	Variance:	7684742 µm^2
Mean/Median Ratio:	2.351	C.V.:	142%
Mode:	2828 µm	Skewness:	2.235 Right skewed
d_{10}:	6.498 µm	Kurtosis:	4.580 Leptokurtic
d_{50}:	831.1 µm		
d_{90}:	5975 µm		
Specific Surf. Area	4272 cm^2/ml		

% <	10	25	60	75	90
Size µm	6.498	287.6	1251	2423	5975

30#a.$02

Particle Diameter µm	Volume %
1.000	2.63
2.000	3.95
5.000	3.24
10.00	1.46
15.00	1.09
20.00	0.72
25.00	1.00
40.00	0.37
50.00	0.30
60.00	0.27
70.00	0.12
75.00	0.11
80.00	0.20
90.00	82.4

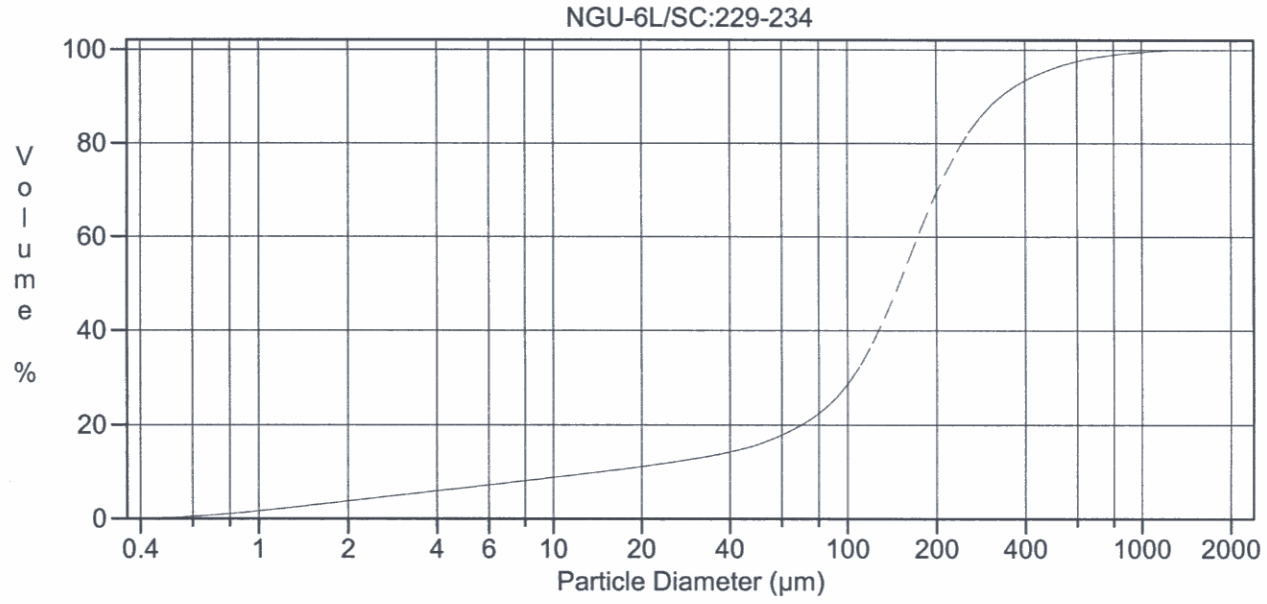

Volume Statistics (Arithmetic) 29#.$02

Calculations from 0.375 µm to 2000 µm

Volume	100.0%		
Mean:	177.0 µm	95% Conf. Limits:	0-483.0 µm
Median:	149.8 µm	S.D.:	156.1 µm
D(3,2):	16.76 µm	Variance:	24371 µm^2
Mean/Median Ratio:	1.182	C.V.:	88.2%
Mode:	168.8 µm	Skewness:	2.671 Right skewed
d_{10}:	14.88 µm	Kurtosis:	11.85 Leptokurtic
d_{50}:	149.8 µm		
d_{90}:	332.2 µm		
Specific Surf. Area	3580 cm^2/ml		

% <	10	25	60	75	90
Size µm	14.88	89.33	173.3	221.1	332.2

29#.$02

Particle Diameter µm	Volume %
1.000	2.14
2.000	2.85
5.000	2.17
10.00	1.28
15.00	1.02
20.00	0.88
25.00	2.23
40.00	1.67
50.00	1.94
60.00	2.15
70.00	1.18
75.00	1.27
80.00	2.83
90.00	74.8

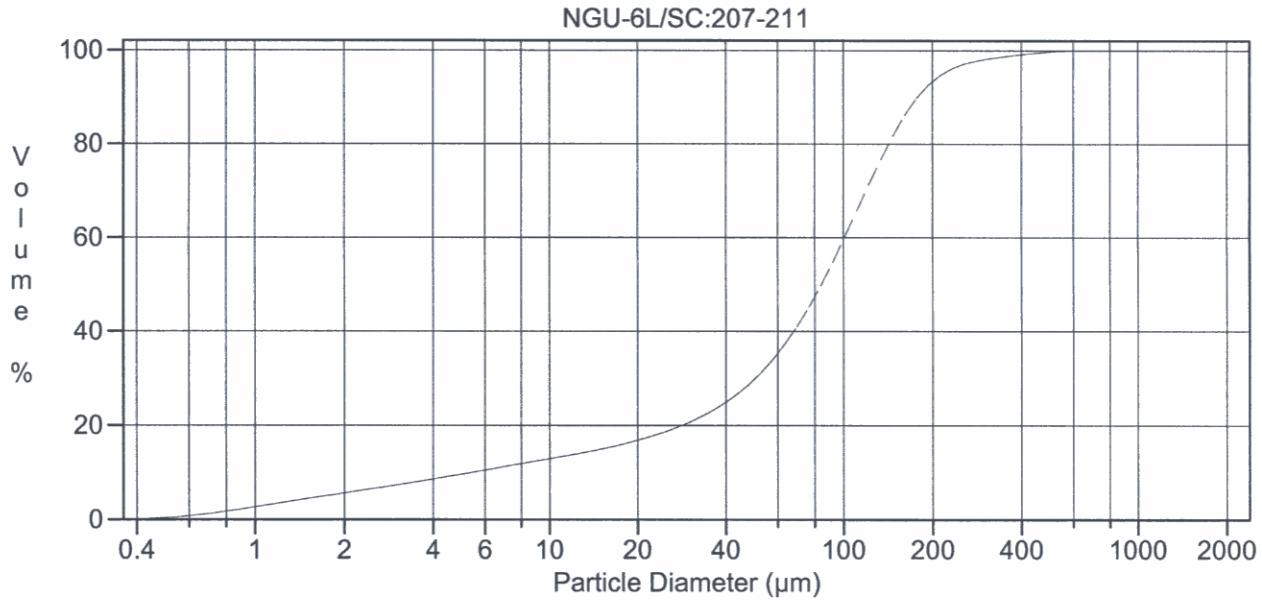

Volume Statistics (Arithmetic) 28.$02

Calculations from 0.375 µm to 2000 µm

Volume	100.0%		
Mean:	93.83 µm	95% Conf. Limits:	0-243.9 µm
Median:	84.40 µm	S.D.:	76.59 µm
D(3,2):	10.98 µm	Variance:	5866 μm^2
Mean/Median Ratio:	1.112	C.V.:	81.6%
Mode:	116.3 µm	Skewness:	1.862 Right skewed
d_{10}:	5.466 µm	Kurtosis:	6.989 Leptokurtic
d_{50}:	84.40 µm		
d_{90}:	178.4 µm		
Specific Surf. Area	5464 cm^2/ml		

% <	10	25	60	75	90
Size µm	5.466	40.40	101.0	130.2	178.4

28.$02

Particle Diameter µm	Volume %
1.000	3.00
2.000	3.99
5.000	3.29
10.00	2.04
15.00	1.88
20.00	1.87
25.00	6.16
40.00	4.90
50.00	5.50
60.00	5.92
70.00	3.06
75.00	3.08
80.00	6.15
90.00	46.6

NGU-6L/SC:191-196

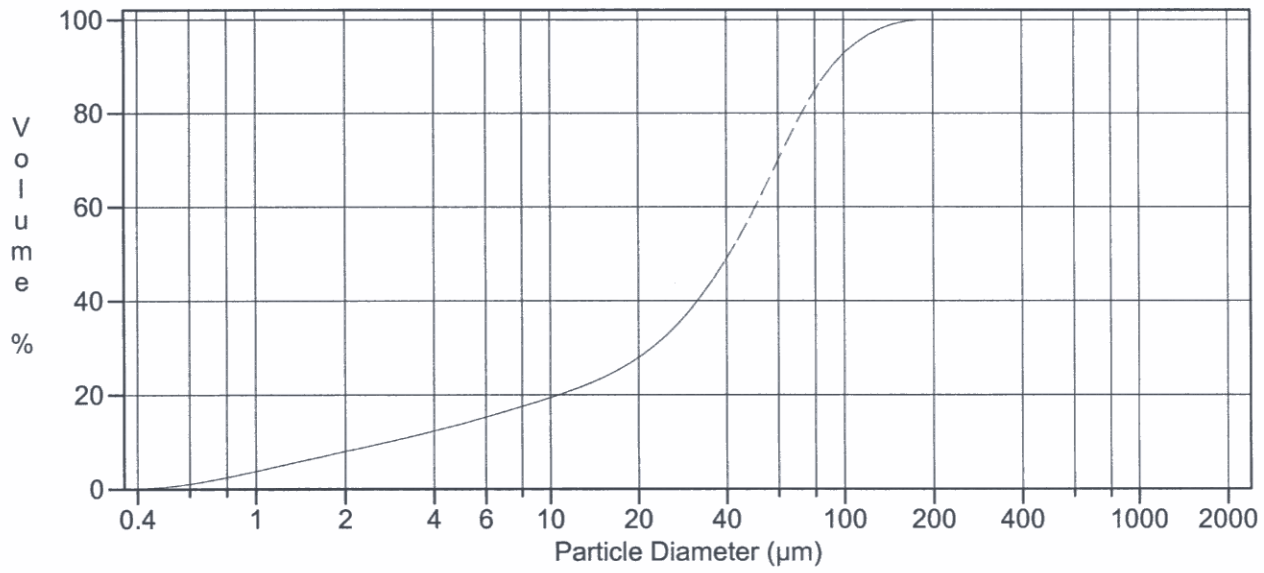

Volume Statistics (Arithmetic) 27.$02

Calculations from 0.375 µm to 2000 µm

Volume	100.0%		
Mean:	45.14 µm	95% Conf. Limits:	0-113.1 µm
Median:	41.04 µm	S.D.:	34.66 µm
D(3,2):	7.509 µm	Variance:	1201 μm^2
Mean/Median Ratio:	1.100	C.V.:	76.8%
Mode:	60.52 µm	Skewness:	0.833 Right skewed
d_{10}:	2.817 µm	Kurtosis:	0.564 Leptokurtic
d_{50}:	41.04 µm		
d_{90}:	91.41 µm		
Specific Surf. Area	7991 cm^2/ml		

% <	10	25	60	75	90
Size µm	2.817	16.81	50.29	65.87	91.41

27.$02

Particle Diameter µm	Volume %
1.000	4.25
2.000	5.93
5.000	5.52
10.00	4.11
15.00	4.33
20.00	4.83
25.00	16.2
40.00	10.8
50.00	10.1
60.00	8.58
70.00	3.46
75.00	2.94
80.00	4.66
90.00	10.6

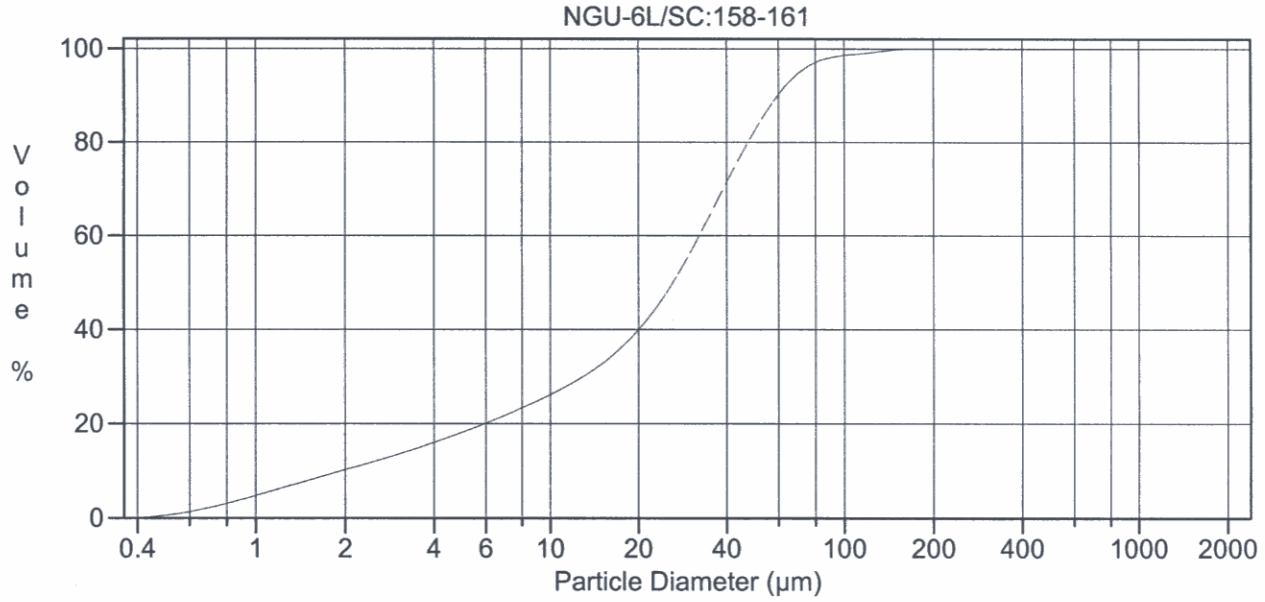

Volume Statistics (Arithmetic) 26.$02

Calculations from 0.375 µm to 2000 µm

Volume	100.0%		
Mean:	29.47 µm	95% Conf. Limits:	0-77.43 µm
Median:	26.33 µm	S.D.:	24.47 µm
D(3,2):	5.845 µm	Variance:	598.5 µm^2
Mean/Median Ratio:	1.120	C.V.:	83.0%
Mode:	37.96 µm	Skewness:	1.407 Right skewed
d_{10}:	1.968 µm	Kurtosis:	3.796 Leptokurtic
d_{50}:	26.33 µm		
d_{90}:	59.84 µm		
Specific Surf. Area	10265 cm^2/ml		

% <	10	25	60	75	90
Size µm	1.968	9.181	32.40	42.95	59.84

26.$02

Particle Diameter µm	Volume %
1.000	5.45
2.000	7.97
5.000	8.01
10.00	6.50
15.00	7.19
20.00	7.99
25.00	23.5
40.00	11.3
50.00	7.58
60.00	4.64
70.00	1.34
75.00	0.93
80.00	1.08
90.00	1.92

NGU-6L/SC:123-126

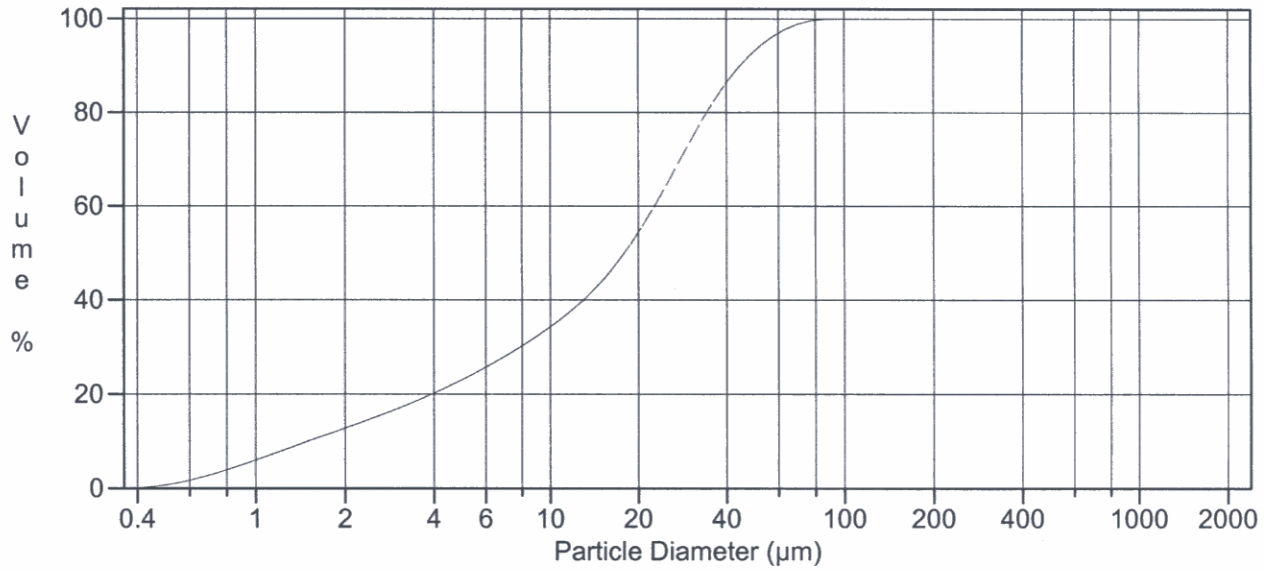

Volume Statistics (Arithmetic) 25#.$02

Calculations from 0.375 µm to 2000 µm

Volume	100.0%		
Mean:	20.77 µm	95% Conf. Limits:	0-54.41 µm
Median:	18.01 µm	S.D.:	17.17 µm
D(3,2):	4.688 µm	Variance:	294.7 µm^2
Mean/Median Ratio:	1.153	C.V.:	82.7%
Mode:	28.69 µm	Skewness:	0.931 Right skewed
d_{10}:	1.514 µm	Kurtosis:	0.541 Leptokurtic
d_{50}:	18.01 µm		
d_{90}:	44.66 µm		
Specific Surf. Area	12800 cm^2/ml		

% <	10	25	60	75	90
Size µm	1.514	5.758	22.80	30.97	44.66

25#.$02

Particle Diameter µm	Volume %
1.000	6.79
2.000	10.3
5.000	11.2
10.00	9.67
15.00	10.3
20.00	10.2
25.00	21.9
40.00	6.82
50.00	3.73
60.00	2.02
70.00	0.51
75.00	0.31
80.00	0.26
90.00	0.049

NGU-6L/SC:93-96

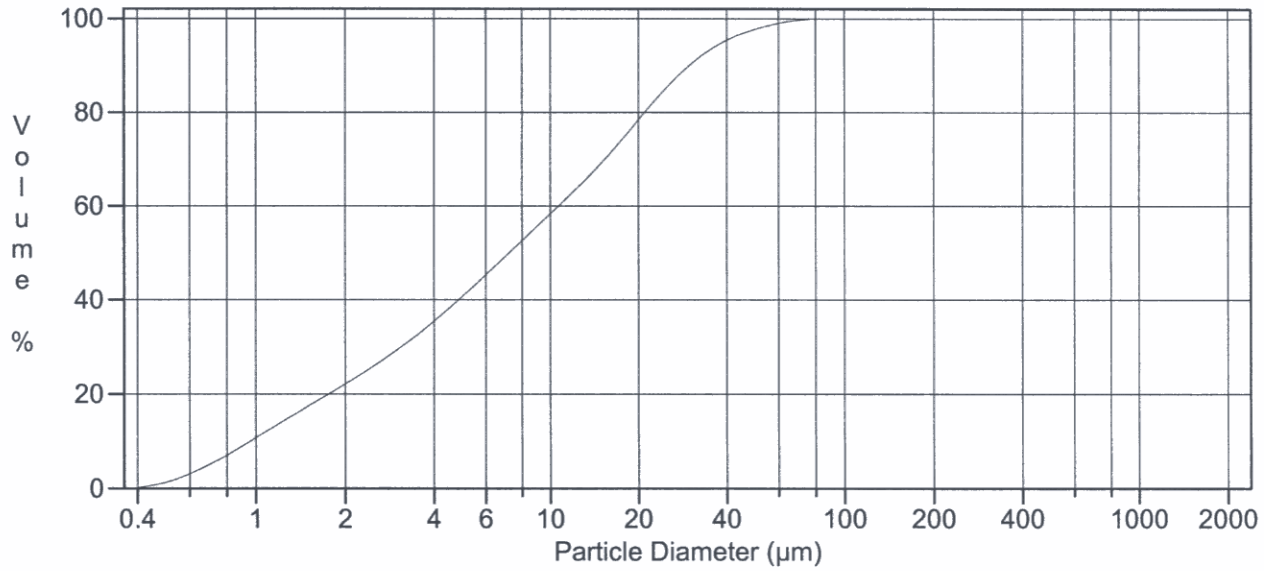

Volume Statistics (Arithmetic) 24.$02

Calculations from 0.375 µm to 2000 µm

Volume	100.0%		
Mean:	12.20 µm	95% Conf. Limits:	0-38.04 µm
Median:	7.247 µm	S.D.:	13.18 µm
D(3,2):	2.885 µm	Variance:	173.7 µm^2
Mean/Median Ratio:	1.684	C.V.:	108%
Mode:	19.76 µm	Skewness:	1.755 Right skewed
d_{10}:	0.962 µm	Kurtosis:	3.538 Leptokurtic
d_{50}:	7.247 µm		
d_{90}:	29.90 µm		
Specific Surf. Area	20799 cm^2/ml		

% <	10	25	60	75	90
Size µm	0.962	2.381	10.71	18.12	29.90

24.$02

Particle Diameter µm	Volume %
1.000	11.4
2.000	18.6
5.000	17.6
10.00	10.9
15.00	9.12
20.00	7.06
25.00	10.0
40.00	2.36
50.00	1.27
60.00	0.71
70.00	0.16
75.00	0.090
80.00	0.060
90.00	0.0060

NGU-6L/SC:77-82

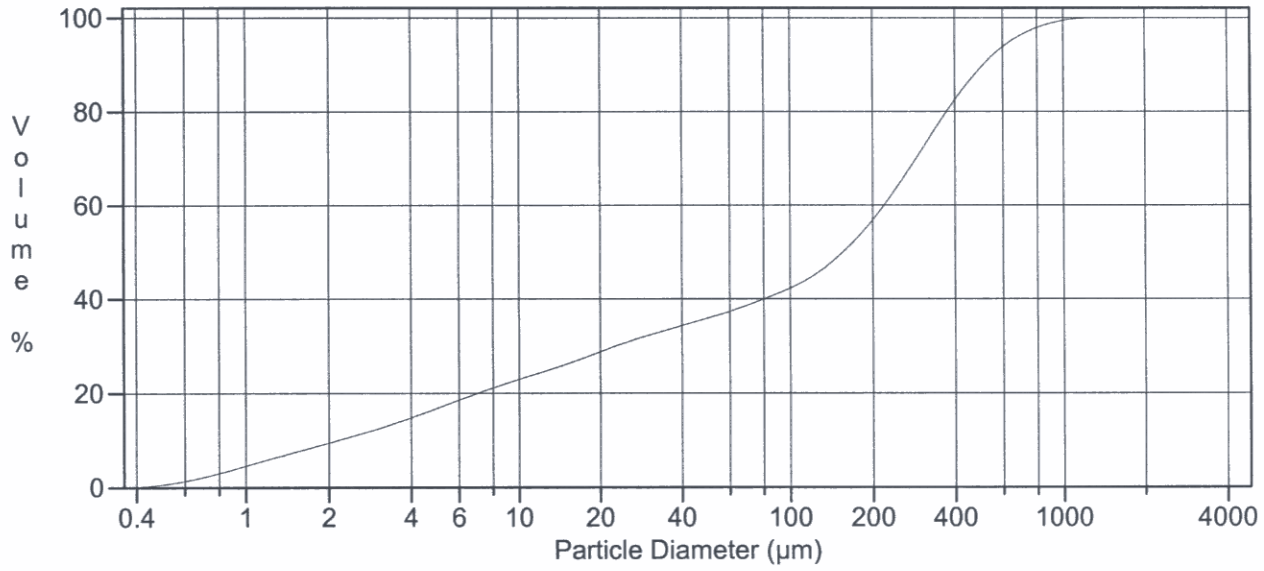

Volume Statistics (Arithmetic) 23a.$02

Calculations from 0.375 µm to 4000 µm

Volume	100.0%		
Mean:	209.3 µm	95% Conf. Limits:	0-653.2 µm
Median:	156.8 µm	S.D.:	226.5 µm
D(3,2):	6.930 µm	Variance:	51281 µm^2
Mean/Median Ratio:	1.335	C.V.:	108%
Mode:	295.5 µm	Skewness:	1.803 Right skewed
d_{10}:	2.189 µm	Kurtosis:	8.386 Leptokurtic
d_{50}:	156.8 µm		
d_{90}:	511.1 µm		
Specific Surf. Area	8658 cm^2/ml		

% <	10	25	60	75	90
Size µm	2.189	13.15	221.0	328.3	511.1

23a.$02

Particle Diameter µm	Volume %
1.000	4.88
2.000	7.40
5.000	6.11
10.00	3.19
15.00	2.64
20.00	2.01
25.00	3.54
40.00	1.57
50.00	1.43
60.00	1.36
70.00	0.64
75.00	0.61
80.00	1.18
90.00	58.9

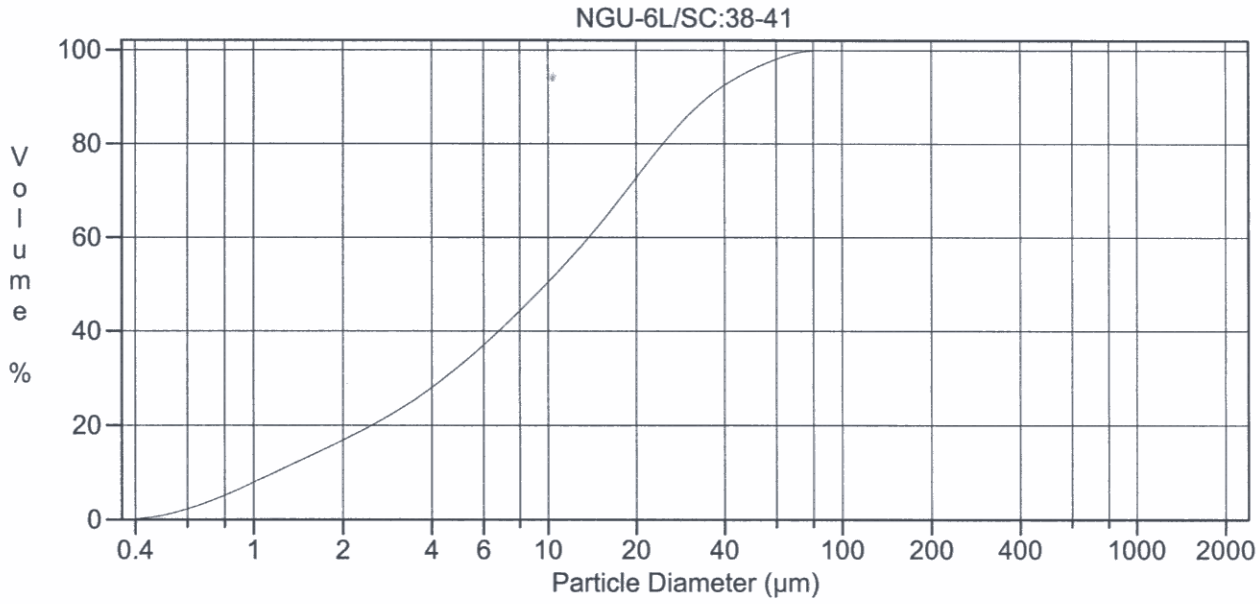

Volume Statistics (Arithmetic) 22.$02

Calculations from 0.375 µm to 2000 µm

Volume	100.0%		
Mean:	14.83 µm	95% Conf. Limits:	0-44.24 µm
Median:	9.860 µm	S.D.:	15.01 µm
D(3,2):	3.568 µm	Variance:	225.2 μm^2
Mean/Median Ratio:	1.504	C.V.:	101%
Mode:	19.76 µm	Skewness:	1.578 Right skewed
d_{10}:	1.186 µm	Kurtosis:	2.529 Leptokurtic
d_{50}:	9.860 µm		
d_{90}:	35.43 µm		
Specific Surf. Area	16818 cm^2/ml		

% <	10	25	60	75	90
Size µm	1.186	3.428	13.83	21.44	35.43

22.$02

Particle Diameter µm	Volume %
1.000	8.96
2.000	15.8
5.000	17.8
10.00	12.2
15.00	9.94
20.00	7.79
25.00	12.1
40.00	3.41
50.00	2.16
60.00	1.32
70.00	0.32
75.00	0.18
80.00	0.13
90.00	0.013

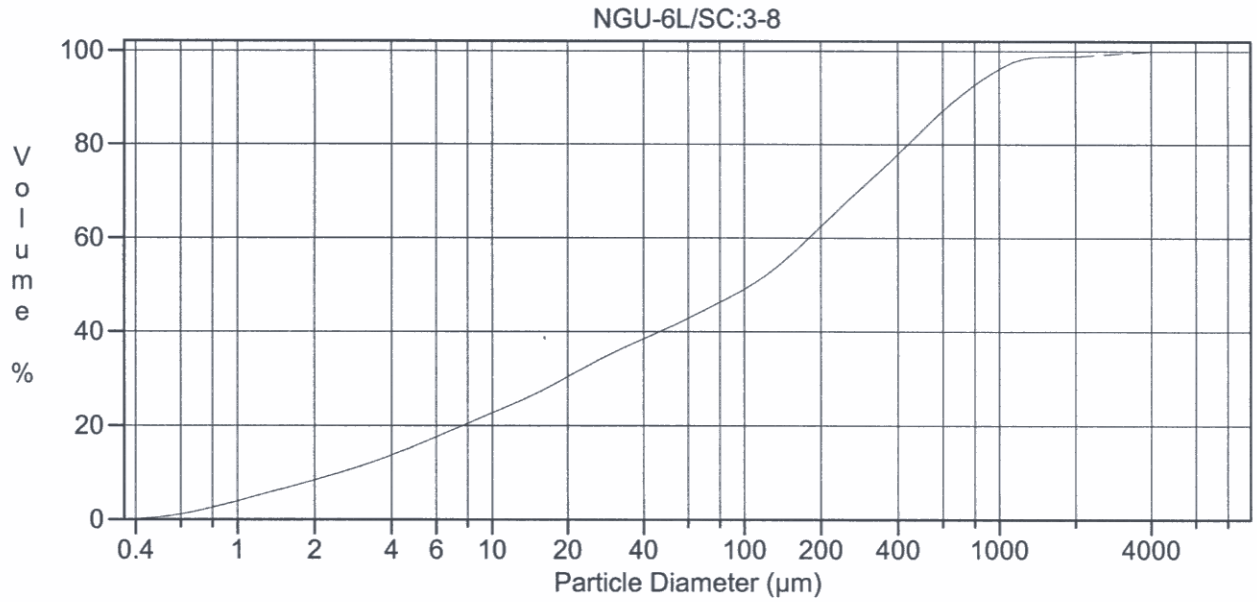

Volume Statistics (Arithmetic) 21a.$02

Calculations from 0.375 µm to 8000 µm

Volume	100.0%		
Mean:	258.6 µm	95% Conf. Limits:	0-1102 µm
Median:	107.6 µm	S.D.:	430.6 µm
D(3,2):	7.412 µm	Variance:	185378 µm^2
Mean/Median Ratio:	2.403	C.V.:	167%
Mode:	471.1 µm	Skewness:	4.838 Right skewed
d_{10}:	2.540 µm	Kurtosis:	38.85 Leptokurtic
d_{50}:	107.6 µm		
d_{90}:	692.7 µm		
Specific Surf. Area	8095 cm^2/ml		

% <	10	25	60	75	90
Size µm	2.540	12.66	179.8	353.9	692.7

21a.$02

Particle Diameter µm	Volume %
1.000	4.49
2.000	7.35
5.000	6.91
10.00	4.19
15.00	3.52
20.00	2.82
25.00	5.26
40.00	2.31
50.00	2.02
60.00	1.83
70.00	0.83
75.00	0.77
80.00	1.44
90.00	52.4

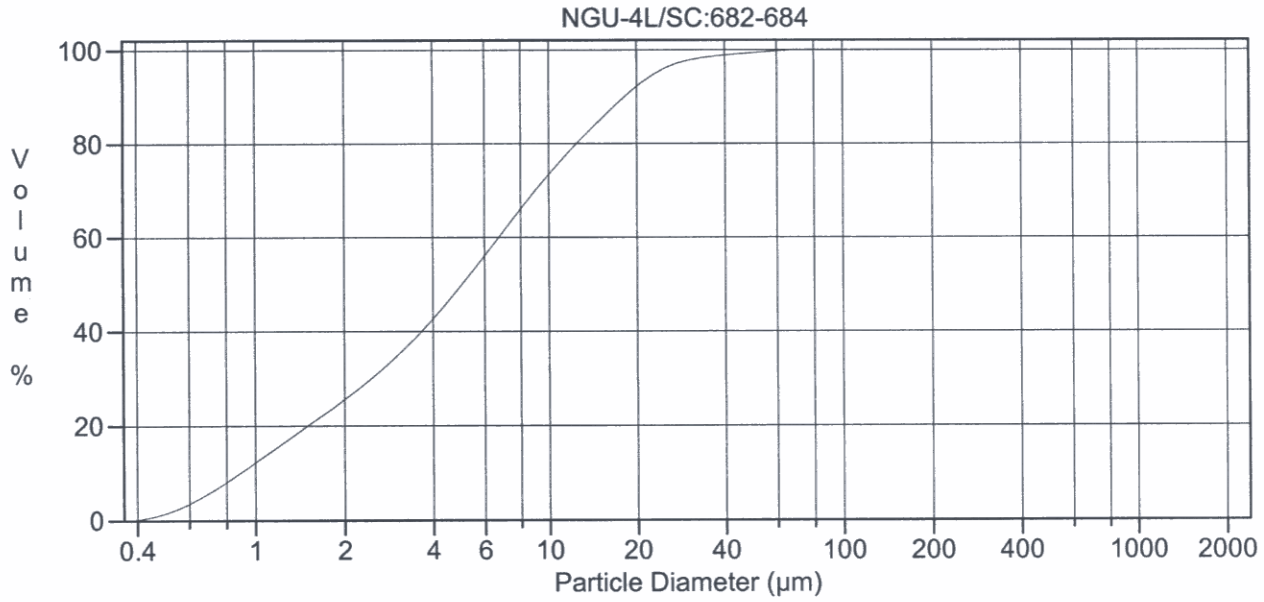

Volume Statistics (Arithmetic) 18.$02

Calculations from 0.375 µm to 2000 µm

Volume	100.0%		
Mean:	7.801 µm	95% Conf. Limits:	0-24.71 µm
Median:	5.043 µm	S.D.:	8.627 µm
D(3,2):	2.476 µm	Variance:	74.43 µm^2
Mean/Median Ratio:	1.547	C.V.:	111%
Mode:	6.452 µm	Skewness:	2.712 Right skewed
d_{10}:	0.893 µm	Kurtosis:	11.46 Leptokurtic
d_{50}:	5.043 µm		
d_{90}:	18.28 µm		
Specific Surf. Area	24236 cm^2/ml		

% <	10	25	60	75	90
Size µm	0.893	1.955	6.736	10.56	18.28

18.$02

Particle Diameter µm	Volume %
1.000	13.3
2.000	24.2
5.000	23.6
10.00	11.6
15.00	7.12
20.00	3.96
25.00	2.76
40.00	0.51
50.00	0.38
60.00	0.23
70.00	0.046
75.00	0.022
80.00	0.012
90.00	0.00090

NGU-4L/SC:665-668

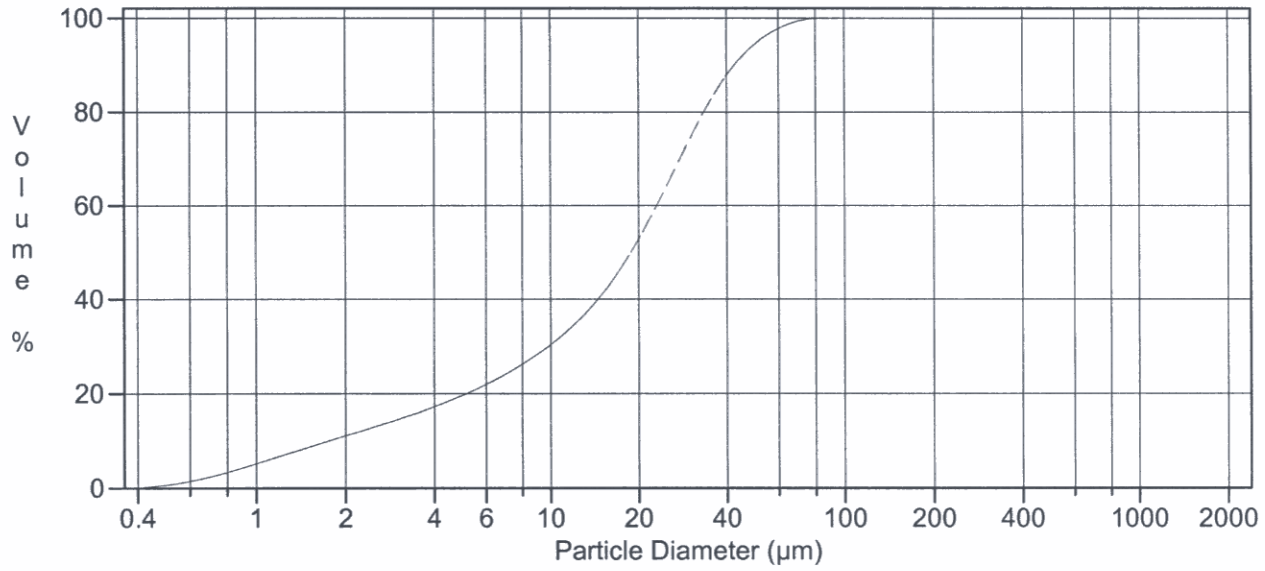

Volume Statistics (Arithmetic) 20.$02

Calculations from 0.375 µm to 2000 µm

Volume	100.0%		
Mean:	20.90 µm	95% Conf. Limits:	0-52.21 µm
Median:	18.90 µm	S.D.:	15.97 µm
D(3,2):	5.231 µm	Variance:	255.1 µm^2
Mean/Median Ratio:	1.106	C.V.:	76.4%
Mode:	26.14 µm	Skewness:	0.837 Right skewed
d_{10}:	1.768 µm	Kurtosis:	0.467 Leptokurtic
d_{50}:	18.90 µm		
d_{90}:	42.65 µm		
Specific Surf. Area	11470 cm^2/ml		

% <	10	25	60	75	90
Size µm	1.768	7.455	23.17	30.48	42.65

20.$02

Particle Diameter µm	Volume %
1.000	5.93
2.000	8.55
5.000	10.7
10.00	10.7
15.00	11.6
20.00	11.5
25.00	23.7
40.00	6.62
50.00	3.28
60.00	1.62
70.00	0.36
75.00	0.20
80.00	0.13
90.00	0.015

NGU-4L/SC:631-633

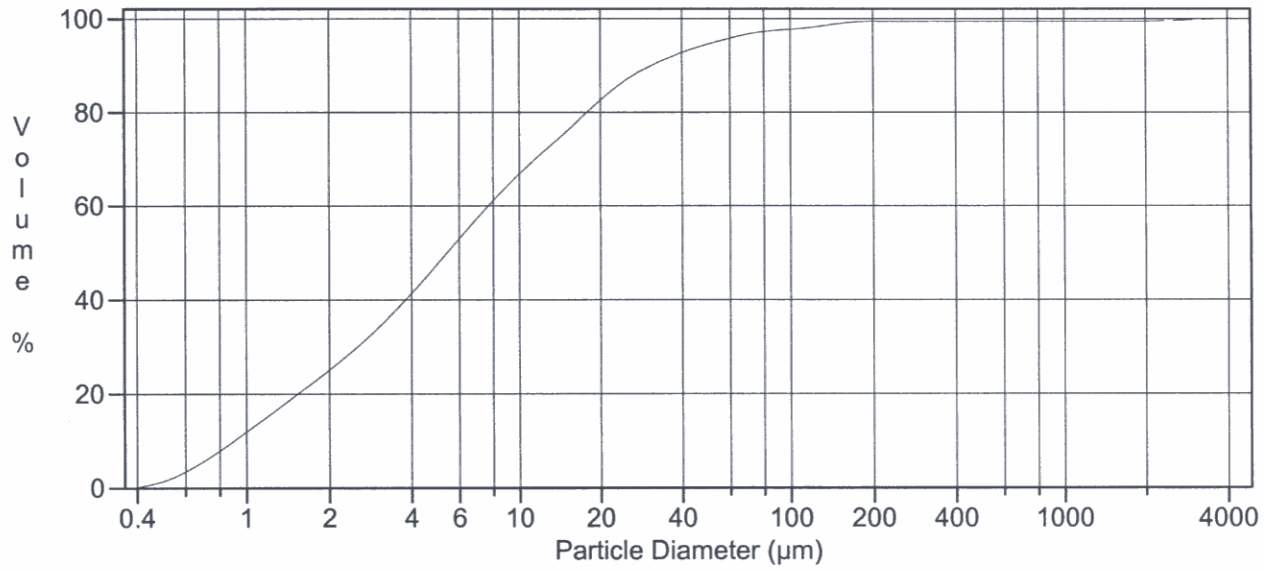

Volume Statistics (Arithmetic) 19a.$02

Calculations from 0.375 µm to 4000 µm

Volume	100.0%		
Mean:	30.80 µm	95% Conf. Limits:	0-472.9 µm
Median:	5.435 µm	S.D.:	225.6 µm
D(3,2):	2.587 µm	Variance:	50888 µm^2
Mean/Median Ratio:	5.667	C.V.:	732%
Mode:	5.355 µm	Skewness:	12.21 Right skewed
d_{10}:	0.906 µm	Kurtosis:	148.4 Leptokurtic
d_{50}:	5.435 µm		
d_{90}:	31.04 µm		
Specific Surf. Area	23192 cm^2/ml		

% <	10	25	60	75	90
Size µm	0.906	2.005	7.719	14.45	31.04

19a.$02

Particle Diameter µm	Volume %
1.000	13.1
2.000	22.6
5.000	19.1
10.00	9.17
15.00	6.66
20.00	4.47
25.00	5.73
40.00	1.81
50.00	1.25
60.00	0.90
70.00	0.30
75.00	0.23
80.00	0.30
90.00	2.52

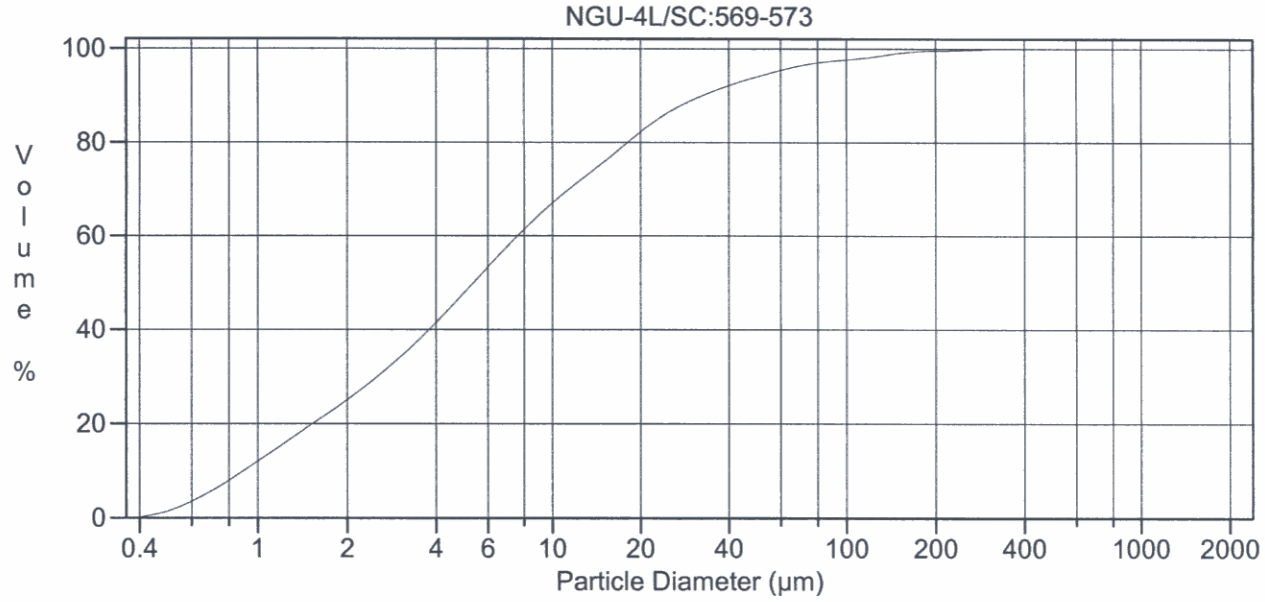

Volume Statistics (Arithmetic) 17.$02

Calculations from 0.375 µm to 2000 µm

Volume	100.0%		
Mean:	14.52 µm	95% Conf. Limits:	0-71.76 µm
Median:	5.384 µm	S.D.:	29.20 µm
D(3,2):	2.575 µm	Variance:	852.9 µm^2
Mean/Median Ratio:	2.697	C.V.:	201%
Mode:	5.355 µm	Skewness:	5.426 Right skewed
d_{10}:	0.900 µm	Kurtosis:	39.95 Leptokurtic
d_{50}:	5.384 µm		
d_{90}:	32.81 µm		
Specific Surf. Area	23303 cm^2/ml		

% <	10	25	60	75	90
Size µm	0.900	1.996	7.619	14.49	32.81

17.$02

Particle Diameter µm	Volume %
1.000	13.1
2.000	22.8
5.000	19.1
10.00	8.81
15.00	6.38
20.00	4.29
25.00	5.62
40.00	1.93
50.00	1.37
60.00	1.00
70.00	0.35
75.00	0.27
80.00	0.38
90.00	2.67

NGU-4L/SC:562-566

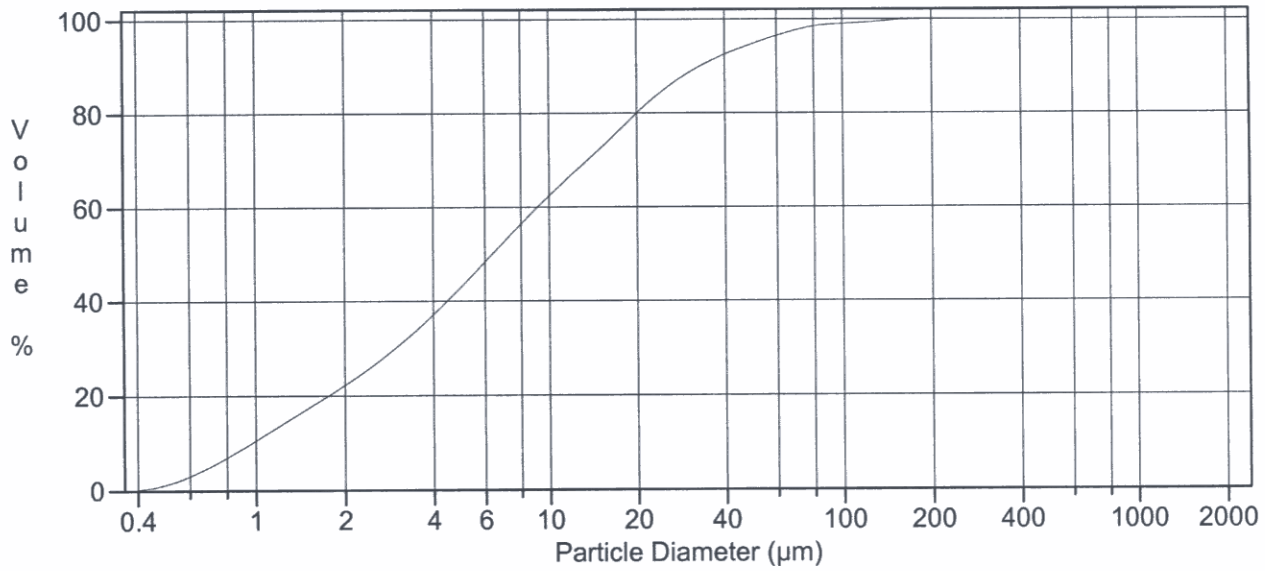

Volume Statistics (Arithmetic) 16.$02

Calculations from 0.375 µm to 2000 µm

Volume	100.0%		
Mean:	13.58 µm	95% Conf. Limits:	0-53.14 µm
Median:	6.389 µm	S.D.:	20.19 µm
D(3,2):	2.840 µm	Variance:	407.5 μm^2
Mean/Median Ratio:	2.125	C.V.:	149%
Mode:	5.878 µm	Skewness:	3.695 Right skewed
d_{10}:	0.973 µm	Kurtosis:	18.97 Leptokurtic
d_{50}:	6.389 µm		
d_{90}:	33.12 µm		
Specific Surf. Area	21130 cm^2/ml		

% <	10	25	60	75	90
Size µm	0.973	2.339	9.153	16.61	33.12

16.$02

Particle Diameter µm	Volume %
1.000	11.7
2.000	20.9
5.000	19.3
10.00	10.1
15.00	7.45
20.00	5.28
25.00	7.32
40.00	2.30
50.00	1.65
60.00	1.23
70.00	0.43
75.00	0.32
80.00	0.39
90.00	1.23

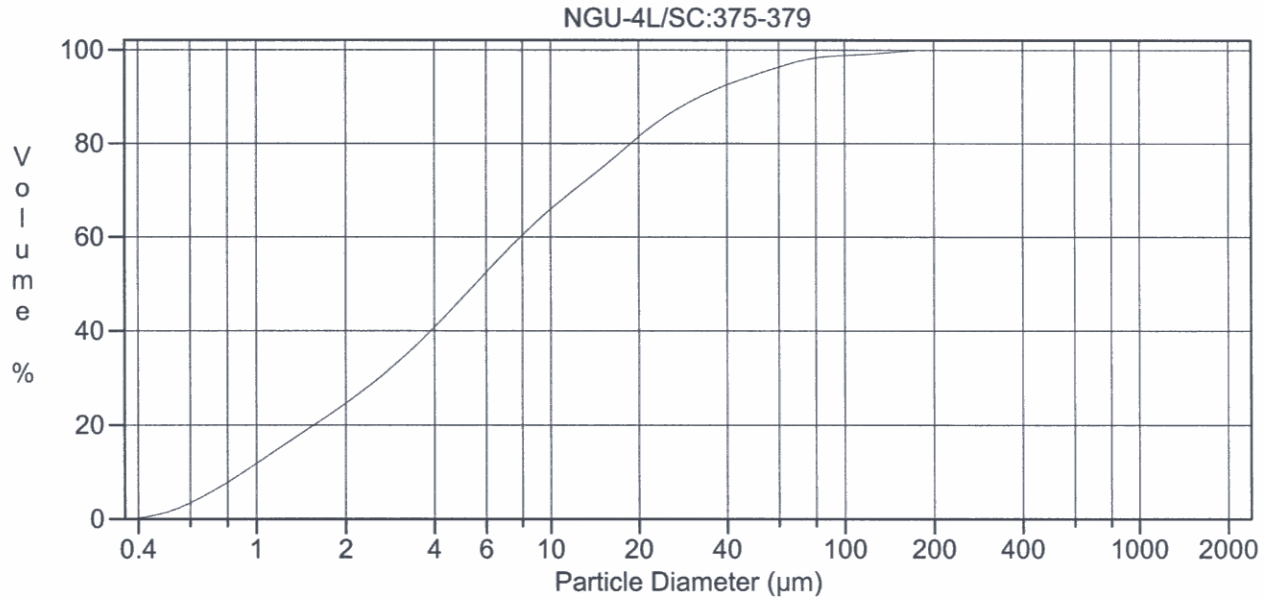

Volume Statistics (Arithmetic) 15.$02

Calculations from 0.375 µm to 2000 µm

Volume	100.0%		
Mean:	13.04 µm	95% Conf. Limits:	0-53.85 µm
Median:	5.539 µm	S.D.:	20.82 µm
D(3,2):	2.613 µm	Variance:	433.5 µm^2
Mean/Median Ratio:	2.354	C.V.:	160%
Mode:	5.355 µm	Skewness:	3.855 Right skewed
d_{10}:	0.908 µm	Kurtosis:	19.93 Leptokurtic
d_{50}:	5.539 µm		
d_{90}:	32.54 µm		
Specific Surf. Area	22960 cm^2/ml		

% <	10	25	60	75	90
Size µm	0.908	2.046	7.913	15.19	32.54

15.$02

Particle Diameter µm	Volume %
1.000	12.8
2.000	22.5
5.000	18.8
10.00	8.87
15.00	6.60
20.00	4.64
25.00	6.53
40.00	2.19
50.00	1.62
60.00	1.23
70.00	0.43
75.00	0.31
80.00	0.38
90.00	1.35

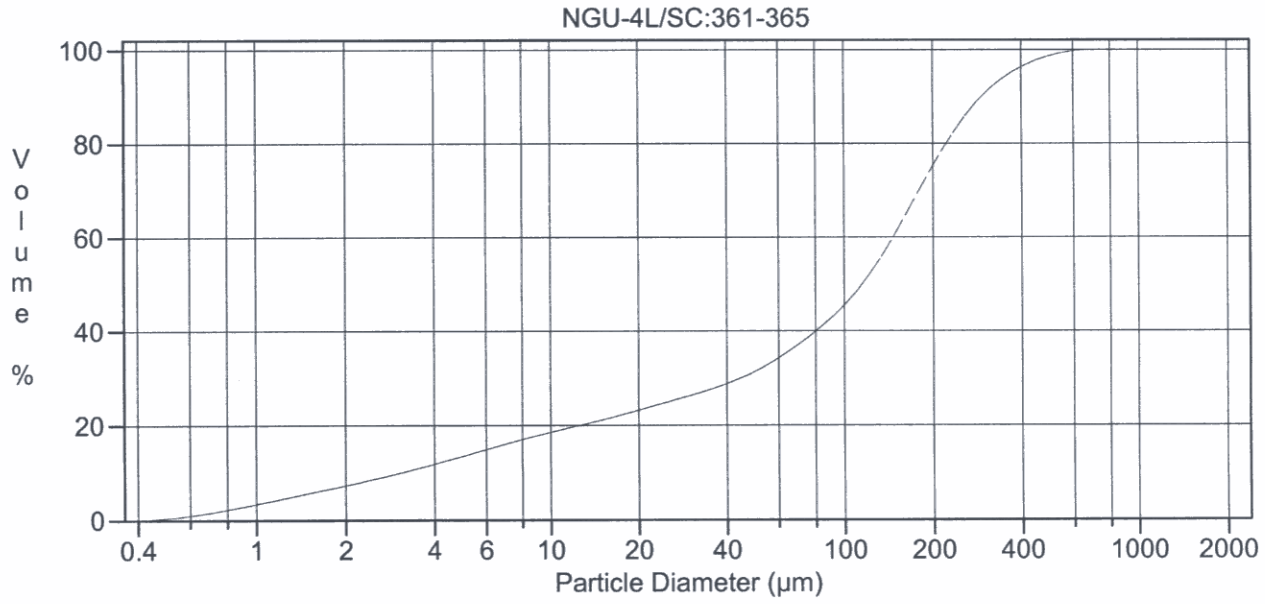

Volume Statistics (Arithmetic) 14.$02

Calculations from 0.375 µm to 2000 µm

Volume	100.0%		
Mean:	133.7 µm	95% Conf. Limits:	0-371.5 µm
Median:	115.5 µm	S.D.:	121.3 µm
D(3,2):	8.643 µm	Variance:	14714 μm^2
Mean/Median Ratio:	1.157	C.V.:	90.7%
Mode:	168.8 µm	Skewness:	1.153 Right skewed
d_{10}:	3.107 µm	Kurtosis:	1.516 Leptokurtic
d_{50}:	115.5 µm		
d_{90}:	294.0 µm		
Specific Surf. Area	6942 cm^2/ml		

% <	10	25	60	75	90
Size µm	3.107	25.68	146.8	199.3	294.0

14.$02

Particle Diameter µm	Volume %
1.000	3.93
2.000	6.17
5.000	5.03
10.00	2.57
15.00	2.06
20.00	1.70
25.00	3.91
40.00	2.62
50.00	2.82
60.00	2.87
70.00	1.41
75.00	1.39
80.00	2.76
90.00	57.4

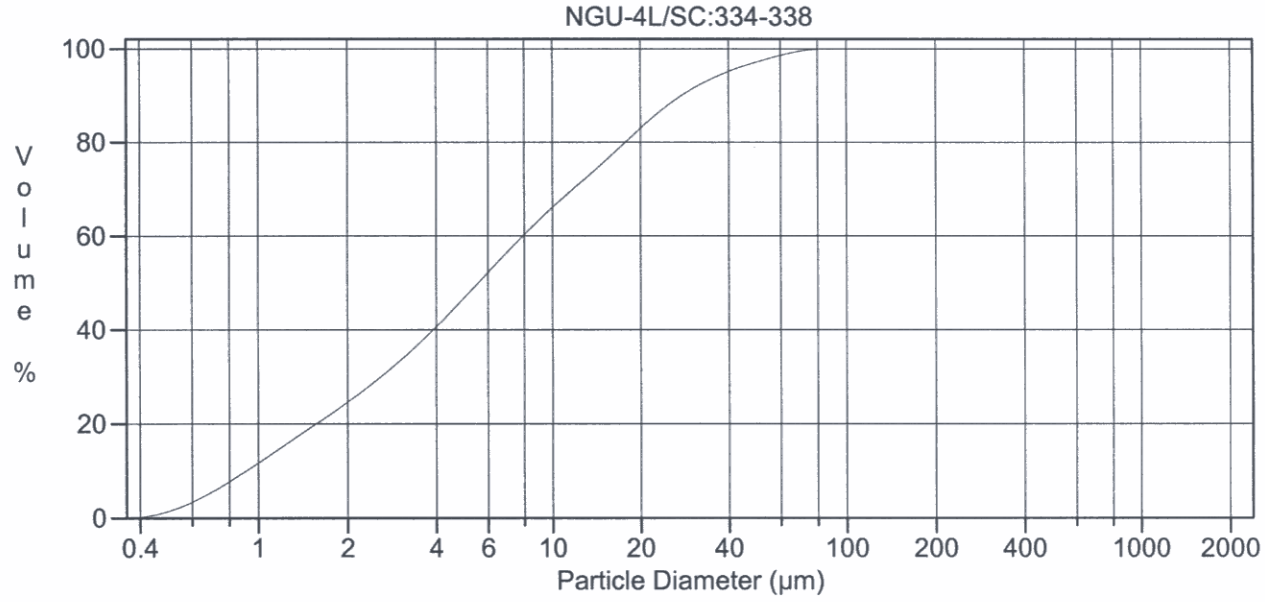

Volume Statistics (Arithmetic) 13.$02

Calculations from 0.375 µm to 2000 µm

Volume	100.0%		
Mean:	10.88 µm	95% Conf. Limits:	0-37.23 µm
Median:	5.580 µm	S.D.:	13.44 µm
D(3,2):	2.616 µm	Variance:	180.7 µm^2
Mean/Median Ratio:	1.949	C.V.:	124%
Mode:	5.355 µm	Skewness:	2.240 Right skewed
d_{10}:	0.914 µm	Kurtosis:	5.704 Leptokurtic
d_{50}:	5.580 µm		
d_{90}:	27.78 µm		
Specific Surf. Area	22934 cm^2/ml		

% <	10	25	60	75	90
Size µm	0.914	2.050	7.943	14.61	27.78

13.$02

Particle Diameter µm	Volume %
1.000	12.9
2.000	22.3
5.000	19.2
10.00	9.64
15.00	7.23
20.00	5.15
25.00	7.07
40.00	2.05
50.00	1.38
60.00	0.93
70.00	0.26
75.00	0.15
80.00	0.12
90.00	0.018

NGU-4L/SC:194-198

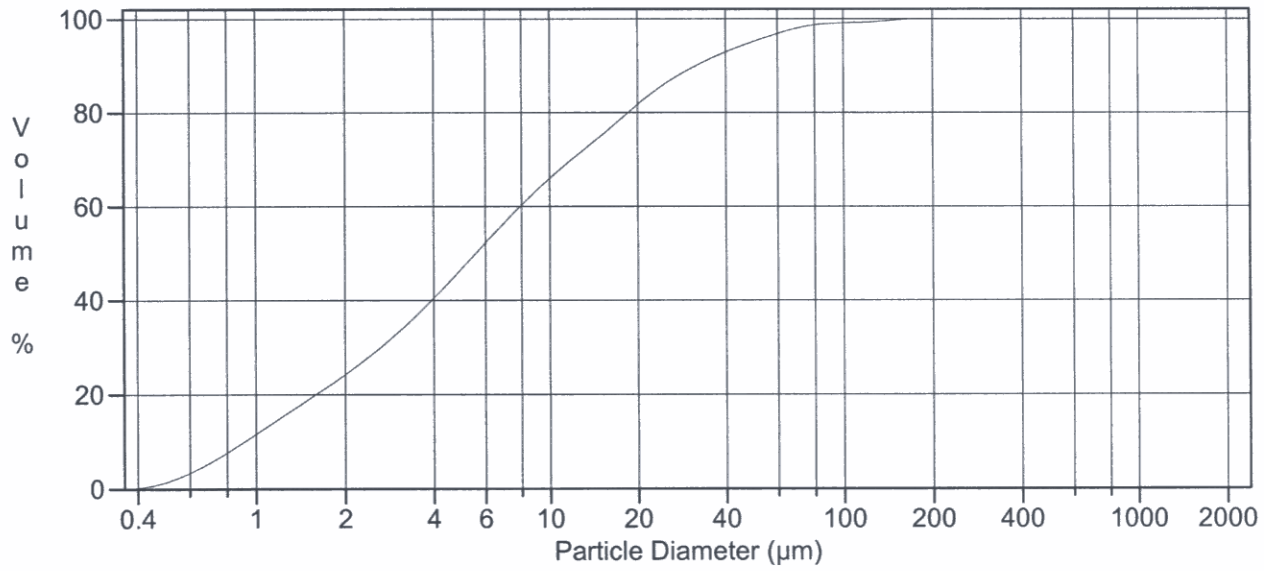

Volume Statistics (Arithmetic) 12.$02

Calculations from 0.375 µm to 2000 µm

Volume	100.0%		
Mean:	12.64 µm	95% Conf. Limits:	0-50.88 µm
Median:	5.583 µm	S.D.:	19.51 µm
D(3,2):	2.638 µm	Variance:	380.5 µm^2
Mean/Median Ratio:	2.265	C.V.:	154%
Mode:	5.355 µm	Skewness:	3.807 Right skewed
d_{10}:	0.918 µm	Kurtosis:	20.18 Leptokurtic
d_{50}:	5.583 µm		
d_{90}:	31.90 µm		
Specific Surf. Area	22742 cm^2/ml		

% <	10	25	60	75	90
Size µm	0.918	2.089	7.937	15.03	31.90

12.$02

Particle Diameter µm	Volume %
1.000	12.6
2.000	22.6
5.000	19.2
10.00	9.06
15.00	6.65
20.00	4.63
25.00	6.61
40.00	2.29
50.00	1.66
60.00	1.19
70.00	0.39
75.00	0.27
80.00	0.30
90.00	1.07

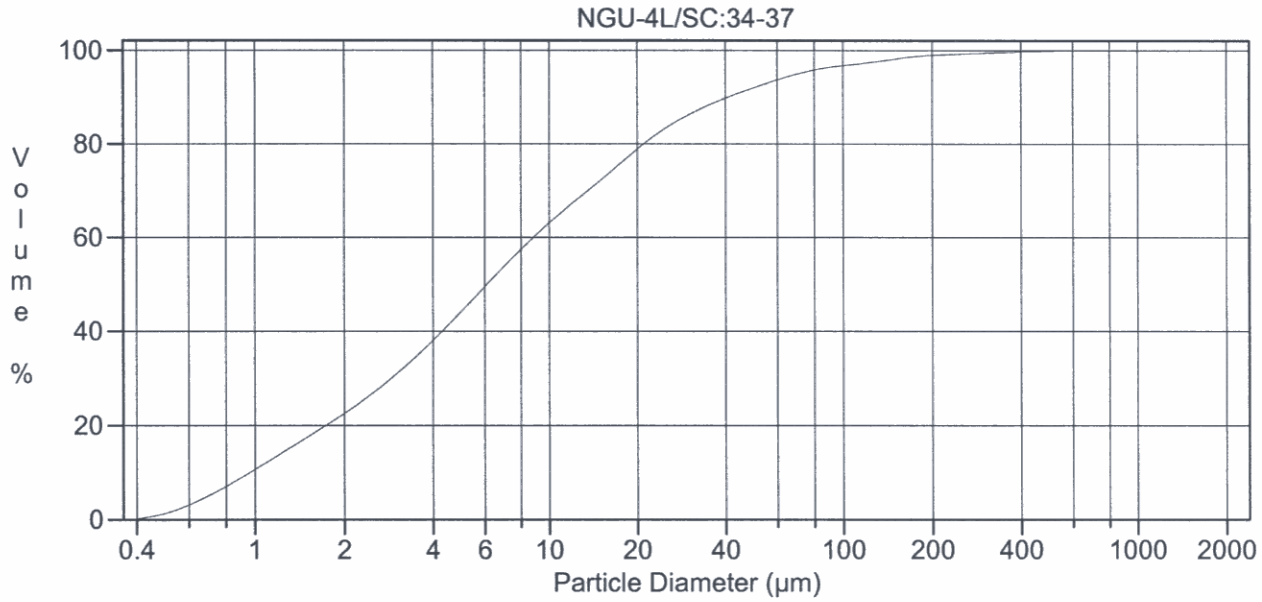

Volume Statistics (Arithmetic) 11.$02

Calculations from 0.375 µm to 2000 µm

Volume	100.0%		
Mean:	18.75 µm	95% Conf. Limits:	0-106.3 µm
Median:	6.132 µm	S.D.:	44.66 µm
D(3,2):	2.808 µm	Variance:	1994 μm^2
Mean/Median Ratio:	3.059	C.V.:	238%
Mode:	5.355 µm	Skewness:	6.851 Right skewed
d_{10}:	0.964 µm	Kurtosis:	62.08 Leptokurtic
d_{50}:	6.132 µm		
d_{90}:	40.98 µm		
Specific Surf. Area	21366 cm^2/ml		

% <	10	25	60	75	90
Size µm	0.964	2.285	8.854	16.97	40.98

11.$02

Particle Diameter µm	Volume %
1.000	11.9
2.000	21.7
5.000	18.9
10.00	9.15
15.00	6.62
20.00	4.55
25.00	6.42
40.00	2.22
50.00	1.65
60.00	1.28
70.00	0.48
75.00	0.38
80.00	0.56
90.00	3.67

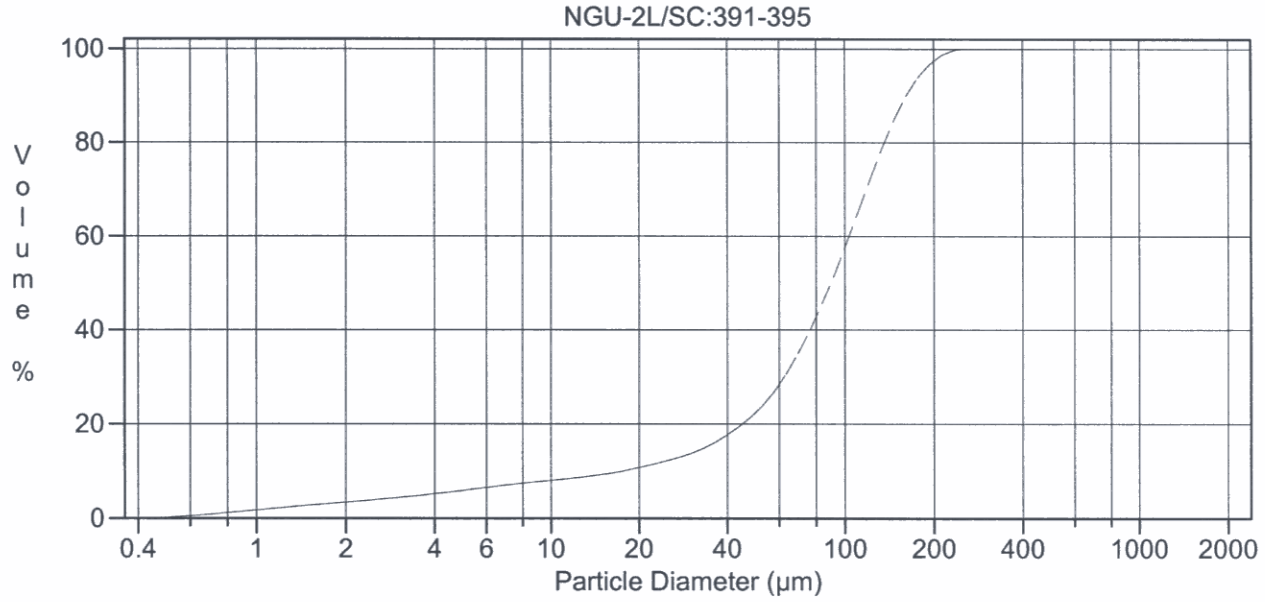

Volume Statistics (Arithmetic) 10.$02

Calculations from 0.375 µm to 2000 µm

Volume	100.0%		
Mean:	91.59 µm	95% Conf. Limits:	0-194.6 µm
Median:	89.84 µm	S.D.:	52.54 µm
D(3,2):	16.27 µm	Variance:	2760 µm^2
Mean/Median Ratio:	1.019	C.V.:	57.4%
Mode:	116.3 µm	Skewness:	0.242 Right skewed
d_{10}:	17.80 µm	Kurtosis:	-0.384 Platykurtic
d_{50}:	89.84 µm		
d_{90}:	161.6 µm		
Specific Surf. Area	3687 cm^2/ml		

% <	10	25	60	75	90
Size µm	17.80	54.72	103.7	127.0	161.6

10.$02

Particle Diameter µm	Volume %
1.000	1.67
2.000	2.50
5.000	2.12
10.00	1.25
15.00	1.44
20.00	1.49
25.00	5.45
40.00	4.78
50.00	5.89
60.00	6.98
70.00	3.71
75.00	3.72
80.00	7.42
90.00	49.9

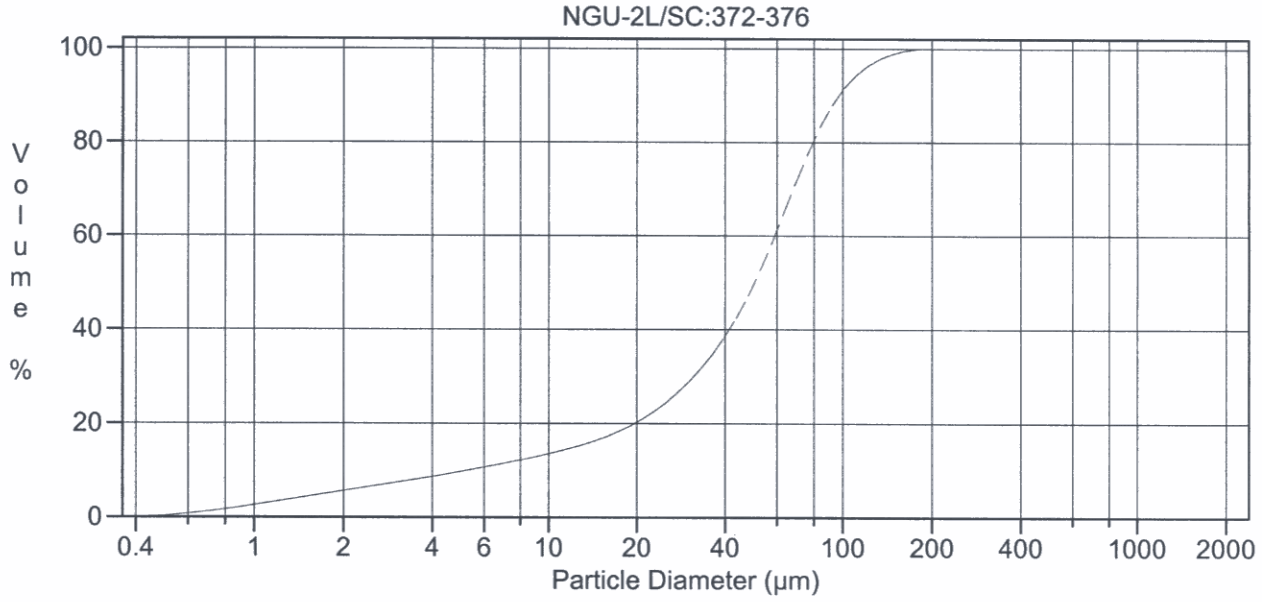

Volume Statistics (Arithmetic) 9.$02

Calculations from 0.375 µm to 2000 µm

Volume	100.0%		
Mean:	52.22 µm	95% Conf. Limits:	0-120.2 µm
Median:	50.46 µm	S.D.:	34.67 µm
D(3,2):	10.17 µm	Variance:	1202 µm^2
Mean/Median Ratio:	1.035	C.V.:	66.4%
Mode:	66.44 µm	Skewness:	0.602 Right skewed
d_{10}:	5.351 µm	Kurtosis:	0.306 Leptokurtic
d_{50}:	50.46 µm		
d_{90}:	97.36 µm		
Specific Surf. Area	5897 cm^2/ml		

% <	10	25	60	75	90
Size µm	5.351	25.87	59.08	73.51	97.36

9.$02

Particle Diameter µm	Volume %
1.000	3.03
2.000	4.08
5.000	3.84
10.00	3.14
15.00	3.52
20.00	4.06
25.00	14.2
40.00	11.0
50.00	11.6
60.00	10.7
70.00	4.56
75.00	3.96
80.00	6.35
90.00	13.3

NGU-2L/SC:323-327

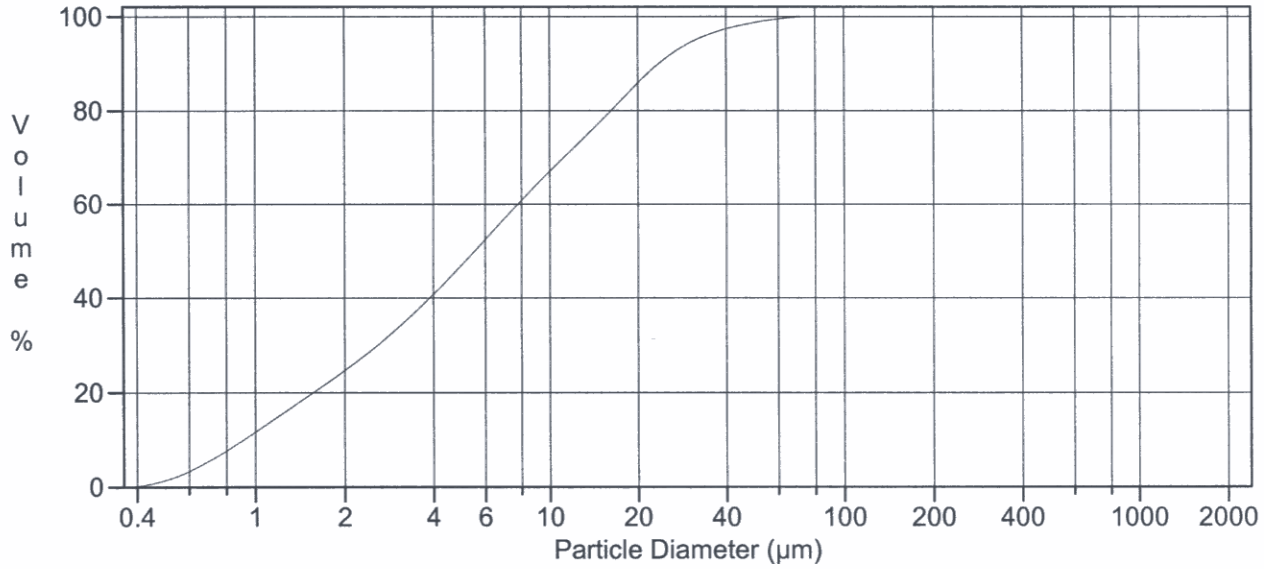

Volume Statistics (Arithmetic) 8#.$02

Calculations from 0.375 µm to 2000 µm

Volume	100.0%		
Mean:	9.658 µm	95% Conf. Limits:	0-31.29 µm
Median:	5.545 µm	S.D.:	11.04 µm
D(3,2):	2.601 µm	Variance:	121.8 µm^2
Mean/Median Ratio:	1.742	C.V.:	114%
Mode:	5.878 µm	Skewness:	2.195 Right skewed
d_{10}:	0.917 µm	Kurtosis:	6.238 Leptokurtic
d_{50}:	5.545 µm		
d_{90}:	23.68 µm		
Specific Surf. Area	23070 cm^2/ml		

% <	10	25	60	75	90
Size µm	0.917	2.039	7.801	13.55	23.68

8#.$02

Particle Diameter µm	Volume %
1.000	13.0
2.000	22.3
5.000	20.0
10.00	10.8
15.00	8.04
20.00	5.46
25.00	6.13
40.00	1.33
50.00	0.74
60.00	0.40
70.00	0.087
75.00	0.045
80.00	0.028
90.00	0.0024

NGU-2L/SC:299-303

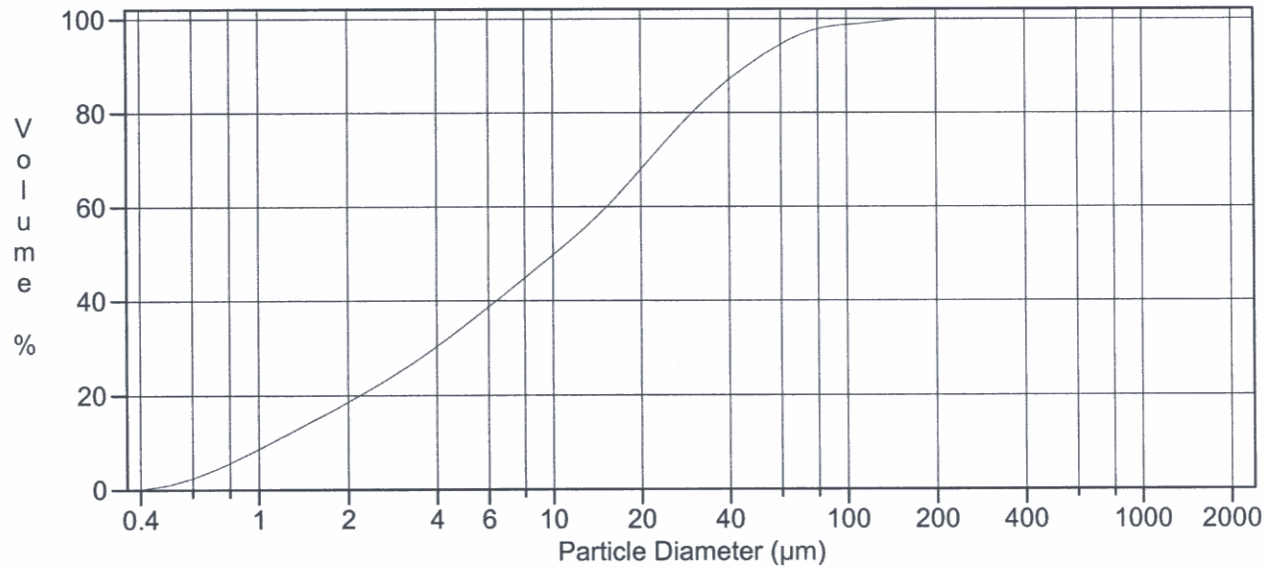

Volume Statistics (Arithmetic) 7.$02

Calculations from 0.375 µm to 2000 µm

Volume	100.0%		
Mean:	18.37 µm	95% Conf. Limits:	0-62.84 µm
Median:	10.16 µm	S.D.:	22.69 µm
D(3,2):	3.404 µm	Variance:	514.6 μm^2
Mean/Median Ratio:	1.809	C.V.:	123%
Mode:	21.69 µm	Skewness:	2.539 Right skewed
d_{10}:	1.109 µm	Kurtosis:	9.147 Leptokurtic
d_{50}:	10.16 µm		
d_{90}:	46.48 µm		
Specific Surf. Area	17628 cm^2/ml		

% <	10	25	60	75	90
Size µm	1.109	3.003	15.35	25.30	46.48

7.$02

Particle Diameter µm	Volume %
1.000	9.96
2.000	16.2
5.000	14.9
10.00	9.72
15.00	8.40
20.00	6.88
25.00	12.3
40.00	4.38
50.00	3.07
60.00	2.13
70.00	0.69
75.00	0.50
80.00	0.62
90.00	1.65

NGU-2L/SC:275-279

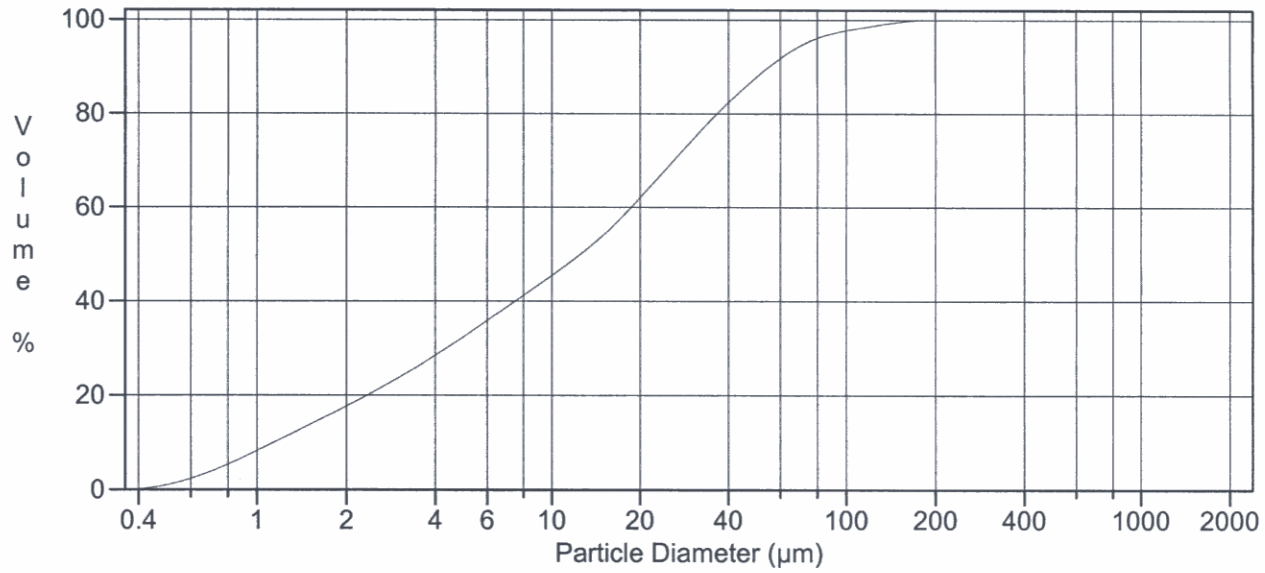

Volume Statistics (Arithmetic) 6.$02

Calculations from 0.375 µm to 2000 µm

Volume	100.0%		
Mean:	21.94 µm	95% Conf. Limits:	0-73.92 µm
Median:	12.58 µm	S.D.:	26.52 µm
D(3,2):	3.608 µm	Variance:	703.2 μm^2
Mean/Median Ratio:	1.744	C.V.:	121%
Mode:	23.81 µm	Skewness:	2.256 Right skewed
d_{10}:	1.146 µm	Kurtosis:	6.692 Leptokurtic
d_{50}:	12.58 µm		
d_{90}:	55.32 µm		
Specific Surf. Area	16629 cm^2/ml		

% <	10	25	60	75	90
Size µm	1.146	3.269	18.76	30.89	55.32

6.$02

Particle Diameter µm	Volume %
1.000	9.46
2.000	14.8
5.000	13.0
10.00	8.60
15.00	7.88
20.00	6.80
25.00	13.6
40.00	5.47
50.00	3.91
60.00	2.75
70.00	0.94
75.00	0.73
80.00	1.01
90.00	2.89

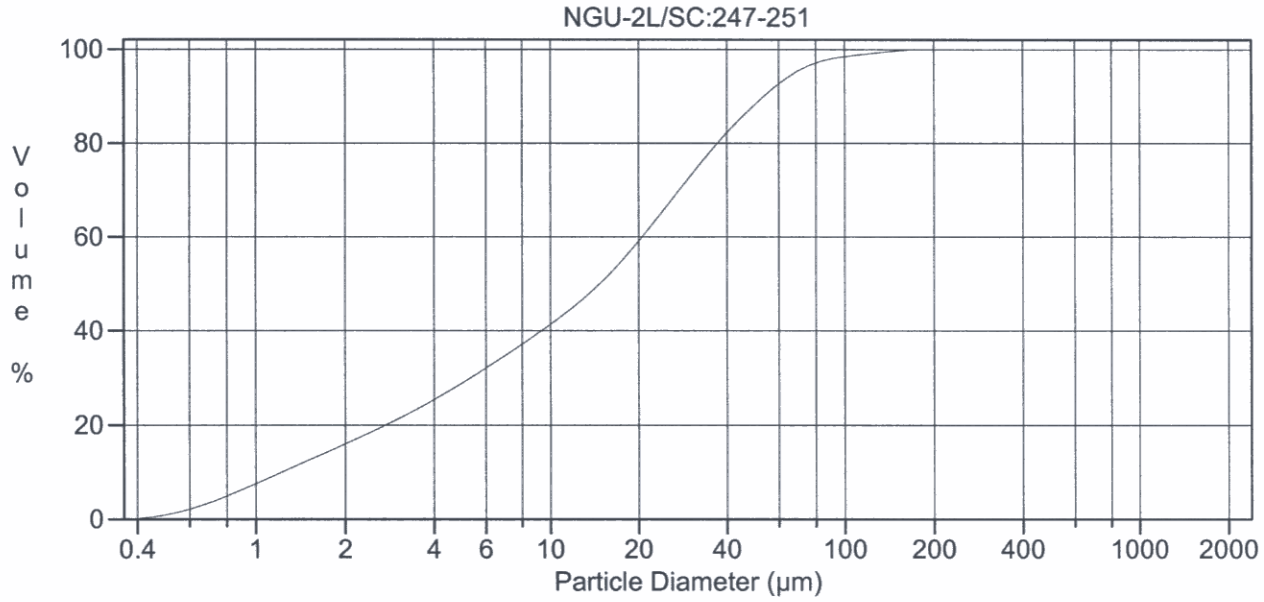

Volume Statistics (Arithmetic) 5.$02

Calculations from 0.375 µm to 2000 µm

Volume	100.0%		
Mean:	22.16 µm	95% Conf. Limits:	0-69.91 µm
Median:	14.80 µm	S.D.:	24.36 µm
D(3,2):	3.919 µm	Variance:	593.5 µm^2
Mean/Median Ratio:	1.497	C.V.:	110%
Mode:	26.14 µm	Skewness:	2.086 Right skewed
d_{10}:	1.227 µm	Kurtosis:	6.371 Leptokurtic
d_{50}:	14.80 µm		
d_{90}:	53.50 µm		
Specific Surf. Area	15311 cm^2/ml		

% <	10	25	60	75	90
Size µm	1.227	3.912	20.66	32.02	53.50

5.$02

Particle Diameter µm	Volume %
1.000	8.46
2.000	12.9
5.000	12.4
10.00	9.07
15.00	8.57
20.00	7.60
25.00	15.6
40.00	6.16
50.00	4.28
60.00	2.89
70.00	0.93
75.00	0.69
80.00	0.89
90.00	2.01

NGU-2L/SC:223-227

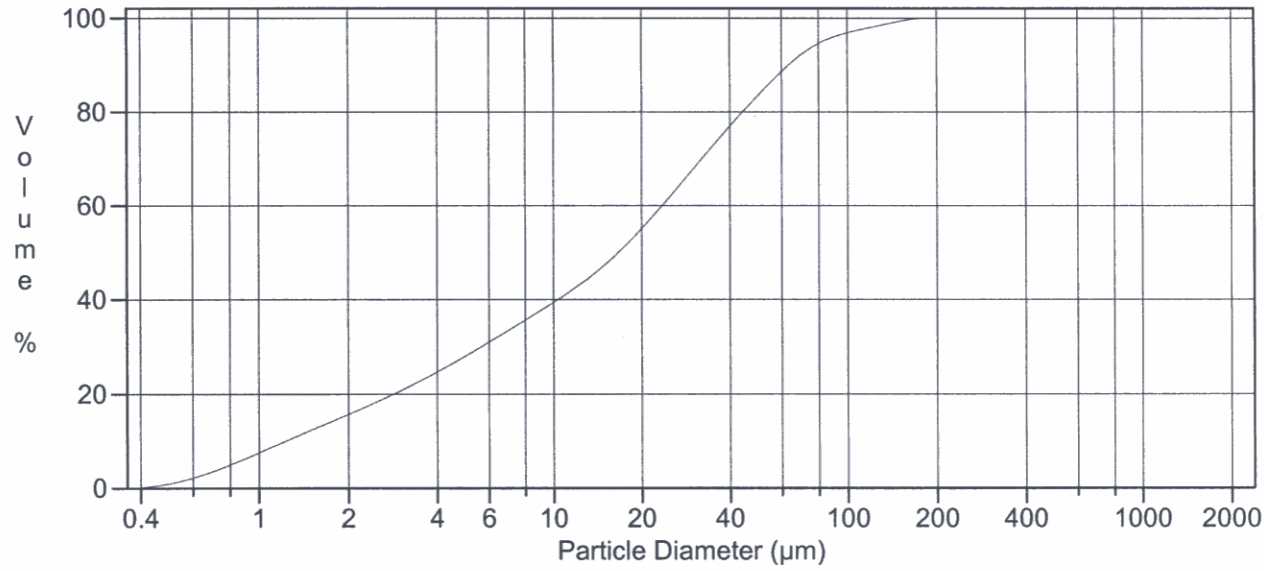

Volume Statistics (Arithmetic) 4#.$02

Calculations from 0.375 µm to 2000 µm

Volume	100.0%		
Mean:	26.13 µm	95% Conf. Limits:	0-83.96 µm
Median:	16.73 µm	S.D.:	29.51 µm
D(3,2):	4.026 µm	Variance:	870.7 µm^2
Mean/Median Ratio:	1.561	C.V.:	113%
Mode:	31.50 µm	Skewness:	1.971 Right skewed
d_{10}:	1.237 µm	Kurtosis:	4.913 Leptokurtic
d_{50}:	16.73 µm		
d_{90}:	63.54 µm		
Specific Surf. Area	14902 cm^2/ml		

% <	10	25	60	75	90
Size µm	1.237	4.103	23.62	37.75	63.54

4#.$02

Particle Diameter µm	Volume %
1.000	8.16
2.000	12.4
5.000	11.3
10.00	7.97
15.00	7.63
20.00	6.87
25.00	15.0
40.00	6.64
50.00	5.02
60.00	3.67
70.00	1.30
75.00	1.02
80.00	1.44
90.00	4.07

NGU-2L/SC:146-150

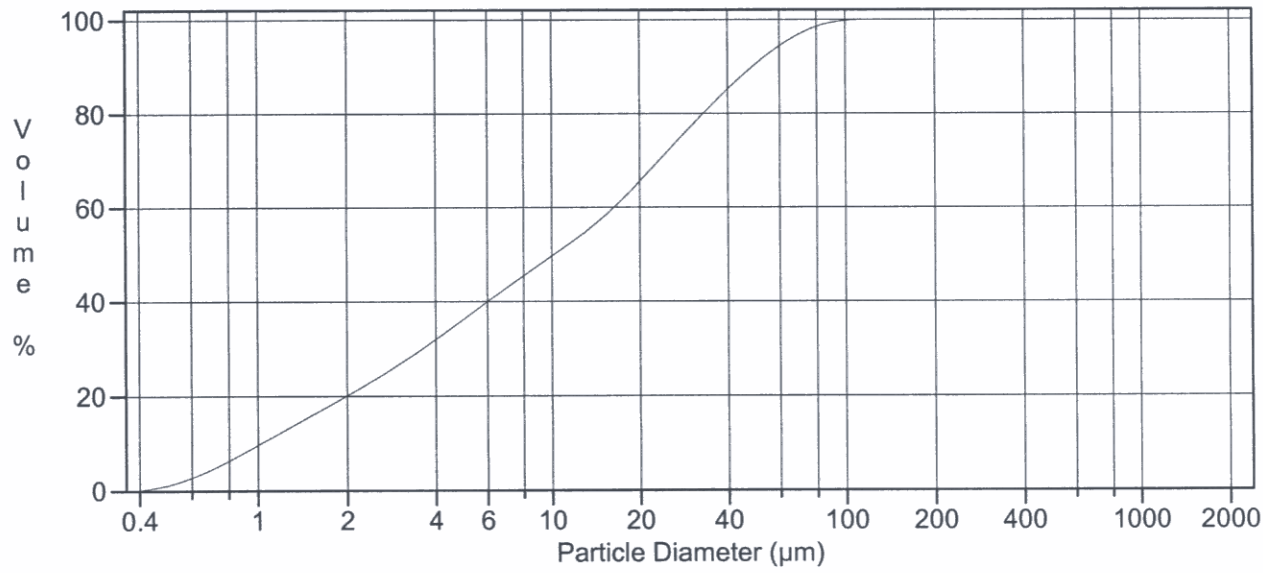

Volume Statistics (Arithmetic) 3.$02

Calculations from 0.375 µm to 2000 µm

Volume	100.0%		
Mean:	18.45 µm	95% Conf. Limits:	0-58.66 µm
Median:	10.24 µm	S.D.:	20.52 µm
D(3,2):	3.229 µm	Variance:	420.9 µm^2
Mean/Median Ratio:	1.803	C.V.:	111%
Mode:	23.81 µm	Skewness:	1.517 Right skewed
d_{10}:	1.031 µm	Kurtosis:	2.063 Leptokurtic
d_{50}:	10.24 µm		
d_{90}:	48.83 µm		
Specific Surf. Area	18583 cm^2/ml		

% <	10	25	60	75	90
Size µm	1.031	2.737	16.42	27.79	48.83

3.$02

Particle Diameter µm	Volume %
1.000	10.5
2.000	16.2
5.000	13.4
10.00	8.21
15.00	7.60
20.00	6.54
25.00	13.2
40.00	5.39
50.00	3.76
60.00	2.58
70.00	0.87
75.00	0.67
80.00	0.89
90.00	0.71

NGU-2L/SC:69-73

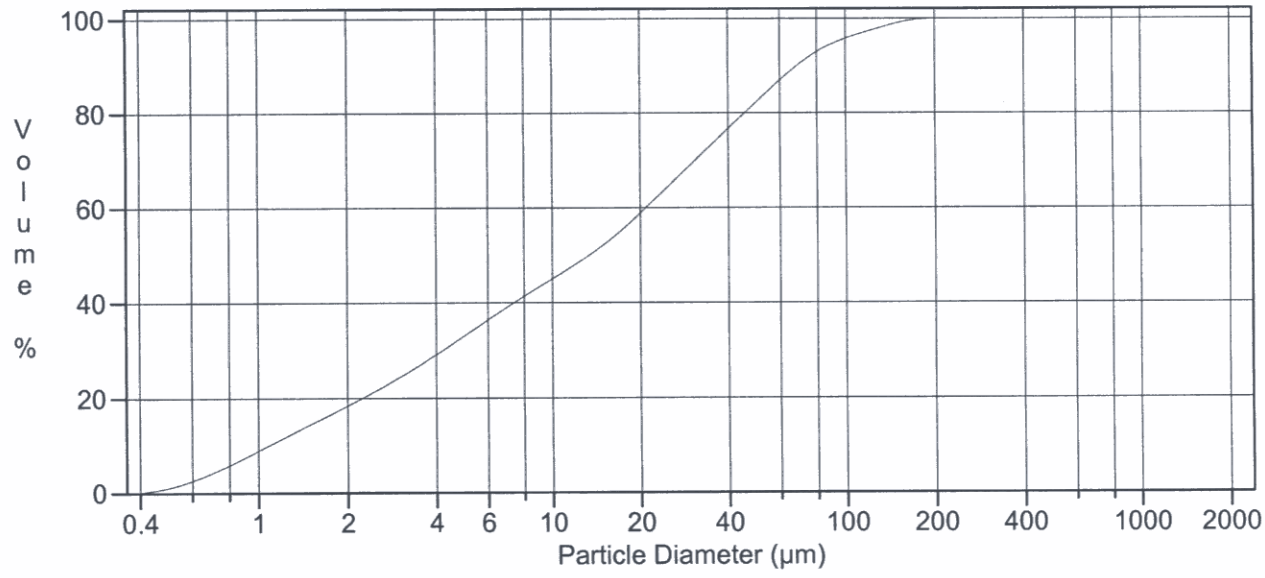

Volume Statistics (Arithmetic) 2.$02

Calculations from 0.375 µm to 2000 µm

Volume	100.0%		
Mean:	26.17 µm	95% Conf. Limits:	0-89.87 µm
Median:	13.46 µm	S.D.:	32.50 µm
D(3,2):	3.519 µm	Variance:	1057 μm^2
Mean/Median Ratio:	1.944	C.V.:	124%
Mode:	34.58 µm	Skewness:	1.997 Right skewed
d_{10}:	1.090 µm	Kurtosis:	4.521 Leptokurtic
d_{50}:	13.46 µm		
d_{90}:	68.79 µm		
Specific Surf. Area	17049 cm^2/ml		

% <	10	25	60	75	90
Size µm	1.090	3.138	21.04	37.67	68.79

2.$02

Particle Diameter µm	Volume %
1.000	9.52
2.000	14.7
5.000	11.9
10.00	7.14
15.00	6.62
20.00	5.72
25.00	12.1
40.00	5.68
50.00	4.56
60.00	3.57
70.00	1.35
75.00	1.11
80.00	1.69
90.00	5.46

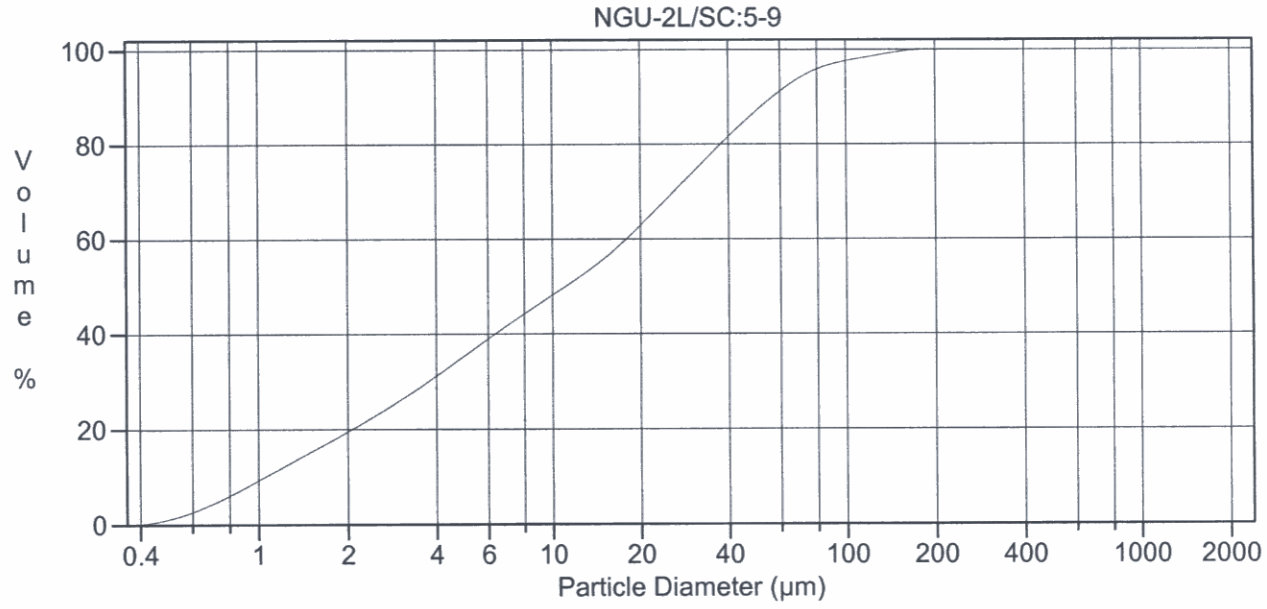

Volume Statistics (Arithmetic) 1#.$02

Calculations from 0.375 µm to 2000 µm

Volume	100.0%		
Mean:	21.94 µm	95% Conf. Limits:	0-75.85 µm
Median:	11.14 µm	S.D.:	27.50 µm
D(3,2):	3.333 µm	Variance:	756.4 µm^2
Mean/Median Ratio:	1.970	C.V.:	125%
Mode:	31.50 µm	Skewness:	2.234 Right skewed
d_{10}:	1.057 µm	Kurtosis:	6.380 Leptokurtic
d_{50}:	11.14 µm		
d_{90}:	56.86 µm		
Specific Surf. Area	18001 cm^2/ml		

% <	10	25	60	75	90
Size µm	1.057	2.845	17.99	31.46	56.86

1#.$02

Particle Diameter µm	Volume %
1.000	10.2
2.000	15.9
5.000	12.8
10.00	7.62
15.00	7.01
20.00	6.04
25.00	12.7
40.00	5.57
50.00	4.07
60.00	2.88
70.00	0.99
75.00	0.77
80.00	1.08
90.00	3.15

NGU-6L/SC:552-556

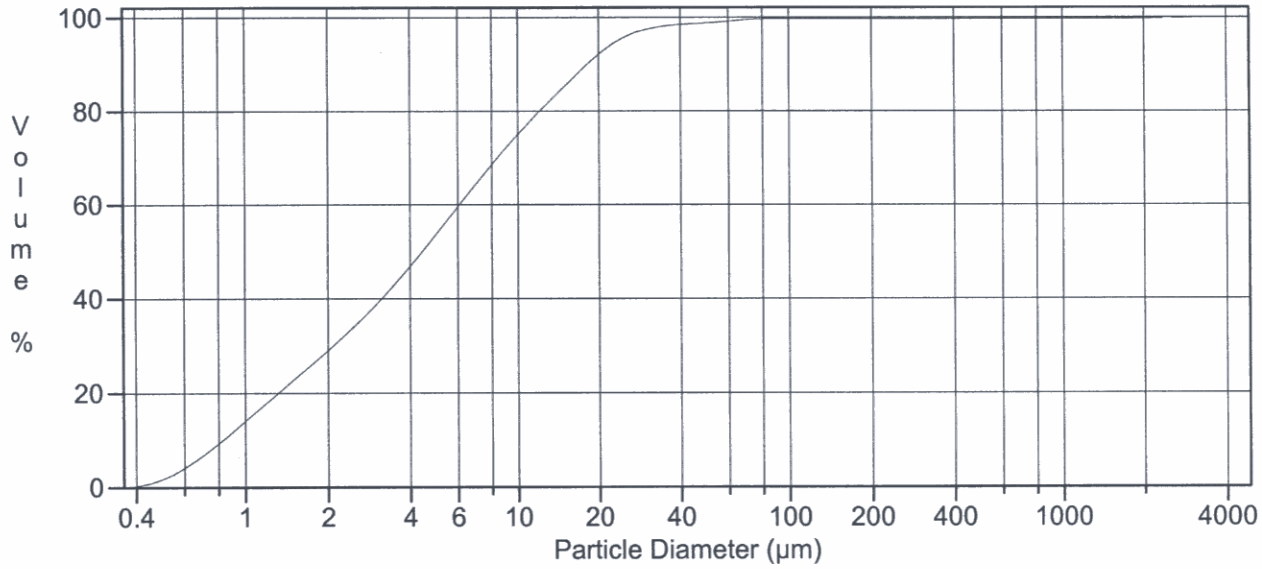

Volume Statistics (Arithmetic) 35a.$02

Calculations from 0.375 µm to 4000 µm

Volume	100.0%		
Mean:	17.62 µm	95% Conf. Limits:	0-349.2 µm
Median:	4.455 µm	S.D.:	169.2 µm
D(3,2):	2.270 µm	Variance:	28626 µm^2
Mean/Median Ratio:	3.954	C.V.:	960%
Mode:	5.878 µm	Skewness:	16.51 Right skewed
d_{10}:	0.833 µm	Kurtosis:	271.2 Leptokurtic
d_{50}:	4.455 µm		
d_{90}:	18.23 µm		
Specific Surf. Area	26426 cm^2/ml		

% <	10	25	60	75	90
Size µm	0.833	1.670	6.101	10.04	18.23

35a.$02

Particle Diameter µm	Volume %
1.000	15.0
2.000	24.7
5.000	21.3
10.00	10.4
15.00	6.74
20.00	3.77
25.00	2.59
40.00	0.36
50.00	0.34
60.00	0.33
70.00	0.10
75.00	0.058
80.00	0.042
90.00	0.36

APPENDIX 4

Lithostratigraphic, sediment density, magnetic susceptibility and X-ray imagery (XRI) logs of lake cores

Legend

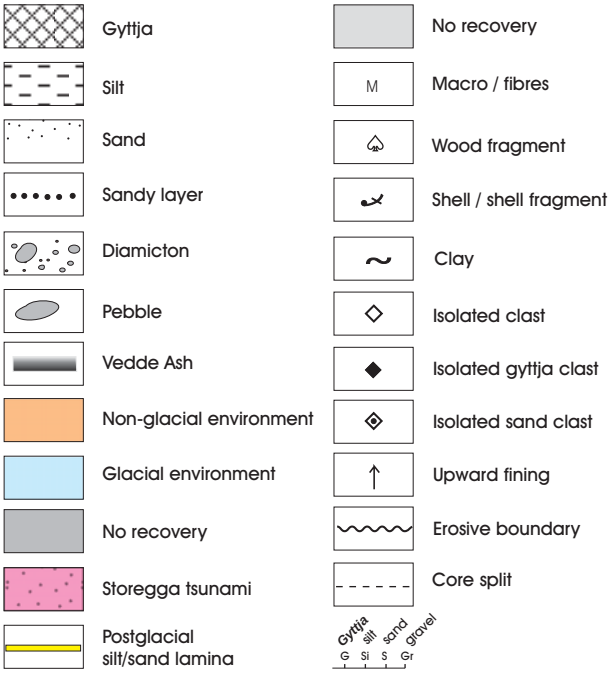
Gyttja
Silt
Sand
Sandy layer
Diamicton
Pebble
Vedde Ash
Non-glacial environment
Glacial environment
No recovery
Storegga tsunami
Postglacial
silt/sand lamina
No recovery
M
Macro / fibres
Wood fragment
Shell / shell fragment
Clay
Isolated clast
Isolated gyttja clast
Isolated sand clast
Upward fining
Erosive boundary
Core split
Gyttja
silt
sand
gravel
G
Si
S
Gr

Storsætervatnet, S1

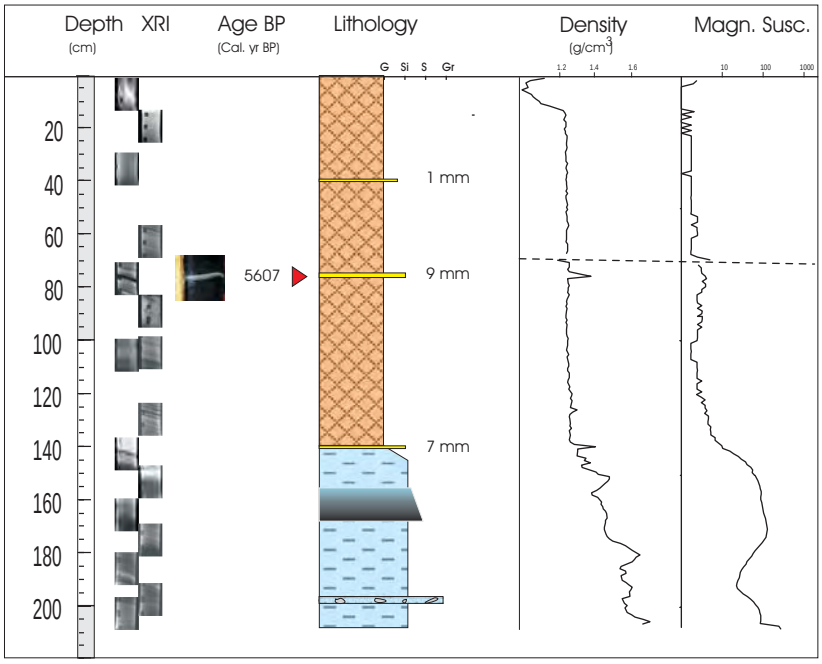

Storsætervatnet, S2

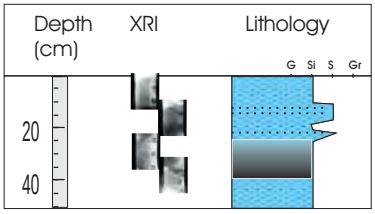

Storsætervatnet, S3

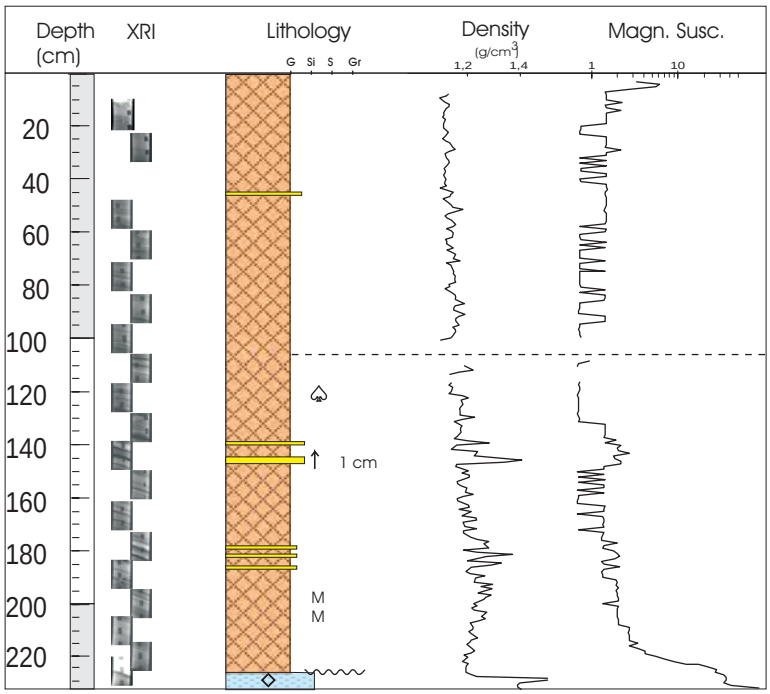

Storsætervatnet, S4

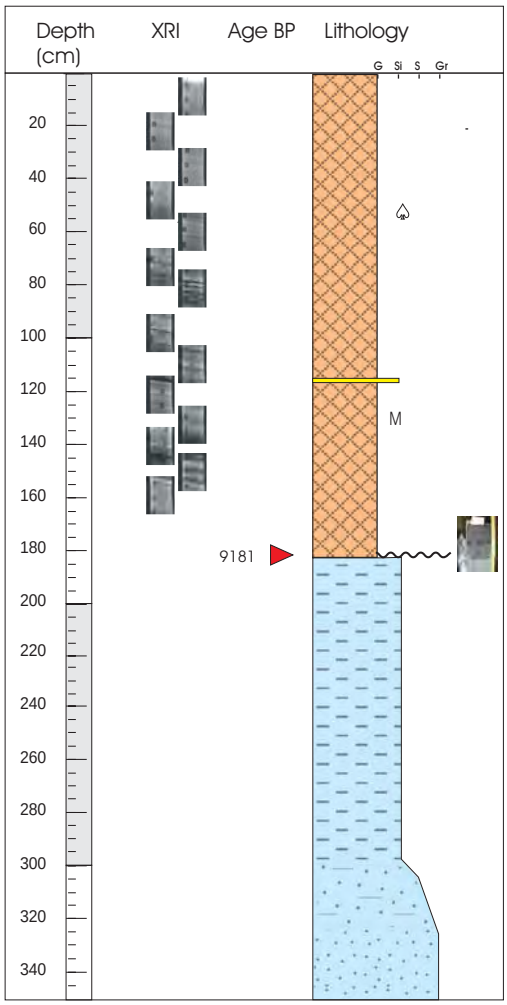

Storsætervatnet, S5

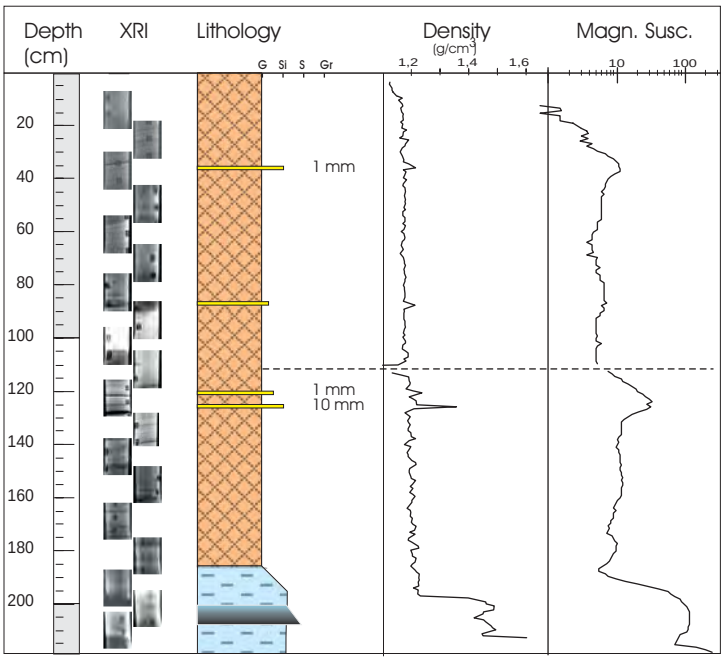

Storsætervatnet, S6

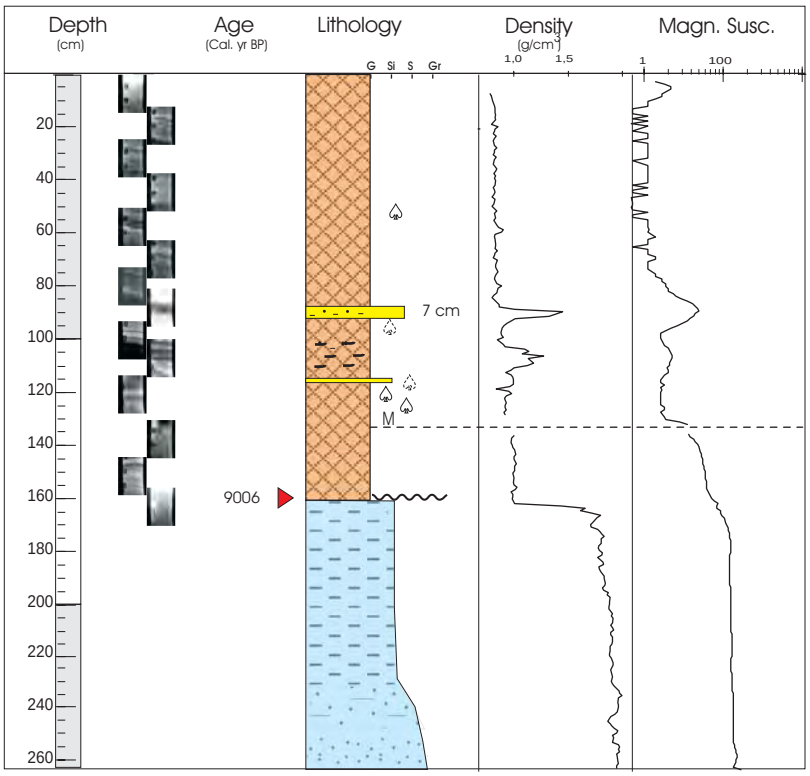

Storsætervanet, S7

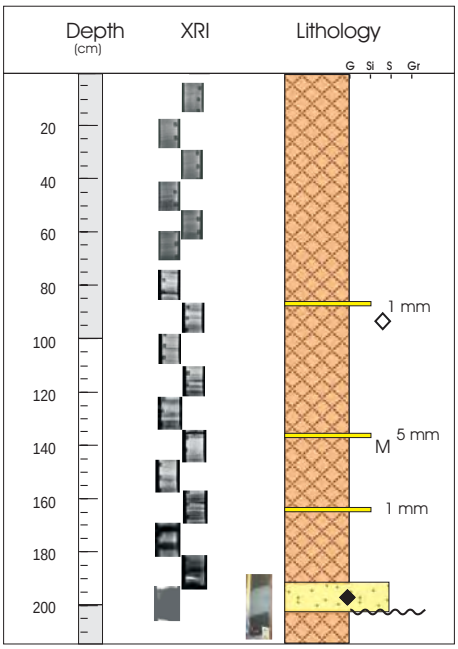

Storsætervatnet, S8

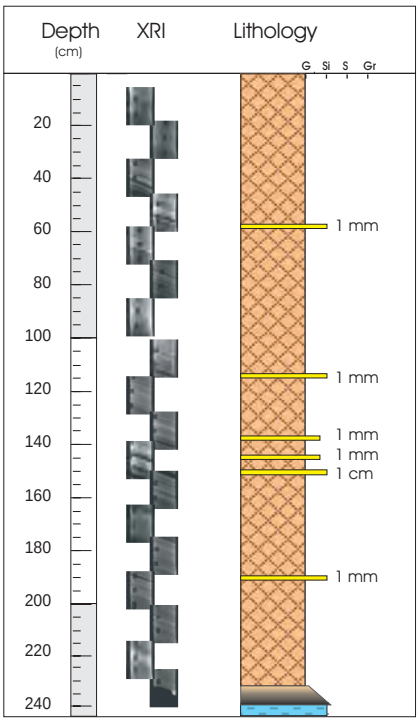

Storsætervatnet, S9

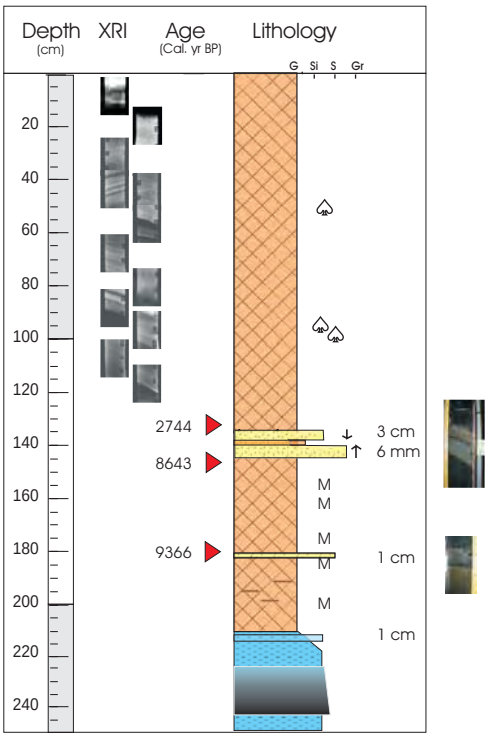

Storsætervatnet, S10

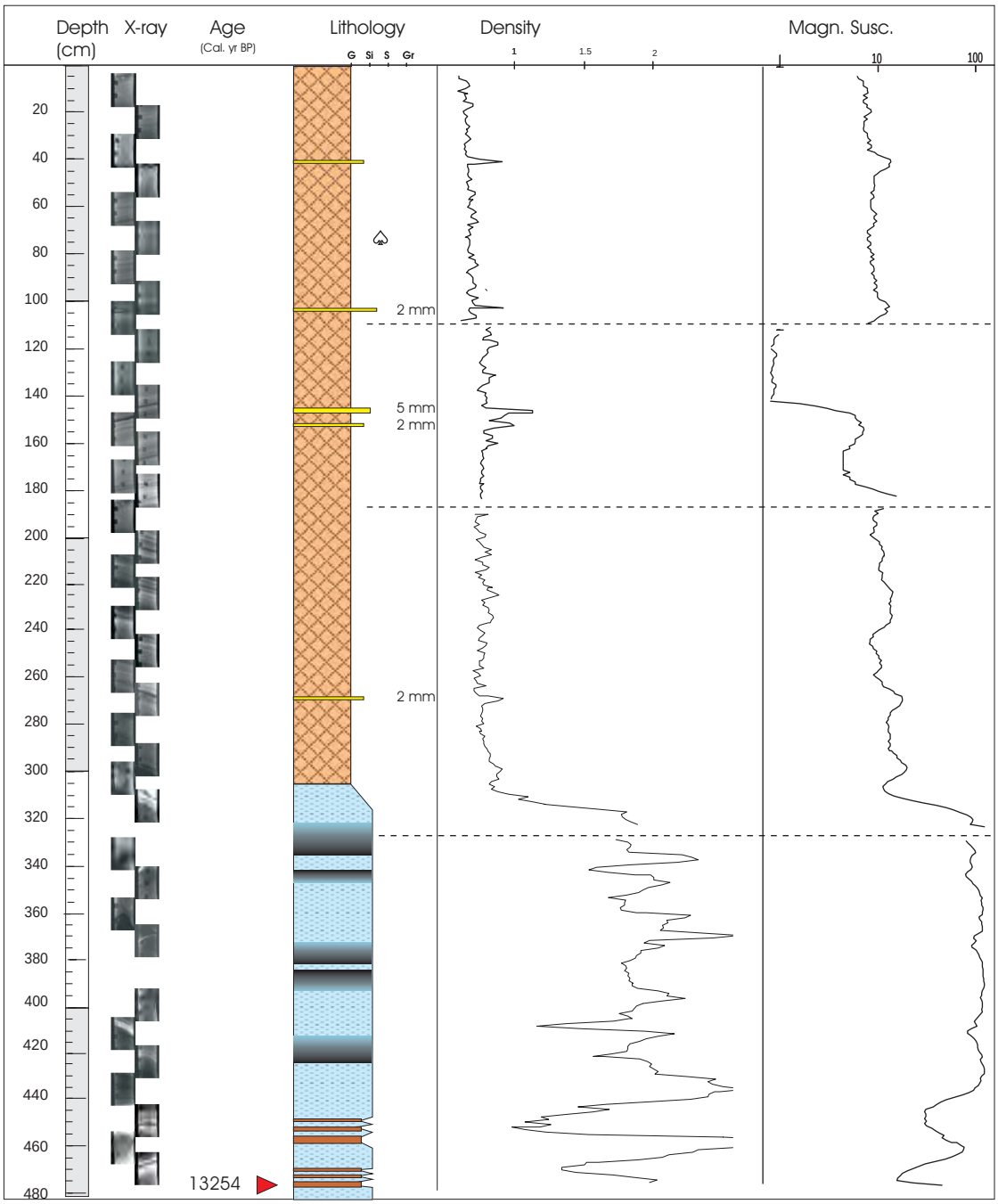

Medvatnet, M1

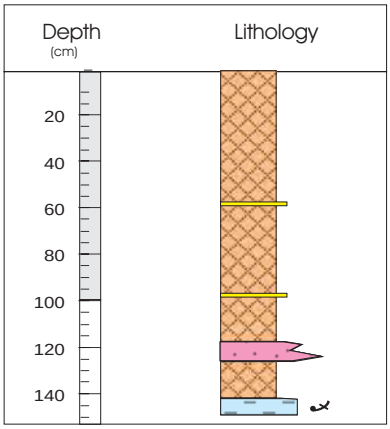

Medvatnet, M2

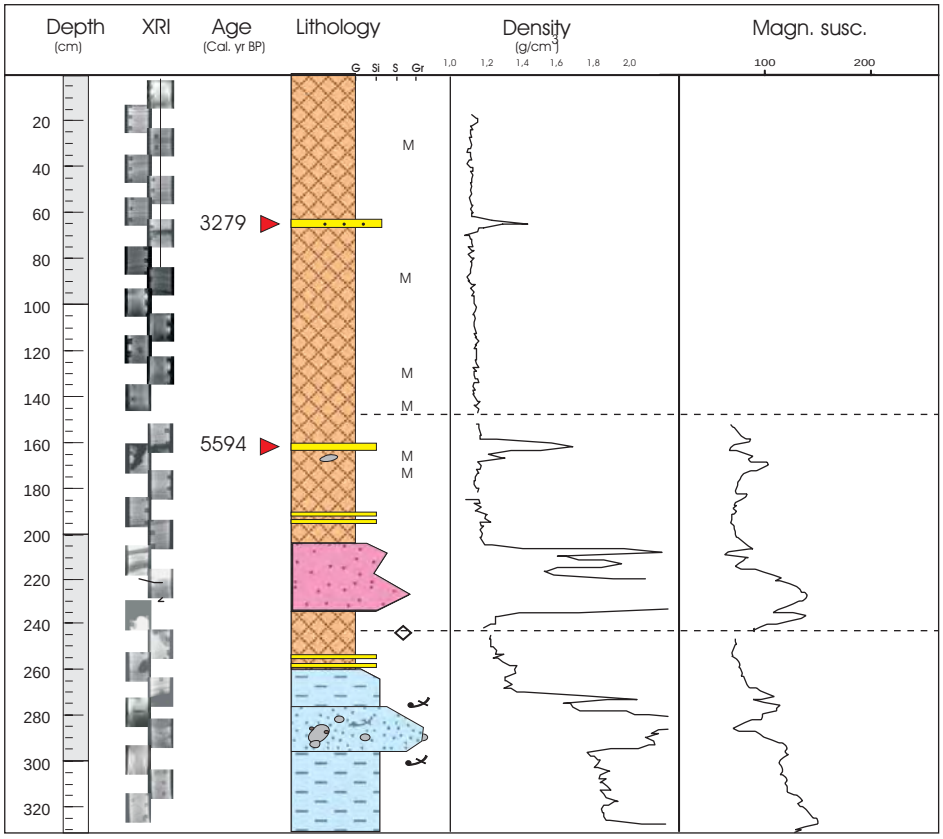

Medvatnet, M3

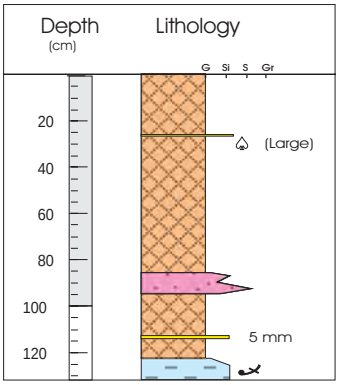

Medvatnet, M4

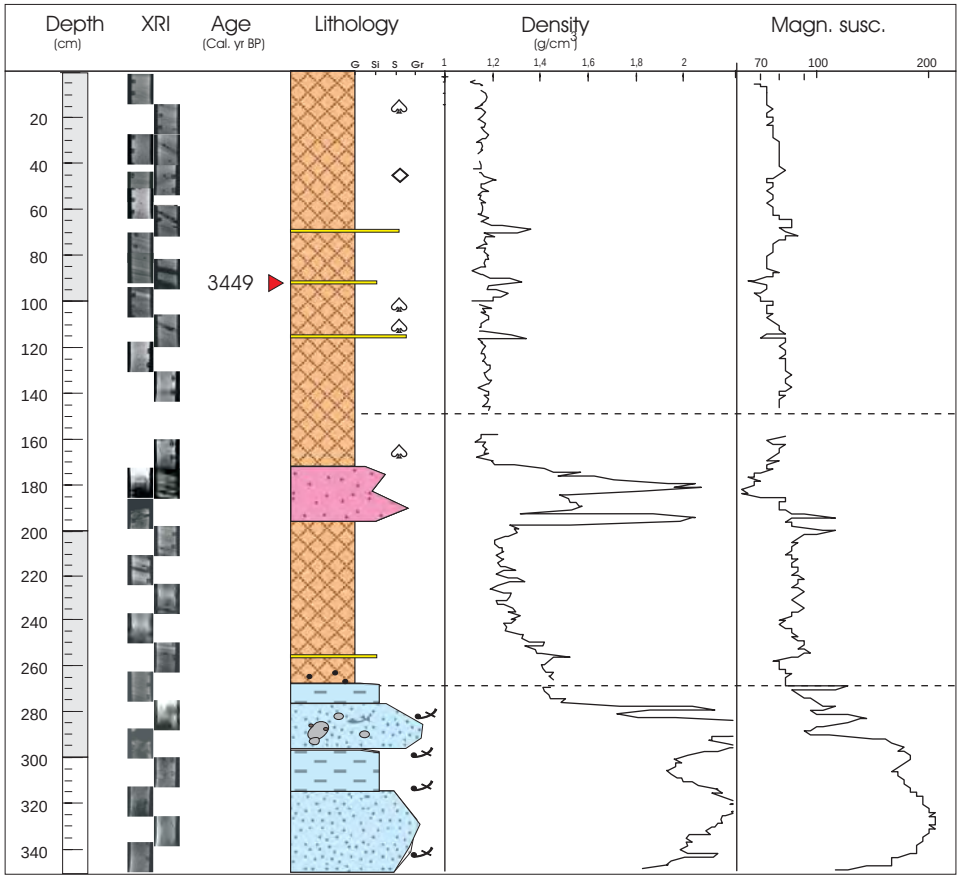

Medvatnet, M5

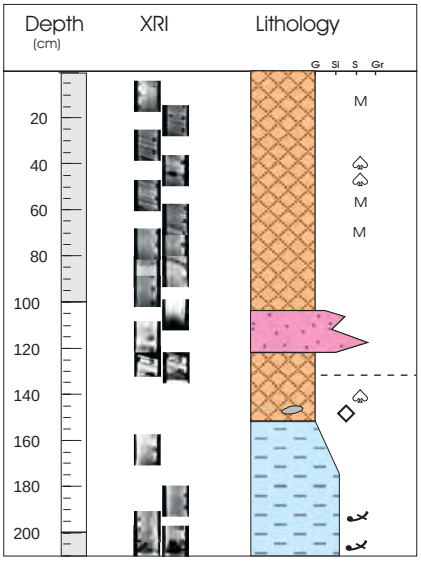

Medvatnet, M6

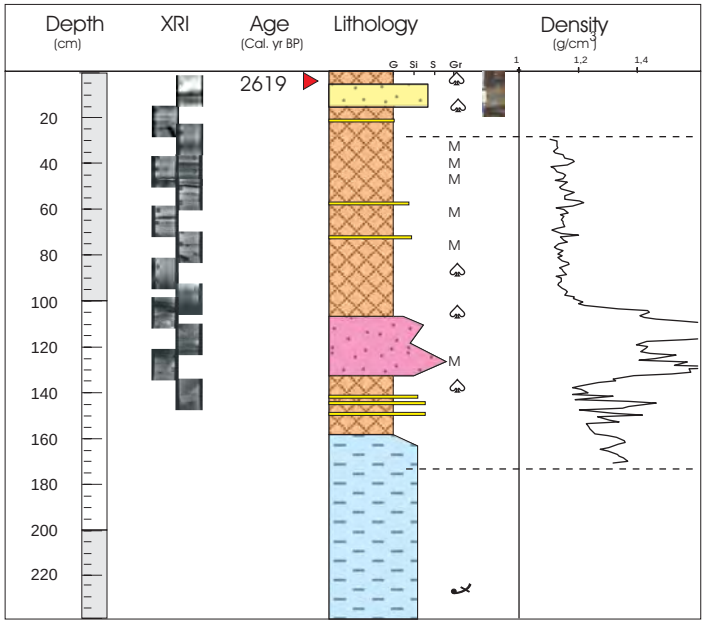

Nedstevatnet, N1

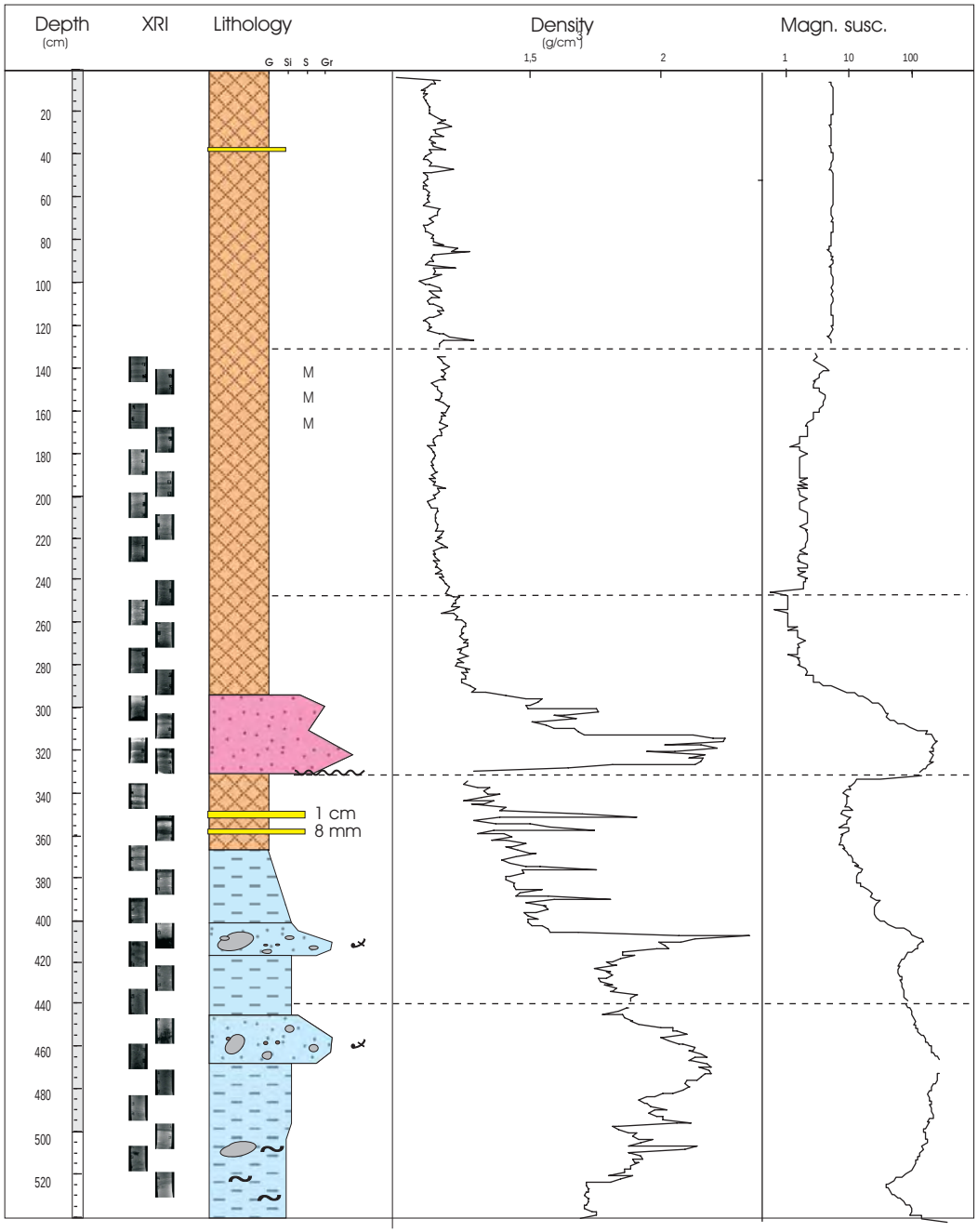

Nedstevatnet, N2

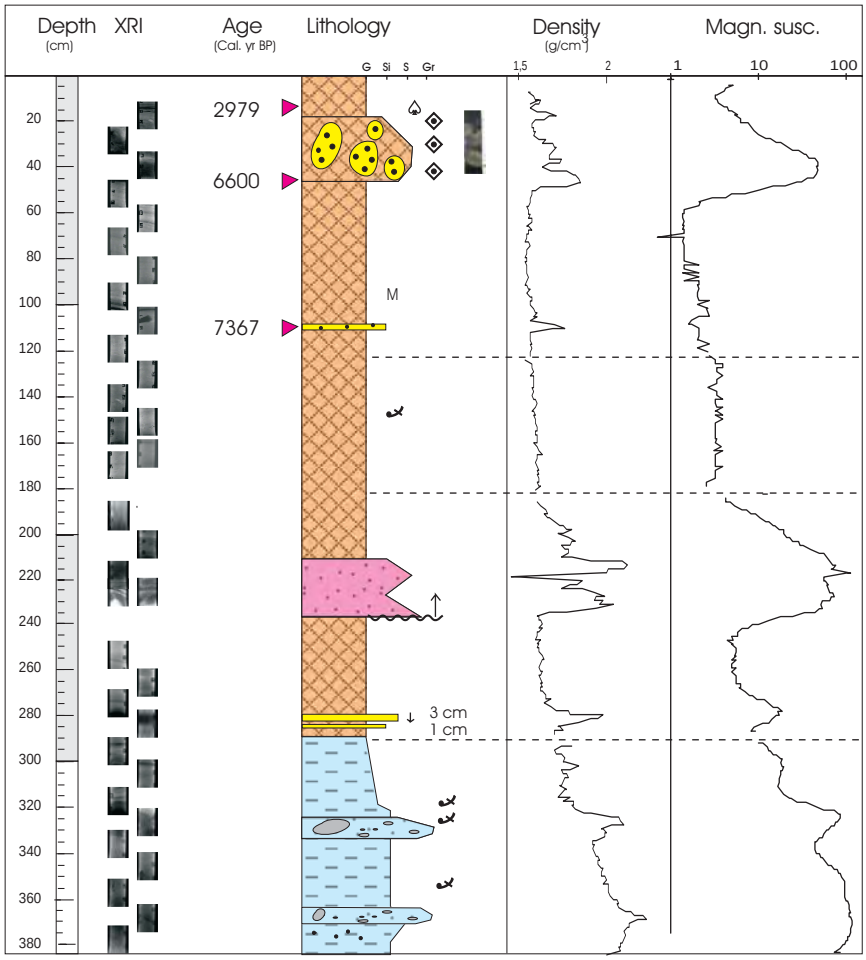

Nedstevatnet, N3

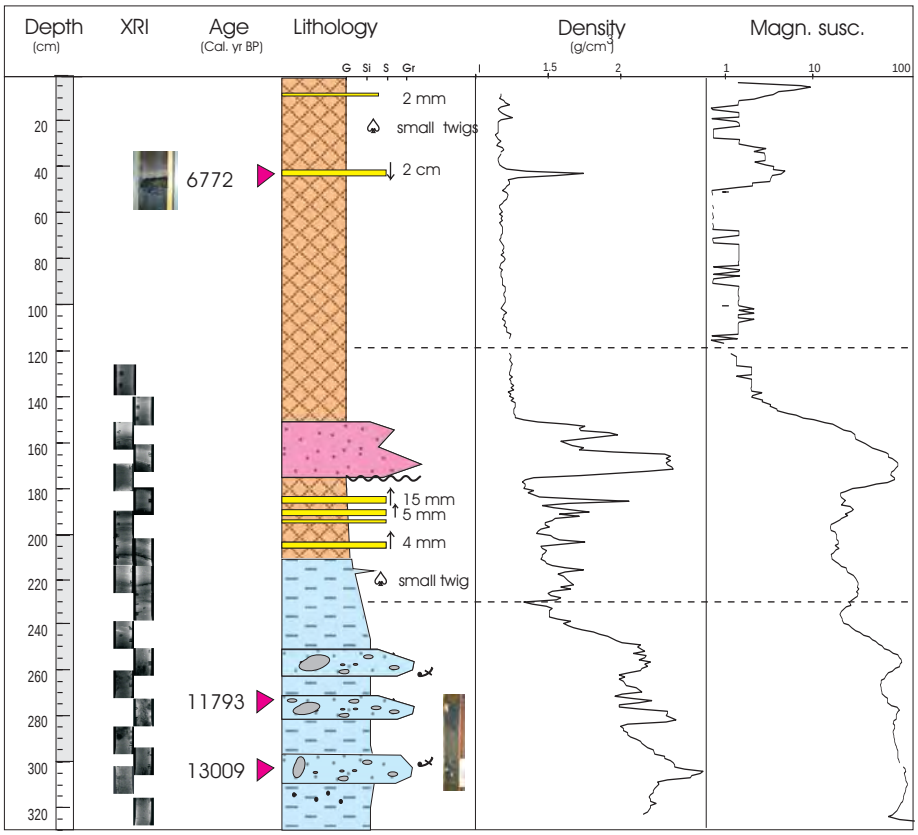

Nedstevatnet, N5

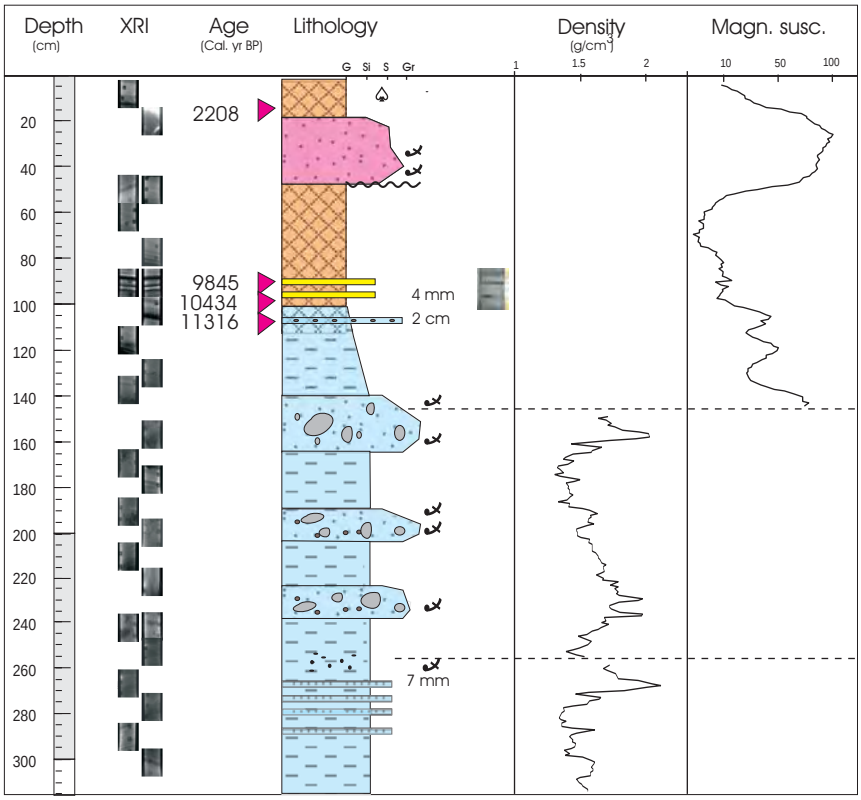

Rotevatnet, R1

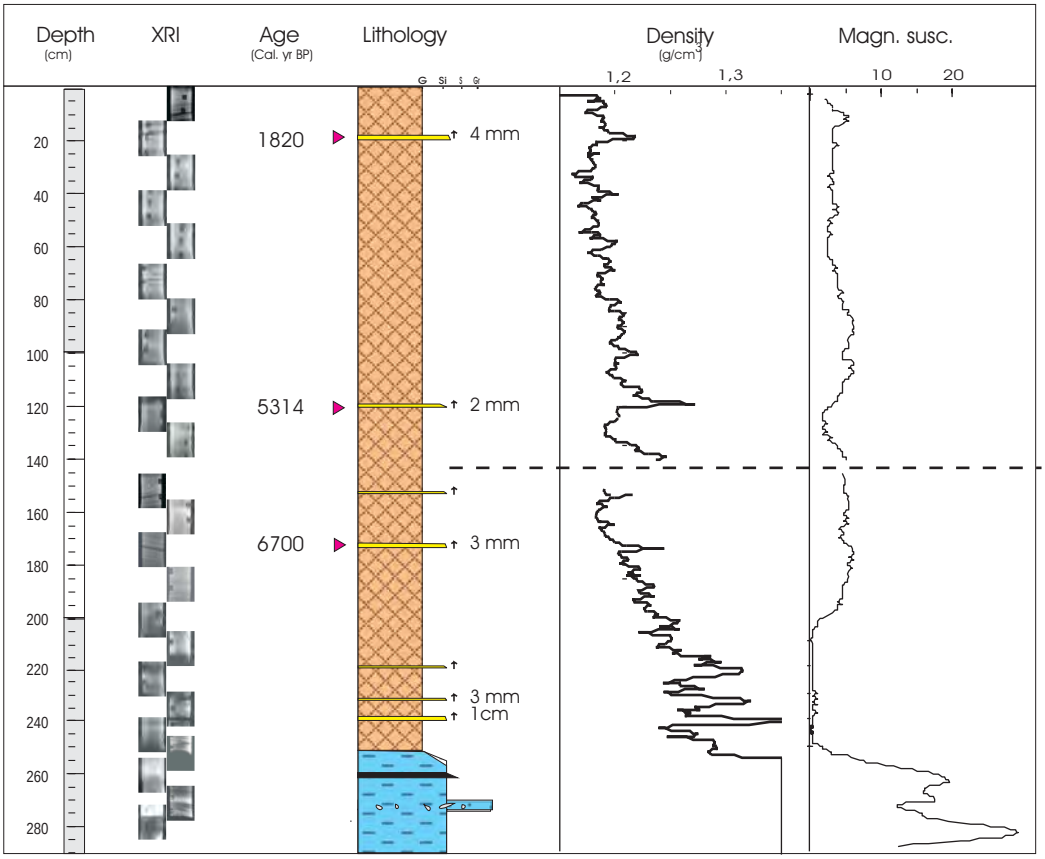

Rotevatnet, R2

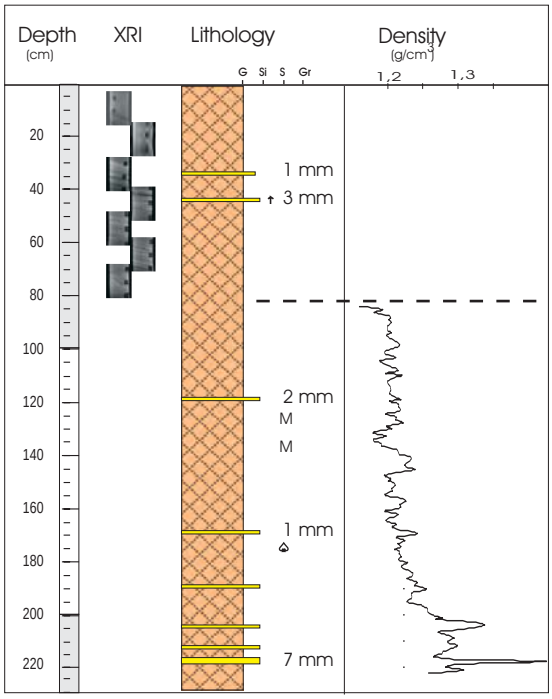

Rotevatnet, R3

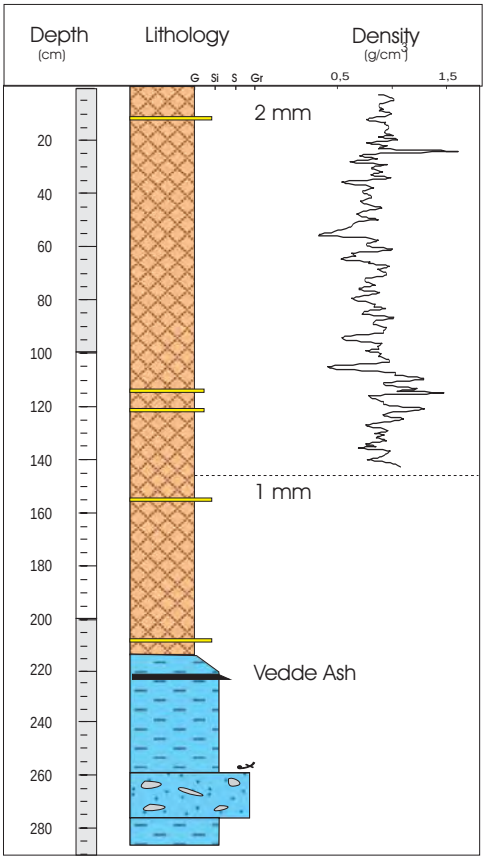

Hovdevatnet, H1

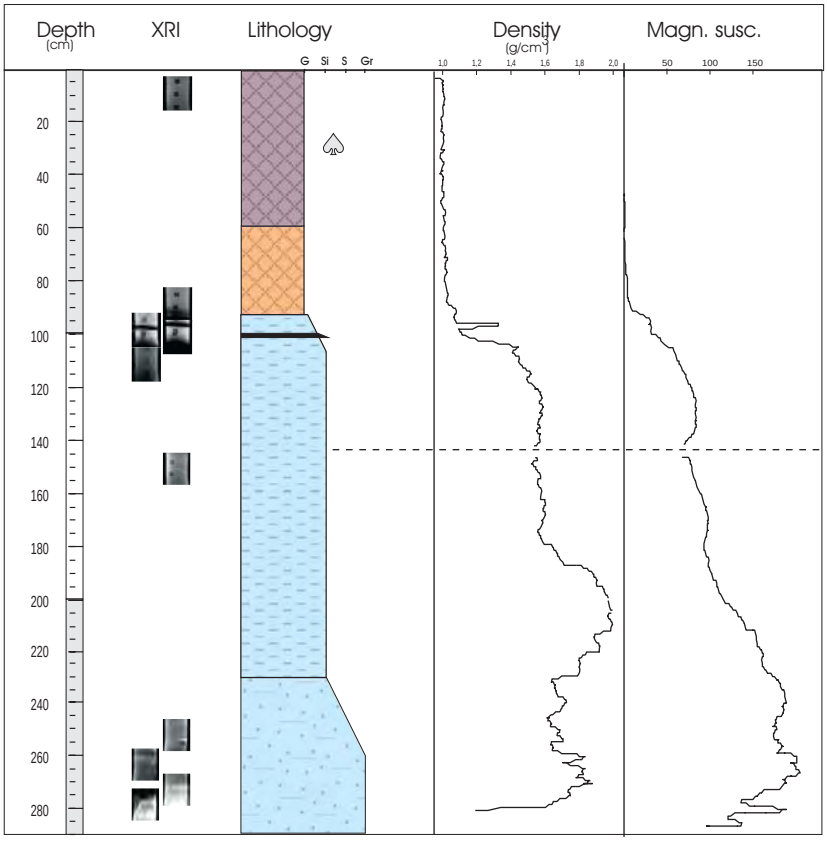

Hovdevatnet, H2

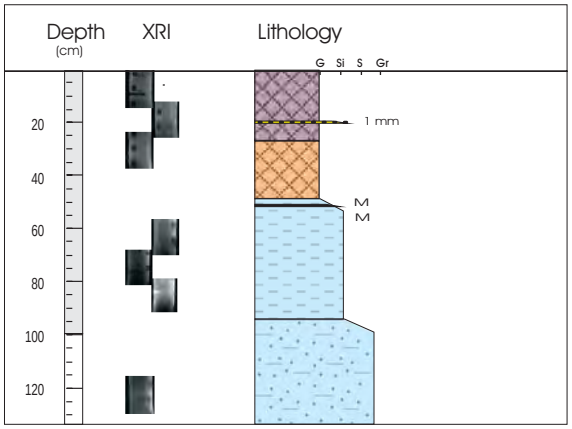

Hovdevatnet, H3